2015

Distributions of glycine betaine and the methylamines in coastal waters: analytical developments and a seasonal study

Cree, Charlotte

DISTRIBUTIONS OF GLYCINE BETAINE AND THE METHYLAMINES IN COASTAL WATERS: ANALYTICAL DEVELOPMENTS AND A SEASONAL STUDY

by

Charlotte Cree

A thesis submitted to Plymouth University

in partial fulfilment for the degree of

DOCTOR OF PHILOSOPHY

Biogeochemistry Research Centre

Plymouth University

In collaboration with

Plymouth Marine Laboratory

September 2014

'To strive, to seek, to find and not to yield!'

Alfred Lord Tennyson

Abstract

Distributions of glycine betaine and the methylamines in coastal waters: analytical developments and a seasonal study

Charlotte Cree

A novel technique comprising solid phase microextraction and gas chromatography has been developed to analyse the three methylamines (monomethylamine, dimethylamine and trimethylamine) at the concentrations expected in seawater. The volatility of the methylamines was exploited and allowed the headspace pre-concentration and gas chromatographic separation of the analytes. This method achieved limits of detection of 0.43 nmol dm^{-3}, 2.50 nmol dm^{-3} and 0.37 nmol dm^{-3} for monomethylamine, dimethylamine and trimethylamine, respectively, which are lower than any previously reported for seawater. This technique was applied to natural samples collected from the Western English Channel (WEC) and the methylamines were successfully quantified.

A liquid chromatography-mass spectrometry method was used to analyse glycine betaine in marine particulates. The volume filtered during sample collection was found to be critical in achieving accurate measurements of glycine betaine. Large filter volumes (1 L) significantly decreased observed concentrations compared to smaller volumes, and 10 mL was the optimised amount filtered. The difference in concentrations was attributed to large water volumes causing cell damage and loss of glycine betaine to the dissolved phase. Cell resilience was thought to play a role in the differences observed; for example, diatoms with their rigid silica cell walls were hypothesised to be more resilient to filtration stress.

A seasonal study was carried out in the WEC using both 1 L and 10 mL samples and maximum glycine betaine concentrations were 50 nmol dm^{-3} and 484 nmol dm^{-3} in the 1 L and 10 mL samples, respectively. The latter concentrations were more than an order of magnitude higher than all previous measurements. Seasonality was observed and a significant correlation was found with chlorophyll *a*. Statistics were applied to the phytoplankton biomass data and contributions

from specific phytoplankton taxa were identified, including from *Prorocentrum minimum* and *Chaetoceros socialis*.

Table of Contents

List of Figures

List of Tables

ACKNOWLEDGMENTS

A PhD is generally thought of as one person's labour of love. To a certain extent this is true, however it could not happen without the help and support of a great many people. First and foremost, my greatest thanks must go to my supervisors Mark Fitzsimons and Ruth Airs. To Mark, for always having an open door and providing the guidance I needed to navigate the minefield of methylamine analysis. To Ruth, for always reassuring me that I could do it and for marking thesis drafts in multi-coloured pens to soften the blow! Thanks also to Anthony Lewis and Steve Archer for providing valuable insight and advice throughout this challenging project.

Thanks must also go to my colleagues in the Biogeochemistry Research Centre and at PML, who have made the many hours in the lab far more bearable. Special thanks go to Dr Paul Sutton, who has always been so generous with his time and knowledge; everything I know about GC analysis I learnt from you. Thanks also to Professor Steve Rowland for funding the purchase of the nitrogen-phosphorus detector that proved so valuable to this project.

Thank you to the technical staff at Plymouth University: Andrew, Andy, Claire and Ian, who always had time to help and answer my endless supply of stupid questions. My seasonal study was improved immeasurably by the fantastic work of the WCO, so thank you to the crew and scientists who sample every week. This includes, but is not limited to: Claire Widdicombe, Glen Tarran, Denise Cummings and Carolyn Harris.

I could not have gotten this far without the immense amount of support I have always received from my friends. Thank you to Debs for the emergency hot chocolates and record rainfall in Durban. Thanks also to Claire and Morwenna for the endless cups of tea and coffee. To Matt (and of course Tom) for picking me up when I fell, and for never failing to make me laugh. And of course to Steph, for smiling through the tears and dancing in the rain.

Thank you finally to my parents and sister Alice, for never letting me believe I couldn't do anything I ever wanted. Mum and dad, you taught me to live my life with courage and conviction and I could not have done this without your constant love and support.

AUTHOR'S DECLARATION

At no time during the registration for the degree of Doctor of Philosophy has the author been registered for any other University award without prior agreement of the Graduate Committee

Work submitted for this research degree at the Plymouth University has not formed part of any other degree either at Plymouth University or at another establishment

This study was financed with the aid of a studentship from the Natural Environment Research Council and carried out in collaboration with Plymouth Marine Laboratory.

A programme of advanced study was undertaken, with relevant scientific seminars and conferences attended at which work was often presented.

Word count of main body of thesis: 44278

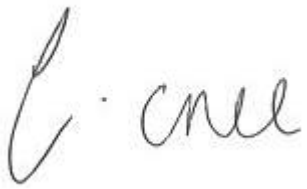

Signed:

Date: 29th May 2015

PRESENTATIONS AND CONFERENCES ATTENDED

2014 Challenger Conference for Marine Science, Plymouth UK: Oral and poster presentations.

2014 International Symposium on DMSP and related compounds Barcelona, Spain: Oral and poster presentations.

2013 British Organic Geochemistry Conference, Plymouth, UK: Poster

2012 6th Annual PlyMSEF Conference, Plymouth, UK: Oral presentation.

2012 Biogeochemistry Research Centre Conference, Plymouth, UK: Oral presentation.

2012 Challenger Conference for Marine Science, Norwich, UK: Oral and poster presentations.

2012 British Organic Geochemistry Conference, Leeds, UK: Oral presentation.

2011 5th Annual PlyMSEF Conference, Plymouth, UK: Oral presentation.

2011 Biogeochemistry Research Centre Conference, Plymouth, UK: Oral presentation.

2010 Biogeochemistry Research Centre Conference, Plymouth, UK: Oral presentation.

PAPERS

Cree, C., Airs, R.L., Archer, S.D., Fitzsimons, M.F. A seasonal study of particulate glycine betaine in the Western English Channel. Environmental Chemistry. *In preparation.*

Cree, C., Airs, R.L., Fitzsimons, M.F. Development and application of solid phase microextraction to the measurement of methylamines in seawater. Environmental Chemistry. *Submitted.*

Cree, C., Airs, R.L., Archer, S.D., Fitzsimons, M.F. A review of analytical techniques for the analysis of methylated amines in marine systems. Trends in Analytical Chemistry. *In preparation.*

LIST OF COMMON ABBREVIATIONS

ANOVA	analysis of variance	LoQ	limit of quantification
ACN	acetonitrile	MA	methylamines
CCN	cloud condensing nuclei	MLD	mixed layer depth
CERN	European Organisation for Nuclear Research	MMA	monomethylamine
CLOUD	Cosmics Leaving OUtdoor Droplets	MS	mass spectrometry
CPA	cyclopropylamine	NPD	nitrogen-phosphorus detector
DEA	diethylamine	NPF	new particle formation
DIC	dissolved inorganic carbon	ODS	octadecasilyl
DMA	dimethylamine	PAR	peak area ratio
DMS	dimethylsulphide	PAR	photosynthetically active radiation
DMSP	dimethylsulphoniopropionate	PDMS	polydimethylsiloxane
DOC	dissolved organic carbon	phytC	phytoplankton biomass carbon
DON	dissolved organic nitrogen	PON	particulate organic nitrogen
DVB	divinylbenzene	PTFE	polytetrafluorothylene
ESI	electrospray ionisation	QA	quaternary amine
FID	flame ionisation detector	RSD	relative standard deviation
FMOC	9-fluorenylmethyl chloroformate	SPE	solid phase extraction
GBT	glycine betaine	SPME	solid phase microextraction
GC	gas chromatography	SST	sea surface temperature
GF/F	glass fibre filter	SW	seawater
HPLC	high-performance liquid chromatography	TDN	total dissolved nitrogen
HPW	high purity water	TMA	trimethylamine
IC	ion chromatography	TMAO	trimethylamine N-oxide
IS	internal standard	UV	ultraviolet
LC-MS	liquid chromatography mass spectrometry	VOC	volatile organic compounds
LLE	liquid-liquid extraction	WCO	western channel observatory
LoD	limit of detection	WEC	western English channel

Chapter 1

Introduction

Chapter Outline

This chapter introduces glycine betaine and the methylamines and their role in the marine environment. The osmotic role of glycine betaine is discussed and the cycling of these nitrogenous compounds in marine systems is examined. Finally, a potential role for the methylamines in atmospheric chemistry is explored.

Summary

Nitrogen is a dynamic element in marine systems. It is primarily used as a nutrient, but it may have a climatic role. For example, the quaternary amine glycine betaine, produced by phytoplankton, degrades to produce the methylamines. These volatile constituents of the nitrogen cycle are able to cross the air-sea interface where they affect atmospheric chemistry and influence cloud formation by acting as a source of base to the atmosphere. This characteristic makes the methylamines potentially significant for climate regulation which, in turn, will affect algal productivity. The cycling of the methylamines on a global scale is poorly understood and the predicted changes in climate make an understanding of their role in marine systems a key research goal.

1.1 Nitrogen in the Marine Environment

The nitrogen (N) cycle is one of the most complex cycles in the marine environment and plays an important role in maintaining the biogeochemical balance of this element via a myriad of chemical transformations. The dominant form of nitrogen in marine systems is gaseous molecular nitrogen (N_2), which accounts for more than 95% of the nitrogen present (Karl and Michaels, 2001). The stability of the nitrogen triple bond means that this form of nitrogen is inert to all but the specialised N_2-fixing organisms, such as some species of cyanobacteria. As a result, forms of 'fixed' nitrogen, such as nitrate, nitrite and ammonium, in addition to dissolved organic nitrogen (DON) and particulate organic nitrogen (PON), serve as a nitrogen source for most primary production. Nitrogen availability is dependent on two broadly-defined sources for primary production: new nitrogen and regenerated nitrogen (Karl and Michaels, 2001). New nitrogen in the system comprises nutrient input from outside the euphotic zone whilst regenerated nitrogen takes the form of inorganic nutrients recycled from organic matter within the euphotic zone. The resulting biogeochemical cycle, represented in Figure 1.1, is complicated by the diversity of compounds formed and the transfers involved (Capone, 2008).

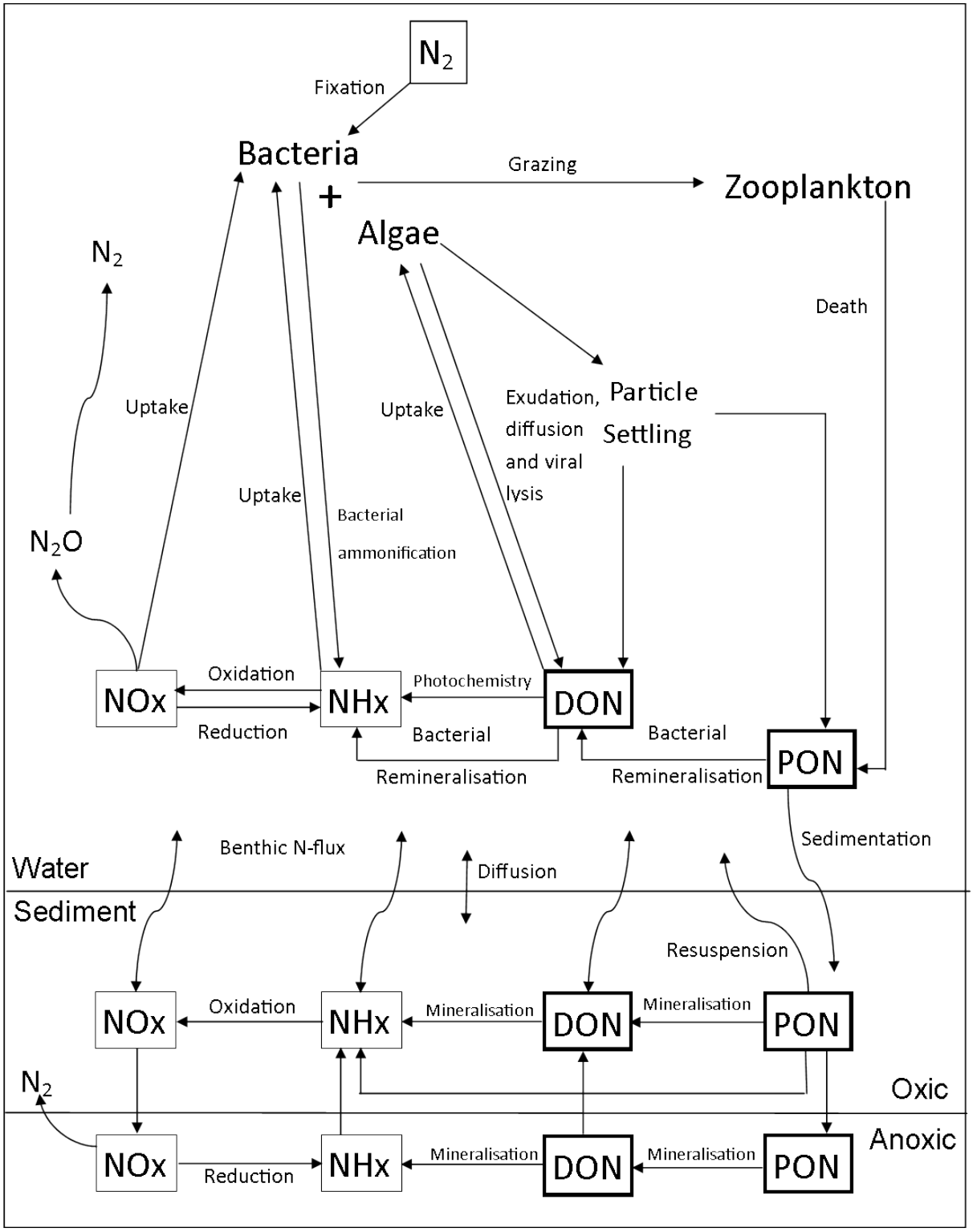

Figure 1.1: Biogeochemical cycle of N, highlighting its role in the sediment and the water column. DON: dissolved organic nitrogen; PON: particulate organic nitrogen; adapted from Worsfold et al. (2008)

1.1.1 Dissolved Organic Nitrogen

Many studies have focused on inorganic nitrogen because of its demonstrated contribution to primary production (Capone, 2008). However, interest in DON as a source of nitrogen for biological productivity is increasing. DON makes up a considerable proportion of total nitrogen (TN), comprising up to 60-69% of total dissolved nitrogen (TDN) in some rivers, estuaries and surface ocean waters (Bronk, 2002). The average composition of nitrogen pools in ocean, coastal and estuarine waters, demonstrating the percentage contribution of DON, is illustrated in Figure 1.2.

DON was previously believed to be a refractory pool and unavailable as a source of nitrogen for primary production (Berman and Bronk, 2003). However, more recent studies found that DON was rapidly cycled in aquatic ecosystems, indicating that the DON pool contained a labile component. It was later concluded that up to 70% of DON is bioavailable (Bronk, 2002). The identification of bioavailable DON species has meant that the DON pool is increasingly being recognised as a dynamic constituent of the marine nitrogen cycle.

The DON pool is a heterogeneous mix of biologically-labile species and refractory compounds. It is chemically complex and, although a large number of molecules have been identified (e.g. urea, dissolved combined amino acids, humic substances and nucleic acids), a significant proportion remains unidentified. For example, in ocean environments less than 14% of DON is identifiable at the molecular level (Cape et al., 2011; Worsfold et al., 2008). This lag in addressing DON cycling can be attributed, in part, to limitations in analytical methods. All

current methods of quantifying total DON involve measuring TDN and then subtracting the DIN fraction, which comprises NH_4^+ and combined NO_2^-/NO_3^- measurements (Bronk, 2002). This approach combines the analytical error and uncertainty of three analyses: TDN, NH_4^+ and NO_2^-/NO_3^- and, as such, is problematic.

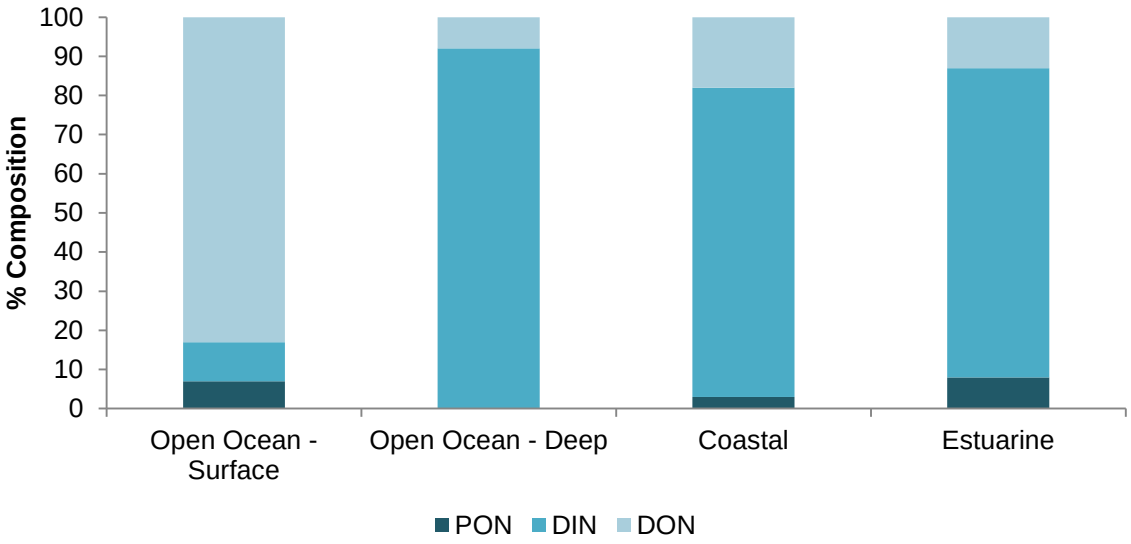

Figure 1.2: Average composition of nitrogen pools in open ocean surface water, open ocean deep water, coastal and estuarine waters, modified from Berman and Bronk (2003). PON: particulate organic nitrogen; DIN: dissolved organic nitrogen and DON: dissolved organic nitrogen.

The cycling of DON in marine systems can be understood as comprising two main parts: sources and sinks. Sources of DON to aquatic systems are both abiotic and biotic (Berman and Bronk, 2003). Abiotic sources of DON include atmospheric inputs, sediment and run-off from terrestrial regions. In estuarine and coastal waters the composition of the DON pool is heavily influenced by its catchment area. Sediment release can also be an important source of DON, particularly in shallow coastal and estuarine environments (Fitzsimons et al.,

2006). For example, in shallow Danish coastal waters the release of DON from sediment was estimated to be twice that of DIN (Lomstein et al., 1998).

Biotic sources of DON include phytoplankton, bacteria, zooplankton and viral lysis events (Berman and Bronk, 2003). Extracellular release from phytoplankton occurs via either passive diffusion or active exudation, whilst meso- and macrozooplankton are able to release DON by faecal pellet dissolution, excretion and sloppy feeding and bacterial action could also release DON (Berman and Bronk, 2003). Viral lysis events can release DON and affects both autotrophs and heterotrophs. These processes are summarised in Figure 1.3a.

Four primary DON sinks exist: bacterial uptake, photochemical decomposition, abiotic adsorption and phytoplankton uptake (Figure 1.3b). A major loss of nitrogen from the DON pool occurs through bacterial uptake and degradation to ammonium, which can be assimilated by bacteria and phytoplankton or oxidised to nitrate. Dissolved organic matter can photo-degrade to produce biologically-available nitrogen, including dissolved ammonium, primary amines and nitrite (Bushaw-Newton and Moran, 1999; Bushaw et al., 1996; Moran and Zepp, 1997). Components of the DON pool can be removed by adsorption to colloids (Schuster et al., 1998) and sub-micron particles (Nagata and Kirchman, 1996). Phytoplankton are able to utilise DON as a source of nitrogen; for example 50% of daily phytoplankton demand in the North Pacific could potentially be met by remineralisation of the DON pool (Benner et al., 1997)

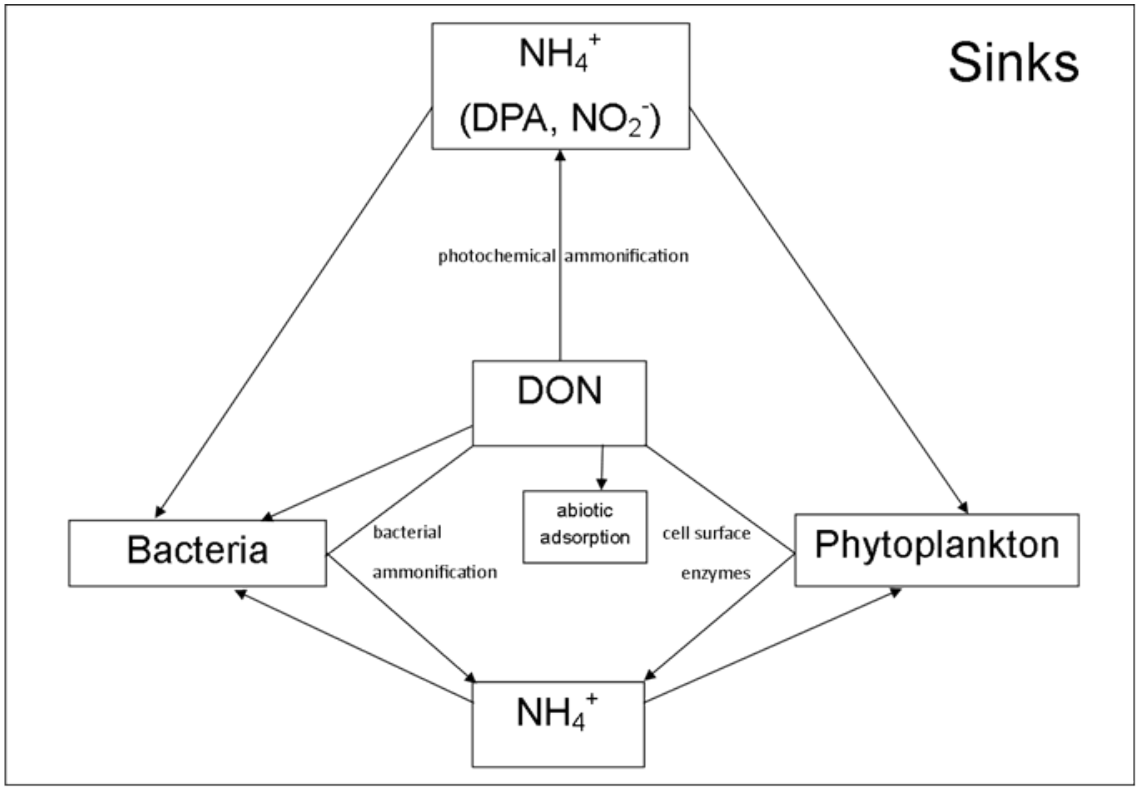

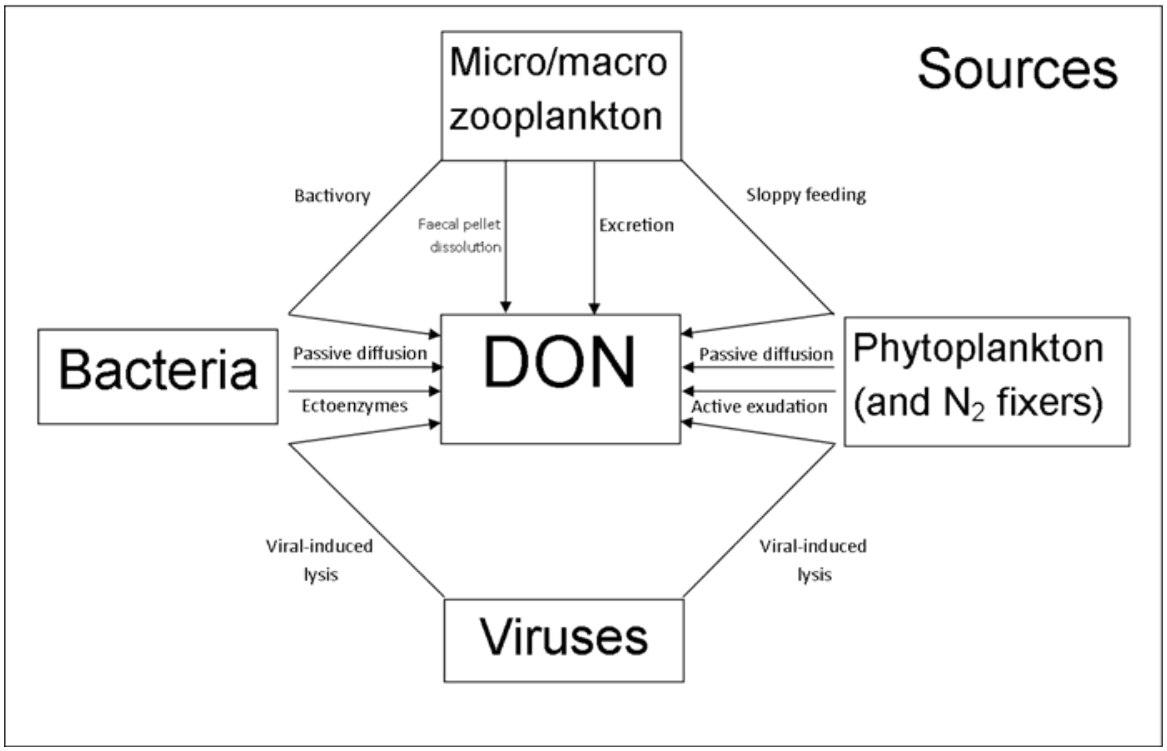

Figure 1.3: a) Sources of DON in aquatic systems b) Sinks of DON in aquatic systems. DPA: dissolved primary amines, adapted from Bronk (2002)

1.1.2 Microbial Ecology and the Nitrogen Cycle

The term microbes is used to cover all single-celled organisms: autotrophic and heterotrophic prokaryotes, such as bacteria and cyanobacteria; autotrophic and heterotrophic eukaryotes, such as algae and phagotrophic protists as well as viruses. Microbes are ubiquitous in the marine environment, diverse in nature and very important to the functioning of marine systems. Microbial activities include photosynthesis, organic carbon degradation, nitrogen fixation, nitrification and denitrification and play a key role in the nitrogen cycle. Most transformations between fixed nitrogen species are mediated by marine organisms, either as part of their metabolism to obtain nitrogen for synthesis or to gain energy for growth (Table 1.1) (Capone, 2008).

Table 1.1: Microbial mediated nitrogen cycle processes

Process	Organisms	Biogeochemical Role
NO_3^- assimilation	Phytoplankton	Source of N
NO_2^- assimilation	Phytoplankton	Source of N
NH_4^+ assimilation	Phytoplankton Bacteria	Source of N
Ammonification	Bacteria Zooplankton	Release of N
Denitrification	Bacteria	Electron acceptor
Anammox	Bacteria	Source of energy
N_2 fixation	Cyanobacteria	Source of N

As nitrogen fixation can only be carried out by specialised nitrogen-fixers most marine microbes need to utilise ‘prefixed’ nitrogen from their environment to meet their nitrogen requirements. As a consequence, and due to the nitrogen-limited characteristic of many ecosystems, nitrogen is thought to be a limiting factor in phytoplankton growth (Ryther and Dunstan, 1971; Sharp, 1983).

1.2 Glycine Betaine

1.2.1 Function

The primary role of glycine betaine (GBT) (Figure 1.4A) in phytoplankton is as an osmolyte (Dickson and Kirst, 1986; King, 1988a). Aquatic organisms face unique biological pressures due to water stresses such as high or fluctuating salinity, desiccation and freezing (Yancey et al., 1982) and in order to survive in this medium, cells must maintain an intracellular osmotic pressure greater than that of the exterior (Welsh, 2000). Consequently, the ability to adapt to fluctuations in the osmolarity of the growth medium is vital for growth and survival. Prokaryotes, plants and animals show remarkably similar responses to osmotic stress, with each utilising organic salts and a group of low molecular weight organic molecules as osmolytes (Yancey et al., 1982). Inorganic salts, such as KCl, can be used and a positive correlation between intracellular K^+ concentrations and tolerance of high salinity has been reported (Csonka, 1989). However use of this osmolyte can present difficulties as cells exhibit a narrow range of adaptation (Welsh, 2000). For example, halobacterial cell envelopes are structurally unstable outside a limited range of inorganic salt concentrations.

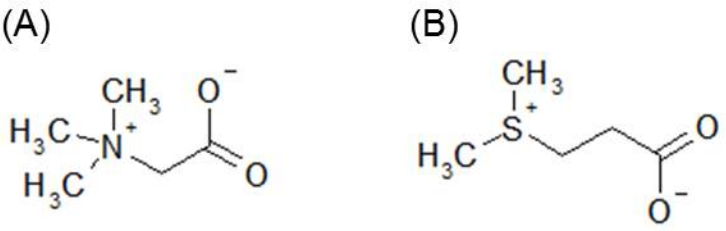

Figure 1.4: The structures of: (A) glycine betaine and (B) dimethylsulphoniopropionate

A number of low molecular weight organic osmolytes are synthesised or accumulated by organisms for use in osmoregulation (Burg and Ferraris, 2008; Welsh, 2000). They are often termed compatible solutes as they can be accumulated to high concentrations without disturbing cell chemistry, such as DNA replication and cellular metabolism. Such compounds include polyhydric alcohols (e.g. glycerol), free amino acids, quaternary amines (e.g. betaines) and urea (Dickson and Kirst, 1986; Yancey et al., 1982). Solutes that are non-charged or zwitterionic are often favoured over ionic solutes. For example, the zwitterionic GBT ($(CH_3)_3N^+CH_2O_2^-$, Figure 1.4A) is the preferred compatible solute in most eubacterial species and allows the highest levels of osmotolerance (Poolman and Glaasker, 1998). Utilising compatible solutes such as glycine betaine alters a small fraction of cell macromolecular structure instead of having to modify a vast number of proteins in order to cope with high or fluctuating salt concentrations (Yancey et al., 1982).

In addition to their osmotic function, compatible solutes have a number of other proposed uses (Welsh, 2000). Firstly, as they are often accumulated to high concentrations in cell cytoplasm, they could represent significant intracellular stocks of carbon and nitrogen (Galinski and Trüper, 1982; Liss et al., 1997; Turner et al., 1988). For example, *Ectothiorhodospira halochloris*, (a

haloalkophilic phototrophic bacterium,) synthesises GBT (1N atom) as its major compatible solute, but can also produce two minor solutes, trehalose (0N atoms) and ectoine (2N atoms). During periods of nitrogen repletion ectoine is accumulated and trehalose pools are minimal or absent. During periods of nitrogen depletion trehalose is accumulated to replace ectoine; this latter process is thought to liberate the nitrogen in ectoine for cell growth (Liss et al., 1997; Turner et al., 1988). Similarly, dimethylsulfoniopropionate- (DMSP) synthesising micro-algae may accumulate nitrogenous compatible solutes, such as GBT and proline, when fixed nitrogen is abundant (Figure 1.4B). These nitrogenous pools can then be replaced by DMSP when nitrogen becomes more limited (Liss et al., 1997).

Secondly, compatible solutes can provide protection against stresses other than osmotic stress. For instance the disaccharide trehalose is associated with increased thermotolerance in bacteria, yeast, fungal and slime mould cells (Hottiger et al., 1987). Compatible solutes can also provide protection against freezing. Sugars and polyols especially, have been found to increase the resistance of microbial cells to freezing (Welsh, 2000).

Thirdly, compatible solutes can be released to the environment by passive diffusion, during ‘sloppy’ grazing and cell lysis. These compatible solutes are then available for scavenging by other members of the community for use as compatible solutes or as sources of carbon, nitrogen and energy. Microorganisms possess transport systems to scavenge compatible solutes that they are unable to synthesise themselves. For example, many heterotrophic bacteria that are

incapable of synthesising GBT possess GBT transport systems (Booth and Higgins, 1990; Higgins et al., 1987; Poolman and Glaasker, 1998; Record Jr et al., 1998). GBT transport systems are also capable of accumulating other compatible solutes. This ability was demonstrated in natural seawater samples where DMSP and GBT were observed to compete for the same transport systems (Kiene et al., 1998). In natural ecosystems the ability to scavenge compatible solutes may provide an ecological advantage as uptake from the environment is a relatively low-energy process compared to *de novo* biosynthesis. Organic osmolytes are thought to be functionally interchangeable with cells that are capable of being protected by a variety of compatible solutes (Burg and Ferraris, 2008). For example, growth of *Escherichia coli* in saline media was improved by addition of osmolytes, which were not normally utilised by the bacteria, to the growth media (Hanson et al., 1991).

A further role of GBT may be the protection of cells in higher plants and cyanobacteria against photo-oxidative stress and photo-inhibition by protecting Photosystem II (PSII), the first protein complex in the light-dependent reactions of photosynthesis (Kondo et al., 1999; Papageorgiou and Murata, 1995; Prasad and Saradhi, 2004). GBT is thought to act as a protein-stabilising osmolyte in higher plants and cyanobacteria (Papageorgiou and Murata, 1995) and was observed to enhance and stabilise the oxygen-evolving activity of PSII protein complexes. Furthermore, GBT was thought to accelerate recovery of PSII from a photo-inactivated state (Prasad and Saradhi, 2004). Although this effect has not been studied in phytoplankton, photosynthesis observed in the cyanobacterium *Synechococcus,* when modified to accumulate GBT, was more tolerant to light

levels than control cells (Deshnium et al., 1997). In addition to protecting cells from light stress GBT has been proposed to stabilise the action of antioxidant enzymes. This was demonstrated in transgenic wheat species (Liang et al., 2009) and resulted in a higher tolerance for salt stress than the wild-type species.

1.2.2 The relationship between GBT and DMSP

The similarities in structure and properties of DMSP and GBT were noted during early studies of marine osmolytes (Challenger, 1951) (Figure 1.4). Both DMSP and GBT are energetically expensive to produce, with each ultimately requiring reductive assimilation and subsequent methylations. Production of GBT and DMSP therefore involves the dedication of significant amounts of energy and cell resources. Allocation of cellular nitrogen to GBT production is particularly interesting as nitrogen is considered to be a limiting factor in many marine ecosystems. A reciprocal relationship between DMSP and GBT in marine phytoplankton has been proposed (Andreae, 1986) where, in nitrogen-limited conditions, DMSP would be preferentially synthesised over nitrogen containing osmolytes. Investigations into this proposed relationship are discussed further in Section 1.2.4.

1.2.3 Production of GBT

Biosynthesis

GBT can either be taken up directly from the environment or synthesised. Studies of biosynthesis have primarily been carried out in higher plants and in bacteria. Two primary precursors of GBT have been identified: choline and glycine (Nyyssölä et al., 2000). The most common synthetic pathway is conversion of

choline, via a two-step process, with betaine aldehyde as an intermediate. This pathway has been observed in both bacteria and higher plants, with the differences observed in the enzymes involved. Bacteria and higher plants use betaine dehydrogenase in the conversion of betaine aldehyde to GBT (Lamark et al., 1991; Velasco-García et al., 1999). Divergence occurs in the choline to betaine aldehyde conversion. Gram negative bacteria, such as *Escherichia coli*, use a choline dehydrogenase (Boch et al., 1996; Pocard et al., 1997) while Gram positive bacteria, such as *Bacillus subtilis*, utilise an alcohol dehydrogenase (Boch et al., 1996) and plants use a choline monooxygenase (Weretilnyk and Hanson, 1989).

An alternative pathway involving a three-step methylation from glycine has been identified in extreme halophiles (Nyyssölä et al., 2000). The reaction is catalysed by two methyltransferases: *glycine sarcosine methyltransferase* and *sarcosine dimethyl methyltransferase*. This pathway is less commonly observed, which is because methylation reactions are highly energetically expensive.

Biosynthesis of GBT has not been studied in marine phytoplankton. Synthetic routes can therefore only be inferred from the studies carried out in higher plants and bacteria. However, as both the indicated precursors, choline and glycine are known to be present in phytoplankton (Airs and Archer, 2010) the presence of similar reaction pathways is probable.

1.2.4 GBT in Phytoplankton Cultures

The most extensive knowledge of GBT in marine systems has come from four culture studies (Keller et al., 1999b; Keller et al., 1999a; Spielmeyer et al., 2011; Spielmeyer and Pohnert, 2012). The quantitative significance of GBT and DMSP was investigated in six batch cultured species of phytoplankton (Keller et al., 1999b). GBT was observed in three of the six species cultured: the dinoflagellate *Amphidinium carterae*, the prymnesiophyte *Chrysochromulina sp*. and the cocolithophore *Emiliania huxleyi* (Table 1.2). The GBT concentrations were highly variable in terms of species and the growth cycle but evidence indicated that the presence of GBT was related to nitrogen availability. The prymnesiophyte *Chrysochromulina sp*., for example, contained significant concentrations of GBT (172.3 µM) during exponential phase growth which rapidly diminished as the cells entered stationary phase (4.0 µM) (Keller et al., 1999b); a change which coincided with nitrogen limitation. In addition, *Emiliania huxleyi* produced maximum levels of GBT when the cells were nitrogen-replete and maintained a low level throughout the stationary phase, when nitrogen levels were diminished (Keller et al., 1999b).

No clear relationship between GBT and DMSP was observed in the cultures studied (Keller et al., 1999b). Consequently, additional culture experiments were carried out to further investigate a potential relationship (Keller et al., 1999a). Three species, *Thalassiosira pseudonana*, *Emiliania huxleyi* and *Amphidinium carterae* were studied using nitrogen-limited chemostat cultures. A reciprocal relationship between GBT and DMSP was identified in *Thalassiosira pseudonana* with GBT dominating under nitrogen-replete conditions and DMSP dominating

under nitrogen-deficient conditions. This relationship was not observed in the other two species studied. The DMSP and GBT concentrations did not vary in a systematic way with nitrogen availability in *Amphidinium carterae* and the DMSP concentrations observed in *Emiliania huxleyi* remained constant despite changes in GBT concentration, which increased during the highest growth rate (Keller et al., 1999a). However, the addition of nitrate to the nitrogen-limited cultures resulted in increased GBT concentrations in all three species providing additional evidence that GBT production is sensitive to nitrogen availability.

Twenty one microalgal species were cultured by Spielmeyer et al. (2011) and eight species were observed to produce GBT including prymnesiophytes, a cryptophyte and a dinoflagellate (Table 1.2). Interestingly, the data from the separate culture studies (Keller et al., 1999b; Spielmeyer et al., 2011) were often conflicting. For example, 7 pg GBT per cell was observed in *Prorocentrum minimum* by Spielmeyer et al. (2011) but was absent in the cultures analysed by Keller et al. (1999b). This could indicate that GBT is not only species-specific but also strain-specific. However, the two studies employed different methods and different limits of detection were reported: 47 ng on column (Keller et al., 1999b) and 0.7 ng on column (Spielmeyer et al., 2011) which may have affected the measurements. No definitive link between taxonomic groups and GBT production was observed in these studies. However, all of the prymnesiophytes and dinoflagellates studied produced GBT.

Based on limited studies of other taxonomic groups, such as halophytes and cyanobacteria, GBT could make up a significant percentage (up to 20%) of

cellular nitrogen (Cavalieri and Huang, 1981; King, 1988b). However, N-osmolytes typically contributed less than 2% of cellular organic nitrogen (ca. 7% in *Chrysochromulina spp*.) in studies by Keller et al. (1999b). This percentage is approximately similar to the percentage contribution of the methylamines to marine sediments. DMA and TMA, extracted using hydrochloric acid (HCl) were observed to contribute approximately 0.5% of total organic nitrogen (Lee and Olson, 1984). However, HF extractions were found to recover an order of magnitude more aliphatic amines than HCl extractions (Lee, 1988). This indicated that the MAs could constitute approximately 5% of total organic nitrogen in marine sediments. Further work is required to ascertain the contribution of nitrogen-osmolytes to cellular nitrogen.

The effect of temperature on GBT concentration has also been studied (Spielmeyer and Pohnert, 2012). Two diatoms, *Thalassiosira pseudonana* and *Phaeodactylum tricornutum*, and the cocolithophore *Emiliania huxleyi,* showed a significant increase in GBT content with increasing temperature. The molar concentrations of GBT indicated a pronounced temperature dependence of GBT. Notably, a protein stabilising effect of GBT at elevated temperatures had been observed in higher plants (Papageorgiou and Murata, 1995).

Table 1.2: Summary of particulate GBT (GBT_p) concentrations measured in algal cultures; E = exponential growth phase; S = stationary growth phase.

		GBT Concentration (nmol dm^{-3})	
Class	Species	Keller et al., 1999b	Spielmeyer 2011
Pavlovophyceae	*Pavlova lutheri*		0.25 (E)
Cryptophyceae	*Rhodomonas sp.*		0.95 (E)
Coscinodiscophyceae	*Thalassiosira weissflogii*		1.43 (E)
	Cryptochloris sp.		0.066 (E)
Cocolithophyceae	*Isochrysis galbana*		0.12 (E)
Bacillariophyceae	*Phaeodactylum tricornutum*		1.55 (E)
Dinophyceae	*Prorocentrum minimum*		0.11 (E)
Coscinodiscophyceae	*Thalassiosira pseudonana*		0.59 (E)
Prymnesiophyceae	*Chrysochromulina*	172 (E)	
		4 (S)	
Cocolithophyceae	*Emiliania huxleyi*	32.6 (E)	
		8.1 (S)	
Dinophyceae	*Amphidinium carterae*	2.7 (E)	
		15 (S)	

1.2.5 GBT in Seawater Particulates

The first known study of particulate GBT (GBT_p) in natural phytoplankton populations involved sample collection and analysis at four depth profiles in the Gulf of Maine (Table 1.3) (Keller et al., 2004). GBT_p concentrations of 0-15 nmol dm^{-3} were observed at the four sites but no pattern of distribution was observed. Maximum concentrations of 15 nmol dm^{-3} were observed in the surface waters of the Georges Basin which decreased with depth. Contrastingly, maximum concentrations of 15 nmol dm^{-3} were also observed but at a depth of 100 m in the Wilkinson Basin. Subsequently, a maximum concentration of 18 nmol dm^{-3} was observed in particulates collected from the Western English Channel (Airs and Archer, 2010) (Table 1.3). This concentration was very similar to those observed by Keller et al. (2004). Particulate samples taken in the tropical North Atlantic Ocean contained maximum GBT_p concentrations of 2.2 nmol dm^{-3} in surface water (Airs and Archer, 2010).

Similar GBT_p concentrations for coastal waters were reported in both studies, with lower concentrations observed in oceanic samples, which are expected to contain less biomass.

Table 1.3: GBT_p concentrations measured in natural phytoplankton populations

Location	Keller et al., 2004 (nmol dm^{-3})	Airs and Archer, 2010 (nmol dm^{-3})
Gulf of Maine	0-15	
Western English Channel		18
North Atlantic		2.2

1.2.6 GBT Degradation in the Marine Environment

The degradation pathways of quaternary amines in the water column are poorly understood. Incubation studies using ^{14}C-GBT demonstrated that, once released, GBT is rapidly turned over (0.5-11 hours) in coastal seawater (Kiene and Hoffmann Williams, 1998). Size fractionation indicated that sub-micrometer organisms (thought to be bacteria) were primarily responsible for this uptake (Kiene and Hoffmann Williams, 1998). During the first few hours of incubation over 80% of the isotope was recovered as untransformed ^{14}C-GBT. There were two potential reasons for this; firstly, a lack of constitutive ability to rapidly degrade intracellular GBT and secondly, purposeful accumulation of GBT for osmotic reasons. As the incubations proceeded beyond 4-5 hours the ^{14}C-GBT$_p$ concentrations started to drop but appeared to stabilize at around 1-3 nmol dm^{-3}. The concentration of retained ^{14}C-GBT appeared to be related to salinity as, when the salinity of the incubation was artificially raised, the concentration of ^{14}C-GBT retained within the cell increased. The maximum GBT uptake rates were calculated and were found to range between: 0.39-44 nmol L^{-1} h^{-1}. The observed rates were thought to be influenced by temperature, the number of microorganisms present and the level of transportation and degradation enzymes in these organisms. Further studies looking at temperature dependence found the optimum temperature for uptake and degradation were close to the *in situ* water temperature during sample collection (Kiene and Hoffmann Williams, 1998). This suggested a degree of adaptation by the microbial communities.

GBT can be degraded both aerobically and anaerobically (Figure 1.5) (Bernard et al., 1986; King, 1984). Aerobic degradation has been studied primarily in

terrestrial bacteria and occurs via a series of demethylation reactions to produce glycine (Chlumsky et al., 1995; Smith et al., 1988; Wargo et al., 2008). The resulting glycine is channelled into the Krebs cycle via pyruvate. There is no experimental evidence, however, to demonstrate that marine microorganisms use this pathway for GBT oxidation.

Anaerobic degradation is a more complicated process and involves two pathways. Anaerobic fermentation in marine sediments produces TMA and acetate, with further degradation to DMA and MMA (Chen, 2012; Chen et al., 2011; King, 1984; Welsh, 2000). In the surface ocean this process can take place in anoxic microsites such as detrital particles and the digestive systems of zooplankton (King, 1984). The second pathway involves sequential demethylation by two groups of bacteria: homoacetogens and sulphate reducers (Chen, 2012; Chen et al., 2011; Heijthuijsen and Hansen, 1989; Möller et al., 1984; Müller et al., 1981; van der Maarel et al., 1996) and proceeds via two key intermediates: dimethylglycine and sarcosine.

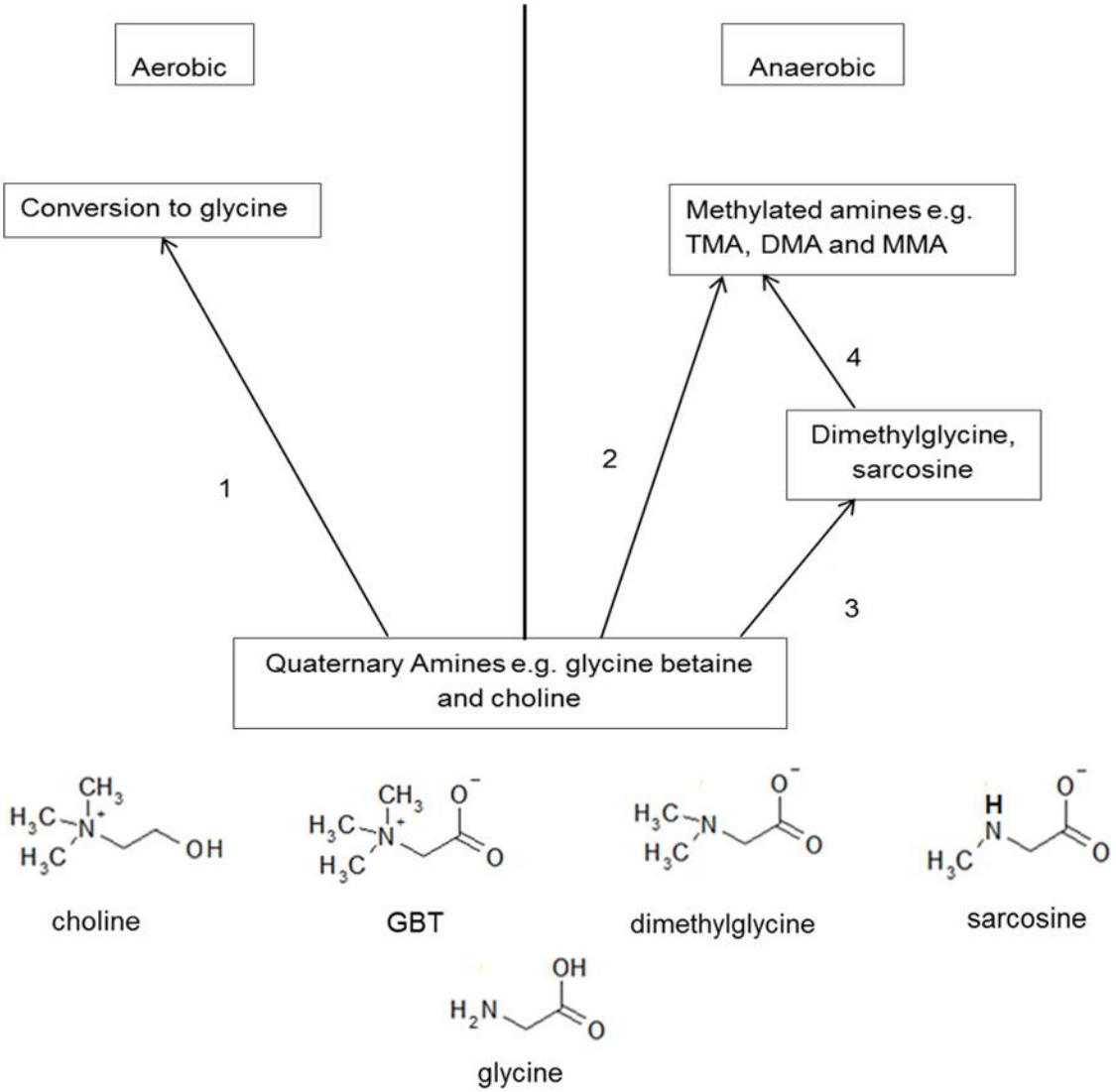

Figure 1.5: Microbial metabolism of the quaternary amines in terrestrial systems. Aerobic degradation through demethylation (1) or anaerobic degradation through reductive cleavage (2) or demethylation (3) followed by further conversion to small methylated amines (4)

1.3 The Methylamines

1.3.1 Production

The major source of MAs is thought to be the biological degradation of quaternary amines (QAs) such as GBT. Anaerobic fermentation or reduction of GBT takes place in sediment and in anoxic microsites in the water column producing trimethylamine (TMA) and acetate (King, 1984). This primary reductive cleavage pathway is mediated by the selenium-containing enzyme: *glycine betaine reductase*. Under anaerobic conditions the TMA is used by methanogens to produce methane (King, 1984). In aerobic conditions the TMA can be further catabolised to produce trimethylamine N-oxide (TMAO), dimethylamine (DMA), monomethylamine (MMA) and, ultimately, ammonium (Figure 1.6) (Chen et al., 2011). A few studies have analysed MA concentrations in the marine environment and these are summarised below.

MA in Marine Sediments

Anaerobic processes play a key role in MA production and one of the main locations for anaerobic production is marine sediments. Studies in the Oglet Bay saltmarsh, situated on the northern shore of the Mersey estuary (NW England) found sediment concentrations of 0-11, 0-0.81 and 0.01-0.81 µmol g^{-1} dry weight for MMA, DMA and TMA respectively (Fitzsimons et al., 1997). These values were similar to those of Yang et al. (1994) who reported MA concentrations and uptake rates in Flax Pond, USA, New York. This study demonstrated a strong seasonal variation in the abundance and biological uptake of the MAs, with both concentrations and uptake higher in summer than in winter (Yang et al., 1994) (Table 1.4). DMA was found to be the most abundant MA (15-180 nmol dm^{-3})

with the highest uptake rate (0.1-12 nmol dm^{-3} h^{-1}), while MMA and TMA both had lower concentrations (5-60 nmol dm^{-3}) and uptake rates (0.01-2.4 nmol dm^{-3} h^{-1}) (Yang et al., 1994).

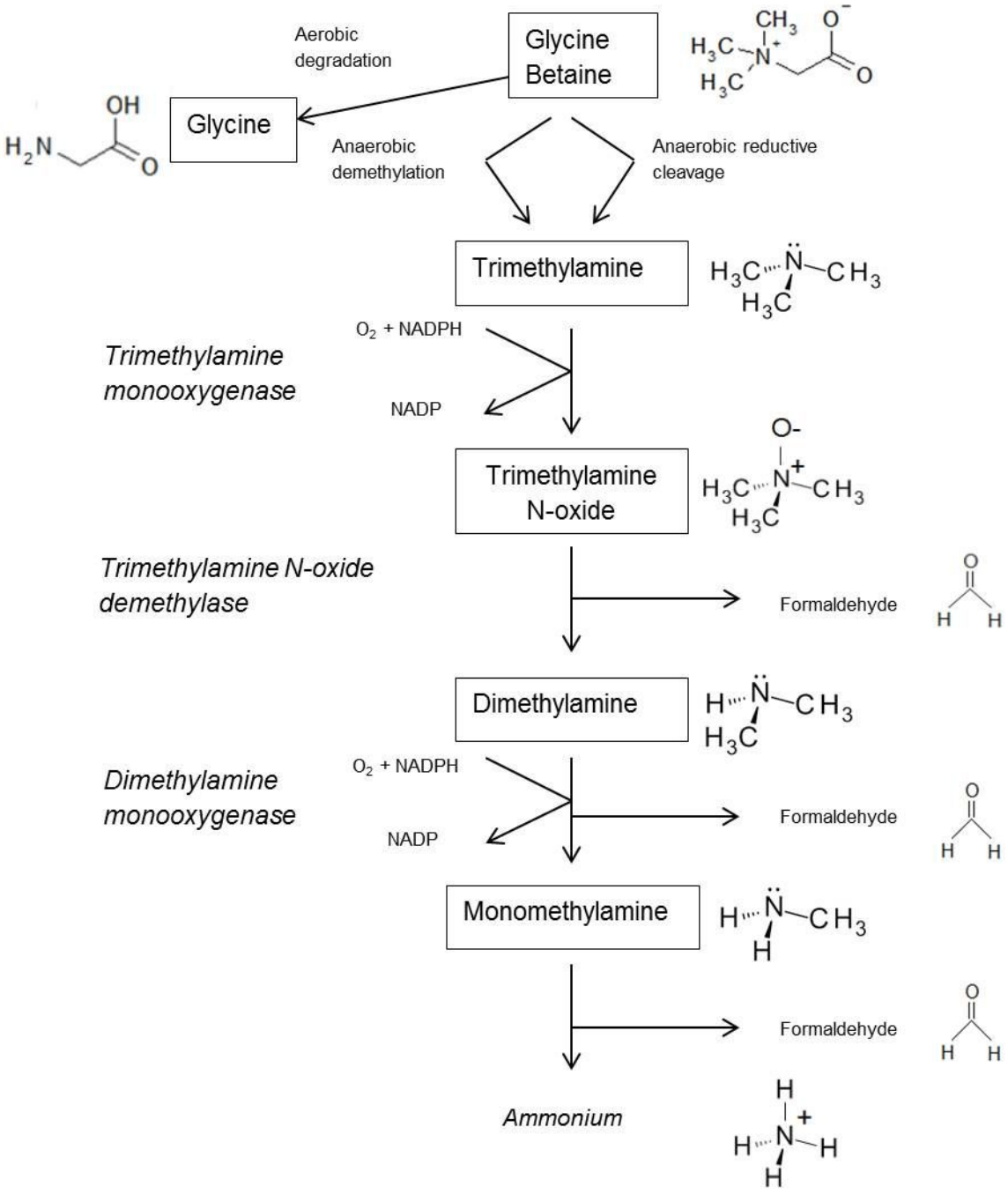

Figure 1.6: Proposed pathway of trimethylamine oxidation in surface waters; adapted from Chen et al. (2011)

MAs in Aquatic Systems

Few reports of MA concentrations in aquatic systems are available. Dissolved MAs were found to be ubiquitous in the photic zone of the Arabian Sea (Gibb et al., 1999a; Gibb et al., 1999b). MMA was reported to be the most abundant MA with TMA present at the lowest concentrations (< 4 nmol dm^{-3}). The concentrations of MMA and DMA were highest in shallow, productive coastal waters compared to offshore waters, whilst TMA concentrations were low (< 4 nmol dm^{-3}) in both the coastal upwelling and offshore regions (Gibb et al., 1999b). In deep waters all three MAs were present in low concentrations (MMA<10, DMA<5, TMA<2 nmol dm^{-3}). This minimal presence below the photic zone suggested that the MAs were closely involved with euphotic zone processes. MMA and DMA vertical concentration maxima were observed to coincide with the chlorophyll *a* (Chl *a*) maxima in both coastal and offshore waters whilst TMA concentration maxima occurred below the Chl *a* maximum at the base of the temperature and oxygen gradients (Gibb et al., 1999b).

A degree of diatom-specific MMA, and to a lesser extent DMA, production was inferred through pigment studies (Gibb et al., 1999b). Diatoms are adapted to high nitrogen abundance and dominate phytoplankton assemblage in coastal waters. In more oligotrophic offshore conditions, taxonomic shifts to phytoplankton more adapted to reduced nitrogen availability (such as Prymnesiophytes) occur, which was reflected in lower dissolved MA concentrations (Gibb et al., 1999b). Additional pigment analysis in the latter study implied that phytogenic MA production was weighted towards primary amines as

the pigment concentrations correlated better with MMA concentrations than total MA concentrations (Gibb et al., 1999b).

MMA and DMA concentrations have been reported to correlate strongly with zooplankton biomass (Gibb et al., 1999b). This correlation of zooplankton presence and aqueous MMA and DMA concentrations has also been observed for DMS (Welsh, 2000). Ambient DMS release increased 24-fold when dinoflagellates (which are ecologically important DMS producers) were subject to copepod grazing (Dacey and Wakeham, 1986). Whilst MMA and DMA concentrations correlated strongly with zooplankton abundance, TMA concentration was inversely related to zooplankton biomass, which indicated its removal from the aqueous phase. This concurs with studies that observed that copepods oxidised ^{14}C-TMA from seawater and accumulated it as TMAO (Strom, 1979; 1980).

Table 1.4: Summary of previous water column MA studies (nd = not determined)

Author (year)	Location (Number of Samples)	Concentration (nmol dm^{-3})		
		MMA mean±σ	DMA mean±σ	TMA mean±σ
Gibb et al. (1999b)	Arabian Sea – Coastal			
	Aug-Oct 1994 (30)	12±20	3.0±4.1	0.10±0.37
	Nov-Dec 1994 (27)	22±13	4.2±2.8	0.45±0.81
	Arabian Sea – Offshore			
	Aug-Oct 1994 (82)	6±7	2.9±2.8	0.05±0.21
	Nov-Dec 1994 (44)	12±7	2.9±1.6	0.13±0.24
	Gulf of Oman			
	Aug-Oct 1994 (40)	11±9	2.8±3.1	0.18±0.42
	Nov-Dec 1994	nd	nd	nd
Van Neste et al. (1987)	Pacific Hawaii - Coastal (9)	52±20	1.5±2.0	12±3.0
	Atlantic-Massachusetts - Coastal (3)	200±58	8.9±4.4	41±27
Abdul Rashid et al. (1991)	Irish Sea	0-619	0-100	0-4
Yang et al., (1993; 1994)	Flax Pond, New York	5-60	15-180	<3-80
Gibb (1994)	Mediterranean – Offshore	7.5±5.5	4.6±3.0	1.4±1.6
	Mediterranean - Coastal	18±10	12±11.4	10±6.9

MAs in Algal Culture

MAs are produced by phytoplankton either through direct emission or by degradation of quaternary amines, such as choline and glycine betaine, via Hoffmann elimination (King, 1988b). In addition, zooplankton and organisms at higher trophic levels are proposed to contribute to MA cycling through grazing and excretion (King, 1988b).

A limited number of culture studies of MA production have been carried out to try to identify potential contributors to MA production and concentration. MA production per cell in algal cultures, was observed to increase with increasing NO_3^- concentration in the culture medium (Abdul Rashid et al., 1991). This concurs with observations in the Arabian sea, where the highest MA concentrations were observed in a nutrient-rich upwelling area (Gibb et al., 1999b). In addition, MMA was found to be the most abundant MA, accounting for 86-90% of the total MA concentration in culture studies (Abdul Rashid et al., 1991). This was followed by DMA, which accounted for 1.7-12% of the total MA concentration with TMA the lowest proportion (0.2-3%). This study also demonstrated that concentrations of MMA, DMA and TMA reached 92-136, 5-37 and 0.7-4 times higher in bacteriostatic cultures, respectively, than those measured in non-bacteriostatic conditions. This indicated that heterotrophic bacteria were able to utilise MAs preferentially (i.e. MMA>DMA>TMA)(Abdul Rashid et al., 1991).

1.3.2 The fate of MAs in the marine environment

The fate of the MAs in the environment is governed by two primary processes: loss to the atmosphere and turnover by microorganisms. The MAs' volatile nature allows their transfer across the sea-air interface (Van Neste et al., 1987). Once they have crossed the sea-air interface they are proposed to act as a source of base in the atmosphere (discussed in detail in Section 1.4).

Turnover by microorganisms is thought to account for a significant loss of MAs from the marine environment. MMA uptake (measured using ^{14}C MMA) has been demonstrated in several classes of phytoplankton, including dinoflagellates, cocolithophores (Balch, 1986) and diatoms (Wheeler and Hellebust, 1981). In addition, the uptake of MAs has been demonstrated in heterotrophic bacteria (Budd and Spencer, 1968), non-methylotrophs (Bicknell and Owens, 1980), methylotrophs (Budd and Spencer, 1968) and methanogens (Winfrey and Ward, 1983).

Knowledge of the fates of MAs in the marine environment is limited to a few studies (Abdul-Rashid, 1990; Gibb et al., 1999a). Further work is required to fully understand uptake and turnover of the MAs and to begin to quantify the contribution of MAs from aqueous systems to the atmosphere.

1.4 Atmospheric Chemistry

1.4.1 Physical Aspects of Sea-Air Exchange

The flux of a trace gas across the sea-air interface is calculated from its measured (or estimated) concentration gradient across and the transfer velocity. A ‘two-phase’ resistance model of gas exchange (Liss and Slater, 1974) is commonly applied. This model assumes the transfer velocity represents the conductivity of the layers either side of the interface with respect to the gas of interest. The transfer velocity is expected to be controlled by processes disturbing the molecular diffusion layers. For water-soluble molecules the rate of mass transfer is dominated by air-side resistance and for sparingly soluble molecules the rate of mass transfer is controlled by water-side resistance.

1.4.2 Marine Aerosol

There are two major forms of atmospheric aerosol: primary and secondary. Primary aerosols are particulates that are emitted directly into the atmosphere such as sea-salt, dust and soot. Secondary aerosols are particulates that are formed in the atmosphere by gas-to particle conversion (Kulmala, 2003). In the atmosphere, aliphatic amines are able to undergo oxidation by OH and NO_3 radicals and O_3, leading to the formation of organic nitrogen-containing species which can be partitioned to the particle phase, becoming part of the atmospheric aerosol.

Atmospheric aerosols affect global climate in two ways: directly, by scattering or absorbing incoming solar radiation, and indirectly, by acting as cloud condensing nuclei (CCN). CCN increase cloud albedo and affect precipitation patterns (Bzdek

et al., 2011). Marine aerosols influence both direct and indirect radiative forcing where the direct effect describes aerosols scattering and absorbing short wave and long wave radiation, and the indirect effect describes how aerosols modify the properties of clouds (IPCC, 2007).

New particle formation (NPF) is a phenomenon that can impact upon CCN density and is thought to have two main steps: nucleation and growth. There are four main proposed nucleation mechanisms: 1) homogeneous nucleation involving binary mixtures of water and sulphuric acid; 2) homogeneous ternary (water-sulphuric acid-ammonia) nucleation; 3) ion-induced nucleation and 4) homogeneous nucleation involving iodide species. Nucleation and particle growth are likely to be decoupled under atmospheric conditions. Competition between particle growth and scavenging by larger pre-existing particles determines the actual production rate of observable particles (Kulmala, 2003).

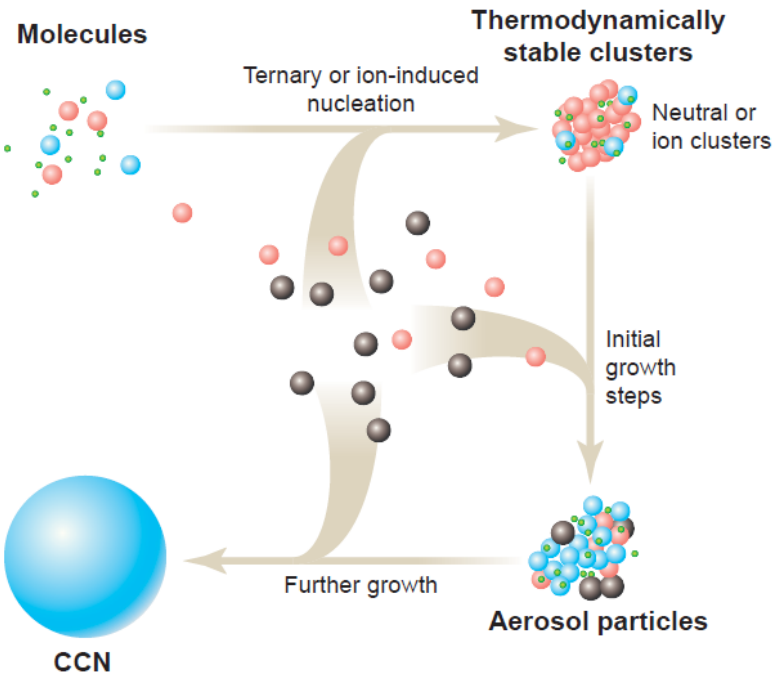

Figure 1.7: Summary of CCN formation, taken from Kulmala (2003)

Experimental and theoretical studies have demonstrated that binary sulphuric acid-water nucleation alone cannot explain most of the NPF events in the atmosphere (Kulmala et al., 2004; Laakso et al., 2007). These observations indicate that other compounds are required to stabilise the clusters. Contributions from ions, ammonia and organic compounds have been proposed to participate in particle nucleation (Kurten et al., 2008). Ammonia was proposed as a potential stabilising compound and laboratory and theoretical experiments have investigated its potential effect (Kurten et al., 2008). Experimental studies found that ammonia had a clear enhancing effect on sulphuric acid-water nucleation, enhancing nucleation by 1-2 orders of magnitude (Ball et al., 1999). However, this effect was moderate and not enough to explain the observed particle formation rates in the atmosphere (Antitila et al., 2005; Ball et al., 1999; Nadykto and Yu, 2007; Torpo et al., 2007).

Another proposed source of base stabilisation was the aliphatic amines. Like ammonia, amines can form nitrate and sulphate salts under atmospheric conditions. Proton affinity data indicated that proton transfer should occur more easily for amine-acid clusters than for ammonia-acid clusters, leading to stronger binding (Hunter and Lias, 1998).

Density functional theory was applied to study the thermochemistry of pre-nucleation clusters (Nadykto et al., 2011; Nadykto et al., 2014). These computational studies found that amines form strong hydrogen-bonded complexes with pre-nucleation sulphuric acid-water clusters and that the stability of sulphuric acid-amine-water complexes were higher than sulphuric acid-ammonia-water complexes. However, this study concluded that the enhancement in stability due to the amines was not large enough to overcome the difference in typical atmospheric concentrations of ammonia and amines. Further laboratory experiments observed that, under atmospherically relevant concentrations, TMA enhanced sulphuric acid-water nucleation but the effect was moderate and similar to that of ammonia (Erupe et al., 2011). It was concluded that the stabilising effect of amines was unlikely to exceed that of ammonia.

Additional computational and experimental studies examined the structure and formation thermodynamics of dimer clusters of sulphuric acid with amines and ammonia (Kurten et al., 2008). The amines formed stronger clusters than ammonia, as predicted by the proton affinity data (Hunter and Lias, 1998). The computed free energies for complex formation showed that amines were more effective than ammonia at enhancing the addition of sulphuric acid molecules to

both neutral and ionic clusters. These results indicated that both neutral and ion-induced nucleation mechanisms involving sulphuric acid are likely to be enhanced much more effectively by amines than by ammonia, even after the differences in their atmospheric concentrations were taken into account (Kurten et al., 2008). Further laboratory experiments carried out in the Cosmics Leaving OUtdoor Droplets (CLOUD) chamber at the European Organization for Nuclear Research (CERN) provided the first direct evidence of the effect of the MAs on particle nucleation (Almeida et al., 2013). This study found that DMA concentrations above 3 parts per trillion by volume enhanced nucleation rates by more than a 1000 fold over ammonia. The new enhanced nucleation rates were enough to explain observed NPF events. Molecular analysis of the clusters revealed that the faster nucleation was explained by base-stabilisation of the acid-amine pairs which reduced evaporation. This study also concluded that the contribution of ion-induced nucleation was small.

The lack of sensitive experimental methods to monitor the very first steps of particle formations limits the understanding of the significance of amines to NPF events. Most of the uncertainties involved in thermodynamic calculations of nucleation events are associated with the first few steps (Nadykto et al., 2014). If these uncertainties could be reduced then the calculations could be better constrained and the understanding of NPF events increased.

1.4.3 Methylamines in Marine Aerosol

A number of studies have analysed MA concentrations in the atmosphere, including both gas phase and particulate phase concentrations. Studies in the Arabian Sea revealed that concentrations of total NH_3 were 10-100 times greater

than the MAs (Gibb et al., 1999a). In contrast to the aqueous phase, where MMA concentrations dominated the MA budget (Gibb et al., 1999b), DMA concentrations rivalled and often exceeded those of MMA in the gas phase (Table 1.5). This difference in MA ratio was supported by a study of atmospheric aliphatic amines at Cape Verde (Muller et al., 2009), which found DMA concentrations to be 3-11 times higher than MMA concentrations, depending on the season. The biggest difference was evident in May 2007 (Table 1.6). The Cape Verde study also quantified diethylamine (DEA) and found concentrations of this analyte to be three times higher than those of MMA. Studies carried out in the North Atlantic Ocean (Facchini et al., 2008) found both DMA and DEA present at concentrations up to 66 ng m^{-3}; unfortunately MMA wasn't measured and so could not be compared.

Table 1.5: Atmospheric gaseous and aerosol concentrations of NH_3 and MAs (LoD = limit of detection; 2.3, 0.81 and 0.21 pmol m^{-3} for MMA, DMA and TMA respectively)

Source	Location	Ammonia	MMA	DMA	TMA
Gas Phase (pmol m^{-3})					
Gibb et al. (1999a)	Arabian Sea (Aug–Oct)	346-1726	37-177	16-65	<LoD-1.4
	Arabian Sea (Nov-Dec)	2454-5625	50-241	50-870	<LoD-13
Gronberg et al. (1992)	Coastal Malmo, Sweden	nd	200±50	50±20	390±140
Van Neste et al. (1987)	Rhode Island	nd	11±5	93±51	30±19
	Hawaii	nd	52±12	240±40	100±40
Particulate Aerosol Phase (pmol m^{-3})					
Gibb et al. (1999a)	Arabian Sea (Aug-Oct)	943-4095	<LoD-189	23-96	0.3-13
	Arabian Sea (Nov-Dec)	5909-8619	81-146	81-379	2-15

Although 30% of atmospheric amines are thought to be derived from marine sources, knowledge of such sources is extremely limited (Facchini et al., 2008). Studies carried out at Cape Verde and the North Atlantic Ocean, both sites remote from significant anthropogenic contamination, indicated that MA concentrations in the atmosphere had a biogenic source (Table 1.6). The Cape Verde study found that MA concentrations correlated strongly with high near-surface Chl *a* concentrations, determined by ocean colour satellites indicating high primary productivity (Muller et al., 2009). Exact sources of amines at Cape Verde were undetermined but high amine concentrations during algal blooms supported the hypothesis that marine biological activity was a source of MAs. Furthermore, the highest amine concentrations were determined in fine particles, suggesting that the presence of amines in the particle phase was via reaction of gas phase amines with acidic sub-micrometer particles.

Table 1.6: Summary of aliphatic amine concentrations measured in sub-micrometer aerosol at Cape Verde, taken from Muller et al. (2009)

	Aliphatic Amine Concentration (pg m^{-3})		
	Average	Maximum	Minimum
	May 2007 (n=11)		
MMA	20	10	30
DMA	220	130	360
DEA	60	5	110
	June 2007 (n=10)		
MMA	60	10	120
DMA	200	50	390
DEA	80	60	140
	December 2007 (n=24)		
MMA	180	2	520
DMA	570	100	1400
DEA	320	90	760

DMA and DEA concentrations in the North Atlantic aerosol were measured by Muller et al. (2009) and found to range from 6-66 ng m^{-3} during periods of high biological activity and from 0.4-20 ng m^{-3} during periods of low biological activity. These observations further supported the hypothesis that DMA and DEA in aerosol samples had biogenic oceanic sources and were produced through the reaction of gaseous amines with sulphuric acid or acidic sulphates.

The exchange of MAs across the sea-air interface is likely to represent a small but important loss from the aqueous cycle, contributing a potentially important source of base to the remote atmosphere. However these fluxes are currently poorly characterised, which makes their influence on atmospheric composition complex and uncertain.

1.5 Aims and Objectives

Distribution and cycling of the MAs in marine systems have been investigated previously (Fitzsimons et al., 2005; Gibb et al., 1999b) but the link between quaternary amines and their atmospherically-active MA derivatives, and the possible climatic implications of MA diffusion across the sea-air interface has not been examined. However, before the significance of the MAs to potential climate regulation can be robustly quantified, a better understanding of the QAs and MAs must be gained.

Aim 1: To measure MA concentrations in seawater

> ***Objective 1:*** Develop a combined pre-concentration and chromatographic method to measure MA concentrations at levels expected in the Western English Channel.

Aim 2: To optimise the measurement of GBT in seawater

> ***Objective 2:*** To determine an appropriate filter volume for maximum GBT recovery.

Aim 3: To elucidate seasonal variability of GBT concentrations in the Western English Channel

> ***Objective 3:*** To carry out a seasonal study of particulate GBT concentrations in the Western English Channel and analyse the data in relation to phytoplankton taxonomic succession and other physico-chemical variables measured.

Chapter 2

Review of analytical methods for determination of the methylamines

Chapter Outline

This chapter reviews the approach that will be taken to the quantification of methylamines in seawater. This approach comprises a pre-concentration step, a chromatographic step and a detection step. Techniques that have been applied by previous studies are outlined and gas chromatography with a pre-concentration step identified as a suitable approach.

2.1 Introduction

Analysis of the methylamines (MAs) is particularly challenging due to their polarity, aqueous solubility and volatility. The purpose of this review was to evaluate reported techniques for resolving and quantifying low molecular weight amines at environmentally relevant concentrations (nmol dm^{-3}-μmol dm^{-3}) according to the requirements of the project aims.

No single reported technique appeared to be capable of fulfilling these criteria for all of the analytes of interest. The approach taken, therefore, involved a combination of techniques which, in conjunction, were capable of analysing MAs in marine water samples. The approach comprised three main stages: a pre-concentration step, a separation step and a detection step. The pre-concentration step was employed to extend the linear range of response and to lower the limit of detection. The chromatographic step was used to resolve the three MAs and ensure that they eluted separately from any potential interfering compounds and the detector chosen to provide a fast, sensitive and selective response to the MAs.

2.2 Pre-concentration

Common analytical problems associated with the measurement of analytes in seawater include matrix effects, resulting in high limits of detection. A matrix effect occurs when non-target components of a sample interfere with determination of the analytes (Kuráň and Soják, 1996). To address this, sample pre-concentration can be performed, which often incorporates a clean-up step to reduce matrix interference. Sample pre-treatment is often the most time-

consuming and challenging step of the analytical procedure, making the availability of efficient sample preparation methods and consumables a priority for suppliers. The choice of pre-concentration technique has depended on the type of matrix involved along with the concentration and volatility of the compounds to be analysed.

Sample pre-treatment and pre-concentration often involves extracting the chosen analyte from the sample matrix and transferring it to a new matrix that contains fewer interferents, while achieving a higher final concentration. Classically, extractions of organic analytes have been carried out using liquid-liquid extraction (LLE), which utilises an organic solvent to extract analytes from an aqueous sample. LLE is highly versatile and potentially selective but is not easily automated and the pre-concentration factor is limited. The main disadvantage in LLE is the use of organic solvents which can be expensive, toxic and difficult to dispose of (Demeestere et al., 2007). A number of alternatives to LLE are described below.

2.2.1 Headspace Extractions

Headspace pre-concentration techniques exploit the ability of volatile compounds to partition between the aqueous and gaseous phases (Biziuk and Przyjazny, 1996; Dewulf and Van Langenhove, 1999; Kuráň and Soják, 1996). Volatile compounds migrate from an aqueous sample into a smaller volume headspace where they can be sequestered (e.g. in aqueous acid or onto a solid sorbent). There are two primary methods of headspace pre-concentration: static and dynamic.

Static headspace pre-concentration is an equilibrium method using a sealed system and a trap. The sample is heated and the analytes diffuse from the liquid phase into the gaseous phase where they are trapped. Static headspace pre-concentration was used by Abdul Rashid et al. (1991) for the analysis of MAs in sediment and pore water samples, involving micro-diffusion in a Cavett flask. Samples were placed in the flask and adjusted to pH 12 to deprotonate the MAs, then heated to 60°C in a fan oven; this promoted MA diffusion into the gas phase where they were trapped in a small-volume aqueous acid trap. Samples were then analysed using packed column GC-nitrogen phosphorus detector (NPD) and this approach achieved LoDs of approximately 17-32 nmol dm^{-3}. Subsequent detection limits of 9-22 nmol dm^{-3} were reported in Fitzsimons et al. (2006) using the same method.

The dynamic headspace method, also known as purge and trap, is a modification of the static headspace method where a dynamic equilibrium is established to promote analyte transfer to the headspace. Conventional dynamic headspace analysis, first described by Swinnerton et al. (1962), extracts dissolved volatile organic compounds (VOCs) by passing a stream of inert gas through an aqueous sample held within a container. The gas stream, enriched with the VOCs, leaves the purge vessel and is passed through a trap, for example, a cold, sorbent or acid trap, where the analytes are retained (Demeestere et al., 2007; Dewulf and Van Langenhove, 1999; Jakubowska et al., 2009; Kuráň and Soják, 1996). Dissolved VOCs can be almost completely removed from the sample as the inert gas constantly strips them from solution. The continuous stripping of the compounds from solution makes dynamic headspace sampling theoretically more

sensitive than static headspace, which relies on an equilibrium being established. Dynamic headspace extraction was applied to extract six alkylamines (including the MAs) from cosmetic products by Zhong et al. (2012). The cosmetic samples were homogenised and added to base modified (2g lithium hydroxide) aqueous samples (10 mL). The samples were then purged with nitrogen gas (0.8 mL min^{-1}) and trapped in 10 mL of 50 mM acetic acid. The purge and trap system was coupled with ion chromatography to achieve limits of detection of 0.64-0.78 µmol dm^{-3}.

Dynamic headspace extractions have two main drawbacks, foaming of the sample and the analyte transfer time, both of which limit sample throughput (Dewulf and Van Langenhove, 1999). Static headspace is limited by the marginal equilibrium changes caused by the trapping process compared to the constant shifting of the equilibrium, created by sweeping the system with an inert gas during dynamic headspace extraction. A higher pre-concentration factor can therefore be achieved using the latter option.

2.2.2 Solid Phase Extraction

Solid phase extraction (SPE) is a sample preparation technology which partitions organic compounds dissolved in an aqueous sample between a solid sorbent and a liquid phase (Jakubowska et al., 2009). SPE uses the affinity of analytes in a sample for the solid phase, to separate the different components. Either the desired analyte or undesired impurities are retained on the stationary phase. If the portion retained on the stationary phase includes the analyte then a separate

elution can be carried out to collect and pre-concentrate the analyte, separated from any impurities (Figure 2.1).

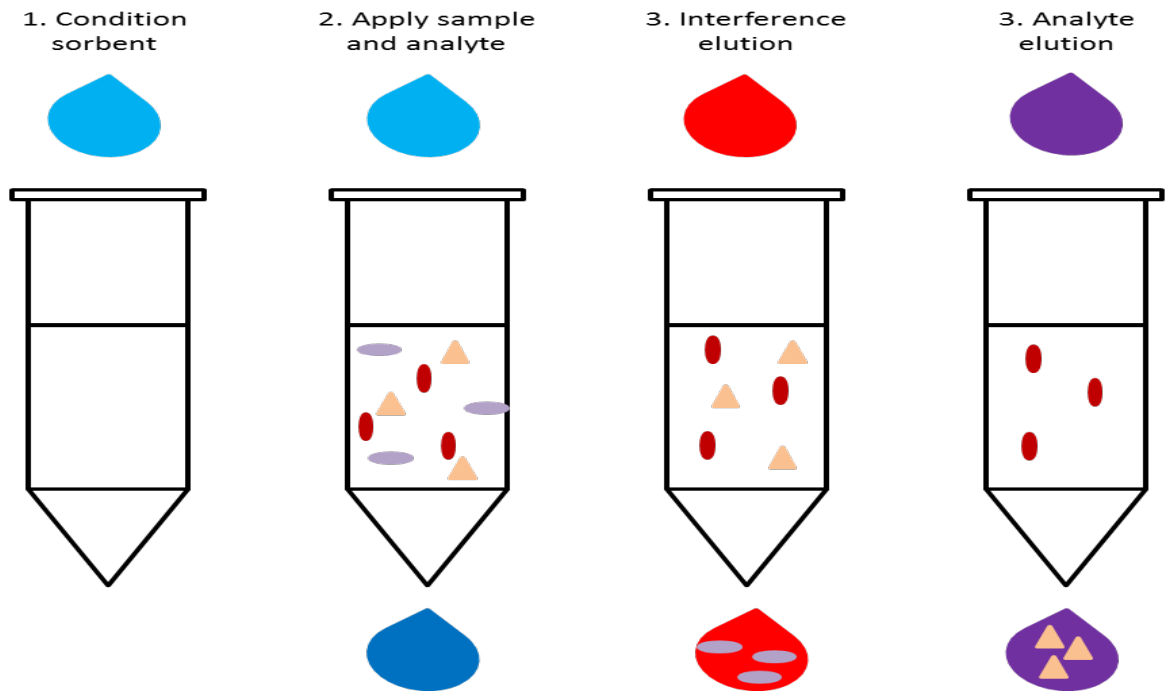

Figure 2.1: Solid Phase Extraction method of action

SPE pre-concentration has been applied to the analysis of TMA in aqueous samples using HPLC with 9-fluorenylmethyl chloroformate (FMOC) derivatisation (Chafer-Pericas et al., 2004). Using direct analysis (without preconcentration) TMA could be determined over the range 4.2-169.5 µmol dm^{-3} with a detection limit of 0.8 µmol dm^{-3}. Pre-concentration using C18 SPE cartridges lowered the range of detection to 0.84-16.9 µmol dm^{-3} with a limit of detection of 84.7 nmol dm^{-3}. The trapped analytes were then released by solvent desorption for analysis.

2.2.3 Solid Phase Microextraction

Solid phase microextraction (SPME) is a solvent-free extraction process that simultaneously extracts and pre-concentrates analytes from aqueous samples or

a sample headspace (Pawliszyn, 1997). The analytes partition between the sample and a polymer coated fibre stationary phase, the choice of which depends on the compounds to be analysed. A 1 cm length of fused silica fibre, coated with the chosen polymer, is bonded to a stainless steel plunger and installed in a holder similar to a syringe (Figure 2.2).

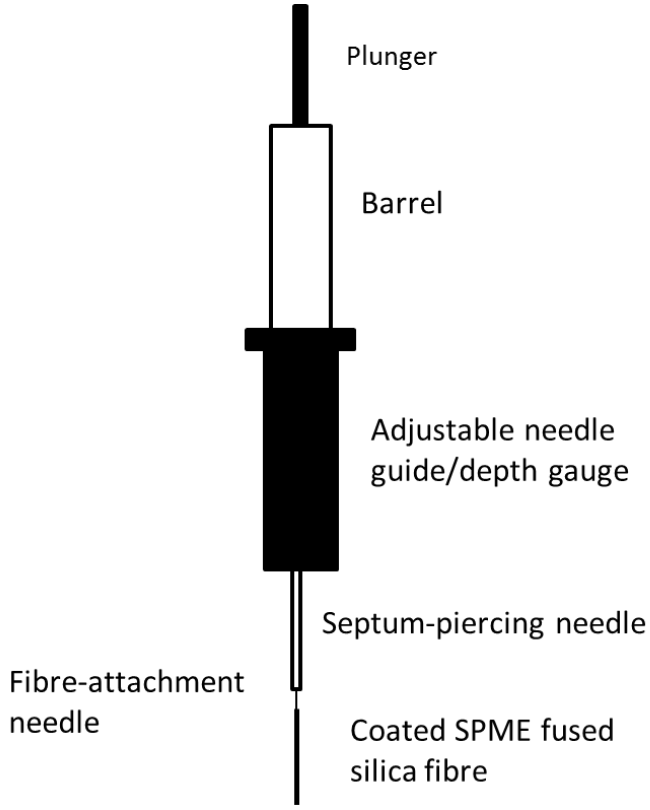

Figure 2.2: Solid Phase Microextraction fibre and holder (adapted from Sigma Aldrich), not to scale

The plunger moves the fused silica fibre into and out of a protective hollow needle. The needle is used to pass the fibre through a septum sealing a sample vial; the plunger is then depressed and the fibre exposed to the sample (direct SPME) or the sample headspace (Pawliszyn, 1997). Over time, which is optimised, the organic analytes adsorb to the fibre and an equilibrium is established. Once the equilibrium is established the fibre is rehoused and removed from the vial. The needle is subsequently injected into a GC, the fibre

exposed and the analytes thermally desorbed. Desorption depends on the boiling point of the analyte, the coating of the fibre and the temperature of the injection port. When analysing sewage-polluted water, Abalos et al. (1999) applied SPME extraction, in conjunction with GC, to the quantification of the MAs. A polydimethylsiloxane (PDMS) fibre was chosen and exposed to the headspace of a 20 mL water sample for 30 minutes. The MAs were desorbed from the fibre in the GC injector at 220°C over a 5 minute period. This approach achieved limits of detection of approximately 0.19-0.87 μmol dm^{-3}. In addition, SPME was applied to the HPLC analysis of the three MAs in aqueous samples (Herraez-Hernandez et al., 2006). Carbowax-templated resin SPME fibres were used to preconcentrate the samples and allowed limits of detection of 161 nmol dm^{-3} and 111 nmol dm^{-3} for MMA and DMA respectively and 4.2 μmol dm^{-3} for TMA to be achieved. However, the derivatisation process employed for the analysis (detailed in Section 2.3.2) converts TMA to the DMA-derivative which makes their concurrent analysis in natural samples impossible.

Direct solution extraction is the more widely used application of SPME but it reduces the lifetime of the fibre, whilst headspace-SPME (HS-SPME), which is more suitable for volatile compounds such as the MAs, extends the fibre lifetime. In addition, headspace extraction provides a cleaner sample and minimises the likelihood of extracting interfering analytes. In HS-SPME two mass transfer steps occur (Figure 2.3), the first between the sample and the headspace and the second between the headspace and the fibre coating (Silva et al., 2004). Maximum extraction occurs when equilibrium is reached between the three phases. The time required for the system to reach equilibrium depends on the

rate of the two mass transfer steps. To achieve high accuracy and precision it is often more important to keep sampling time and other parameters consistent than achieving maximum recovery.

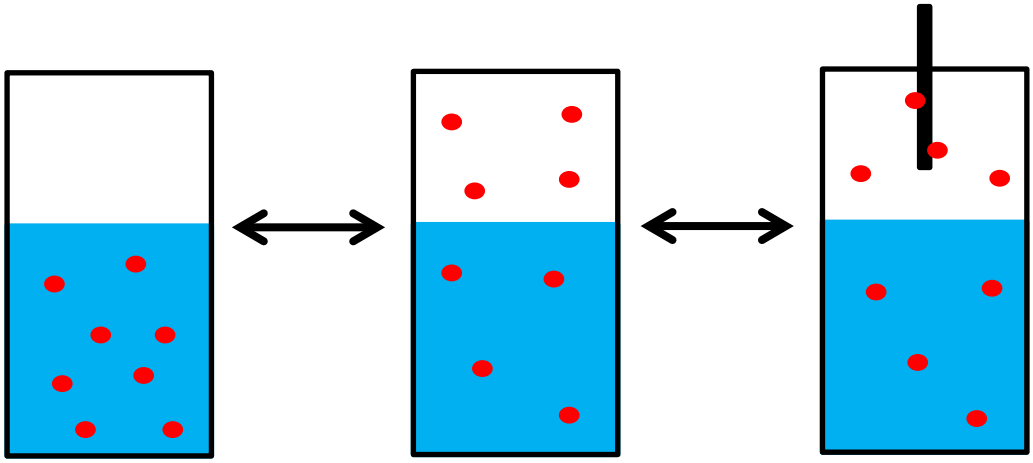

Figure 2.3: Head Space-Solid Phase Microextraction equilibrium processes

The main disadvantages of SPME are the limited lifetime of the relatively expensive fibres, degradation of fibres with increased usage, and bleeding of the SPME coating into the GC inlet.

2.2.4 Membrane Extraction

Membrane extraction utilises porous and nonporous (semi-permeable) membranes to separate VOCs in aqueous solutions (Jakubowska et al., 2005; Jönsson and Mathiasson, 2001; Kuráň and Soják, 1996). Porous membranes use size exclusion to separate compounds (i.e. molecules with diameters smaller than the membrane pores can pass through the membrane). In contrast, nonporous membranes use differences in solubility and diffusion rates to separate molecules. The aqueous sample (donor phase) is brought into contact with a membrane and the VOCs permeate selectively through the membrane into

a gaseous or aqueous phase (acceptor phase) on the other side (Jönsson and Mathiasson, 2001). Membrane extraction was applied to the analysis of MAs in seawater by Gibb et al. (1995) using micro porous PTFE to mediate gas exchange for flow injection gas diffusion and analysis by ion chromatography (IC). Seawater samples were treated with alkaline EDTA to convert the MAs to the volatile form required for gaseous diffusion while chelated Mg^{2+} and Ca^{2+} to prevent their precipitation as $Ca(OH)_2$, and $Mg(OH)_2$. The MAs diffused selectively across a gas-permeable microporous PTFE Goretex membrane into a recirculating acidic 'acceptor' stream where the MAs were reprotonated and preconcentrated (Figure 2.4). The acidic acceptor solution was then injected onto an IC column. This method achieved limit of detections of 3-5 nmol dm^{-3} with relative standard deviations of 1-6% at 1 µmol dm^{-3}.

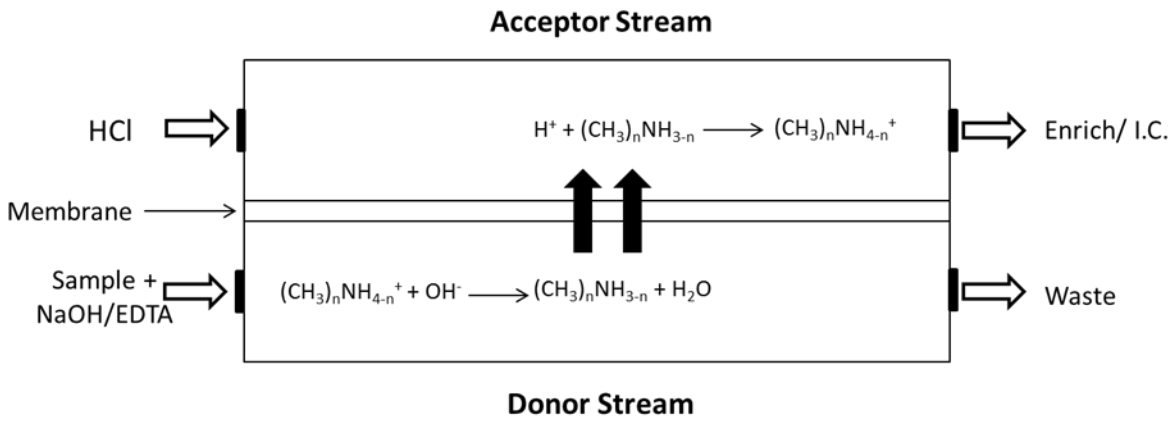

Figure 2.4: Schematic diagram of the speciation and diffusion of the MAs across the Goretex membrane (Gibb et al., 1995)

Pre-concentration of the MAs from pore water samples was also achieved using a diffusion technique (Yang et al., 1993) combining a Perspex diffusion chamber with a Teflon membrane. An initial diffusion step was carried out by treating the donor stream with sodium hydroxide to convert the cationic MAs to their free

form. The MAs then diffuse across the membrane into an acidic acceptor stream. Sodium chloride was added to the acceptor stream to balance the osmotic pressure. The initial diffusion step was carried out for 24 hours at 55°C. A second diffusion step then transferred the amines from the acidic saline solution to a more dilute acidic solution. This diffusion step was carried out for 12 hours at 55°C. Pre-concentrated samples were then analysed using GC-NPD. This technique achieved sub micro-molar LoDs and was capable of analysing MA concentrations as low as 10 nmol dm^{-3} (Yang et al., 1993). Despite the success of this method and its ability to measure low nanomolar concentrations of MAs the time taken for each diffusion step was prohibitive and the method was not widely adopted.

2.3 Chromatography and Detection

Chromatography is a technique which resolves analytes based upon their partition between two phases (mobile and stationary) in a dynamic system (Skoog et al., 2004). Three main forms of chromatography have been reported for detection of the MAs: GC, HPLC and IC.

2.3.1 Gas Chromatography

Gas chromatography has been applied to the analysis of low molecular weight amines, capitalising on their volatile nature. However, GC analysis is complicated by the basic nature of the amines which, due to the influence of the amino group, causes strong adsorption characteristics. The amino group introduces a dipole which is responsible for strong interactions with silanol groups and siloxane bridges in the stationary phase. This results in nonlinear adsorption effects such as tailing (de Zeeuw et al., 2000). There are two main ways of preventing these unfavourable adsorptions: derivatise the amine or deactivate the system.

Derivatisation is used to neutralise the unfavourable effects of the amino group and can improve detection and separation of these compounds. There are a number of ways to derivatise amines but all methods are labour-intensive and have a number of drawbacks. These include: incomplete reaction, unstable derivatives and the need for extra purification steps. In addition, tertiary amines (e.g. TMA) cannot be derivatised using standard reagents available for this purpose. Carbamate formation is one of the few methods available for derivatization of TMA but this would not be a one step process (daCosta et al., 1990). Alternatively, deactivation of the chromatographic system can be performed (de Zeeuw et al., 2000). There are a range of commercially available

ultra-inert liners and columns especially designed for this purpose, but other methods include deactivating the system with a highly polar amine such triethylamine. The triethylamine interacts with all silanol groups and stops the other amines interacting with them. This approach only works for separations occurring below approximately 150°C as above this temperature the deactivation ceases to occur. Alternatively, deactivation can be carried out with caustic inorganic substances such as sodium or potassium hydroxide which shield the silanol groups and siloxane bridges. However, these chemicals cause column degradation and consequently reduce column lifetime (de Zeeuw et al., 2000). Sodium hydroxide has been successfully applied to GC analysis of the MAs by reducing adverse interactions between the amines and the GC (Abdul Rashid et al., 1991). A column packed with untreated porous packing (Chromosorb 103) was pH modified with potassium hydroxide, this allowed the successful resolution of the three MAs, treated with sodium hydroxide to maintain the MAs in their free form.

Another factor to consider when analysing highly volatile amines is their retention on the column. The MAs have low boiling points which increases their affinity for the mobile phase and if the stationary phase cannot sufficiently retain the MAs then resolution will be limited (Abalos et al., 2001). There are a number of commercially available columns designed for amine analysis: thick film base deactivated polyethylene glycol columns, base-modified porous polymer columns, non-polar methyl (phenyl) silicone phase columns and deactivated methyl/phenyl type stationary phases (Abalos et al., 2001; de Zeeuw et al., 2000). Several thick film fused silica columns have also been developed based

on base modified polyethylene glycol such as the CP-Wax 51. Separation on these columns was possible and the amines eluted as symmetrical peaks, although the retention of volatiles amines was difficult to achieve. As non-bonded columns these columns were also water intolerant which was problematic for the analysis of aqueous samples (Abalos et al., 2001; de Zeeuw et al., 2000). Porous polymers are stable, inert and fully water resistant materials; however, separation on porous polymer columns, such as the CP-PoraPLOT column, have required very high operating temperatures (de Zeeuw et al., 2000). At these temperatures the dipole-dipole interaction and adsorptive effects were reduced (Abalos et al., 2001; de Zeeuw et al., 2000). A tailor made PoraPLOT amine capillary column (30 m length, 0.32 mm internal diameter, 10 µm film thickness) was applied to the analysis of MAs in sewage polluted waters (Abalos et al., 1999). This method achieved limits of detection of approximately 0.19-0.87 µM. The non-polar methyl (phenyl) silicone phase has been applied to amine analysis (de Zeeuw et al., 2000). However the stability of non-polar phases to amine analysis is limited and they cannot be modified with basic agents. The acidity of the silica surface interacts detrimentally with the amines; however, despite this, volatile amines can be separated if the film is sufficiently thick (Abalos et al., 2001; de Zeeuw et al., 2000). The latest amine analysis column, the CP Volamine, has employed a multi-purpose deactivation and phase stabilisation to make the methyl/phenyl type stationary phase suitable for amine analysis. The acidic surface has been minimised by chemically bonding the deactivating agent to the silanol groups which has reduced the dipole-dipole interaction and provided shielding to reduce interaction with siloxane bridges. The CP Volamine has a special thick film, optimised to separate volatile amines (de Zeeuw et al., 2000).

The ultimate success of GC analysis is dependent on the efficiency of the detection system and its suitability to the analytes. Two detectors used for analysing amines are the flame ionisation detector (FID) and the nitrogen-phosphorus detector (NPD) (Abalos et al., 1999; Abdul Rashid et al., 1991; daCosta et al., 1990; Van Neste et al., 1987). The FID is widely used in analytical chemistry and is universal for carbon containing analytes. The sample, in a carrier gas, is passed through a hydrogen-air flame. Alone, the hydrogen-air flame creates few ions but when an organic compound passes through the flame the ions produced are increased. A polarizing voltage is used to collect the ions and the current produced is converted to a digital signal for analysis (Fowlis, 1995; Skoog et al., 2004). The NPD is similar to the FID and is a sensitive but specific detector that responds to nitrogen- and phosphorus-containing compounds. The detector comprises a rubidium or caesium chloride alkali bead which is heated by a coil, over which a carrier gas mixed with hydrogen and air passes. The heated bead emits electrons by thermionic emissions which are collected at the anode and provide the background current. When a component that contains nitrogen or phosphorous exits the column, the partially combusted nitrogen and phosphorous materials are adsorbed onto the surface of the bead. This increases the emission of electrons and the current which is then measured. The NPD exhibits greater selectivity and sensitivity towards nitrogen containing compounds and can exclude interfering peaks present from the sample matrix (Fowlis, 1995; Skoog et al., 2004). The NPD has been successfully applied to the analysis of amines (Abalos et al., 1999; Abdul Rashid et al., 1991; Yang et al., 1993).

2.3.2 High Performance Liquid Chromatography

HPLC is a highly versatile form of elution chromatography using a liquid mobile phase. There are two main HPLC set ups: normal-phase and reversed-phase. Normal-phase HPLC uses a highly polar stationary phase such as triethylene glycol and a relatively non-polar mobile phase such as hexane. Reversed-phase HPLC uses a non-polar stationary phase, often a hydrocarbon and a relatively polar mobile phase such as water, methanol and acetonitrile (Skoog et al., 2004). No highly sensitive universal detector, like those found in GC, is available for HPLC. The detector used will, therefore, depend on the nature of the sample. The most widely used detectors for liquid chromatography are: UV-visible, fluorimetric or mass spectrometric (liquid chromatography/mass spectrometry, LC-MS) (Chafer-Pericas et al., 2004).Since short-chain aliphatic amines lack a chromophore and have little fluorescence, they are difficult to detect using common LC detectors and so a chemical derivatization is generally required. Several reagents have been proposed including FMOC, *o*-phtalaldialdehyde and dansylchloride. Derivatization typically proceeds via carbonyl addition, with the amine acting as the nucleophile. However, since proton loss is a pre-requisite step for carbonyl addition, this process is not suitable for tertiary amines (i.e. TMA). As a result, few procedures have been developed or reported for the derivatization of tertiary aliphatic amines. Chafer-Pericas et al. (2006) reported a method for analysis of the MAs involving a derivatisation with 9-fluorenylmethyl chloroformate (FMOC). HPLC was successfully applied to the analysis of the three MAs in aqueous samples using a LiChrospher 100 RP_{18} (125mm × 4mm i.d.) column with a Hypersil C_{18} 30 µm pre-column (Herraez-Hernandez et al., 2006). An acetonitrile-water gradient mobile phase with increasing acetonitrile

content was used with a 1 mL min^{-1} flow rate. SPME was used to pre-concentrate the MAs and on fibre derivatisation using FMOC was carried out to improve the sensitivity of the detector to the MAs. Limits of detection of 111 nmol dm^{-3} – 4.2 µmol dm^{-3} were achieved. However, the derivatization of TMA resulted in its conversion to the DMA-derivative, making analysis of both DMA and TMA as discreet moieties impossible in natural samples.

2.3.3 Ion Chromatography

Ion exchange chromatography (IC) is liquid chromatography employing an ion-exchange resin as the stationary phase to separate charged species based on their interaction with the resin. Thermal conductivity detectors are frequently employed by IC and have many properties of an ideal detector: they are reasonably sensitive, universal for charged species and respond in a predictable way to concentration changes. However, to elute most analyte ions in a reasonable time a high electrolyte concentration is required (Skoog et al., 2004). The high electrolyte concentration required often swamps the analytes' signal during detection so that an extra step is often required.

There are two forms of IC: suppressor based and single-column. In suppressor-based ion chromatography, the ion-exchange column is followed by a suppressor column or membrane. The second column or membrane converts the ions of the eluting solvent to a molecular species that does not interfere with the conductimetric detection of analyte ions (Skoog et al., 2004). Single-column ion-exchange chromatography depends on the small differences in conductivity between sample ions and the eluent ions. Analyte ions are separated on a low-

capacity ion exchanger using a low-ionic strength eluent which does not interfere with conductimetric detection of analyte ions (Skoog et al., 2004).

Concentrations of the MAs in seawater were successfully quantified using IC with a low capacity cation exchange column (Gibb et al., 1995). The solution, pre-concentrated by membrane diffusion, was injected onto the ion exchange column where the MAs were protonated in the acidic eluent to their monovalent alkyl ammonium cations. The retention of the MAs depends upon the degree of aliphatic substitution. With increasing substitution (primary>secondary>tertiary) the hydrophobicity is enhanced and the analytes partition in favour of the stationary phase over the eluent, increasing their retention time (elution order: MMA<DMA<TMA). This method, in conjunction with membrane diffusion pre-concentration, achieved limits of detection of 3-5 nmol dm^{-3} and exhibited linearity between 0-2000 nmol dm^{-3}.

Two additional IC methods were developed for the analysis of MAs in atmospheric gas-particle samples, one method using a standard IC column and another an amine specific column, using a methanesulfonic acid gradient elution (VandenBoer et al., 2012). An online trace cation concentrator column was used with conductivity suppression prior to detection to improve selectivity and detection limits to picomolar levels. Both methods achieved selective and semi-quantitative detection at ambient concentrations, though co-elution prevented unequivocal identification and quantification of peak areas. An outline of method details is presented in Table 2.1.

Table 2.1: A summary of MA analytical methods

Source	Method	Details	Sample Type	Limit of Detection	Recovery
Abdul Rashid et al. (1991)	Cavett flask microdiffusion with GC-NPD analysis	Flask heated at 60°C, diffusion into an acid trap, packed column GC – porous packing modified with NaOH solution	Sediment and pore water	9-22 nmol dm^{-3}	45-73%
Fitzsimons et al. (2006)	Static headspace				
Zhong et al. (2012)	Multi-channel purge and trap with IC analysis	Samples pH-modified with lithium hydroxide, purged at 0.8 mL min^{-1} with nitrogen and trapped in 10 mL of 50 mM acetic acid	Cosmetics	0.64-0.78 µmol dm^{-3}	80.3-105.7%
Chafer-Pericas et al. (2004)	SPE with HPLC	TMA analysed using HPLC with 9-fluorenylmethyl chloroformate (FMOC) derivatisation. Preconcentrated onto C18 SPE cartridges connected on-line to the column	Tap, sea and waste water spiked with TMA	84.7 nmol dm^{-3}	
Herraez-Hernandez et al. (2006)	SPME with HPLC	Analysed the three MAs, derivatised with FMOC using HPLC. Preconcentrated using SPME with Carbowax-templated resin	Spiked tap and river water	111-161 nmol dm^{-3} for MMA and DMA 4.2 µmol dm^{-3} for TMA	
Abalos et al. (1999)	SPME with GC-NPD analysis	Polydimethylsiloxane (PDMS) fibre exposed to the headspace of a 20 mL water sample for 30 minutes, and the MAs then desorbed in the GC inlet liner at 220°C for 5 minutes	Sewage polluted water	0.19-0.87 µmol dm^{-3}	
Gibb et al. (1995)	Membrane extraction with IC analysis	Micro-porous PTFE mediated gas-exchange and eluted in acidic eluent before IC analysis	Seawater	3-5 nmol dm^{-3}	
(Yang et al., 1993)	Membrane extraction with GC analysis	Teflon membrane mediated gas-exchange with elution in acidic eluent before GC analysis	Pore-water	< µmol dm^{-3}	>90%

2.4 Discussion and Conclusions

Three reported methods provided valuable insight into deciding the best approach for analysis of MAs in marine samples: microdiffusion-GC analysis (Abdul Rashid et al., 1991), SPME-GC analysis (Abalos et al., 1999) and flow injection gas diffusion – IC (Gibb et al., 1995).

Static headspace microdiffusion combined with packed column GC-NPD was applied to the analysis of sediment and pore water samples and could reliably achieve LoDs of 9-22 nmol dm-3s (Abdul Rashid et al., 1991; Fitzsimons et al., 2006). This microdiffusion method reported 45-73% recoveries and, as such, leaves scope for improving the limit of detection if the recovery could be increased. Dynamic headspace extraction has the capacity to improve MA recoveries, as purging inert gas through the sample increases the air-water interface and allows better transfer between the liquid and gas phase. For example, Zhong et al. (2012) reported recoveries of 80-105% using a dynamic purge and trap extraction.

SPME pre-concentration and capillary GC-NPD analysis were used to determine concentrations of MAs in seawater samples and limits of detection of 0.19-0.87 µM have been reported (Abalos et al., 1999). As such, SPME offers a reasonable alternative to dynamic headspace extraction. Analysis by GC can resolve the three MAs (Abalos et al., 1999; Abdul Rashid et al., 1991) and, in conjunction with pre-concentration techniques, is capable of nmol dm^{-3} detection.

Pre-concentration coupled with IC was capable of detecting 3-5 nmol dm^{-3} levels of the three MAs, and these low nanomolar levels are more environmentally relevant (Gibb et al., 1995). IC is able to exploit the polar, basic nature of the MAs, which is inhibitive in GC analysis due to adsorptive artefacts, as they are detected as cations in an acidic eluent flow. IC was therefore potentially the method of choice for MA analysis. A significant drawback, however, is that the most successful IC method developed to date used specific bespoke equipment that isn't readily-available. In the nearly twenty years since this method (Gibb et al., 1995) was published it has not been widely adopted, despite increasing interest in cycling of the MAs. To facilitate the continuing interest of the marine analytical community in the MAs, it was felt that a sensitive and robust analytical method which utilised readily-available equipment and instrumentation should be developed, taking into account its ease of use and applicability. Reported methods using GC with a pre-concentration step have all used routine equipment and instrumentation that are readily-available, so development of the analytical method for determination of the MAs was focussed in this area.

Chapter 3

Development of an analytical method for the quantification of dissolved methylamines in seawater

Chapter Outline

This chapter outlines the steps taken to develop a method for the quantification of methylamines in seawater. A gas chromatographic step using a column specifically designed for the separation of volatile amines was developed. Quantification required a preconcentration step to achieve environmentally relevant limits of detection. Preconcentration using a purge and trap method was initially explored but the low recoveries observed precluded its use. A solid phase microextraction method was subsequently developed and applied to the quantification of the methylamines at low nanomolar concentrations in seawater.

3.1 Introduction

Methylamines (MAs) are low molecular weight basic compounds with the general formula $(CH_3)_nNH_{3-n}$. They are analogues of ammonium and undergo extensive hydrogen bonding to form basic solutions (pKa = 9.80-10.77). Their properties are summarised in Table 3.1.

Table 3.1: Structural formulae and properties of the methylamines (MAs)

Variable	Monomethylamine (MMA)	Dimethylamine (DMA)	Trimethylamine (TMA)	Source
Abbreviation	MMA	DMA	TMA	
Chemical Formula	H_3CNH_2	$(H_3C)_2NH$	$(H_3C)_3N$	
Molecular Weight	31.06	45.12	59.11	(Weast, 1986)
BP (°C)	-6.3	7.4	2.9	(Weast, 1986)
Acidity Constant, pK_a (298K, I=0)	10.64	10.77	9.80	(Bates and Pinching, 1984; Smith and Martell, 1975)
Basicity Constant, pK_b (298K, I=0)	3.36	3.23	4.2	Calculated
Solubility Coefficient (298K, I=0)	0.0126	0.0021	0.0015	(Hidy, 1984)

In aqueous solution the MAs partition between their free and protonated forms, with the latter generally accounting for over 90% of the total dissolved concentration at environmentally relevant pH (Gibb et al., 1999a). The ratio of protonated to unprotonated MAs is pH dependant with an increase in pH decreasing the relative abundance of protonated MAs (Table 3.1). At seawater pH (7.8-8.2) the protonated form is dominant (Thurman and Burton, 2001).

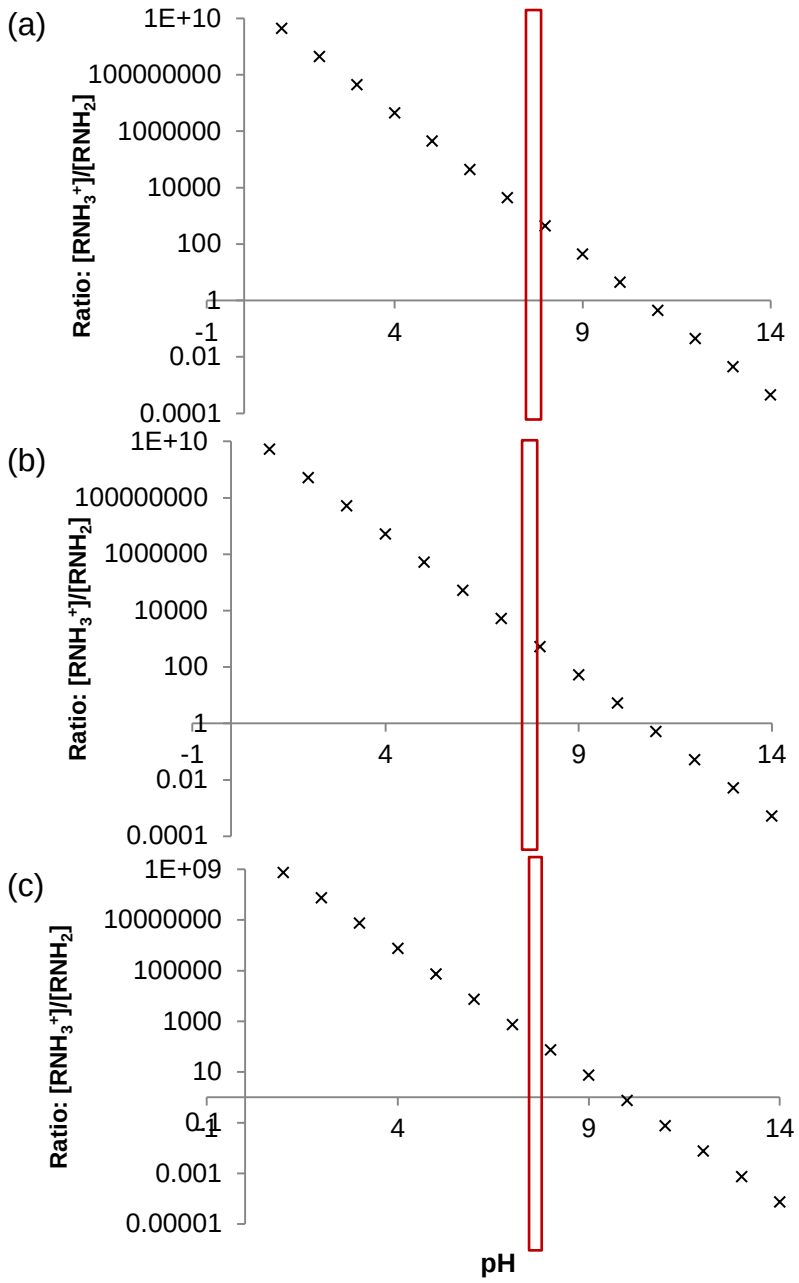

Figure 3.1: The pH dependent ratio of protonated to unprotonated methylamines in aqueous solution for: (A) MMA, (B) DMA and (C) TMA. Red boxes highlight the pH range of seawater

The MAs' volatility (b.p. -6.3 – 7.4°C) makes them suitable for analysis by gas chromatography and this was successfully exploited by Abdul Rashid et al. (1991) and Abalos et al. (1999). However, the MAs basic and polar character makes chromatographic analysis difficult because interactions with chromatographic systems at the injection and separation stages can cause peak-

tailing and reproducibility problems. These problems become more evident with decreasing molecular size as the amino group becomes progressively more influential. Previously published methods for MA analysis (Abalos et al., 1999; Abdul Rashid et al., 1991; for further information see Chapter 2) indicated that these problems could be overcome and as such a GC approach, in conjunction with a pre-concentration step, was selected for application to aqueous samples.

Aim: To analyse MAs in seawater

Objectives:

- To develop a GC method that would resolve and quantify the three MAs, ideally by aqueous injection.
- To develop a pre-concentration method that would take advantage of the MAs volatility and thereby facilitate their analysis at the range of reported environmental concentrations.

3.2 Detection of Methylamines

A sensitive and selective detector that gave a linear response was required for the analysis of the MAs. The flame ionisation detector (FID) and the nitrogen-phosphorus detector (NPD) were available for use in the analysis of MAs. The NPD exhibits greater selectivity and sensitivity than the more commonly used FID. The FID is a universal detector that responds to all hydrocarbon-containing compounds, however, the low molecular weight MAs gave a relatively weak response to the FID. The NPD, in contrast, only responds to nitrogen (or phosphorus) containing compounds, providing improved selectivity through reduced interference from other compounds. The NPD also provides better sensitivity than the FID for nitrogen-containing compounds of up to two orders of magnitude, and was therefore selected for MA analysis.

3.3 Chromatography Development

3.3.1 Sample Matrix

The sample matrix to be used for analysis was an important consideration as it needed to be compatible with both the analytes and the column. To adequately dissolve the MAs, a polar solvent was required; this limited solvent choice to methanol and water. All water used for sample preparation was high purity water (HPW, 18.2 MΩ cm^{-1}). Historically, water has been problematic for GC analysis due to degradation of the column stationary phase and its high expansion coefficient creating over-expansion in the injection liner, which can cause flashback.

The basic character of the amines made analysis difficult. The MAs interact with silanol groups and siloxane bridges causing peak tailing and peak area variability. To overcome these adsorption problems sodium hydroxide has been used in amine analysis (Abdul Rashid et al., 1991; de Zeeuw J., 2000). Sodium hydroxide use is discussed in more detail in Section 3.3.3.

3.3.2 Analytical Column

The first column tested, Rxi5Sil (Thames Restek), is a multipurpose, low polarity silarylene phase column that was designed to be ultra-inert. The phase was similar to the 5% phenyl/ 95% dimethyl polysiloxane used in the Rtx-5 amine column which was reported as being suitable for the separation of amines (Abalos et al., 2001). Pyridine was used to test this column, as it is a nitrogen-containing compound with a higher molecular weight than the MAs and so was expected to give a good response and a well-resolved peak. Indeed, pyridine

gave a large Gaussian peak with a linear response between 0.5-10 mM (R^2=0.9945). Using this column the MAs, however, had short retention times (under 2 minutes), were poorly resolved and gave peak shape with considerable tailing. The short retention time indicated insufficient interaction with the stationary phase.

With the Rxi5Sil column, the MAs eluted in the order MMA; TMA; DMA. This elution corresponded with boiling point order (b.p: DMA = 7.4°C, TMA = 2.9°C, MMA = -6.3°C) and was not in agreement with the expected order of elution based on the relative polarity of the amines (MMA; DMA; TMA). (Abalos et al., 1999; Abdul Rashid et al., 1991). As the smallest molecule, MMA behaviour is most influenced by its polar amine group and, as such, would interact the least with a non-polar or low polarity stationary phase, such as the Rxi5Sil. Consequently, MMA was expected to elute first. In contrast, as the largest molecule, the amine group in TMA would have the least influence on behaviour and, as such, this molecule is comparatively the least polar. This meant that it would interact to a greater extent with a non-polar stationary phase and elute last. Eluting in boiling point order, as they volatilised in the injection liner, was further evidence of limited interaction with the column.

The tailing observed during MA analysis reflected adsorption in the GC injector and on-column, contributing to poor resolution. The tailing was most apparent for MMA. MMA is the most polar MA and, as the lowest molecular weight compound, the amino group has more influence over the physico-chemical behaviour of the molecule, causing the strongest adsorption. The lack of tailing observed using the

Rtx 5 amine column (Abalos et al., 2001), was attributed to its base deactivation and this was a key difference between the Rtx 5 and Rxi5Sil columns. The Rxi-5Sil stationary phase was not base-deactivated but ultra-inert. A base-deactivated column may have produced less tailing and improved separation on the column.

Both methanol and water proved problematic as solvents. When analysed in methanol, DMA gave particularly poor peak shape with no definable peak observed; in water, the MMA peak shape deteriorated. However, as the deterioration of DMA chromatography in methanol was judged to be worse than the deterioration of MMA chromatography in water, water was selected as the injection solvent.

In light of the limitations of the Rxi5Sil column, a CP Volamine column (Agilent) was selected for testing. The CP Volamine column had a methyl/phenyl type stationary phase. The Volamine column incorporated a multi-purpose deactivation, chemically bonded to the silanol groups to reduce dipole-dipole interactions, deactivating the acidic surface of the fused silica and providing a shielding effect to reduce interaction with siloxane bridges. The CP Volamine column was designed to provide a stable stationary phase with a thick film to provide sufficient retention and selectivity for the MAs, in particular to separate DMA and TMA. A further advantage was that it was compatible with aqueous samples.

The CP Volamine column improved retention, with the three MAs eluting between 8 and 11 minutes. Resolution was also improved though the chromatography was

still poor, with significant tailing causing co-elution of TMA and DMA. MMA gave particularly poor chromatography with no discernible peak present. There was also evidence of multiple peaks for each MA.

3.3.3 pH Optimisation

With partial resolution achieved using the CP Volamine column, the use of NaOH to address adsorption problems was investigated. Addition of NaOH to the sample matrix (water) significantly improved both the chromatography and resolution of the three MAs (Figure 3.2). A mixed standard sample was injected and three clearly-resolved peaks were evident with MMA, DMA and TMA eluting at 8.56, 9.88 and 10.36 minutes respectively (Figure 3.2). TMA gave a strong Gaussian peak, while the DMA and MMA peaks tailed slightly without co-eluting. Notably, the order of elution (MMA; DMA; TMA) indicated that the MAs were interacting with the column according to polarity.

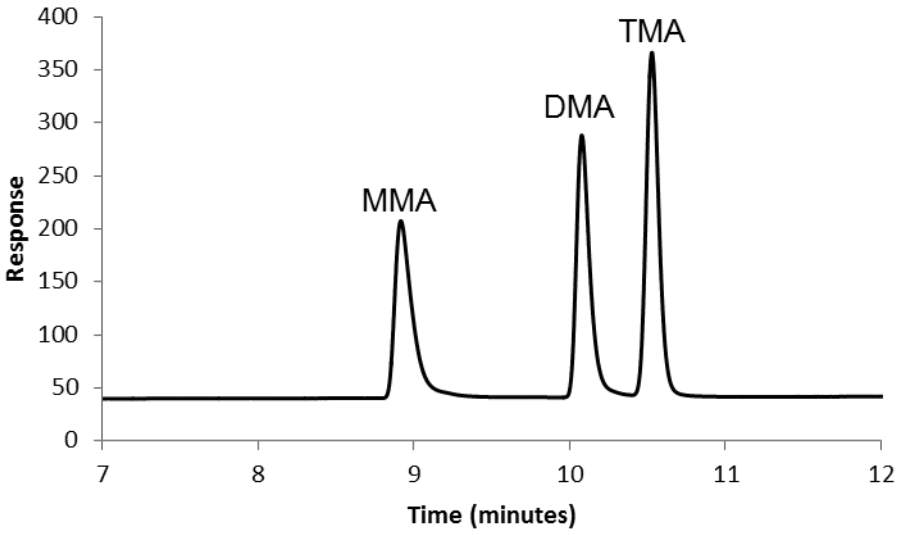

Figure 3.2: A 10 mmol dm^{-3} mixed MA standard chromatogram, analysed by GC-NPD using the CP Volamine column (1µL aqueous injection, inlet temperature: 270°C, detector temperature: 300°C, oven programme: 40-160°C at 10°C min^{-1}, 160-260°C at 15°C min^{-1}, 5 minute hold at 260°C, samples were pH modified with NaOH solution)

A calibration set (0.5-10 mmol dm^{-3}) of mixed MA standard solutions were analysed and showed good linearity (Figure 3.3, MMA R^2=0.96, DMA R^2=0.95, TMA R^2=0.89), with the exception of the 5 mmol dm^{-3} standard solutions.

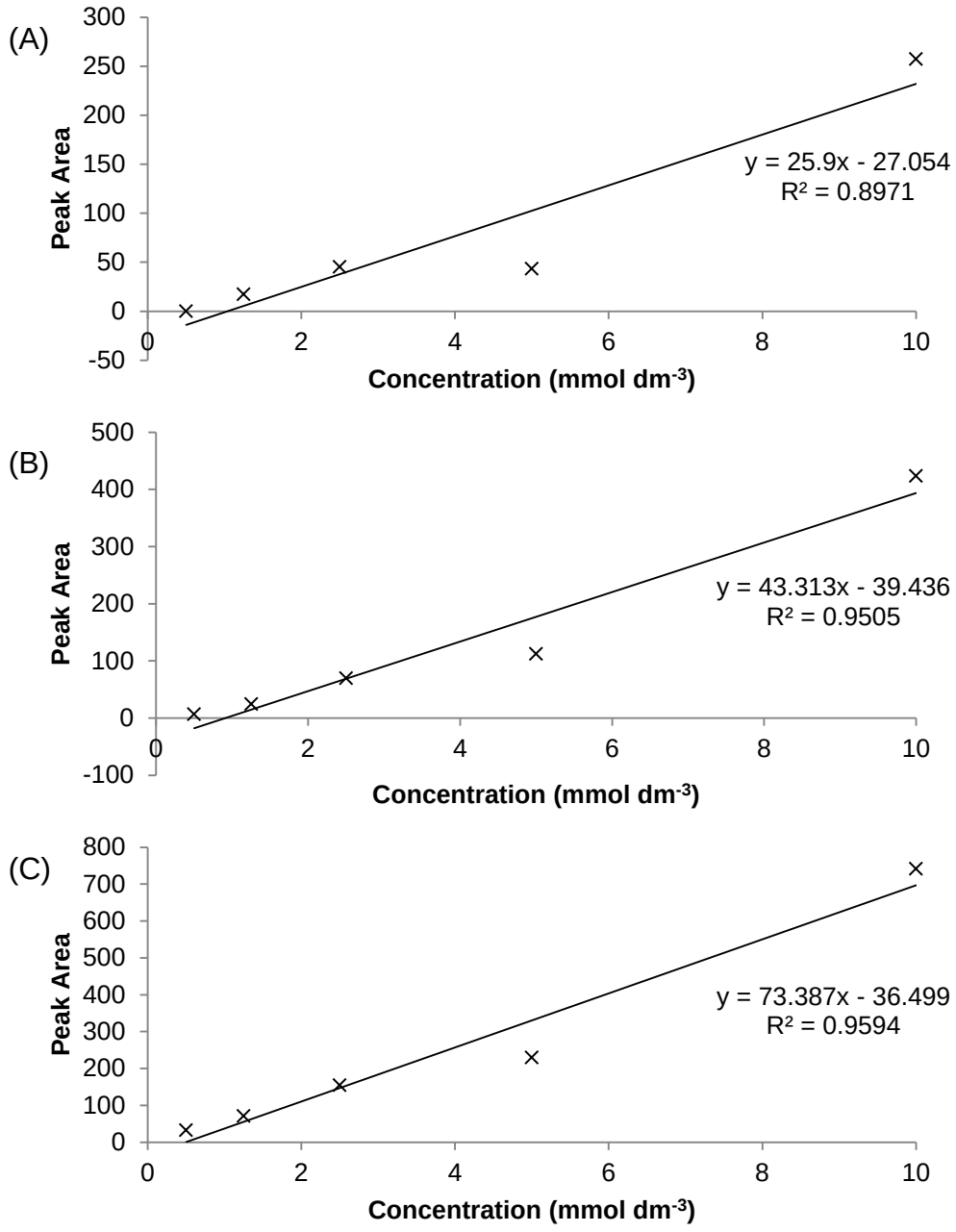

Figure 3.3: Calibrations for: (A) MMA, (B) DMA, (C) TMA for the range: 0.5-10 mmol dm^{-3}. Standard samples were analysed by GC-NPD according to Figure 3.2

The use of NaOH as a source of base during GC analysis can be problematic as it is not sufficiently volatile, it can accumulate at the front of the column where it causes degradation of the stationary phase. As a result, other sources of base to improve chromatography were investigated.

Without NaOH addition, the MAs did not resolve and multiple peaks were evident. A triplicate analysis of a TMA standard showed multiple, inconsistent peaks (Figure 3.4).

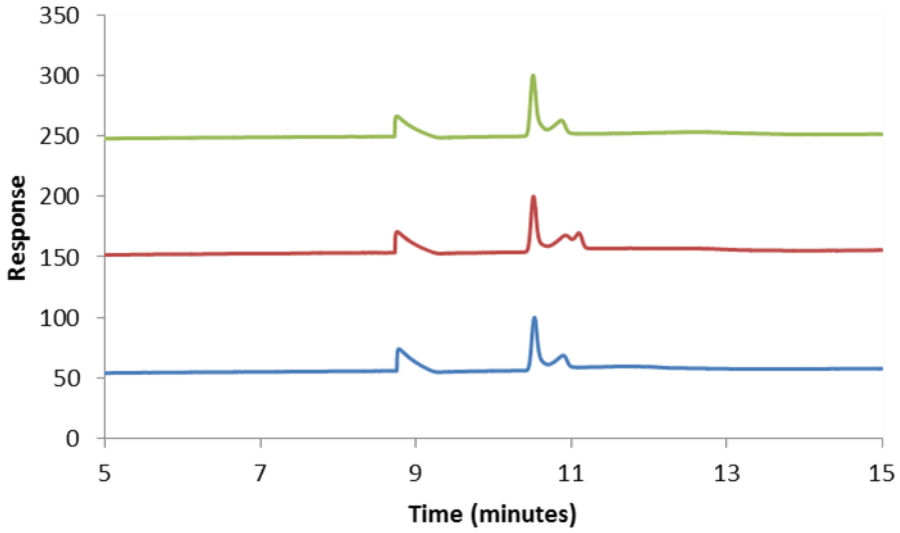

Figure 3.4: Replicate chromatograms for 1 mmol dm^{-3} standard TMA injections analysed using GC-NPD according to Figure 3.2 except without pH modification

The role of NaOH in MA chromatography was twofold. Firstly, to reduce interaction of the MAs with silanol groups and siloxane bridges in the column, and secondly, to deprotonate the MAs. In aqueous samples, MAs partition between their protonated and unprotonated forms. NaOH, as a more basic compound, is thought to act as a competing base and is preferentially protonated over the MAs, converting them to the unprotonated form. Both methanol and water are protic

solvents and, as such, there are protons available to protonate the MAs. This created a pH-dependant equilibrium between their protonated and unprotonated forms, indicating the multiple peaks observed represented both protonated and unprotonated MAs. The use of a CP Volamine column should partially address the unfavourable interactions, as it is multi-purpose deactivated to reduce adverse analyte interaction with the phase. The injection liner was also base-deactivated to minimise sorption within the injector.

Alternative sources of base were investigated. Pyridine, based on the manufacturer's test data, eluted after the MAs. With a pK_b of 8.79, pyridine is a weaker base than the MAs (Table 3.1), but could act as a proton acceptor if present in excess which would shift the MA equilibrium in favour of the unprotonated form. Standards were prepared with the addition of pyridine (pyridine final concentration 6.3 M) and analysed to assess its effect on the chromatography.

The chromatogram resulting from the addition of pyridine to TMA indicated that pyridine forced the TMA into one form over the other, thought to be the unprotonated form (Figure 3.5). The chromatograms obtained with and without the addition of pyridine clearly showed a fluctuation between two peaks, with the latter eluting component dominant in the absence of pyridine (Figure 3.5). With the addition of pyridine, the first peak became dominant, and the poorly-resolved additional peak was reduced in size (Figure 3.5). This suggested that, in the absence of a competing base the MAs fluctuated between protonated and

unprotonated forms and that, in the presence of a competing base, the unprotonated form might be favoured.

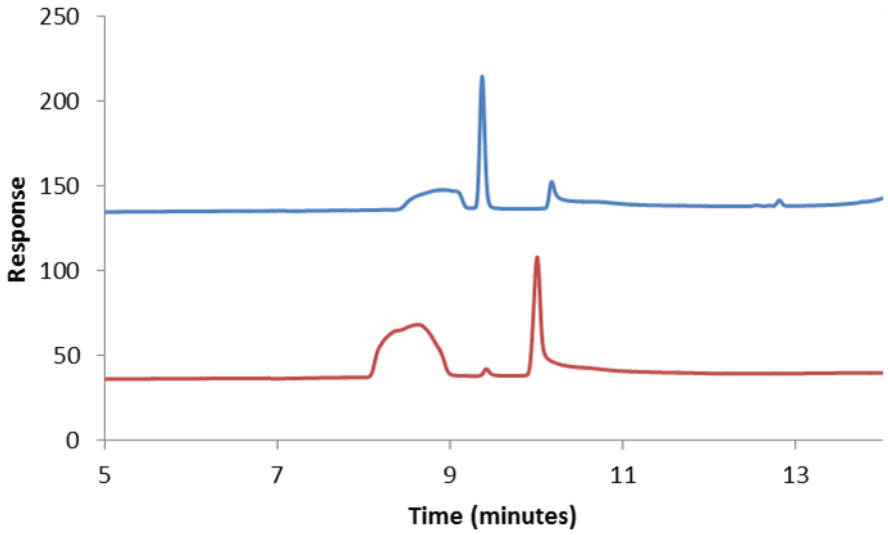

Figure 3.5: Chromatograms from 1 mmol dm^{-3} standard TMA injections in aqueous solution analysed according to Figure 3.2 except without pH modification using NaOH solution (red chromatogram represents TMA analysed with no pH modification and blue chromatogram represents TMA analysed in aqueous solution in the presence of excess pyridine)

The analysis of replicate injections afforded improved chromatography for TMA, with the presence of a single peak (Figure 3.6), but not for MMA and DMA.

In addition, chromatograms of injections of separate MAs, when overlaid indicated that co-elution would still be likely (Figure 3.7). The chromatography was improved compared to that obtained in the absence of base but not sufficiently to achieve resolution of the three MAs, particularly DMA and TMA. The contrasting effect of pyridine addition on MA chromatography may have been related to the fact that pyridine, being less basic than the MAs, was competing for protons but not outcompeting the MAs, even when present in excess.

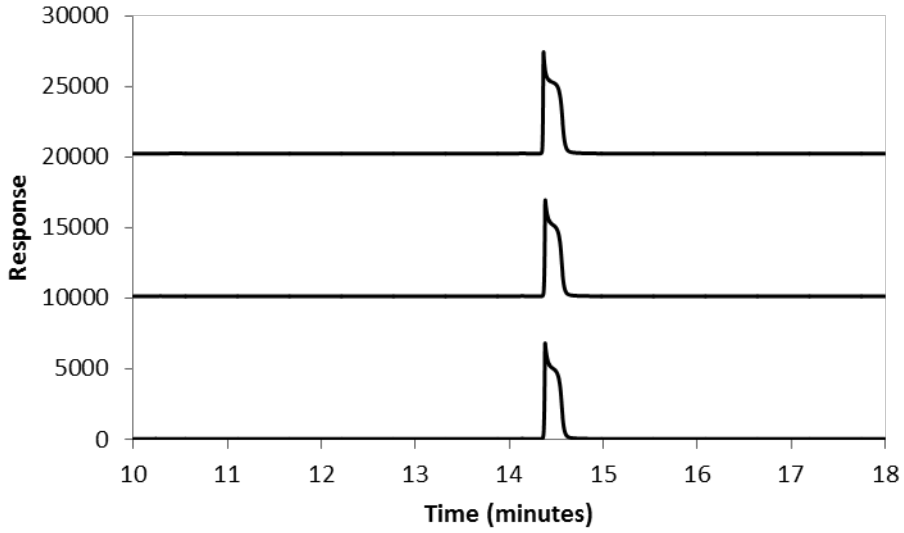

Figure 3.6: Replicate 1mmol dm_{-3} standard TMA injections analysed by GC-NPD according to Figure 3.4 except the aqueous solutions were modified with excess pyrdine

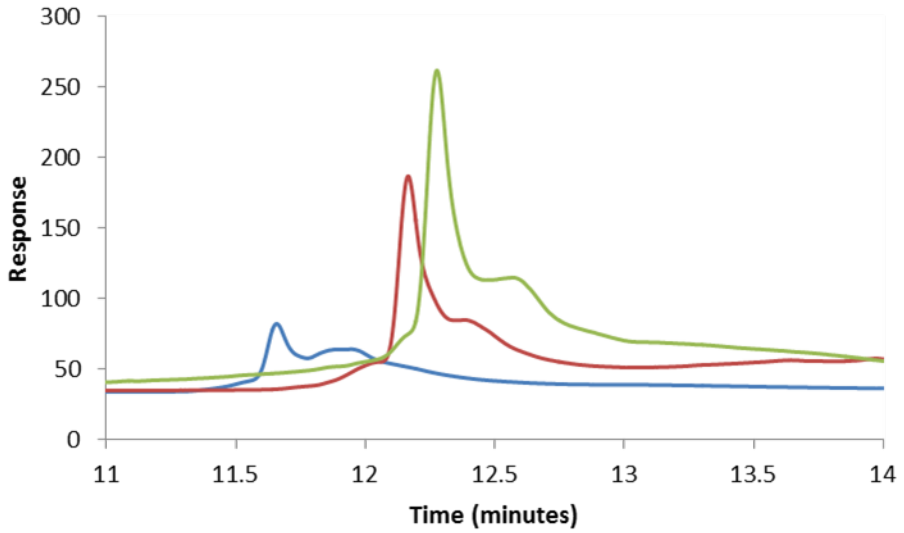

Figure 3.7: Single standard 1 mmol dm^{-3} MA injections (blue=MMA, red=DMA, green=TMA) analysed by GC-NPD according to Figure 3.6 (in the presence of excess pyridine)

With similar basicity to TMA, ammonia (pK_b = 9.25) was also considered. However, ammonia is less basic than DMA and MMA (Table 3.1) and when the MA solutions were spiked with ammonia (final concentration 6 M) no significant improvement was observed.

Given the poor chromatography achieved by substituting NaOH with other bases, alternative ways of using NaOH were investigated. One option was the addition of a guard column, where NaOH could accumulate without damage to the primary GC column. To this end, an additional 2 m of CP Volamine was added to the front of the column to act as a guard column. A mixed standard was analysed and complete resolution was achieved with the MAs eluting in the order of polarity (MMA; DMA; TMA). However, the mixed standard showed a degree of variability in the relative response. Fifteen replicates of mixed MA standard solutions at 10 mmol dm^{-3} concentration were analysed and the peak areas were found to vary substantially (relative standard deviations (RSD) 68-125%; Table 3.3).

To improve precision, the addition of NaOH was standardised, as it had previously been added drop wise to the sample vial. The method was standardised to give a final pH of 13.4 (3 mL of 0.5M NaOH was added to 10 mL of MA solution to give a final NaOH concentration of 0.1M); this significantly improved the RSDs observed (12.9-19.1%; Table 3.3).

Table 3.2: Peak area variability for the MAs analysed using GC-NPD according to Figure 3.2 except for pH modification which was introduced using both drop-wise and standardised NaOH addition, variability expressed as relative standard deviations (RSD) calculated from 10 mmol dm^{-3} mixed MA standard injections (n=9)

Technique	TMA (%)	DMA (%)	MMA (%)
Drop wise NaOH addition	67.9	124.9	118.2
Standardised NaOH addition	19.1	19.0	12.9

Mixed standard and single standard peak areas were compared to see if there was any problematic interaction between the different MAs. TMA and MMA variability were higher in single standards than in the mixed standard but DMA variability was significantly reduced in single standards. This indicated that some form of interaction between the analytes might have been occurring (Table 3.4).

Table 3.3: Mixed and single standard MA variability calculated from peak areas from MA standards analysed by GC-NPD according to Figure 3.2 except with standardised pH modification, variability expressed as relative standard deviations (n=9)

	TMA	DMA	MMA
Mixed Standard RSD (%)	19.13	19.00	12.99
Single Standard RSD (%)	25.93	7.45	22.31

One possible cause of the variation was the relative variability evident in the peak areas. The NPD was expected to give a response that positively correlated with hydrocarbon content. As such, TMA was expected to have the largest peak area and MMA the smallest. However, a fluctuation in relative peak areas was frequently observed, with the MMA peak area being the largest. Replicate analyses of a mixed standard were compared and the fluctuating peak areas were observed (Figure 3.8).

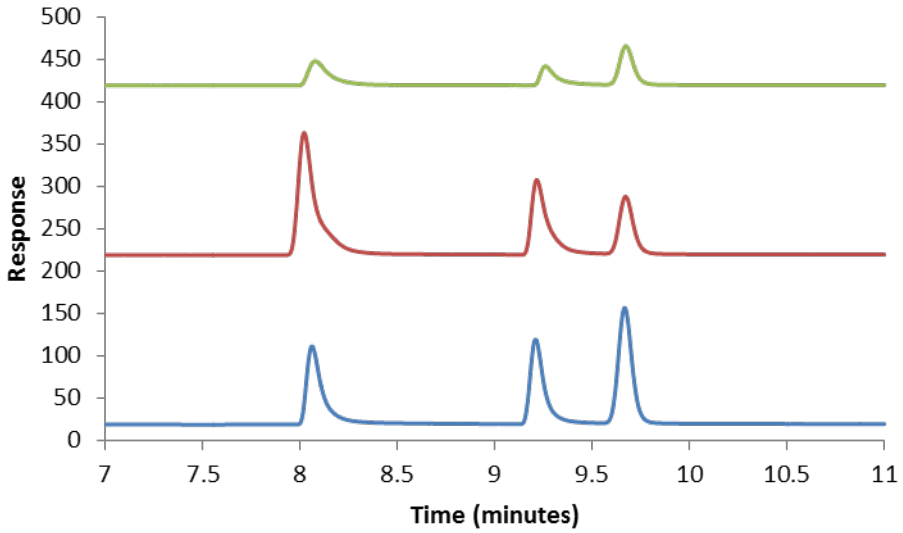

Figure 3.8: Replicate chromatograms from 10 mmol dm^{-3} mixed MA standard injections analysed by GC-NPD according to Figure 3.2 but with standardised pH modification

3.3.4 Addition of an Internal Standard

Quantification of analytes in environmental samples is typically achieved in one of two ways: using an external calibration or through use of an internal standard. An external calibration compares a sample with standards of known concentration to calculate the concentration in the sample. The internal standard (IS) method is used to compensate for potential sources of error. The IS chosen should have similar chemical attributes to the analytes of interest and is added to each sample prior to sample preparation or analysis. Consequently, the IS undergoes the same processes and changes as the analytes. Incorporating the IS into the calibration plot, for example, by using a peak area ratio (peak area ratio = MA peak area: IS peak area) instead of peak area, accounts for procedural error and instrumental fluctuations.

Cyclopropylamine (C_3H_7N; CPA) was selected as an IS for MA analysis as it has not been reported as occurring naturally. It is also a low molecular weight amine that should behave similarly to the MAs, and has been successfully applied in previous studies (Abalos et al., 1999; Abdul Rashid et al., 1991). CPA was analysed by GC and gave a strong, Gaussian response, well resolved from the amines (Figure 3.9) and was linear between 0.5 – 10 mmol dm^{-3} (y = 50.4x – 6.5, R^2 = 0.99).

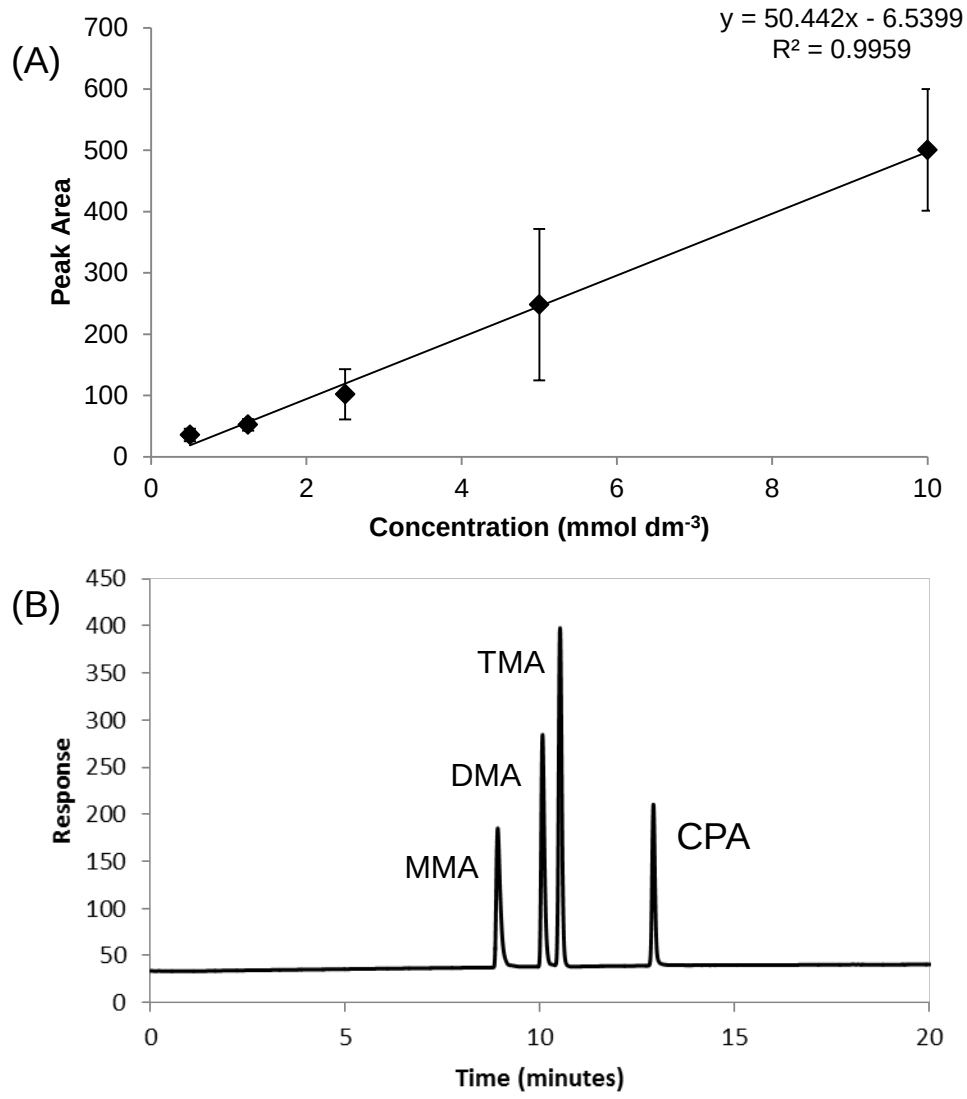

Figure 3.9: (A) CPA calibration and (B) Replicate chromatograms of resolved mixed MA standard with added CPA (n=3) analysed by GC-NPD according to Figure 3.8

Prior to addition of the internal standard, the chromatograms gave variable peak areas with a notable fluctuation between low values and very high values. The addition of an internal standard to account for instrumental fluctuations (using peak area ratio; PAR) reduced the variability; for example, the TMA peak area variability of 16.09% was reduced to 7.82% (Table 3.5). The reduction in variability indicated that the IS was effective in accounting for analytical variability.

Table 3.4: Comparison of peak area variability (expressed as RSD) and peak area ratio (PAR) variability (n=4) from standards analysed by GC-NPD according to Figure 3.8

Concentration (mM)	TMA (%)	TMA PAR (%)	DMA (%)	DMA PAR (%)	MMA (%)	MMA PAR (%)
0.5	29.28	8.75	56.99	19.00	51.30	25.70
1.25	7.29	6.52	17.06	5.60	23.43	13.07
2.5	13.95	11.66	24.76	0.74	30.59	7.35
5	13.56	5.89	16.41	5.61	18.29	7.44
10	16.35	6.28	20.93	0.73	22.10	1.03
Mean	**16.09**	**7.82**	**27.23**	**6.34**	**29.14**	**10.92**

To further reduce the observed variability and to mitigate the effect of water as a solvent and its potential for flashback in the injection liner, the injection volume was reduced to 0.2 µL. The variability was sufficiently reduced (Table 3.6) to allow a calibration to be performed (Figure 3.10). The variability was less than 5% between 2.5-10 mmol dm^{-3} but increased below 2.5 mmol dm^{-3}. However, all RSDs were below 10% and all three calibrations were linear. Notably, the relative peak areas were consistently of the order: MMA < DMA < TMA.

Table 3.5: Variability (expressed as RSD) and linearity of mixed MA standard injections (n = 3) analysed by GC-NPD according to Figure 3.8 except with a reduced injection volume of 0.2 µL

	TMA	DMA	MMA
RSD of peak area ratio (MA:CPA) at 10 mmol dm^{-3}	6.28	0.73	1.03
Calibration R^2 (0.5-10 mmol dm^{-3})	0.9801	0.9844	0.9931

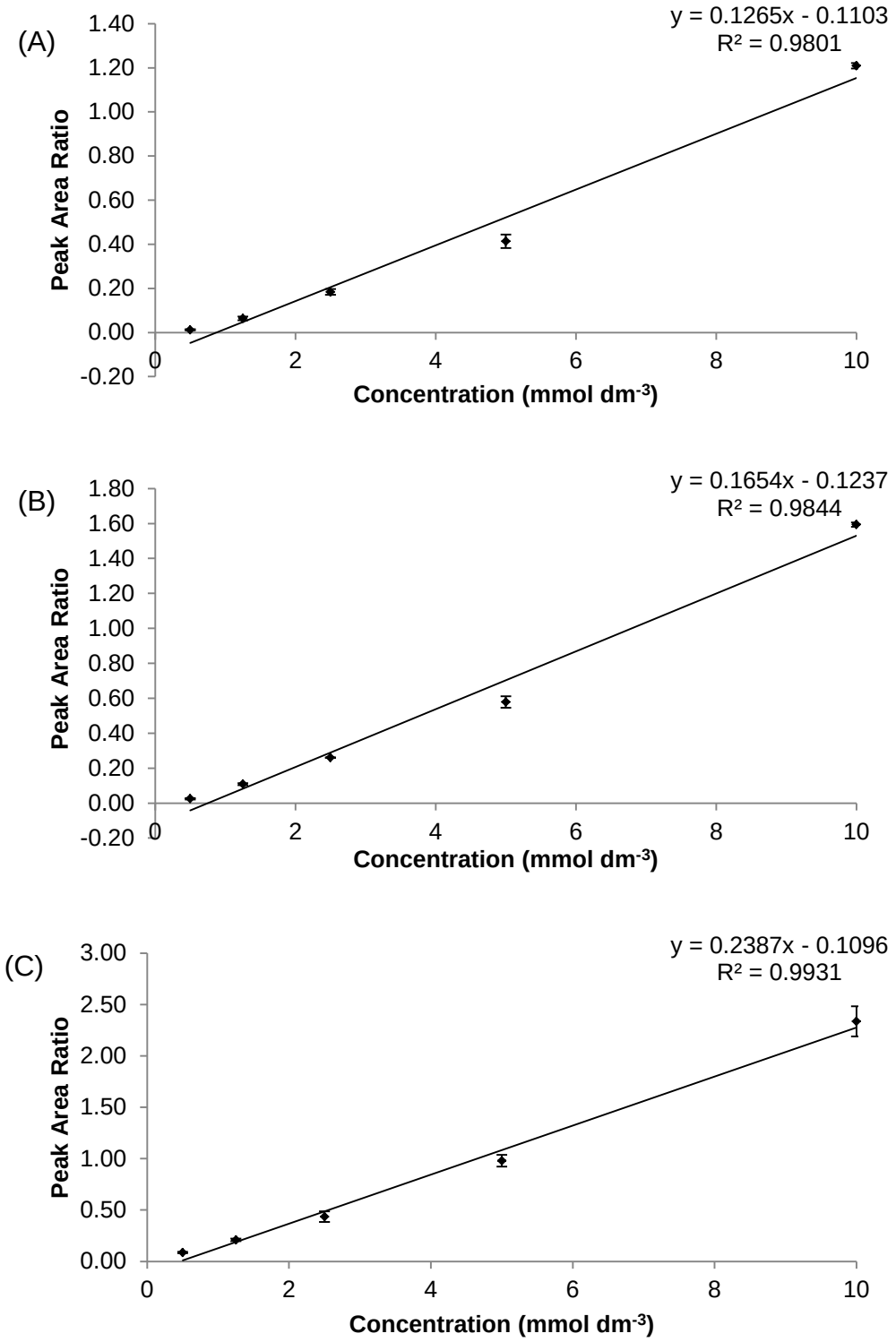

Figure 3.10: Calibrations for (A) MMA, (B) DMA, (C) TMA for the range 0.5-10 mmol dm^{-3} analysed by GC-NPD according to Figure 3.8 except with a reduced injection volume of 0.2 µL

3.4 Pre-concentration via Purge and Trap

Having selected a GC column and injection conditions to satisfactorily resolve the three MAs, the next stage was to develop a pre-concentration method to achieve their analysis at expected environmental concentrations.

3.4.1 Introduction

A previous pre-concentration method for aqueous MAs involved microdiffusion in a Cavett flask (Abdul Rashid et al., 1991), achieving 45-73% recoveries. To try to improve MA recovery, the method was modified to incorporate dynamic headspace pre-concentration. The modifications were based on Dawit et al. (2001). 1-aminopropan-2-one ($CH_3COCH_2NH_2$, APR) was recovered from aqueous samples by injecting acidified water samples into a gas stripping chamber where NaOH was then added to bring the solution to pH 12 (Dawit et al., 2001). The APR was volatilised via deprotonation and stripped from solution using nitrogen gas; the volatile species were passed onto a cartridge to be derivatised for analysis by HPLC. This method achieved 90-100% recoveries from 10 µmol dm^{-3} standard solutions and detection limits of 18 nmol dm^{-3}, using UV-HPLC.

3.4.2 Initial Design

Based on a design reported by Dawit et al. (2001), a three necked round bottom flask was set up. The first neck introduced the nitrogen gas flow; the second was used for NaOH addition to adjust the water pH, while the third acted as a gas outlet to transfer purged analyte to an acid trap via Teflon tubing (Figure 3.11). The NaOH solution (20 mL, 10 M) was added to the water sample to adjust the

sample to pH 13 (pH adjustment discussed in detail below), converting the MAs into the free form to cross the water-air interface, where they could be transferred to an acid trap and protonated. The trap comprised 10 mL of 0.1M HCl (pH 1), with a needle used for venting the trap. The design is illustrated in Figure 3.11.

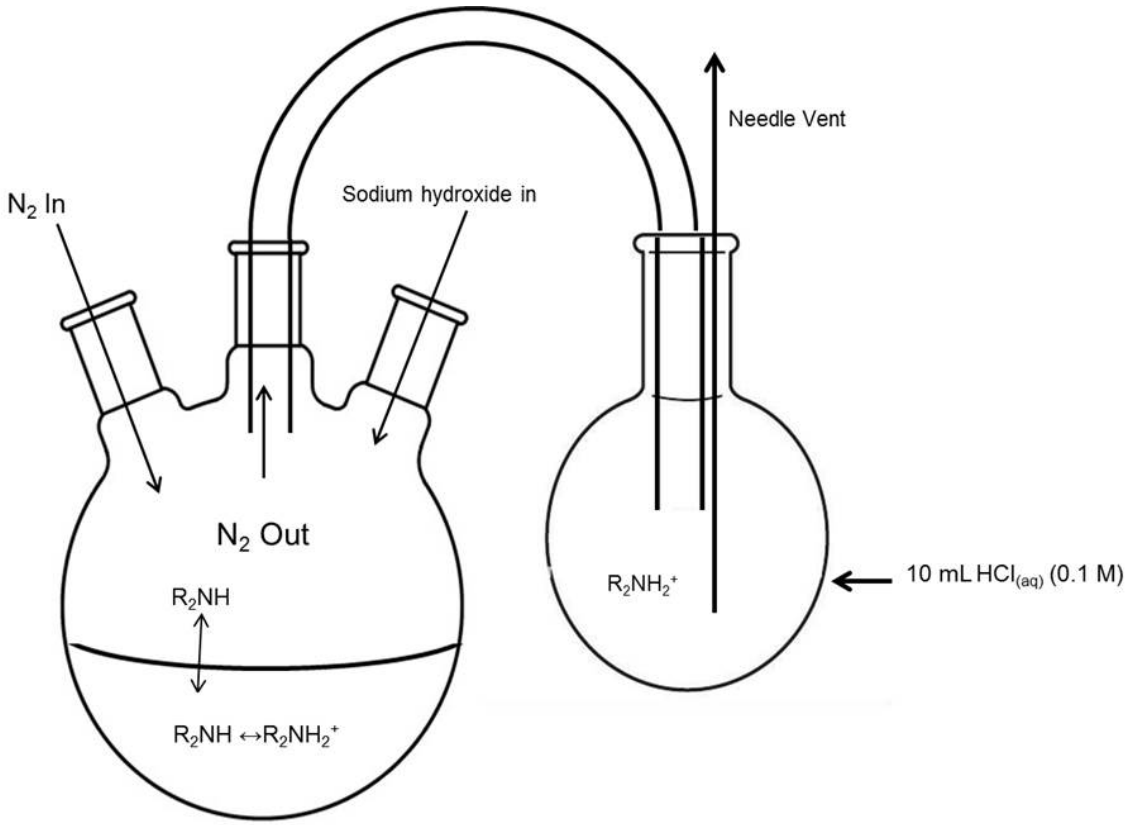

Figure 3.11: Initial design of purge and trap apparatus (not to scale)

The sample matrix had to be considered as the bicarbonate present in seawater would affect the pH of the sample and, as such, the volatility of the MAs. This buffer is created by carbon dioxide exchanging across the air-sea interface (Equation 1) and reacting rapidly with the water (Equation 2).

$$CO_{2(g)} \rightleftharpoons CO_{2(aq)} \qquad \text{Equation 1}$$

$$H_2O + CO_{2(aq)} \rightleftharpoons H_2CO_3$$ Equation 2

This reaction is more rapid than the exchange across the air-sea interface so the formation of H_2CO_3 dominates. The carbonic acid then dissociates in two stages according to the pH of the solution (Equation 3 and Equation 4).

$$H_2CO_3 + H_2O \rightleftharpoons H_3O^+ + HCO_3^-$$ Equation 3

$$HCO_3^- + H_2O \rightleftharpoons H_3O^+ + CO_3^{2-}$$ Equation 4

The relative proportions of the three forms of dissolved inorganic carbon (DIC) namely: H_2CO_3, HCO_3^+, CO_3^{2-} reflect the pH of a water body. The pH of seawater is normally maintained within a relatively narrow range, due to the buffering capacity of HCO_3^- and other alkaline species (Figure 3.12).

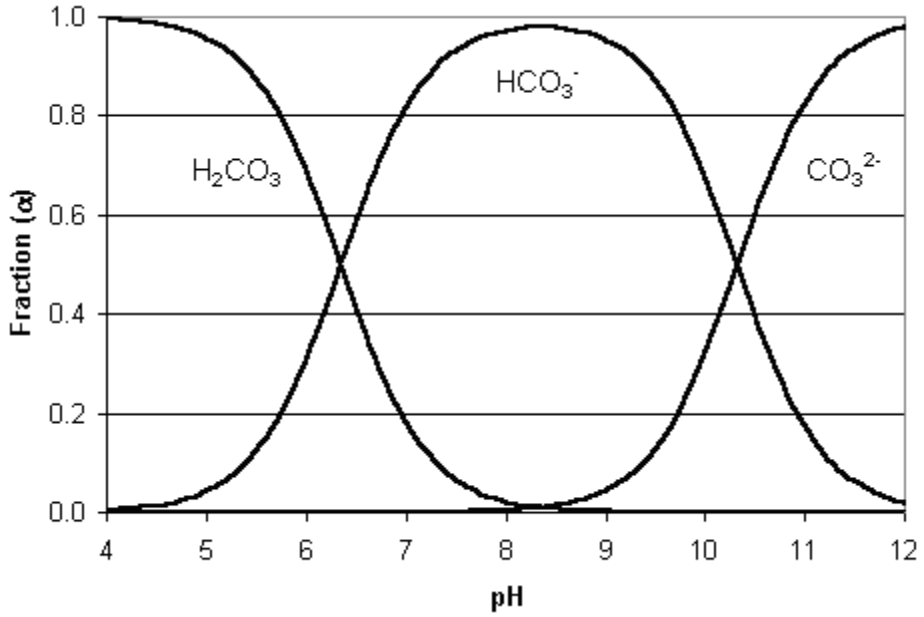

Figure 3.12: Dissolved inorganic carbon (DIC) ion distributions in aqueous solution according to pH

At seawater pH (pH 7.8-8.2) the HCO_3^- dominates, with typical concentrations of approximately 2 mmol dm^{-3}, and buffers the seawater pH (Harrison., 1992). A change in concentration of any DIC species will cause a shift in the equilibrium and alter the concentration of the other ions. At high pH, the bicarbonate ion dissociates to produce H^+ ions and at low pH the bicarbonate combines with excess H^+ ions; both actions buffer the seawater pH. Similarly to the carbonate buffer, at high pH $Mg(OH)_2$ precipitates out of seawater and affects the pH (Equation 5) (Dziubek and Kowal, 1984; Merrill and Jorden, 1975).

$$Mg^{2+}_{(aq)} + 2OH^-_{(aq)} \rightarrow Mg(OH)_{2(s)} \qquad \text{Equation 5}$$

This precipitation begins at pH 9.5 and is largely complete by pH 11-11.5. The precipitation of $Mg(OH)_2$ reduces the pH and so this was also accounted for.

Amines equilibrate in water between protonated and unprotonated forms (Equation 6).

$$RNH_2 + H_2O \rightleftharpoons RN^+H_3 + OH^- \qquad \text{Equation 6}$$

To shift the equilibrium in favour of RNH_2, the carbonate buffer must be exhausted to modify the seawater to a high pH. The amount of NaOH required to overcome the carbonate buffer and the magnesium hydroxide precipitation was investigated and an optimised NaOH concentration calculated (Figure 3.13).

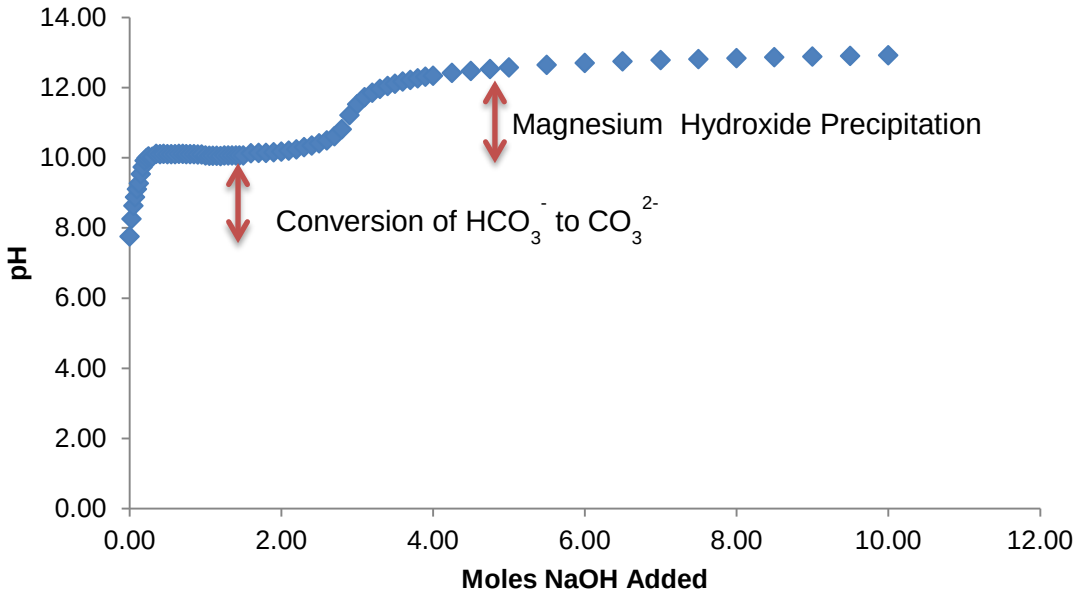

Figure 3.13: Effect of NaOH addition on the pH of a seawater sample

Initial tests were performed using 1 L high purity water (HPW) samples (0 salinity) in a 3 L purge vessel and purged for 1 hour, aiming for a final MA concentration of 10 mmol dm^{-3}. No MAs were detected, however, when the aqueous contents of the acid trap were analysed.

A subsequent adjustment reduced the size of the purge vessel to minimise the headspace above the water sample, in order to improve movement from the purge vessel to the transfer line. This resulted in a 0.2% recovery of TMA (i.e. 0.2% of 10mmol dm^{-3}); a slight improvement. The purge time was then increased to 6 hours to allow further time for MA transfer. This increased TMA recovery to 4%, but this result could not be replicated. Since the NaOH concentration had been optimised, the low recoveries were thought to be due to inefficient transfer from the purge vessel to the acid trap.

The next adjustment was to modify the transfer channel. The initial transfer channel comprised a 20 cm piece of narrow Teflon tubing. This tubing was replaced with a shorter (10 cm), wider piece of tubing, resulting in a shorter transfer channel, minimising the surface area for MA adsorption. However, no improvement resulted. The Teflon tubing was soaked in NaOH solution to minimise adsorption potential, but this did not result in an improved recovery. A conical funnel was then added to the purge vessel end of the transfer tubing (Figure 3.14), to direct gaseous MAs out of the purge vessel and minimise retention of MAs in the headspace.

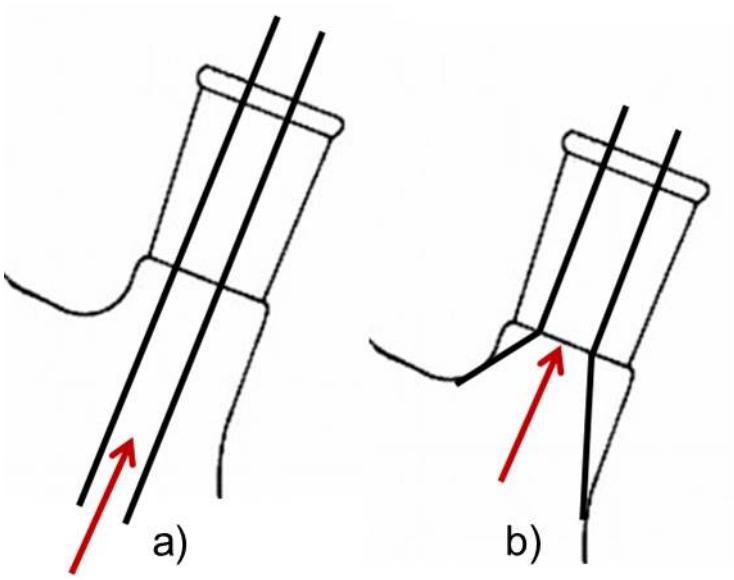

Figure 3.14: Funnel illustration showing: (A) the original design and (B) the funnel added to facilitate transfer of gaseous MAs to the acid trap

The acid trap volume was then reduced to 2 mL, in order to increase the pre-concentration factor. No improvement was observed. Finally, a vacuum step was added via a tube connected to the acid trap flask, which was connected to a vacuum pump to improve transfer of the MAs to the acid trap; no improvement was observed (Figure 3.15).

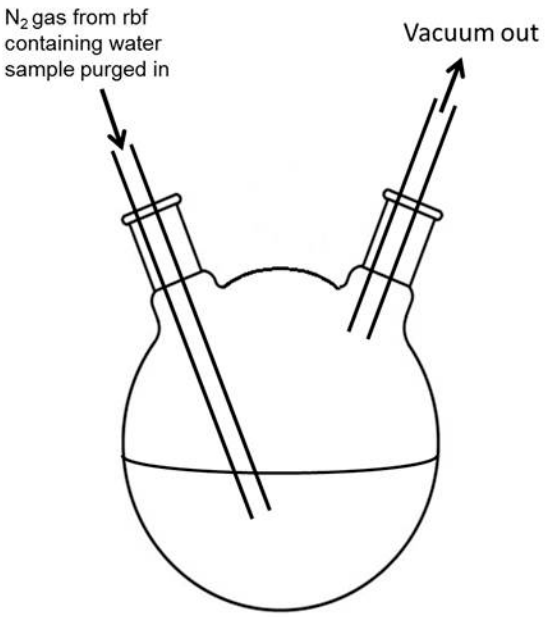

Figure 3.15: Illustration of the vacuum pump set up and its connection to the trap, not to scale

3.4.3 Purge Step Optimisation

There were two key stages of the purge and trap process to be refined: the purge step and the trap step. The purge step was designed to volatilise and then strip the MAs from the sample. The NaOH concentration had been optimised so the next parameter investigated was the gas flow. Initially a qualitatively 'slower' gas flow and lower pressure were used to increase the residence time of the nitrogen bubbles within the sample solution. This did not result in sufficient MA recovery. A 'faster' nitrogen flow was tested, once the system had been 'leak-proofed'. All glass joints were sealed with PTFE liners and clipped, while attachments were held in position using elastic bands. Once the system was leak tight, the faster gas flow rate was tested but did not improve MA recovery.

An important aspect considered when optimising the purge step was airside versus waterside control. The MAs are highly water soluble and, as such, their

mass transfer from water to air should be dominated by airside resistance (Carpenter et al., 2012). In addition, their high solubility meant that they were unlikely to dissolve in the nitrogen bubbled through the solution. This, combined with the need for airside turbulence, meant that disturbing the thin film surface layer of the water should be more effective at promoting transfer across the air-water interface. To test this theory, the target MA concentration was increased to 50 mmol dm^{-3}, to identify incremental changes. Airside turbulence was provided by blowing nitrogen over the surface of the water. This disturbed the thin film surface layer of the water to allow more diffusion of the MAs into the air. Waterside turbulence was provided by blowing nitrogen gas through the water. Airside turbulence resulted in 1.3% TMA recovery but no DMA or MMA, whilst waterside turbulence achieved 1% TMA recovery and no DMA or MMA. Neither method provided significant improvement. A combination of airside and waterside turbulence did not improve recovery further.

To improve diffusion out of the sample the next step was to heat the purge vessel. The purge vessel was heated to 60°C (Abdul Rashid et al., 1991). This improved MA recovery to 4.4%, 1.1% and 0.7% for TMA, DMA and MMA respectively. Notably, this was the first time that DMA and MMA were detected using the purge and trap design.

With no significant difference between waterside and airside turbulence observed, another parameter investigated was the bubble diameter of waterside turbulence nitrogen gas. A frit was used to increase the number of smaller diameter bubbles passing through the sample, to increase the total surface area

of bubbles in contact with the sample. A frit on the nitrogen supply in the purge vessel resulted in recoveries of: 3.4%, 1.4% and 1.5% for TMA, DMA and MMA, respectively. This was an improvement for DMA and MMA but a decrease in recovery for TMA. As a result, a frit was attached to the trap gas supply which improved recoveries to 4.2%, 2.1% and 1.7% for TMA, DMA and MMA respectively. Subsequently, a frit on both the nitrogen supply and the acid trap gas supply was tested but this over-pressurised the system.

3.4.4 Trap Step Optimisation

The low MA recoveries may have been partly due to an inefficient trapping method. The MAs were potentially being volatilised and stripped out of the purge solution and then transferred to the trap vessel where they were not efficiently retained. Two main steps were taken to try and improve the trap step: optimisation of trap volume and trap shape. Firstly, the trap volume was increased to 10mL. The volume had initially been reduced to increase the pre-concentration factor, but was increased to maximise the amount of time the MAs would have to interact with the acid solution. This adaptation did not improve recoveries. The shape of the acid trap was then changed from a round bottom flask to a test tube. This also aimed to increase the amount of time the MAs would be in contact with the acid solution (Figure 3.16). For the same volume of water a longer, thinner vessel would provide a longer path for the bubbles to travel through than a shorter, wider round bottom flask. This was achieved by attaching a glass Pasteur pipette to the Teflon tubing. This added depth and a narrow bubble exit to the transfer channel. The change to the trap vessel achieved a recovery of 4.2%, 3.0% and 2.6% for TMA, DMA and MMA

respectively. The DMA and MMA recoveries were improved, but not the TMA recovery.

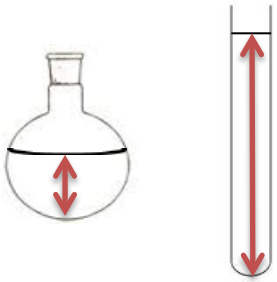

Figure 3.16: Diagrams to illustrate different path length from point of bubble release to the air-water interface in a round bottom flask and a test tube

The results are summarised in Figure 3.17. Though some improvement in recovery was achieved it was still unacceptably low (below 5%).

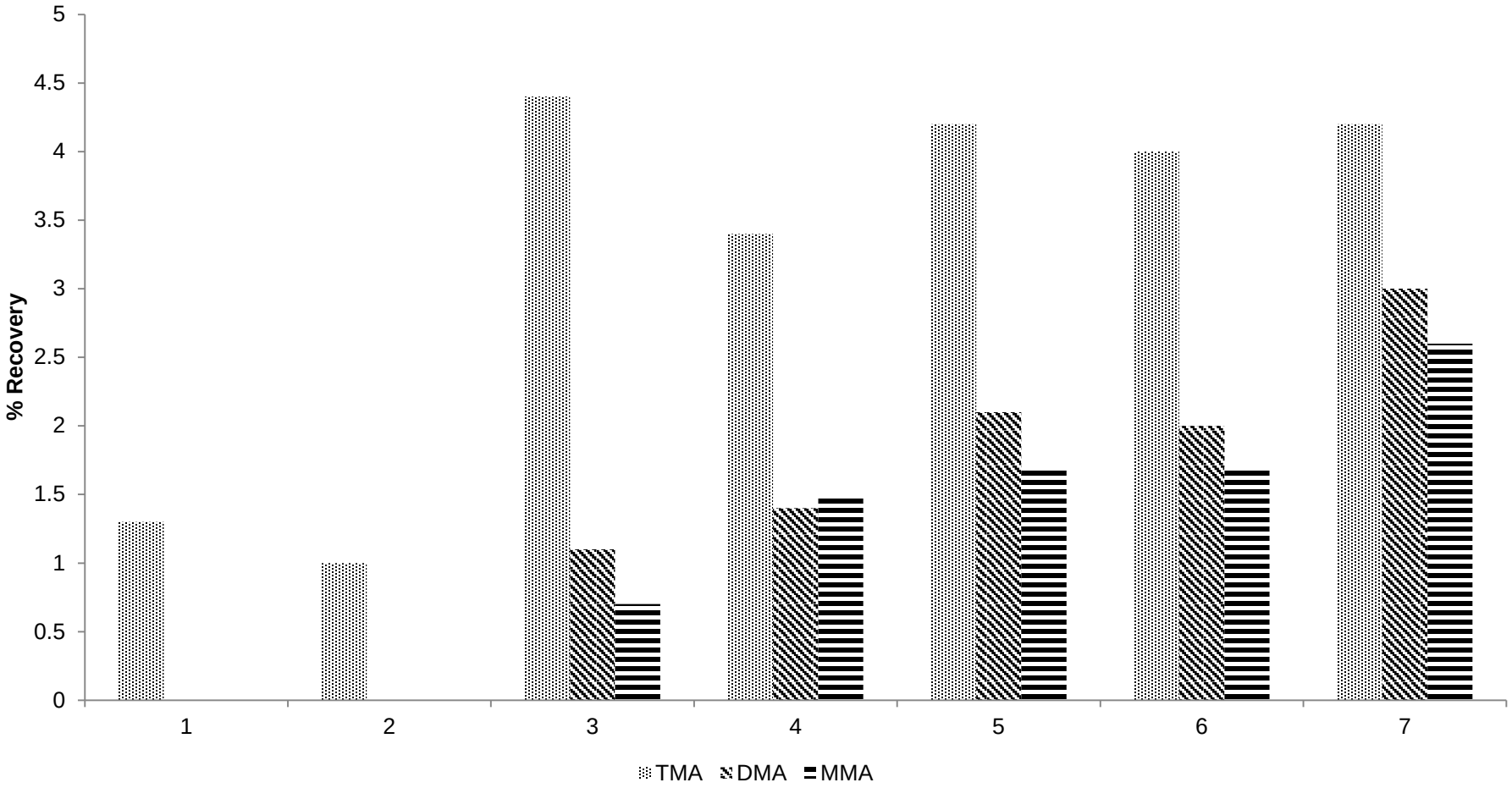

Figure 3.17: Results of the purge and trap experiments. 1) airside turbulence; 2) waterside turbulence; 3) heated purge vessel; 4) frit on nitrogen supply; 5) frit on acid trap; 6) increased trap volume; 7) refinements to trap shape

3.4.5 Potential Improvements to the Purge and Trap Approach

Purge and trap has been successfully applied to the analysis of the MAs in cosmetic products (recoveries of 80.3-105.5%) (Zhong et al., 2012). The main differences between the approach reported in Zhong et al. (2012) and this method were the shape of the purge vessel, the use of lithium hydroxide instead of sodium hydroxide in the purge solution and the presence of acetic acid instead of hydrochloric acid in the acid trap. The shape of the purge vessel reported in Zhong et al. (2012) was longer and thinner than a round bottom flask. This may have affected the residence time of the nitrogen bubbled through the solution, and interaction with the analytes. Interestingly, this method also used waterside turbulence and not airside turbulence.

The use of lithium hydroxide and acetic acid was not expected to improve the recovery to an acceptable level. With such low recoveries from the purge and trap method a new approach was required.

3.5 Solid Phase Microextraction

3.5.1 Introduction

Solid phase microextraction (SPME) was chosen as the next potential pre-concentration method to investigate. SPME has been successfully applied to the analysis of MAs in sewage and wastewater by Abalos et al. (1999).

There are two main methods of SPME extraction: direct (water) and headspace extraction. Direct extraction involves exposing the fibre directly to an aqueous sample. This raises two issues: firstly, as a complex matrix, seawater samples reduce the fibre lifetime and secondly, the pH of the sample need to be considered. The analysis of the MAs required a sample pH of 13.4 which was incompatible with the suitable SPME phases which had upper limits of pH 11. The MAs volatility makes them ideal for headspace analysis. This approach has been reported by Abalos et al. (1999). Headspace extraction was therefore the approach selected for this study.

SPME was not directly compatible with the chromatography method developed for the aqueous injection of MAs since, once the MAs had been extracted, they would be thermally desorbed into the injection liner. This meant that NaOH could not be injected with the sample, raising concerns of adsorption affecting the application of SPME.

3.5.2 Proof of Concept

Historically, SPME sampling had been carried out with small sample volumes. For this reason a proof of concept experiment was carried out with 15 mL samples using 3.2 µmol dm^{-3} mixed MA standards heated at 60°C for 1 hour. The final concentration was calculated from the amount of MAs injected on-column from a 100 mmol dm^{-3} aqueous injection. The solutions were saturated with salt, to promote diffusion by reducing stability and to keep the ionic strength constant between extractions; all samples were adjusted to pH 13.4 with NaOH solution.

The 15 mL extractions were used to test three different fibres: polyacrylate, carboxen/polydimethylsiloxane (carboxen/PDMS) and polydimethylsiloxane/divinylbenzene (PDMS/DVB). The polyacrylate fibre was designed for polar semi-volatiles with molecular weights of 80-300. As expected, this fibre was not suitable for the extraction of the polar, highly volatile MAs. The Carboxen/PDMS was designed to extract gases and low molecular weight compounds with molecular weights of 30-225. This fibre was potentially suitable and proved capable of extracting the MAs; however, during analysis each MA showed multiple peaks and poor chromatography. The PDMS/DVB fibre was designed for volatiles and amines with molecular weights of 50-300. Despite the molecular weight range being above that for MMA and DMA, this fibre was expected to be the most suitable. When single standards were analysed, TMA and DMA appeared as single, tailing peaks, while MMA gave a broad, shallow peak. The poor chromatography was attributed to the absence of NaOH. The PDMS/DVB fibre comprised porous divinylbenzene polymer particles suspended in liquid PDMS polymer. PDMS has an absorptive mode of action and DVB an

adsorptive method of action. The fundamental difference between the two being that, in adsorption, molecules bind directly to a limited number of sites on the surface of a solid while, in absorption, they dissolve into the bulk of the fluid. This means that the saturation point should never be reached. Thus, the dynamic range of adsorption coatings was limited and a linear relationship between the concentration of the analyte in the sample and the amount extracted would be exhibited in a narrow concentration range. Another consequence was that absorption fibres are non-competitive while adsorptive fibres exhibit competitive behaviour. Thus, a molecule with higher affinity for the surface could replace one with a lower affinity.

The DVB blended with PDMS was reported to retain smaller analytes better than PDMS alone so the combination had better affinity for the MAs. The PDMS/DVB fibre was chosen as the most suitable fibre and used for a first mixed standard MA calibration (100 nmol dm^{-3}- 3.2 µmol dm^{-3}, RSDs of 0.7-0.9; Figure 3.18). The MMA peak fully resolved as a broad peak that frequently appeared as two peaks. The DMA and TMA peaks did not fully resolve but were sufficiently resolved to allow robust integration. Notably, when using the PDMS/DVB fibre the DMA peak was consistently larger than the TMA peak. This may indicate that DMA had a higher affinity for the fibre, either preferentially being adsorbed or displacing TMA from adsorption sites.

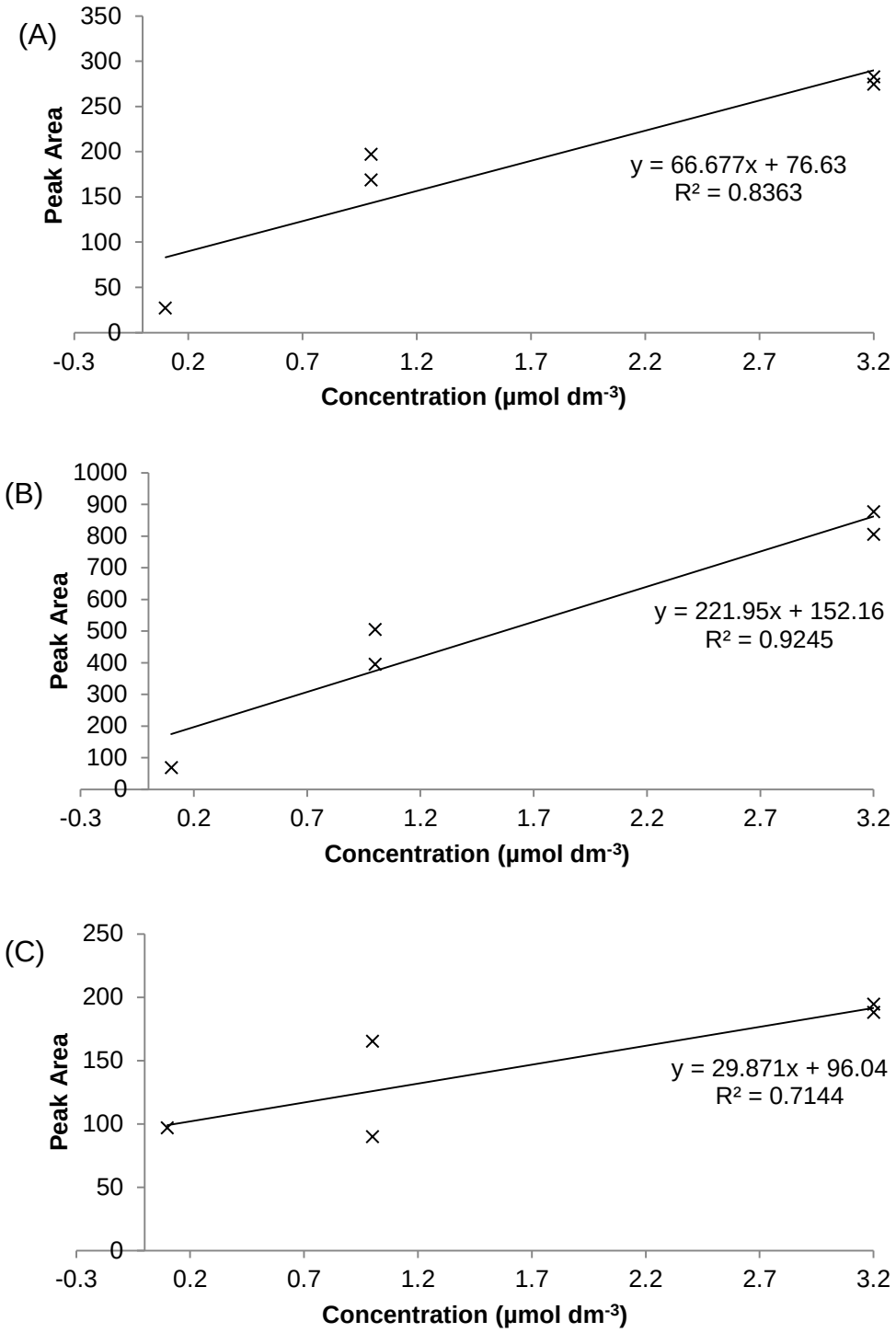

Figure 3.18: Small volume (15 mL) mixed MA standard extractions from HPW heated to 60°C for 2.5 hours to calibrate (A) MMA, (B) DMA, (C) TMA; samples were heated at 60°C for 2.5 hours and analysed by GC-NPD (5 minute thermal desorption in the inlet (270°C) with compounds introduced to column at 1 minute, inlet temperature: 270°C, detector temperature: 300°C, oven programme: 2 minute hold at initial temperature of 50°C then 50-160°C at 10°C/min, 160-260°C at 15°C/min, 5 minute hold at 260°C)

3.5.3. Application of SPME to Seawater Samples

In order to achieve environmentally relevant limits of detection, a larger sample volume was required. However, SPME is not usually applied to large volume extractions and a number of key aspects needed to be investigated and kept constant for scaling up. Firstly, the whole water sample had to be kept homogeneous and secondly, a constant water temperature had to be maintained. One way of keeping the water mixed and temperature consistent was to stir the sample. However, the stirring would need to be kept entirely consistent and, as such, was not introduced as a variable at this stage.

A 1 L volumetric flask was chosen as the extraction vessel, as it allowed the sample volume to be controlled and the headspace to be minimised. However, the volumetric flask did present difficulties for maintaining a constant water temperature. The first heating method chosen was a hot plate. However, even with lagging the hot plate could not maintain an isotherm within the vessel. A water bath was then tried. The water bath was chosen to be large enough to heat the entire water sample but not the headspace. This allowed the water temperature within the flask to be kept constant. The equipment set up is illustrated in Figure 3.19.

Since headspace sampling was being used, consistency of the headspace volume was maintained between samples and slight variations in the water volume (which could be accounted for) were permitted.

Initial tests using 2.5 hour extractions were carried out using 100 nmol dm-3 samples and these gave moderate precision (RSDs: TMA=34%, DMA=15%, MMA=22%, n=6).

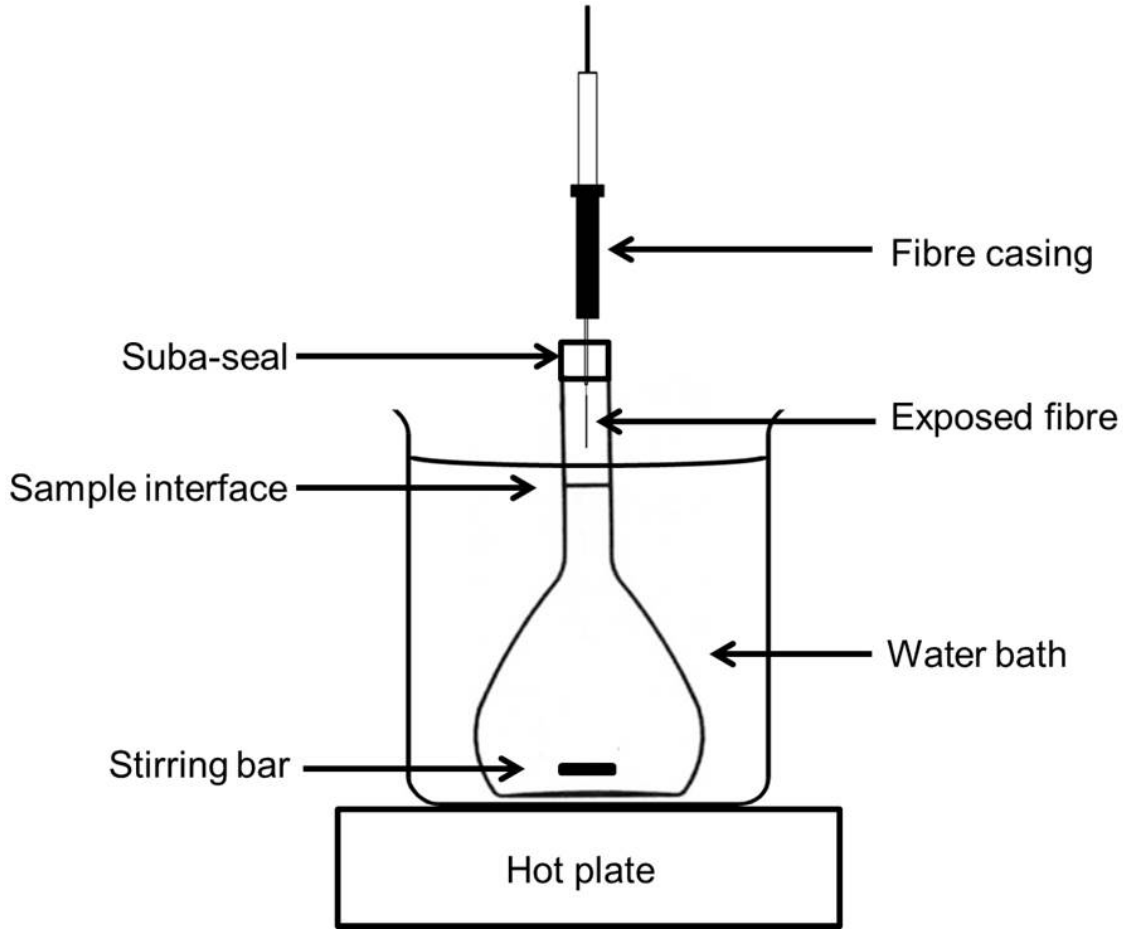

Figure 3.19: The SPME apparatus set up design for analysis of MAs in seawater samples, not to scale

3.5.4 Internal Standard

Due to the suitability of CPA as an IS during GC analysis of aqueous samples, CPA was selected as the IS for SPME. However, extraction of CPA using SPME exhibited high variability. Mixed MA standards (100 nmol dm^{-3}) spiked with CPA (10 nmol dm^{-3}) were extracted (n=8) by SPME and the average RSD for CPA was 135% (Table 3.7). This high variability in the CPA peak area meant that the

calculated peak area ratio, used to account for any instrument variability, was more variable than the raw MA peak areas. For example, the TMA peak area RSD was 35.16% but the TMA peak area ratio (PAR) was 64.03%; practically doubling the variability.

Table 3.6: MA and CPA peak variability (n=8) for 10 nmol dm^{-3} mixed MA standard SPME extractions, peak areas and peak area ratios (PAR) from standards analysed by GC-NPD according to Figure 3.18

	TMA	DMA	MMA	CPA	TMA PAR	DMA PAR	MMA PAR
Average Peak Area	76.81	266.74	81.56	63.95	2.84	10.79	2.73
RSD (%)	35.16	52.19	35.08	135.47	64.03	84.14	66.43

In addition, the presence of CPA increased the variability of the MA peak areas (Table 3.8). For example, the TMA peak area RSD without CPA addition was 24.01%, but with CPA it was 61.57%.

Table 3.7: MA peak area variability for 10 nmol dm^{-3} mixed MA standard SPME extractions with and without internal standard (n=6) from standards analysed by GC-NPD according to Figure 3.18

Peak Area RSD	TMA (%)	DMA (%)	MMA (%)
With Internal Standard	61.57	57.18	60.01
No Internal Standard	24.01	30.02	27.42

This data indicated that CPA was affecting the adsorption and absorption of the MAs to the fibre, possibly by blocking adsorption sites or through displacement of

MAs from sites they already occupied. Since the CPA adversely affected the variability of the MAs, the MA extraction was optimised in the absence of CPA.

3.5.5 Optimisation of Extraction Time

Headspace SPME establishes two equilibria: one between the sample and the headspace, and one between the headspace and the fibre. To achieve consistent results, both equilibria needed to reach steady state before the extraction was completed. Until equilibrium is reached small changes in the extraction time can result in large changes in the amount of analyte absorbed. Once the equilibrium has been reached small changes in time will have a negligible effect on the amount of analyte absorbed (Figure 3.20).

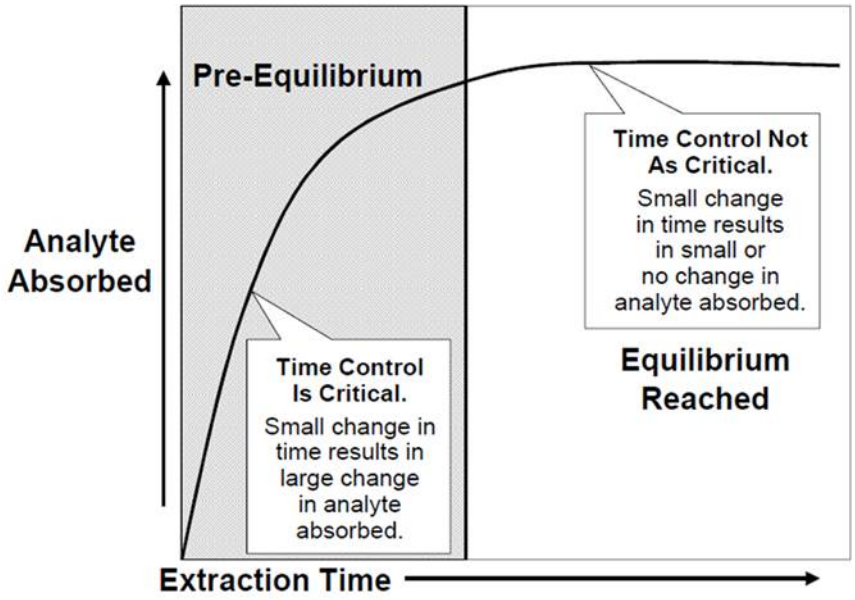

Figure 3.20: Diagram of pre-equilibria and equilibria processes of SPME extraction (taken from Sigma Aldrich)

Extraction profiles were carried out for the three MAs for time periods between 30 minutes and 12 hours (Figure 3.21). The TMA profile showed a plateau in

recovery between 2.5 and 6 hours and an increase at 12 hours, with a 12 hour extraction giving a significantly higher recovery (ANOVA: $F=17.16$ with $df=3$ and $p<0.001$). The DMA profile showed a significantly lower recovery at 30 minutes (ANOVA: $F=12.44$ with $df=3$ and $p<0.001$) and no significant difference between 2.5-12 hours. The MMA profile showed a steady increase in recovery with increasing time with 30 minutes giving a significantly lower recovery, and 12 hours giving a significantly higher recovery (ANOVA: $F=16.84$ with $df=3$ and $p<0.001$). There was no significant improvement in variability to 12 hours and since longer extraction times would limit productivity an extraction time of 2.5 hours was chosen.

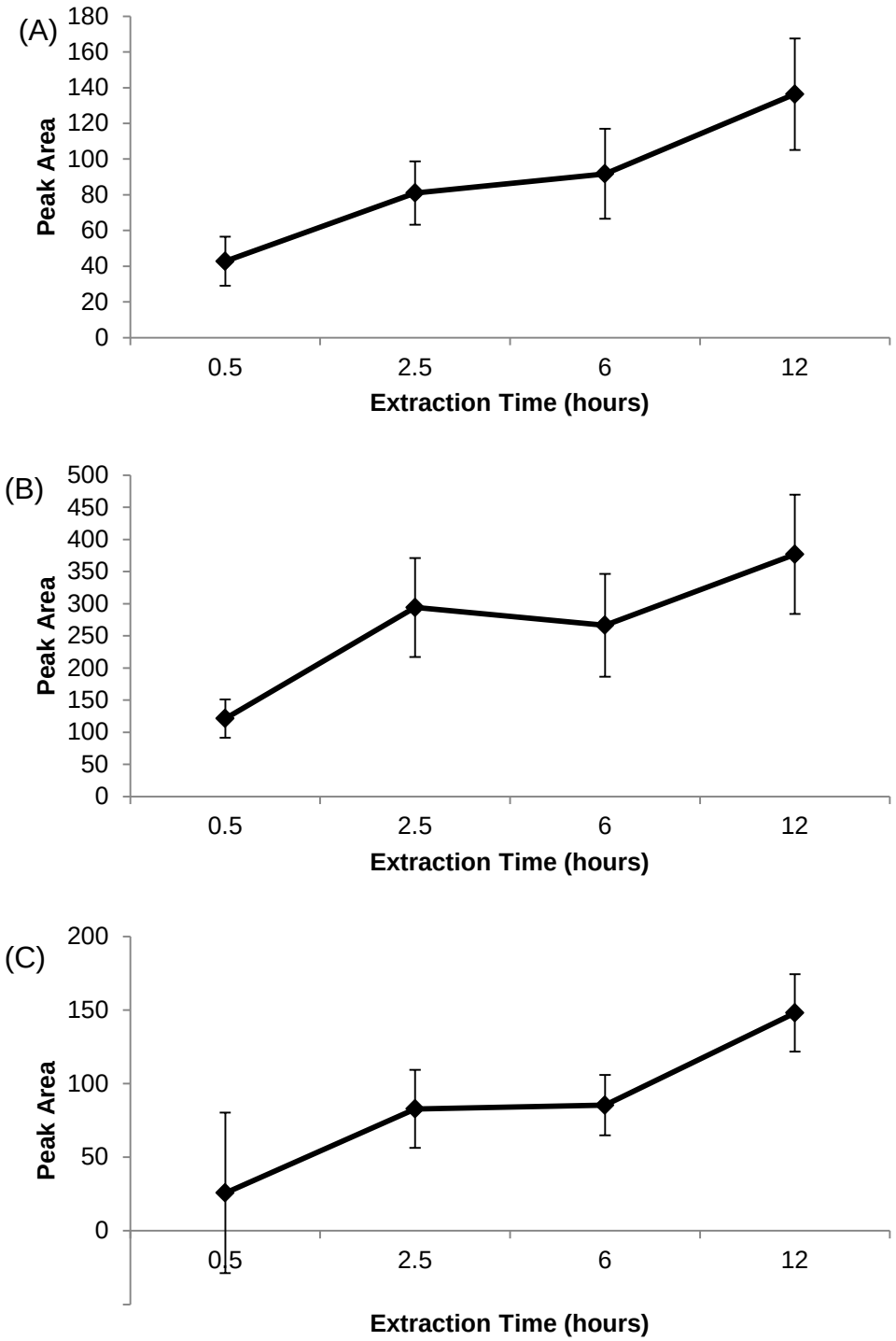

Figure 3.21: Equilibrium time profiles of 50 nmol dm^{-3} mixed MA standards of: (A) MMA, (B) DMA and (C) TMA, extracted from 1 L HPW heated to 60°C for 2.5 hours; error bars denote 1 standard deviation (n=6), standards analysed by GC-NPD according to Figure 3.18

3.5.6 Methods to Maintain an Isotherm in the Sample Solution

To this point the peak areas measured from fibre extracts had shown a high degree of variability with RSDs of 40-48%. One potential cause of this could have been a lack of homogeneity through the water column. One method to increase the homogeneity of the matrix was to add stirring. Stirring had previously been discounted as inconsistent stirring would be detrimental to the reproducibility. However, the use of a volumetric flask meant that a relatively long water column introduced the possibility of temperature and matrix gradients. The effect of stirring on reproducibility was investigated. Recovery was not increased but the variability was reduced (by more than half) for all three MAs (Table 3.9).

Table 3.8: Variability of MA peak areas in stirred and unstirred 50 nmol dm^{-3} mixed MA standards, extracted for 2.5 hours (n=6), standards analysed by GC-NPD according to Figure 3.18

50nmol dm-3, n=6	TMA		DMA		MMA	
	unstirred	stirred	unstirred	stirred	unstirred	stirred
Average Peak Area	94.44	96.26	247.99	242.8	80.84	69.12
RSD	48.37	14.29	40.68	16.66	43.80	18.86

3.5.7 Measurements of MA recoveries from seawater

To take into account matrix effects the quantification and calibration of the MAs had to be replicated using seawater. To compare recovery from HPW and from seawater, a calibration using HPW was carried out (Table 3.10 and Figure 3.22) and compared with a seawater calibration (Table 3.10 and Figure 3.23). Seawater was first pH modified with NaOH to pH 13.4 and purged with nitrogen gas for 1-6 hours before salt was added and the seawater was spiked with MAs.

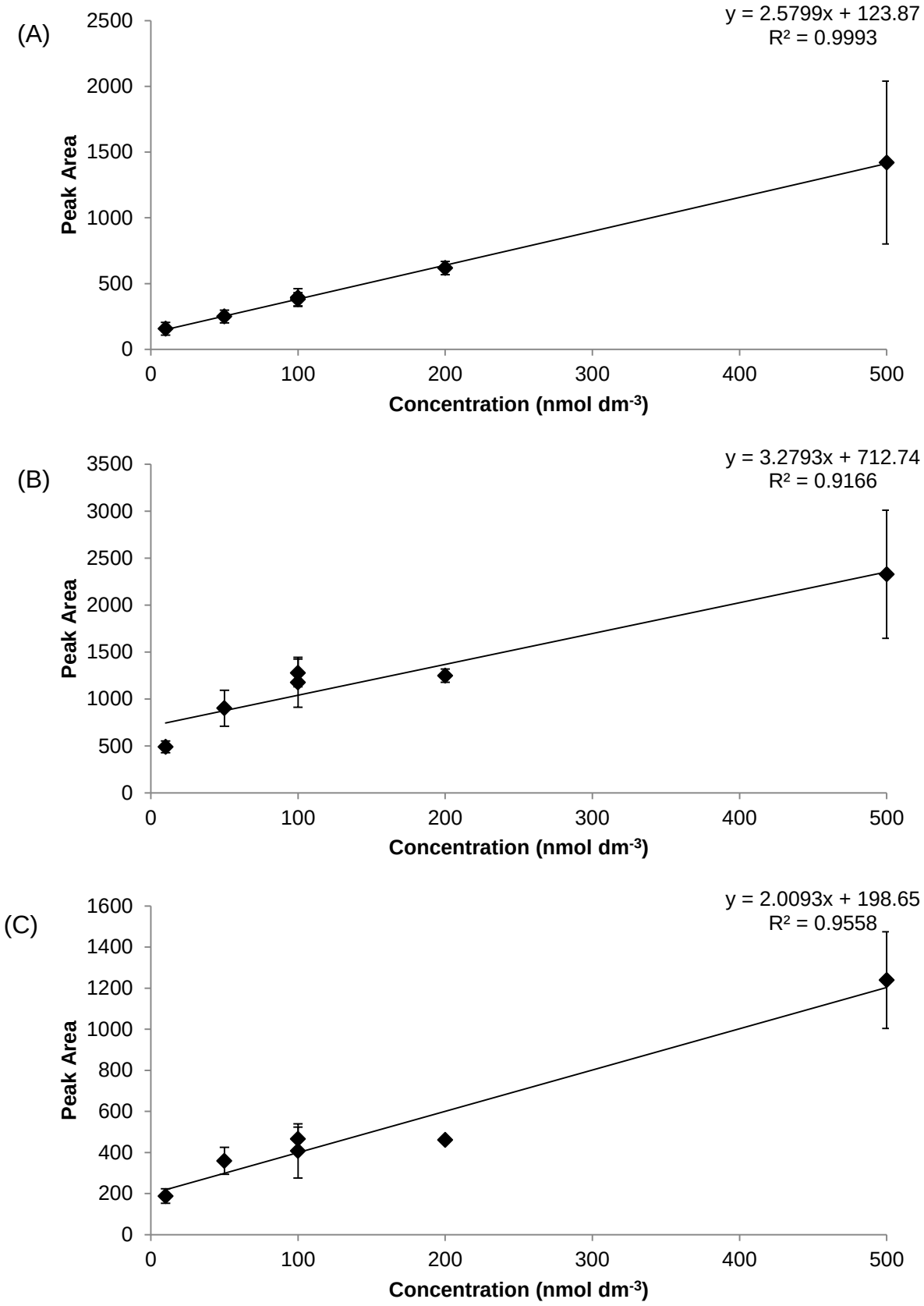

Figure 3.22: Calibration of mixed MA standards of: (A) MMA, (B) DMA and (C) TMA extracted from HPW heated to 60°Cfor 2.5 hours. Error bars denote 1 standard deviation (n=3). Standards analysed by GC-NPD according to Figure 3.18

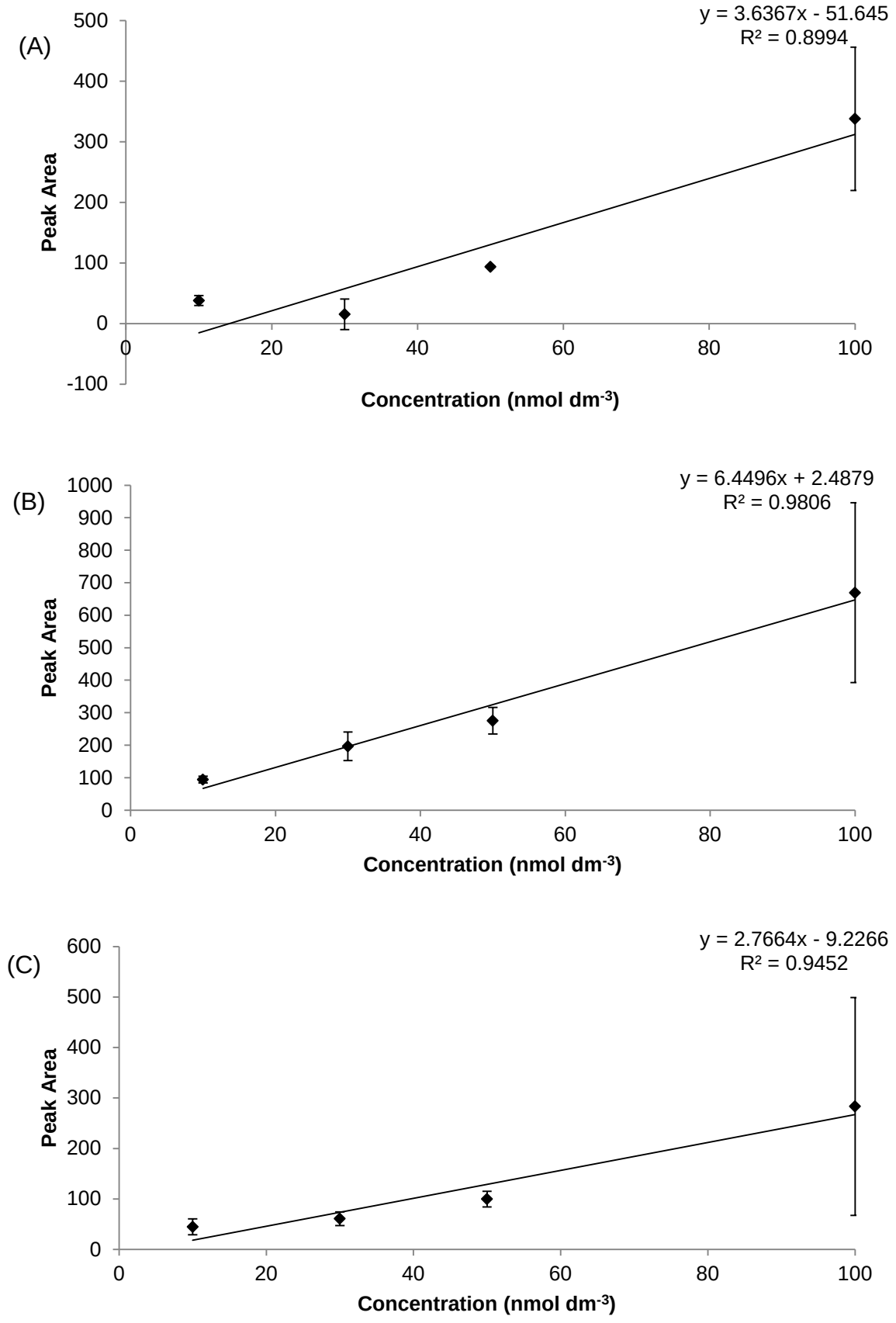

Figure 3.23: Calibration of mixed MA standards of: (A) MMA, (B) DMA and (C) TMA extracted from pre-purged seawater heated to 60°C for 2.5 hours. Error bars denote 1 standard deviation (n=3). Standards analysed by GC-NPD according to Figure 3.18

The chromatography of extracts from seawater was of a similar quality to those from HPW. The MMA peak was broad and frequently showed evidence of two peaks being present whilst the DMA and TMA were not baseline resolved (Figure 3.24).

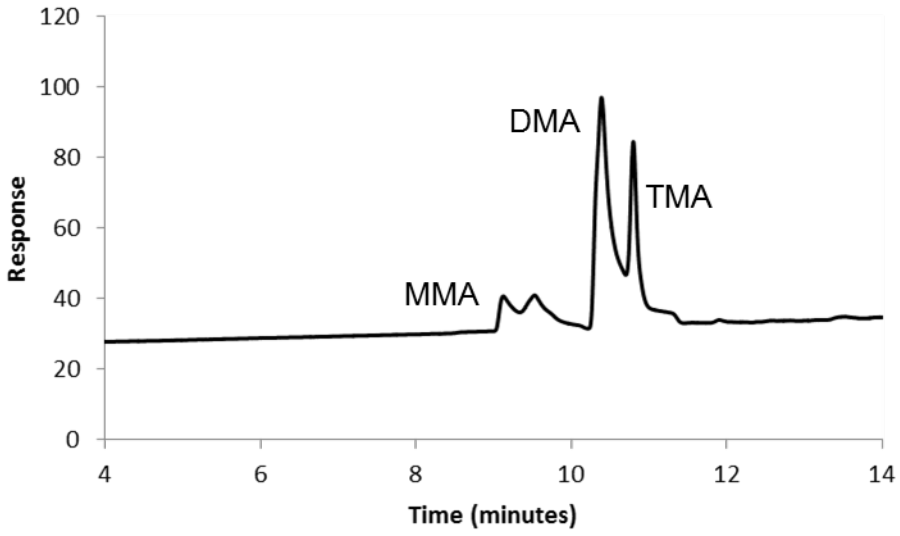

Figure 3.24: 50 nmol dm^{-3} mixed MA standard extracted using the PDMS-DVB fibre from pre-purged seawater for 2.5 hours at 60°C analysed by GC-NPD according to Figure 3.18

On closer inspection of the instrument blanks run before and after the standards and blank extractions from pre-purged seawater, no interfering peaks were seen close to the MMA peak. Both peaks were therefore attributed to MMA and were integrated together (Figure 3.24). Although it is possible to attribute the peak splitting to the attributed to the presence of both protonated and unprotonated MMA it was deemed and unlikely and it was thought more possible that the analyte was being both absorbed and adsorbed to the SPME fibre, leading to different ‘fractions’ on the column. Although baseline resolution was not achieved for DMA and TMA, sufficient resolution was achieved for consistent integration of the two peaks.

The peak areas were smaller in seawater extractions compared with HPW. As seawater is a more complex matrix than HPW, this may have affected the MAs' ability to cross the air-sea interface. Both sets of calibrations were linear but the calibrations using seawater were less reproducible (Table 3.10), potentially due to a matrix effect. The intercept of the calibrations were high which affected the calculated limit of quantification (LoQ).

Table 3.9: Peak area variability, expressed as RSD (%), of mixed MA standards in HPW and seawater, extracted for 2.5 hours (n=3) and analysed by GC-NPD according to Figure 3.18

Concentration (nmol dm^{-3})	TMA (HPW)	TMA (SW)	DMA (HPW)	DMA (SW)	MMA (HPW)	MMA (SW)
10	18.8	35.1	12.8	10.7	31.1	21.6
30		22.4		22.5		25.2
50	18.2	15.4	21.2	14.8	19.3	1.7
100	12.4	76.2	11.6	41.3	13.2	35.1
100	32.2		22.6		17.3	
200	2.4		5.7		8.1	
500	18.9		29.31		43.6	

The variability in peak areas observed was considerable (Table 3.10). One potential reason for this was variation in the physical conditions. For instance, the stirred water bath was made up of two parts: the water bath and the stirring hot plate. As the hot plate didn't automatically adjust to reach a set water temperature, the temperature settings had to be manually adjusted. This meant that any variability in the hot plate temperature might not be accounted for. A second potential variable was the stirring. The stirring had to be consistent. In addition, any variability in the 2.5 hour extraction period could have affected the precision of the results. A further issue that may have affected the variability was

foaming. The seawater samples foamed at the headspace interface. The extent of the foaming was inconsistent between samples and the consistency of the foam was changeable. The variable extent of the foaming meant that the headspace volume was inconsistent which might have contributed to the variability. The consistency of the foam may have affected the ability of the MAs to diffuse across the air-water interface so different foam consistencies could also have contributed to variability in the results. No method was found to improve the extent and consistency of the foaming.

3.5.8 Method Validation

To test the validity of a method a number of parameters must be considered, including specificity, precision, linear range and limits of detection (Ellison and Williams, 2012). Specificity describes the ability of a method to reliably quantify the analyte in the presence of interferences. The SPME-NPD approach gave very specific results for two reasons. Firstly, the SPME headspace sampling ensured that only volatile compounds were extracted. Secondly, the NPD detector detected only nitrogen-containing compounds. These two factors, combined with careful method development to identify the MA peaks, ensured that the peaks observed during analysis were those of the MAs. The linear range of an analytical method represents the range of concentrations over which the sensitivity of the detector is constant whilst the working range describes the concentrations over which samples can be expected to provide acceptable results. The linear and working range of the SPME-NPD method was 10-100 nmol dm^{-3} (Figure 3.23). The precision

describes the closeness of agreement between a series of measurements obtained from multiple sampling of the same homogeneous sample. The precision and particularly the repeatability of the results was assessed and evaluated with RSDs under 10% considered good and under 20% acceptable. The high variability in the peak areas had improved with experience and practice and the sources of variability were identified and reduced, where possible. The precision and LoD were investigated using a mixed MA standard calibration (1-10 nmol dm^{-3}; Table 3.11 and Figure 3.25 and 3.26). All three MAs gave good or acceptable RSDs apart from the lowest concentration MMA standard.

Table 3.10: Peak area variability (expressed as RSD) of mixed MA standard extractions from pre-purged seawater heated at 60°C for 2.5 hours (n=3) and analysed by GC-NPD according to Figure 3.18

Concentration (nmol dm-3)	MMA (%)	DMA (%)	TMA (%)
10	12.21	3.39	1.62
5	8.99	10.98	6.25
2.5	13.62	16.26	9.13
1	27.98	15.40	7.31

The limit of detection (LoD) describes the lowest concentration that can confidently be detected by the analytical method. There are a number of ways of calculating the LoD: 1) using the slope and standard deviation of the calibration; 2) an instrumental method which calculates the signal to noise ratio (S:N) with 3:1 considered the LoD (Ellison and Williams, 2012). The NPD detector provides very low noise levels (e.g. Figure 3.24), so an instrumental method was not considered appropriate. A non-

instrumental method was applied using the standard deviation and slope (Equation 7) to calculate the LoDs (Table 3.12).

$$LoD = \frac{3\sigma}{S}$$ Equation 7

Where σ = standard deviation of the lowest concentration calibration point and

S = slope of the calibration line of best fit

Table 3.11: MA limits of detection calculated from mixed MA standard calibration curves using Equation 7

	MMA	DMA	TMA
Calculated LoD (nmol dm^{-3})	0.43	2.50	0.37

The calculated LoDs were an improvement on those reported previously (Gibb et al., 1995) using flow injection extraction – ion chromatographic analysis, which were 3-5 nmol dm^{-3}.

Robustness, or ruggedness refers to how consistently a method performs when small changes in the environment or operating conditions occur (Ellison and Williams, 2012). The GC analysis was considered robust. GC analysis of the MAs using aqueous injection modified with NaOH gave consistent results with two CP Volamine columns, with a guard column added and with replacement NPD beads. Additionally, the quality of analysis was not significantly changed by different injection or heating programmes. GC analysis using thermal desorption from the SPME fibre gave poorer chromatography but the results obtained were consistent, with both replacement NPD beads and a new NPD not affecting the analysis. The SPME extraction was less robust and required the physical

conditions to be kept highly consistent to obtain acceptable precision. The heating temperature and extraction time were particularly important to achieving consistent results and even small changes or fluctuations had a relatively large impact on results. When the physical conditions were kept consistent the SPME-NPD analytical method gave reproducible results across the course of a week and, as such, showed acceptable levels of robustness.

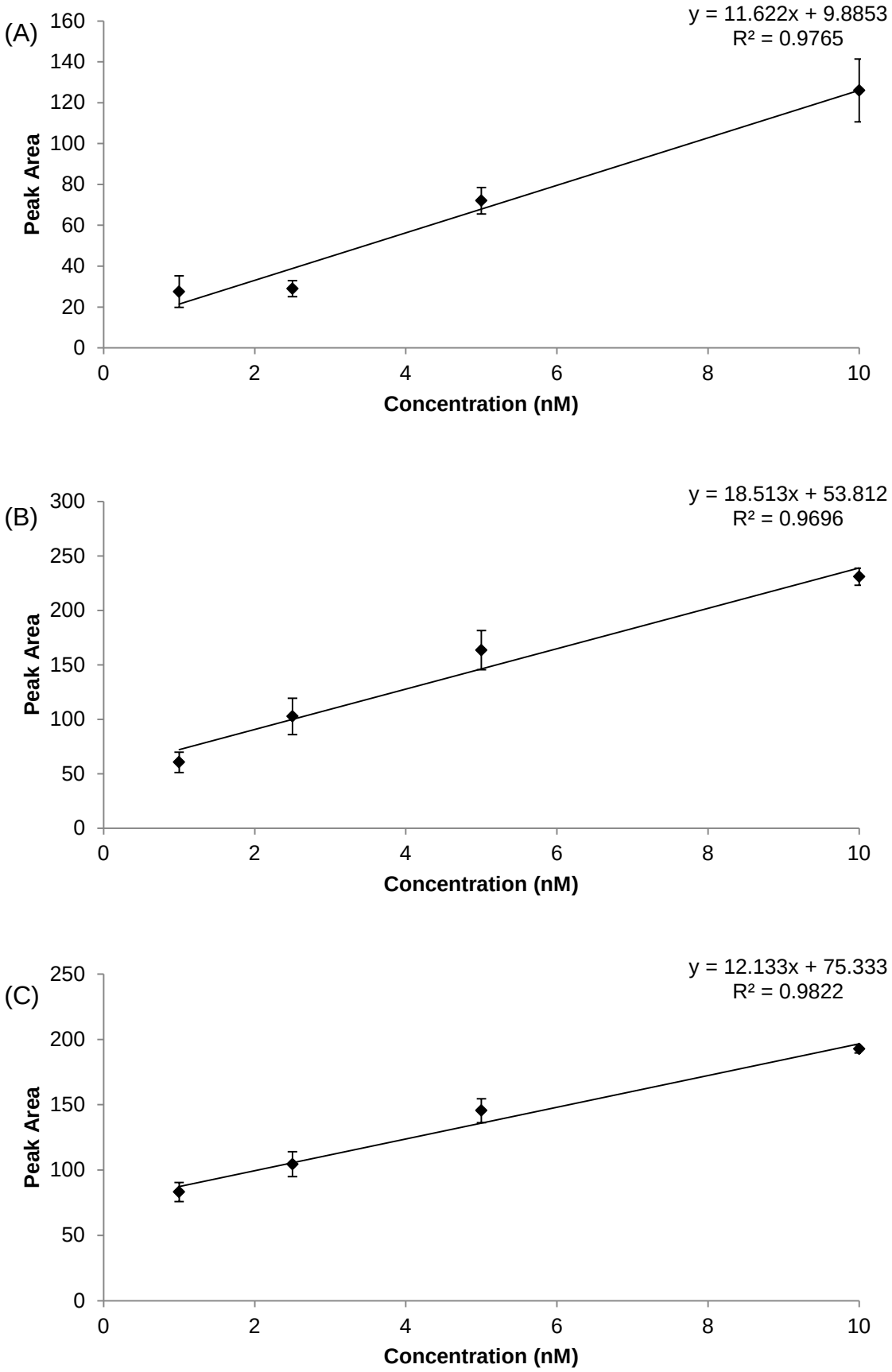

Figure 3.25: Calibration of: (A) MMA, (B) DMA and (C) TMA extracted using a PDMS-DVB fibre from pre-purged seawater for 2.5 hours, heated at 60°C and analysed by GC-NPD according to Figure 3.18. Error bars denote 1 standard deviation (n=3)

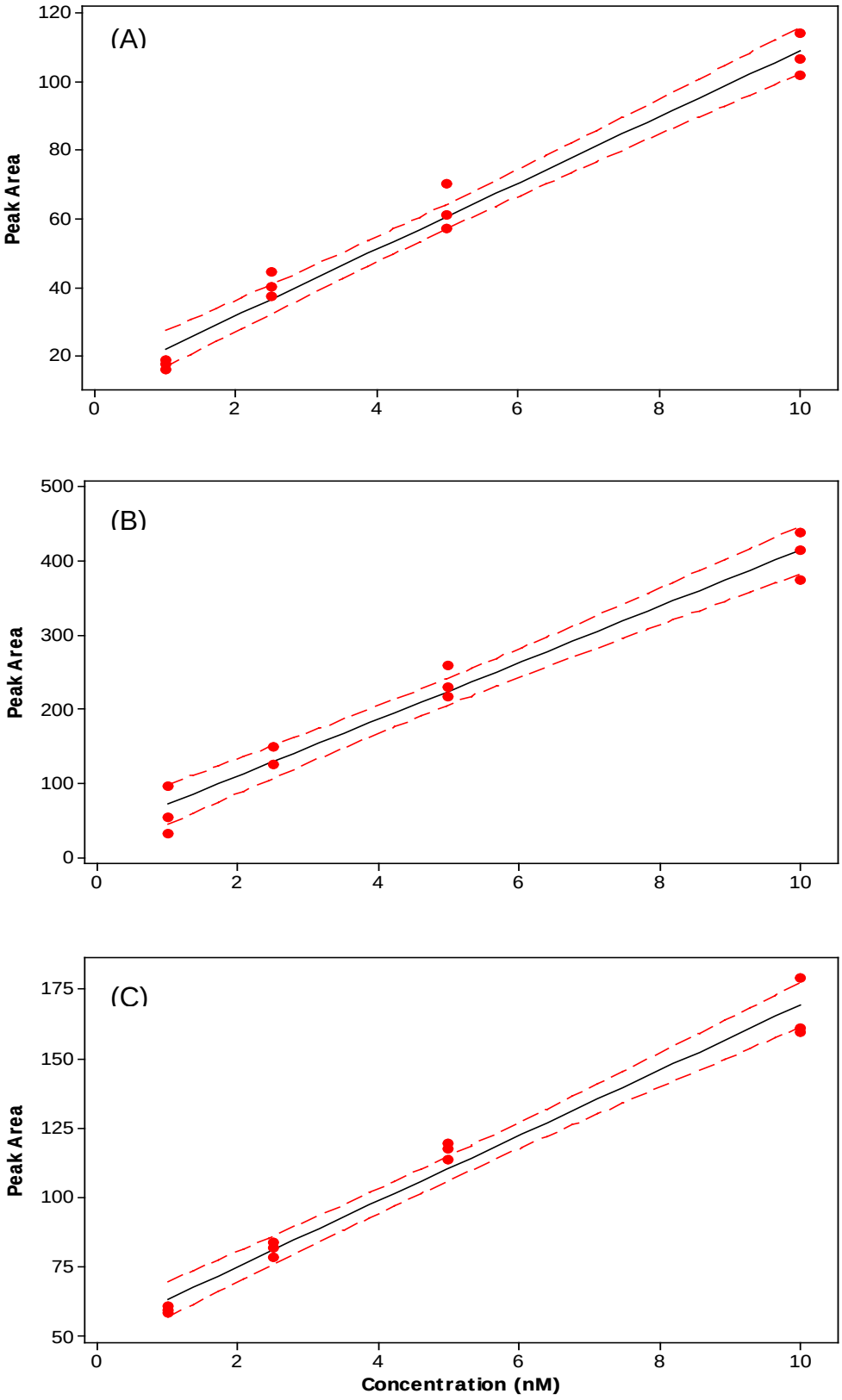

Figure 3.26: Calibration of: (A) MMA, (B) DMA and (C) TMA extracted using a PDMS-DVB fibre from pre-purged seawater for 2.5 hours, heated at 60°C and analysed by GC-NPD according to Figure 3.18. Red dashed line denotes 95% confidence interval

3.5.9 Application to Natural Samples

A sampling procedure was developed to allow the application of the SPME method to the analysis of MAs in seawater. The MAs are volatile compounds and, as such, any sampling method needed to minimise loss of the MAs across the water-air interface, as well as preventing microbial uptake and production of the MAs in the sampled seawater. Once the water had been sampled, it had to be stored until analysis so the method of storage also had to minimise any MA loss or degradation. Water was collected by CTD from station L4 (50°15'N, 04°13'W, Western Channel Observatory, http://www.westernchannelobservatory.org.uk/) using HDPE plastic bottles filled to overflowing and stored in the dark until processing (2-4 hours). Samples were then gravity filtered in 1 L volumes using GF/Fs (nominal pore size 0.7 µm) to remove any particulate matter and minimise the number of microbes present and stored in HDPE plastic bottles filled to overflowing. The samples were then either immediately frozen or acidified to pH 1 using hydrochloric acid and stored at 4°C. Acidification converted the MAs into their non-volatile protonated form, which cannot cross the air-water interface and killed any microbial activity. Frozen samples were defrosted overnight in sealed containers and transferred to the volumetric flask where the NaOH solution was added and the flask sealed with a Suba-seal before the sample was mixed (Figure 3.19).

A selection of seawater samples from a seasonal campaign (October 2012-October 2013) at station L4 were analysed. Given the time needed for method development, sampling was begun in parallel. Seven weeks' worth of stored samples (samples were not acidified and were stored

frozen at -20°C, n=3) taken between April and May 2013 during the spring bloom were chosen for analysis, to maximise the probability of finding the highest MA concentrations. However, while the samples appeared to contain MAs, the concentrations were too low to be quantified.

As the samples from 2013 had been stored for a minimum of three months, the method was subsequently applied to freshly-collected samples. These samples were collected at station L4 during April 2014. Four samples were collected using HDPE bottles and filtered immediately (gravity filtration though GF/Fs) after sampling. Two of these samples were kept chilled in HDPE bottles filled to overflowing and analysed on the same day. The second two samples were acidified with hydrochloric acid (pH 1) immediately after filtration, and stored in HDPE bottles, filled to overflowing at 4°C for analysis the following day. When analysed, the two samples that had not been acidified contained unquantifiable levels of all three MAs. One of the two acidified samples showed quantifiable concentrations of the three MAs. However, an instrumental fault meant the data were lost before the chromatographic peaks could be quantified. The second acidified sample was analysed and concentrations of 6, 3 and 20 nmol dm^{-3} were observed for MMA, DMA and TMA respectively (Figure 3.27).

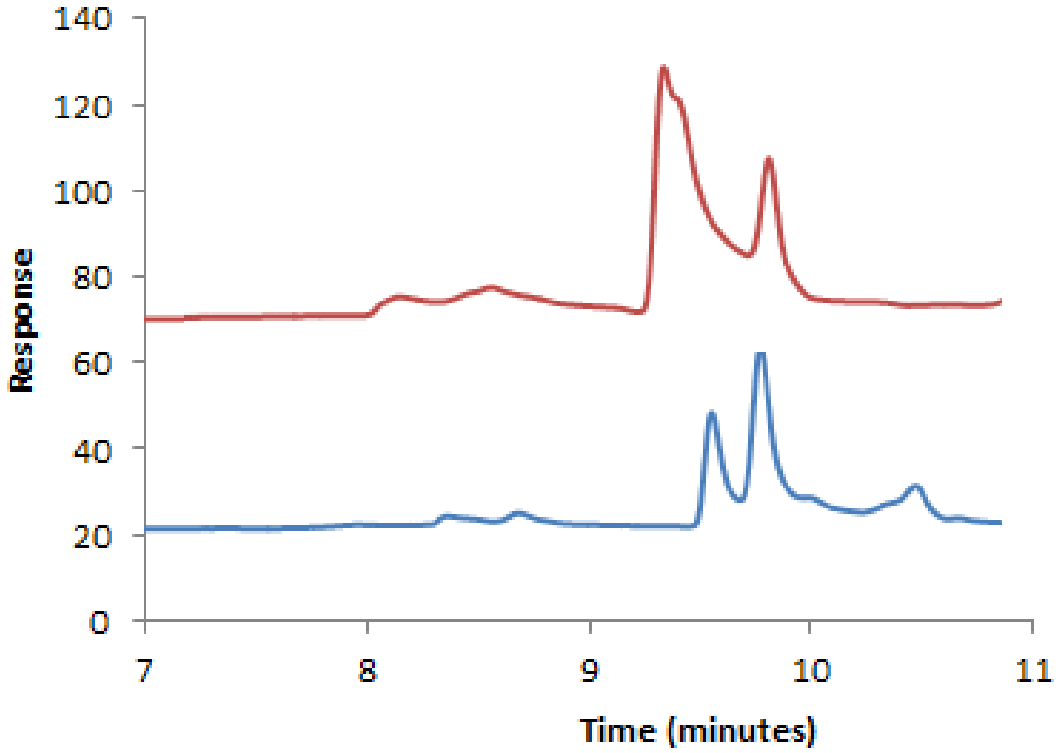

Figure 3.27: Chromatogram of natural sample (blue) taken from the WEC and a 10 nM standard extraction (red), extracted using SPME (PDMS-DVB fibre exposed to the headspace of the sample heated to 60°C for 2.5 hours) and analysed by GC-NPD according to Figure 3.18.

The observed MA concentrations are similar to previous concentrations measured in coastal waters of the UK, Mediterranean and Arabian Sea (Gibb et al., 1995; Gibb et al., 1999b) (Table 3.13).

Table 3.12: Measured concentrations of MA in coastal waters

Coastal Site	MMA (nmol dm^{-3})	DMA (nmol dm^{-3})	TMA (nmol dm^{-3})	Reference
Plymouth Sound	4-23	13-22	0-13	(Gibb et al., 1995)
Mediterranean (Coastal)	4-38	3-15	4-22	(Gibb et al., 1995)
Arabian Sea	6-22	2.9-4.2	0.05-0.81	(Gibb et al., 1999b)
Station L4	3	6	20	This study

The sampling week was chosen due to a substantial bloom event beginning in the previous two weeks. Based on the GBT seasonal study from the previous year, (Chapter 5) the particulate GBT levels took 2-3 weeks to reach their maximum level from the start of the bloom. As GBT is a primary precursor of the MAs the sample week chosen aimed to maximise the probability of finding the highest MA concentrations. Unfortunately the bloom was brief and had declined before sampling occurred. With reduced phytoplankton biomass the MA concentrations would be expected to be lower, which may explain the reduced MA concentration compared to those reported in Gibb (1994).

The MA concentrations in the samples collected during April 2014 were compared with the concentrations measured in the samples collected in 2013. The similarity between the 2013 sample concentrations and the non-acidified samples from 2014 indicated that long term storage was not the primary cause of the low MA concentrations observed in 2013. The non-acidified samples from 2014 were kept chilled in bottles with no headspace and the first sample analysed within two hours of sampling. This reduced the chance for the MAs to cross the air-water interface. The acidified samples were acidified immediately after filtration at the same time as the non-acidified samples were sealed in bottles. This indicated that it is not loss of the MAs into the air that caused the reduced concentration in non-acidified samples compared to acidified samples. Acidification would have killed any microbes not removed by filtration. Filtration was carried out with glass fibre filters (GF/Fs) that have a

nominal pore size of 0.7 µm. 47% of bacterial cells in natural seawater were reported to pass through Whatman GF/F filters (Lee and Fuhrman, 1987). This indicated that microbial turnover of the MAs by bacteria was probably responsible for the reduced MA concentrations in the non-acidified samples. The use of filters with smaller pore sizes than the GF/Fs was contemplated but, based on the filtration artefacts reported in Chapter 4, where large filter volumes were thought to cause cell damage and loss of particulate GBT into the dissolved phase, this option was rejected. Filtering 1 L of water through filters with smaller pore sizes would have subjected the collected particulate matter to even higher pressure. Damaging cells on the filter may have introduced more MAs to the dissolved phase and resulted in over estimates of the dissolved MA concentrations.

3.5.10 Optimised Procedure

Sample Collection

A seawater sample of 1 L volume (n = 3) was collected by CTD (instrument used to measure water column characteristics, as a minimum measuring: Conductivity, Temperature and Depth) then decanted into high density polypropylene (HDPE) bottles and filtered immediately using glass fibre filters (GF/F, nominal pore size 0.7 µm). The filtrate was acidified to pH 1 using concentrated hydrochloric acid (10 mL). Samples were then stored at 4°C prior to analysis.

Sample Pre-concentration by SPME

Samples (850 mL) were transferred to a 1 L volumetric flask and saturated with sodium chloride (approximately 330 g) to maintain a constant ionic strength between samples. Samples were then adjusted to pH 13.4 with sodium hydroxide solution (10 M) and the volumetric flask immediately closed with a Suba-seal. The flask was then placed in a water bath, the SPME needle inserted and the fibre exposed to the headspace.

The flask was heated to 60°C for 2.5 hours before the SPME fibre was retracted within the needle and removed from the flask.

GC Analysis

The SPME needle was inserted into the GC injector containing a narrow SPME liner. The fibre was exposed and the analytes thermally desorbed at 270°C for 5 minutes. The oven was heated from an initial temperature of 50°C (2 minute hold) to 180°C at a rate of 10°C/minute to separate the MAs, which eluted from 8-12 minutes. Finally, the column was heated to 260°C at a rate of 15°C/minute then

held at this temperature for 5 minutes to elute any residual components from the column.

Quantification

Samples were quantified using an external calibration, in accordance with manufacturer guidance. The calibration curve was prepared using GF/F filtered seawater. The filtered seawater was adjusted to pH 13.4 using NaOH solution (10 M) and purged with nitrogen gas for 3-5 hours. Mixed MA standards were spiked into the purged seawater (850 mL, final concentrations 1-10 nM) and extracted using the procedure detailed for natural samples. Replicate concentrations (n = 3) were performed at each concentration and a calibration curve plotted.

Limits of detection were calculated from calibration curves and are as follows: MMA = 0.4 – 2.2 nM, DMA = 1.6-2.5 nM and TMA = 0.4-2.7 nM. The variation between calibration sets indicates that LoDs should be a routine operational measurement in addition to calibration, particularly if analyte concentrations are expected to be close to the LoD.

3.6 Discussion and Conclusions

A method was developed to analyse the MAs in seawater. This method incorporated a SPME pre-concentration step in conjunction with GC-NPD analysis and separation using a volatile amine-specific GC column: CP Volamine (Agilent). The use of CP Volamine stationary phase allowed successful separation of the three MAs and, even though DMA and TMA were not fully resolved, robust quantification was consistently achieved. Headspace SPME extraction successfully pre-concentrated the MAs to allow analysis at environmentally-relevant concentrations. Calculated detection limits were 0.43 nmol dm^{-3}, 2.50 nmol dm^{-3} and 0.37 nmol dm^{-3} for MMA, DMA and TMA, respectively. These values represent an improvement on the previous reported LoDs of 3-5 nmol dm^{-3} (Gibb et al., 1995), by a method which, in any case utilised custom-built equipment that is not readily available.

There are a number of areas that need further work and investigation. Firstly, the method does not currently utilise an internal standard. The IS tested (CPA) proved incompatible with the SPME pre-concentration method causing high degrees of variability. CPA was successfully used to demonstrate amine recovery from seawater samples, and the SPME-GC method showed good reproducibility and robust calibrations. This indicated that the instrument response, using thermal desorption, was relatively stable. With the demonstrated reproducibility and stable instrument response accurate, consistent quantification of the MAs in seawater can be carried out in the absence of an IS. However, to

account for any routine variation in the response of the chromatographic system, another IS could be used. A new IS would need to be similar to the MAs in structure and behaviour, particularly its volatility, but not be present in natural samples; the choice is limited.

The sorption mechanisms controlling interaction of the MAs with the fibre are not yet fully understood. For instance, the effect of CPA on MA reproducibility implies that there was some form of interaction occurring. Similarly, the larger peak areas observed for DMA than for TMA indicated some form of preferential adsorption or displacement. However, the calibrations were reproducible. This indicated that any preferential adsorption occurring was consistent and would not affect the ability of the method to accurately quantify the MAs. Calibrations carried out using single MA standards, as opposed to mixed MA standards, could identify whether DMA is affecting the behaviour and results of TMA and MMA.

Another aspect of this technique that could be improved was the physical set up of the SPME extractions. The use of a water bath to regulate the temperature and stir the heated sample would possibly make controlling the temperature a lot more consistent and accurate. Each simultaneous extraction required a separate water bath. When tested, simultaneous extractions with different water baths did not give consistent results; however, using different fibres and the same bath did. This indicated that different water baths, giving slightly different heating regimes, could significantly change the results achieved. A specially designed sample

vessel could also potentially improve the MA recoveries. The volumetric flask used allowed consistent results but created a long water column, a significant section of which was narrower than the base. Although this allows the headspace to be minimised, it also limits mixing up the water column. A sample vessel that doesn't create a long and narrow column, which would simultaneously minimise the headspace volume, could allow the MAs crossing the water-air interface to be maximised. This could potentially be achieved by coupling dynamic headspace sampling with SPME extraction, creating an equilibrium between the sample and the headspace and then sweeping an inert gas through the headspace to an SPME fibre. Using this approach, the initial headspace wouldn't have to be limited and so the surface of the water could be increased to maximise water to air transfer of the MAs. Another advantage of this is that, by sweeping the headspace with an inert gas, the initial equilibrium would be constantly shifted to allow continual MA transfer into the headspace and increased MA recovery. This method would need to be carefully controlled so that the speed of the gas flow and the volume used were consistent between each extraction. SPME extraction is fundamentally a two-step process: sorption of the analytes to the fibre followed by desorption of the analytes onto the GC (or HPLC). The work carried out to date has focused on sorption of the analytes to the fibre. Desorption of the analytes could also be optimised. For example, the depth, time and temperature of the GC inlet during desorption should be investigated. Optimisation of these parameters is unlikely to significantly affect reproducibility but may improve the limits of detection achieved.

Finally, the analyte recovery could be measured. Analyses were performed using spiked standards which permitted quantification without measuring recoveries. However as SPME is an equilibrium extraction method, recovery is not viewed as critical, and is also difficult to achieve using an identical sample matrix. Measuring sample recovery would require a direct aqueous injection of a standard to gauge the recovery of the analytes using headspace SPME.

This work represents a significant step forward in the use of GC for the analysis of the MAs. The method described herein is more accessible than the IC method reported by Gibb et al. (1995) and improves on the LoDs achieved by microdiffusion-GC (Abdul Rashid et al., 1991). The SPME-GC method makes the analysis of MAs in seawater samples more readily achievable and will allow better understanding of the concentrations and cycling of MAs in marine systems.

Chapter 4

Optimisation of sampling and analysis methods for the measurement of glycine betaine in seawater particulates

Chapter Outline

This chapter outlines the development of a new sampling protocol that employs small volume filtration to reduce cell damage and loss of particulate glycine betaine to the dissolved phase. It then describes ion suppression and its impact on the quantification of glycine betaine by LC-MS. A modified approach is outlined including a mobile phase with a higher aqueous content, used to minimise the impact of the suppression on the quantification of glycine betaine.

4.1 Introduction

Glycine betaine (GBT) is a widely used and highly effective osmolyte in marine organisms. Understanding of the significance of GBT in marine systems is limited due to the difficulties involved in its analysis, including its polar nature and low standing concentrations (nanomolar levels). Consequently, published measurements of particulate GBT (GBT_p) in the environment are scarce.

The first GBT measurements in terrestrial plant material were made using thin layer chromatography (Dickson and Kirst, 1986; Storey and Jones, 1977). Subsequently, an HPLC method for the separation of betaines in plants was developed (Gorham, 1984) using cation exchange chromatography with UV detection at 195 nm. In this study, a range of nitrogen containing osmolytes were separated from plant sap using extraction with either hot methanol or methanol: chloroform: water (12:5:1). The method developed by Gorham (1984) was applied to algal cultures and marine particulate samples (Keller et al., 1999b; 1999a; 2004). This method of analysis, based on UV detection, was limited in two ways. Firstly, seawater and culture extractions contained a number of components that absorbed in the near UV, causing complex chromatograms with peaks that were difficult to distinguish (Airs and Archer, 2010). Secondly, UV detection at 195 nm precludes the use of many organic solvents that absorb in this region. The sensitivity of this method was limited (limit of detection (LoD) of 47 ng on column) and consequently, in order to collect enough particulate matter to achieve an adequate GBT signal, large volumes of seawater (2-4 L) were required.

A liquid chromatography mass spectrometry (LC-MS) approach with electrospray ionisation (ESI) was subsequently applied to GBT analysis (Airs and Archer, 2010). As small, polar molecules that carry a charge, quaternary ammonium compounds, such as GBT, are ideally suited to analysis using ESI. MS analysis had a number of advantages over UV detection. Firstly, the use of a combination of retention time and mass to charge ratio for quantification allowed more selective analysis. Secondly, MS detection permitted the use of more diverse mobile and stationary phases that enabled a different chromatographic approach for the nitrogen-osmolytes. Finally, simultaneous detection of an internal standard, considered essential for reliable quantification using ESI-MS, was permitted. An octadecasilyl (ODS) phase, not fully endcapped (ODS1), was employed for separation (Airs and Archer, 2010). The quaternary amine cation, present in GBT, interacted with the exposed silanol groups, in a similar mechanism to cation exchange chromatography (Evans et al., 2000). Notably, the ODS1 phase permitted separation based on hydrophobicity, an approach used for the structurally similar quaternary ammonium pesticide Chlormequat (Evans et al., 2000). Extraction in methanol: chloroform: water (12:5:1) was employed to allow analysis of culture and marine particulate samples and an improved LoD of 5.3 pg on column was achieved. This represented an improvement in the LoD of approximately four orders of magnitude compared to the method developed by Gorham (1984). With the enhanced LoD an adequate GBT signal could be achieved from particulates collected from smaller sample volumes.

GBT_p levels in culture samples have been analysed using two alternative LC-MS methods. In the first, GBT in particulate extracts was derivatised using 1-

pyrenyldiazomethane to form an ester that could be analysed using reverse phase LC columns (Spielmeyer et al., 2011). This method achieved an LoD of 700 pg on column. The second method described a direct LC-MS approach for DMSP analysis (Spielmeyer and Pohnert, 2010) that was subsequently applied to GBT_p in cell cultures (Spielmeyer and Pohnert, 2012). Hydrophilic interaction liquid chromatography mass spectrometry (HILIC) was applied to particulate extracts and GBT was analysed; however, the linear range of GBT concentrations and LoD were not reported.

In addition to marine particulates, GBT has been analysed in blood plasma, tissue samples and cereals (Holm et al., 2003; Koc et al., 2002). Analysis of choline and its metabolites, including GBT, in tissue samples and cereals was performed by extraction in chloroform and methanol followed by analysis with liquid chromatography-isotope dilution mass spectrometry (Koc et al., 2002) and achieved an LoD of 117 pg on column. The approach used to analyse GBT in blood plasma 'deproteinised' the samples using an acetonitrile extraction followed by separation on a normal phase silica column and analysis using positive ion mass spectrometry (Holm et al., 2003). This approach achieved a linear range between 0.4-400 µM and an LoD of 70 pg on column.

A summary of approaches from previously published methods is detailed in Table 4.1.

Table 4.1: Summary of instrument, sampling, extraction and processing variables for GBT analysis methods modified from Airs and Archer (2010)

Reference	Instrument; detection method; chromatography column	Sample Quantity (sample type)	Extraction Volume (mL)	Additional Sample Processing	Injection Volume (µL)	LoD on column (ng); molarity of solution injected (µmol dm^{-3})	LoD in filtered seawater (nmol dm^{-3})
Airs and Archer (2010)	LC-MS (ion trap); scanning mode; silica (ODS1)	0.15 L (coastal water)	3.0	none	1	0.0053 (0.045)	0.14
Keller et al. (1999b); Keller et al. (2004)	HPLC; UV detection; cation exchange (SCX)	1.00 L (coastal water)	Not stated	Extract evaporate to dryness; re-dissolved in 0.5 mL	100	47 (4.0)	2.00
		0.05 L (cultures)	Not stated			59 (5.0)	2.50
Holm et al. (2003)	LC-MS (triple quadrupole); multireaction-monitoring mode; silica (Hypersil)	30 µL (blood plasma)	n/a	Mixed with acetonitrile, centrifuged	2	0.070 (0.30)	n/a
Koc et al. (2002)	LC-IDMS (liquid chromatography-isotope dilution mass spectrometry)	100 mg (blood plasma or tissue)	400 µL	Extraction in methanol and chloroform followed by centrifugation	10	117	n/a
Spielmeyer and Pohnert (2010); (2012)	UPLC-MS with BEH HILIC column	30-55 mL (culture)	1 mL	100 µL cell extract diluted with acetonitrile/water	1-5 µL	not available	not available
Spielmeyer et al. (2011)	UPLC-MS (Q-ToF); scanning mode; phenyl	0.06-0.7 (cultures)	2.0	Derivatisation with 1-pyrenyldiazomethane	1-7	0.7 (0.2)	n/a

In marine particulate samples, the variability of GBT_p concentrations was higher in extracts collected using vacuum filtration than in samples collected using gravity filtration, due to cell damage during vacuum filtration causing loss into the dissolved phase (Airs and Archer, 2010). Similarly, the filtration method employed was critical for measurements of DMSP (Kiene and Slezak, 2006), particularly for measurements of the dissolved phase. GBT and dimethylsulphoniopropionate (DMSP) play similar intracellular roles within the cell and are expected to be subjected to similar forces during filtration. For analysis of DMSP in the dissolved phase ($DMSP_d$), Kiene and Slezak (2006) demonstrated that the volume of water filtered was a critical factor affecting loss of DMSP from the particulate into the dissolved fraction. Small volume (3.5 mL) gravity drip filtration was recommended to avoid overestimation of $DMSP_d$ concentrations. The effect of filtration as a sampling method on GBT_p remains uncertain. The analytical improvements afforded by the application of LC-MS to measurement of GBT, and the associated improvements in detection limit compared to HPLC (Airs and Archer, 2010), permitted the effect of filtration volume to be investigated as part of the current study.

4.1.1 Aims and Objectives

Aim: To obtain and analyse a representative GBT concentration from marine particulate samples

Objectives:

- To optimise a sampling protocol to obtain representative particulate samples
- To optimise the analytical method for GBT_p analysis

4.2 Effect of filtration volume on observed concentrations of GBT from particulate samples

Seawater from station L4 (50°15'N, 04°13'W, Western Channel Observatory, http://www.westernchannelobservatory.org.uk/) was used as a source of particulates to investigate the effect of filtration method and volume on measured GBT_p concentrations. Water was collected by CTD and decanted into HDPE bottles and stored in the dark until sample processing (approximately 2-4 hours). Gravity filtration using glass fibre filters (GF/F, nominal pore size 0.7 µm) was compared with both low (5-10 mm Hg) and high (30 mm Hg) vacuum filtration (Figure 4.1) using different volumes of seawater. Following filtration, filter papers were flash frozen in liquid nitrogen and stored at -80°C until analysis. Filter papers were then solvent extracted (3 mL, methanol: chloroform: HPW) overnight and clarified using centrifugation and 1 µL injected for analysis by LC-MS according to Airs and Archer (2010) (detailed in Chapter 7).

The effect of filtration method (gravity, low vacuum and high vacuum) on observed GBT_p concentrations was not significant. However, gravity filtration gave lower overall variability for replicate samples (n=3) analysed over the three filtration volumes. For example, an average relative standard deviation (RSD) of 20% was observed in samples collected using gravity filtration compared with 42% for samples collected using high vacuum. This reduced variability is in agreement with the initial observation of improved variability in gravity filtration compared with vacuum filtration reported (Airs and Archer, 2010).

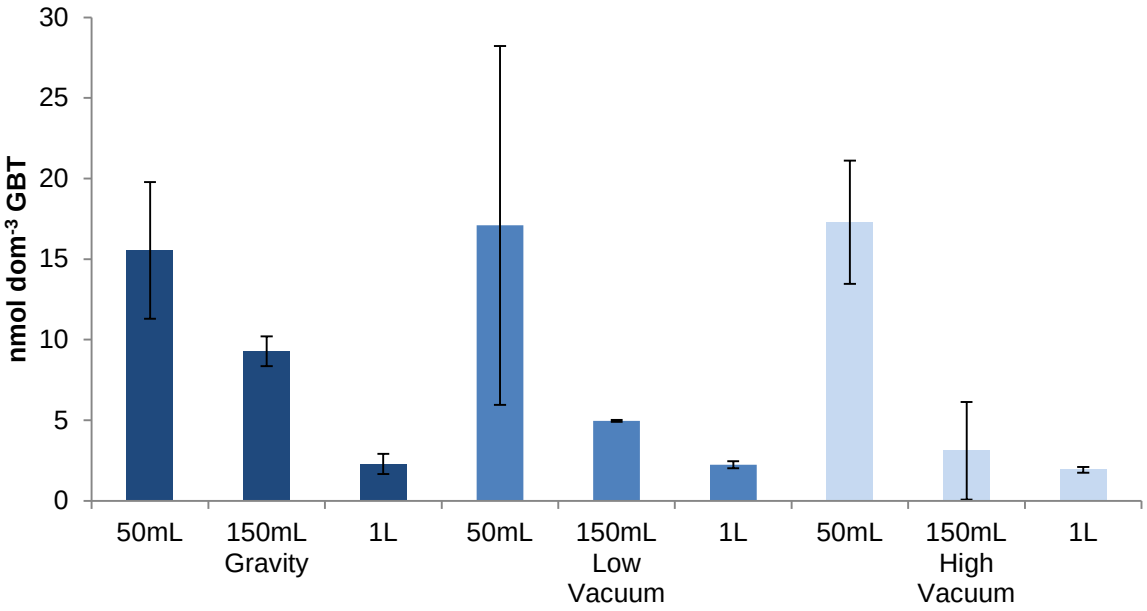

Figure 4.1: Effect of filtration method and sample volume on observed GBTp concentrations in seawater particulates collected from the Western English Channel. Error bars denote ±1 SD (n=3). Filters were solvent extracted (3 mL, methanol: HPW: chloroform) and clarified by centrifugation and 1 µL injected for analysis by LC-MS (Spherisorb ODS1 column, eluent run isocratically at 1 mL min^{-1}. Mobile phase: acetonitrile: methanol: HPW: acetic acid (53: 21: 25: 1) with a final concentration of ammonium acetate of 50 mM, according to Airs and Archer (2010)).

The effect of filtration method on sample analysis was studied in primary production using ^{14}C labelled bicarbonate uptake experiments (Arthur and Rigler, 1967) and in studies of phosphorus uptake (Kuenzler and Ketchum, 1962). A 2% release of dissolved organic carbon (DOC) from cells into the filtrate was observed (Arthur and Rigler, 1967) using gravity filtration compared with a release of up to 36% from vacuum filtered samples. Uptake studies examining the distribution of ^{32}P between the cells and filtrate showed increasing levels of ^{32}P in the filtrate as vacuum pressures were increased (Kuenzler and Ketchum, 1962). This indicated that physical damage to the cells was causing loss into the filtrate. These findings support the hypothesis that the high degree of variability in samples collected by vacuum filtration, reported by Airs and Archer (2010), could be explained by damage to the phytoplankton cells.

The three filtration methods tested showed a significant decrease in observed GBT_p concentrations with increasing filter volume (ANOVA: $F= 7.34$ with $df = 8$ and $p < 0.001$). The 50 mL filtered samples had significantly higher concentrations of GBT_p than 150 mL and 1 L samples. The decrease in GBT_p concentration with increasing filter volume could be attributed to loss to solution through cell damage or breakage, as a result of the large volumes of water passing through the filter. It has been demonstrated that cell resilience is variable between different phytoplankton species (Goldman and Dennett, 1985), with less resilient cells more likely to lose GBT_p to the dissolved phase. In addition, the location of GBT in the cell has not been established, and fractions of varying lability may exist within a cell. If so, then cell damage could have caused loss of more labile GBT fractions to the filtrate. The GBT_p concentrations in the higher volume sample could therefore have represented the GBT present in less labile cells, or less labile pools of GBT_p within the cell, while the samples collected using smaller volumes represented both the labile and less labile GBT_p concentrations.

The length of time cells spend on the filter paper during filtration may also cause loss of GBT. Large filter volumes generally take longer to filter and consequently the cells captured on the filter paper will be subjected to the stress of filtration for longer. The filtration time may therefore have influenced GBT_p concentrations.

Considering the filtration effects on DMSP concentrations observed by Kiene and Slezak (2006) at a range of sample volumes, the effect of filter volume GBT_p concentrations was further investigated using a range of volumes below 100 mL.

Seawater was collected by CTD from station L4 on three separate occasions and particulates were collected using filtration volumes of 10-90 mL. Particulates were collected by gravity filtration using GF/F filters, flash frozen in liquid nitrogen and stored at -80°C until analysis.

A marked increase in the concentration of GBT_p as volume decreased was observed in the three sample sets, specifically 10-30 mL and 20-40 mL (Figure 4.2). Due to the large variability in GBT_p concentrations observed for 10 mL samples from the February 2012 sampling event, the difference on this occasion was not significant (Figure 4.2A, ANOVA: $F=4.62$ with $df=4$ and $p=0.02$). The variability was markedly reduced by increasing the number of replicates and playing close attention to sampling (Figure 4.2B). The reduction in concentration observed between the two lowest volume samples was 53±10% across the three sample sets. Less difference was observed between the second lowest (30/40 mL) and highest sample volumes (70-90 mL) 42±5%. Notably, in March and April (Figure 4.2 A and B), GBT_p concentrations of 336 nmol dm-3 and 173 nmol dm-3, respectively, were observed in the low volume sample extracts. Previous studies of GBT_p in natural samples measured maximum concentrations of 19 nmol dm-3 at the same site (Airs et al., unpublished data). The high sample volumes of 1-4 L used in previous studies of GBT_p in natural samples were likely to have considerably underestimated concentrations of GBT_p.

The effect of filtration volume on analyte losses for studies of primary production using ^{14}C labelled bicarbonate has been discussed (Arthur and Rigler, 1967; Lean and Burnison, 1979; Nalewajko and Lean, 1972). A 6% decrease in ^{14}C

activity collected on filter papers was observed with increasing volumes filtered (5 – 25 mL) (Arthur and Rigler, 1967). It was hypothesised that, as filter volume increased, the pressure differential and the average time spent by phytoplankton cells on the filter surface would increase. As a consequence, increasing filter volumes were expected to increase the relative degree of cell damage. DOC released from cells has been shown to increase by up to a factor of 3 with increasing filter volumes (10-25 mL) (Nalewajko and Lean, 1972). However, Berman (1973) observed no significant difference in ^{14}C bicarbonate uptake by cells and concluded that filtration was an accurate sampling method for analysis of primary production. In summary, water volume appears to be an important factor for sampling phytoplankton, particularly for measurement of analytes such as DMSP and GBT that are easily lost to the dissolved phase.

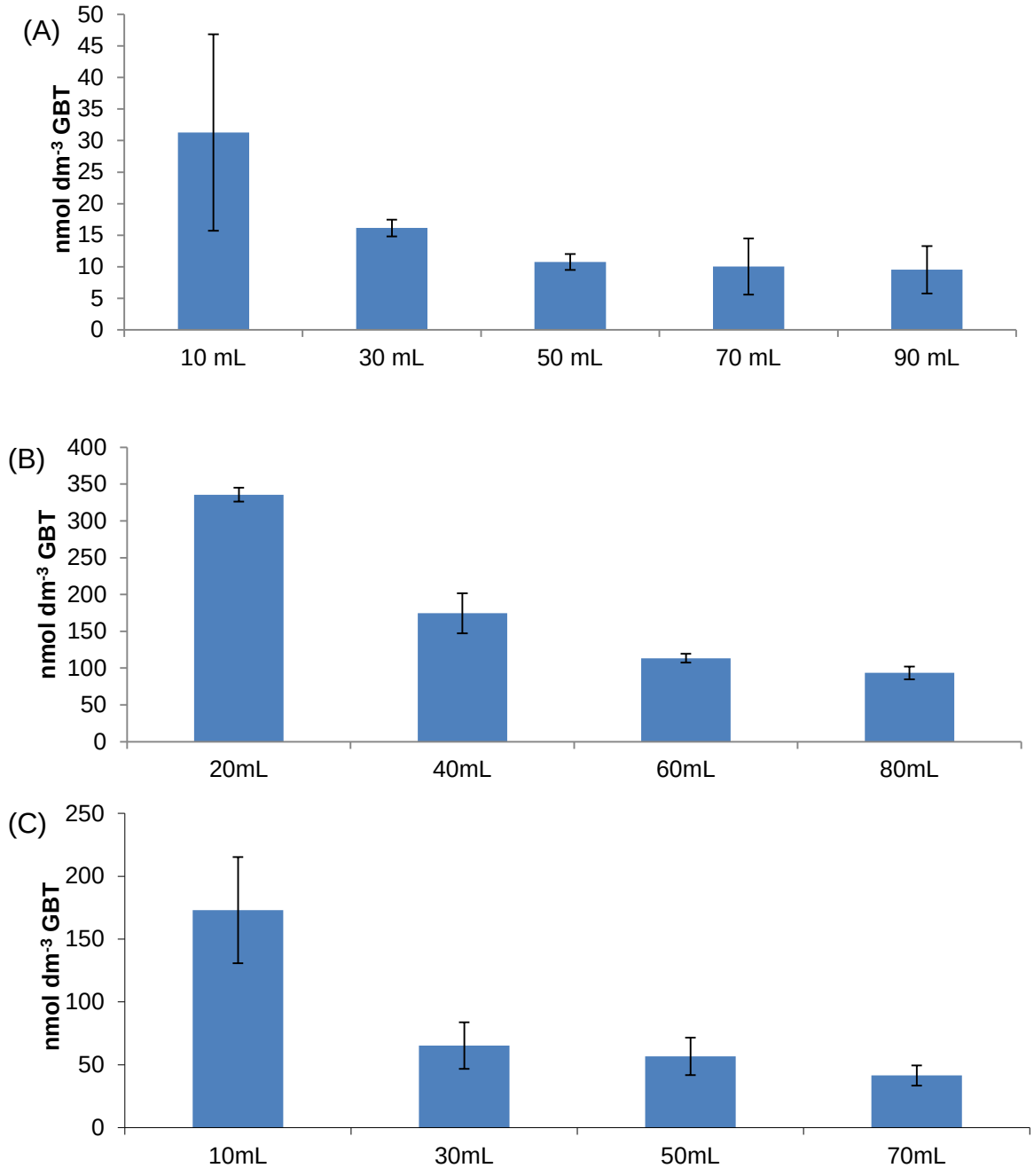

Figure 4.2: Effect of filtration volume on observed GBT_p concentrations in particulate samples collected on (A) February 2012, (B) March 2012 and (C) April 2012 from the Western English Channel. Error bars denote ±1 SD (n=3). Filter papers were extracted and analysed by LC-MS according to Figure 4.1

4.2.1 Potential sources of variability in GBT concentration from low volume particulate samples

As significant variability was observed in GBT_p concentrations from 10 mL particulate samples, potential sources of that variability were considered

Exposure of the filter to air

A marked effect on $DMSP_d$ concentration was observed on exposing the sample filter to air (Kiene and Slezak, 2006). A mean $DMSP_d$ concentration of approximately 2.6 nmol dm^{-3} increased to 15.9 nmol dm^{-3} during filtration of the final 4 mL of water as the filter was exposed to air. The increase in concentration indicated that exposure to air damaged the cellular material, causing release of DMSP to the dissolved phase. Similarly, exposure for as little as 1-2 seconds was sufficient to damage fragile phytoplankton species during studies of ammonium uptake (Goldman and Dennett, 1985). Taken together, these studies indicated that exposure to the air, particularly under vacuum, was likely to cause osmotic shock, leading to cell rupture. Exposure of the filter to air was therefore regarded as a factor that could contribute to variability in GBT_p.

A balance was sought between removing the filter before all the water had passed through and leaving the filter in place for longer than was absolutely necessary. By paying close attention to this aspect of the filtration process, as well as minimising GBT_p losses to the dissolved phase via osmotic shock, the residual water content of the filter paper would be more consistent, reducing uncertainty in the effective extraction volume (volume of extraction solvent + residual water content of filter paper).

GBT peak height variation during LC-MS analysis

A reduced amount of particulate matter was collected from small volume filtrations compared to large volume filtrations. This gave rise to a smaller GBT signal during analysis by LC-MS and increased error involved in integrating a smaller peak.

Phytoplankton assemblage composition

The phytoplankton assemblage within samples is another potential source of variability. Studies of ammonium uptake by phytoplankton have indicated that certain species were more susceptible to cell breakage during filtration (Goldman and Dennett, 1985). *Dunaliella tertiolecta* (a chlorophyte)*, Chroomonus salina* (a cryptophyte) and *Olisthodsicus luteus* (a phytoflagellate) were found to be particularly susceptible to cell breakage when filtered under vacuum, particularly when the filter paper was exposed to air (Goldman and Dennett, 1985). These species were distinguished from the other species tested by the lack of a rigid cell wall. *Dunaliella tertiolecta* lacks a cell wall and its thin outer membrane is sensitive to osmotic shock. Similarly, *Olisthodiscus luteus* is bound by a single membrane and *Chroomonus salina* has a periplast made up of thin, fragile rectangular plates. The lack of a rigid cell wall made these species particularly vulnerable to cell breakage during filtration. In contrast, high ammonium uptake rates were observed in the three diatom species tested: *Phaeodactylum tricomutum, Thalassiosira weissflogii* and *Chaetoceros simplex* (Goldman and Dennett 1985). Diatoms have rigid silica cell walls which were reported to reduce the chance of cell breakage during filtration. The evidence reported to date suggested that phytoplankton resilience to filtration could have implications for

observed effects of filtration volume on GBT_p concentrations, particularly during phytoplankton succession in natural waters, and this was consistent with the results obtained from the volume range experiments (Figure 4.1 and Figure 4.2). As a result, phytoplankton species and biomass were also considered during the seasonal study of GBT_p levels (Chapter 5).

4.3 Contribution of dissolved GBT to measured particulate GBT concentrations

Marine GBT comprises particulate and dissolved forms. The GBT_p accumulated in phytoplankton cells can be released to the dissolved phase in the environment via a number of mechanisms, including passive diffusion, grazing and viral lysis (Welsh, 2000). Once released to the dissolved phase, GBT is expected to form part of the labile fraction of dissolved organic nitrogen (DON) and be rapidly turned over by the microbial community. Concentrations are, therefore, expected to be low, but have not been measured in the marine environment to date. Nevertheless, the potential contribution to GBT_p measurements needs to be established. GBT_d may contribute to GBT_p measurements via interaction with, or adsorption to, particulate matter and the filter paper. A series of experiments was designed to test the potential contribution of GBT_d to observed GBT_p concentrations. Seawater was collected by bucket from Plymouth Sound and used as basis for testing the contribution of dissolved GBT to measured particulate GBT concentrations. Particulates were collected by gravity filtration using GF/F filters, flash frozen in liquid nitrogen and stored at -80°C until analysis. Following filtration, filter papers were flash frozen in liquid nitrogen and stored at -80°C until analysis. Filter papers were then solvent extracted (3 mL, methanol:

chloroform: HPW) overnight and clarified using centrifugation and 1 µL injected for analysis by LC-MS according to Airs and Archer (2010) (detailed in Chapter 7). The experimental design is outlined in Figure 4.3

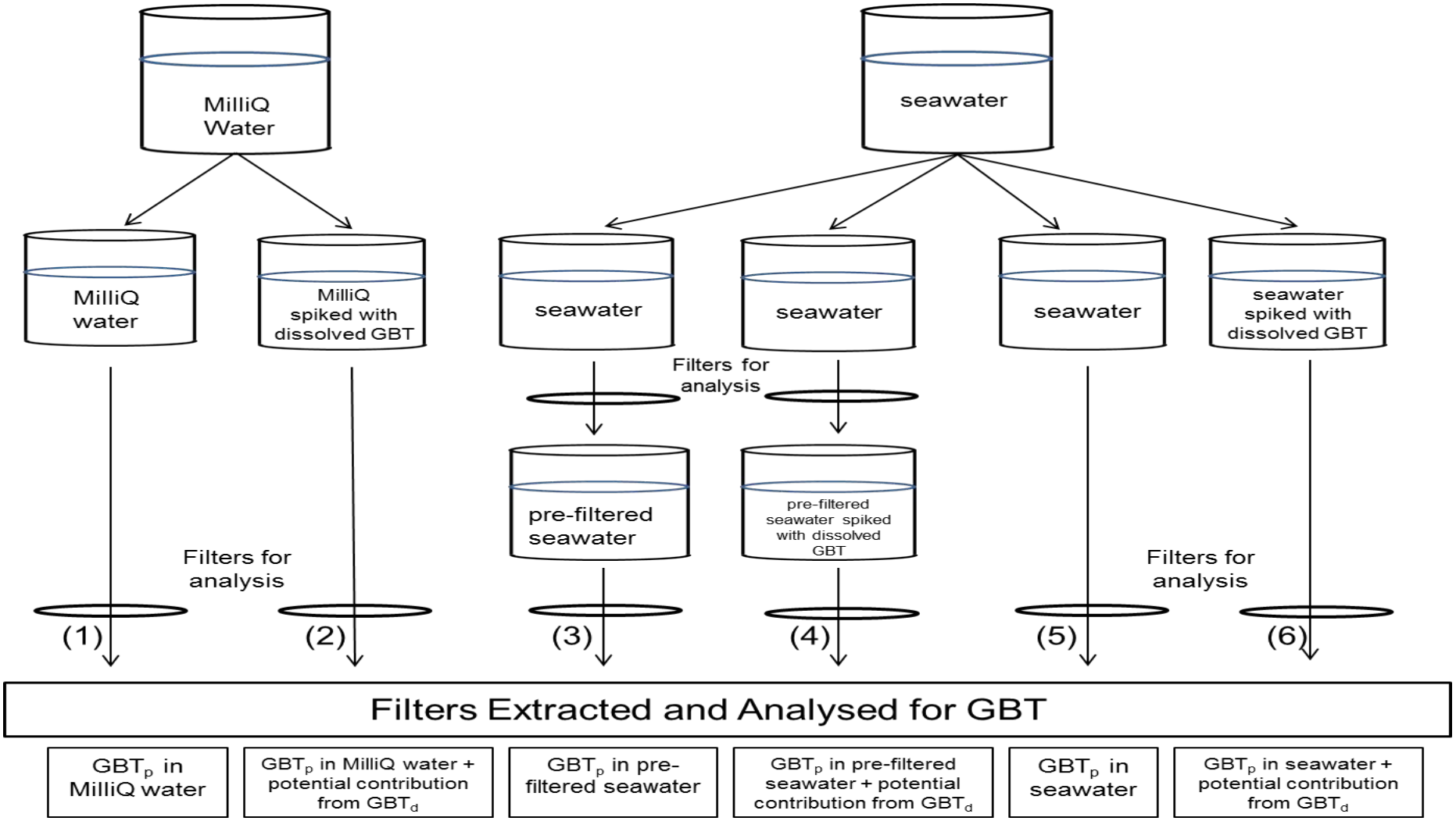

Figure 4.3: Schematic showing the preparation of samples to determine potential contribution of GBT_d to routine GBT_p measurements. Numbers in parentheses refer to the experiment number**.** Filter papers were extracted and analysed according to Figure 4.1

Tests were designed to establish if GBT_d would associate with the filter paper in the absence of any matrix effects or contributions from particulate matter. After establishing no detectable GBT was present in HPW (Figure 4.3, expt. 1), 3 x 1 L aliquots of HPW were spiked with GBT_d, to a final concentration of 30 nmol dm^{-3}, and subjected to the filtering protocol (Figure 4.3, expt. 2). The filters obtained were extracted and analysed by LC-MS and GBT was not detected (Table 4.2) indicating that the GBT added to the HPW did not adhere to filter paper in detectable quantities.

To determine if the seawater matrix affected the potential contribution of measurable GBT_d to levels of GBT_p, the experiment was repeated with seawater from Plymouth Sound (Figure 4.3, expts. 3 & 4). Similarly to experiments 1 and 2, GBT was not detected in the extracts of the filter papers from experiments 3 and 4 (Table 4.2).

Finally, to investigate the potential adherence of GBT_d to particulate matter, seawater with and without added GBT was filtered and the filters extracted and analysed for GBT (Figure 4.3, expts. 5 & 6). Any adherence of the GBT_d to the particulate matter in the seawater would have resulted in an increase in the observed GBT_p concentrations of the spiked compared to the unspiked seawater. The concentration of GBT_p extracted from seawater particulates was 5 nmol dm^{-3}. No increase in the GBT_p signal was observed with addition of GBT_d to the samples (Table 4.2), indicating that there was no measurable contribution from the added GBT_d. In conclusion, GBT_d concentrations up to 30 nmol dm^{-3} did not affect GBT_p measurements.

Table 4.2: The **c**ontribution of GBT_d to measured GBT_p concentrations based on the experiment detailed in Figure 4.3. Error bars denote in ±1 SD (n=3), nd = not detected

	Expt. 1	Expt. 2	Expt. 3	Expt. 4	Expt. 5	Expt. 6
GBT (nmol dm^{-3})	nd	nd	nd	nd	4.52	3.18

4.4 Ion suppression of GBT signal during analysis of natural samples

During analysis of natural samples by LC-MS it was noted that the peak intensity of the internal standard ($_{d11}$-GBT) in sample extracts was substantially reduced compared to calibration standards containing the same concentration of $_{d11}$-GBT. To investigate further, a comparison of the $_{d11}$-GBT peak areas in both natural samples and standards was carried out. The internal standard peak area was reduced, on average, by an order of magnitude between the standards and the natural sample extracts (Table 4.3). The standards gave large, clear Gaussian internal standard peaks whereas in the natural samples the internal standard peaks were substantially smaller and less distinct (Figure 4.4).

Table 4.3: $_{d11}$-GBT (197 pg injected) peak areas in standard solutions and natural sample extracts analysed on the same analytical day

Internal standard peak areas	
Standards	Particulate Extracts
3.7×10^7	1.7×10^6
3.7×10^7	1.6×10^6
3.1×10^7	1.8×10^6

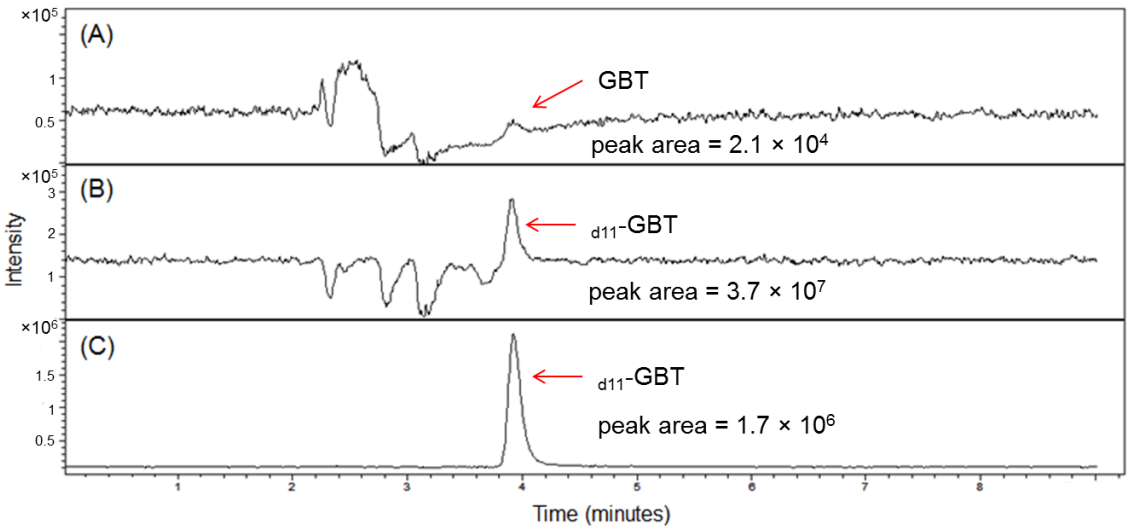

Figure 4.4: Extracted ion chromatogram of (A) *m/z* 118 from a natural sample extract, (B) $_{d11}$-GBT (*m/z* 129, 197 pg injected) from a natural sample extract collected from 10 mL samples and (C) $_{d11}$-GBT (*m/z* 129, 197 pg injected) from a standard. Filter papers extracted and analysed by LC-MS according to Figure 4.1

The reduction in peak area of the $_{d11}$-GBT signal in natural samples compared with calibration standards indicated that the ionisation of GBT was being suppressed in samples, potentially by the sample matrix. Ion suppression is a common problem encountered with LC-MS analysis where the presence of endogenous compounds interfere with analyte ionisation (Bonfiglio et al., 1999; King et al., 2000) To investigate the source of the ion suppression on the internal standard peak areas, extracts from 10 mL and 1 L sample extracts were compared. The intensity of the $_{d11}$-GBT signal from the 10 mL and 1 L samples was approximately equal (Table 4.4). Two potential sources of ion suppression in the samples were the seawater retained in the filter and the particulate matter collected on the filter. The seawater residue retained in the filters (47 mm GF/F) was not expected to differ significantly between filters, nor depend on the volume filtered. The number of phytoplankton cells, however, was expected to be much higher in 1 L samples. As the volume of water filtered did not appear to affect the extent of suppression of the $_{d11}$-GBT signal (Table 4.4), the ion suppression

probably originated from components in the seawater retained on the filter and not from the cells captured on the filter.

Table 4.4: Representative $_{d11}$-GBT peak areas taken from extracted ion chromatogram (*m/z* 129) of extracts obtained from the filtration of 10 mL and 1 L samples and a representative $_{d11}$-GBT peak area from a standard solution. Internal standard solutions were prepared fresh on each analytical day (approximately 197 pg injected); therefore values were based on slightly different $_{d11}$-GBT concentrations

	Average internal standard peak area		Average internal standard peak area in calibration standards
Sample Date	10 mL Natural Samples	1 L Natural Samples	
3rd December 2012	1.7×10^6	1.7×10^6	3.7×10^7
15th April 2013	1.5×10^6	1.5×10^6	
16th September 2013	1.8×10^6	1.4×10^6	

Although the extent of ion suppression was similar between samples, a degree of variability in the *m/z* 129 signal was evident. A comparison of the intra-day variability of the $_{d11}$-GBT peak areas gave RSDs of 26% (n = 30) and 28% (n = 10) in natural samples and standards respectively. The similarity in the variability observed between the standard solutions and natural samples indicated that the intra-day variability was not a consequence of ion suppression. The most likely cause of the variability was fluctuations in the MS response due to ionisation efficiency and detector performance (Mirzaei et al., 2009; Pailleux and Beaudry, 2012). It is for these reasons that internal standard use is considered essential for quantification using ESI-MS.

To investigate reproducibility of the internal standard peak areas with sequential sample analysis, five marine particulate sample extracts were analysed

sequentially by LC-MS. The internal standard peak area diminished rapidly, with the second injection and fifth injections giving a $_{d11}$-GBT peak area that was reduced by > 66 % and an order of magnitude, respectively (Figure 4.5). This indicated that the ion suppression agents were accumulating in the system and having a cumulative effect. This rapid reduction in signal had implications for sample processing as only small numbers of samples could be analysed before the signal became compromised.

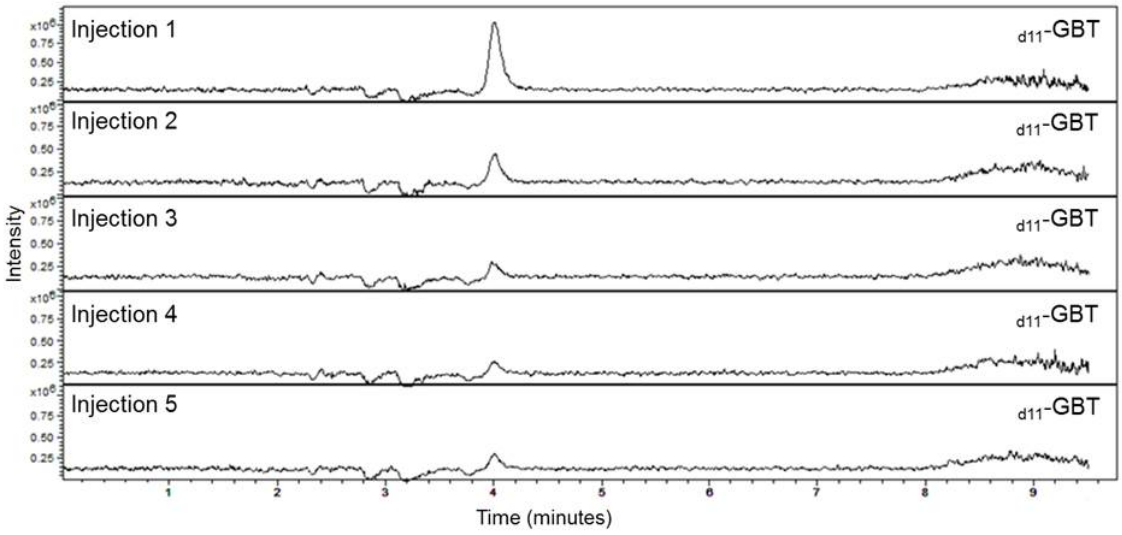

Figure 4.5: Extracted ion chromatogram (*m/z* 129) of five marine particulate sample extracts, analysed consecutively by LC-MS according to Figure 4.1

The relative extent of ion suppression of the GBT signal in particulate extracts collected from 10 mL and 1 L sample volumes was assessed using samples collected from station L4. The filters were extracted and analysed for GBT_p to assess the relative impact of the ion suppression. The particulate extracts from 1 L samples showed clear $_{d11}$-GBT and GBT signals. In contrast, the $_{d11}$-GBT peaks observed in the extracts from 10 mL samples were small and indistinct. The GBT signal observed in the extracts from 10 mL samples often represented the

approximate LoD (signal: noise, 3:1) and, as such, integration of these peaks was not considered analytically robust (Figure 4.6).

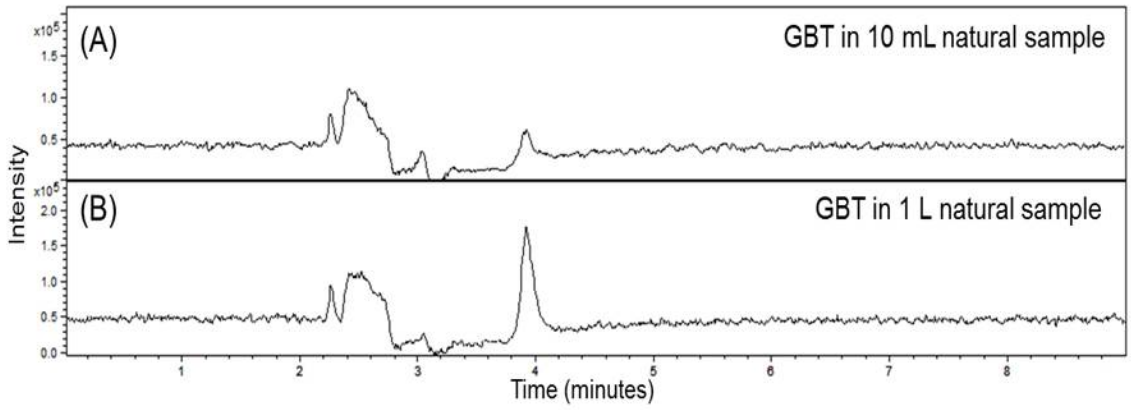

Figure 4.6: Extracted ion chromatogram (*m/z* 118) in (A) a 10 mL natural sample extract and (B) a 1 L natural sample extract from the Western English Channel, analysed by LC-MS according to Figure 4.1

The ion suppression apparent for the 10 mL sample extracts was attributed to the relatively small GBT signal in the 10 mL extracts, compared with the 1 L extracts. Although the 10 mL samples gave higher final concentrations the amount of particulate matter collected was 100 fold less than in the 1 L samples. Consequently, the GBT signal was smaller in the 10 mL extracts. The small GBT signal was then markedly reduced due to ion suppression. The diminished peak areas had implications for the sensitivity of this analytical approach when using small filtration volumes.

The ion suppression observed in the 10 mL sample extracts precluded their analysis pending further investigation of the LC-MS conditions, and efforts were made to reduce the ion suppression so that low volume samples could be analysed. During analysis of GBT, several ions were evident in the mass spectrum, arising from a peak (peak A) eluting just prior to GBT (Figure 4.7). The

size of peak A and the longevity of ions arising from this peak (*m/z* 105, 187, 269) in the mass spectrometer identified it as a candidate contributor to the observed ion suppression. This peak was a source of contaminating ions to the ion source and was particularly problematic as it eluted just prior to GBT. The ions from peak A dominated the mass spectrum as GBT eluted from the column (Figure 4.8). The mass to charge ratio of the ions arising from peak A were coincident with those of sodium acetate clusters (105 = $C_2H_2O_2Na$, 187 = $2(C_2H_2O_2)Na_3$, 269 = $2(C_2H_2O_2)Na_4$) which could be formed during injection by interaction of sodium (from seawater) and acetate (from the mobile phase). These contaminating ions may have contributed to the suppression of GBT ionisation.

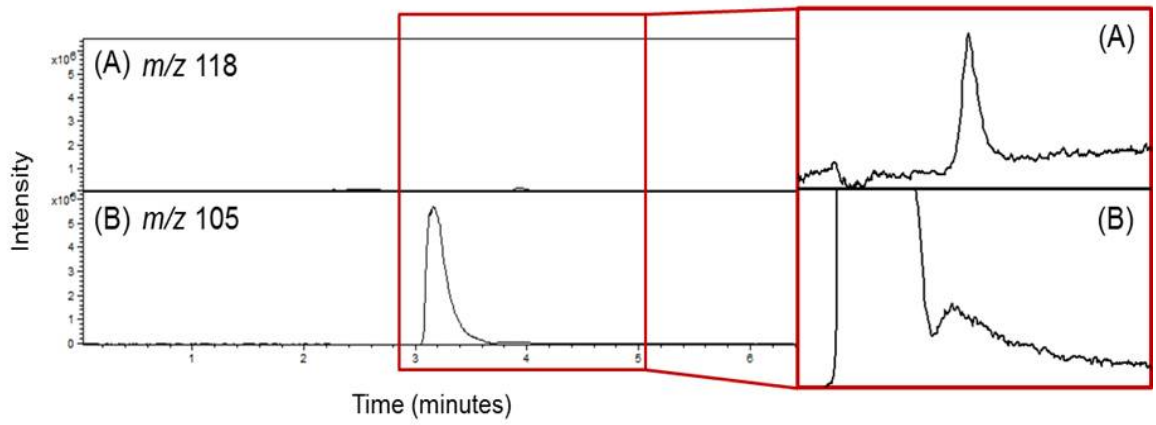

Figure 4.7: Extracted ion chromatogram of (A) *m/z* 118 and (B) contribution of *m/z* 105 to peak A from a 1 L natural sample extract from the Western English Channel, analysed by LC-MS according to Figure 4.1

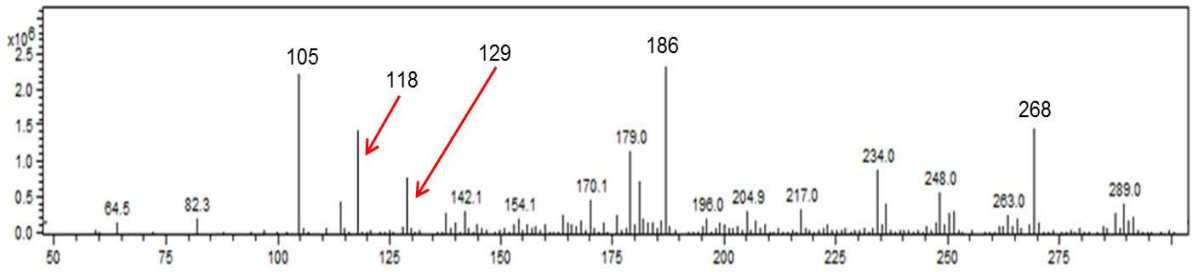

Figure 4.8: Mass spectrum (total ion count) recorded during elution and ionisation of GBT (*m/z* 118) in the ion source during analysis of natural sample by LC-MS according to Figure 4.1

The LC mobile phase composition was altered to affect the relative elution position of GBT and peak A, to minimise potential interference with GBT ionisation. A starting point for the mobile phase composition was 50:50 acetonitrile: HPW (ACN:HPW) as this composition was effective for cleaning the column and source after extract injections.

GBT analysis using 50:50 ACN:HPW as the mobile phase was compared with that used by Airs and Archer (2010) (hereafter Airs and Archer mobile phase) and an increased signal to noise ratio for GBT was observed, although peak tailing was evident. Addition of a small proportion of the Airs and Archer mobile phase to the ACN: HPW composition (Table 4.5) reduced tailing, improving peak shape (Airs et al., personal communication). Notably, with composition B, the elution order of GBT and peak A reversed and consequently, peak A was less likely to affect the ionisation of GBT. GBT was observed to elute as a clear, sharp Gaussian peak with a peak area that was above the signal: noise threshold (3:1) (Figure 4.9). In contrast, during analysis using composition C, peak A eluted prior to the GBT peak and consequently, was expected to affect GBT ionisation (Figure 4.10).

Table 4.5: Solvent compositions of the original (from Airs and Archer, 2010) and modified mobile phase compositions tested for the analysis of GBT_p

Mobile Phase Composition	% Airs and Archer	% ACN:HPW	Acetonitrile (%)	Methanol (%)	HPW (%)	Acetic acid (%)	Final ammonium acetate concentration (mM)
Airs & Archer	100	0	53	21	25	1	50
B	10	90	48.5	2.1	47.5	0.1	5
C	2	98	50.06	0.42	49.5	0.02	1

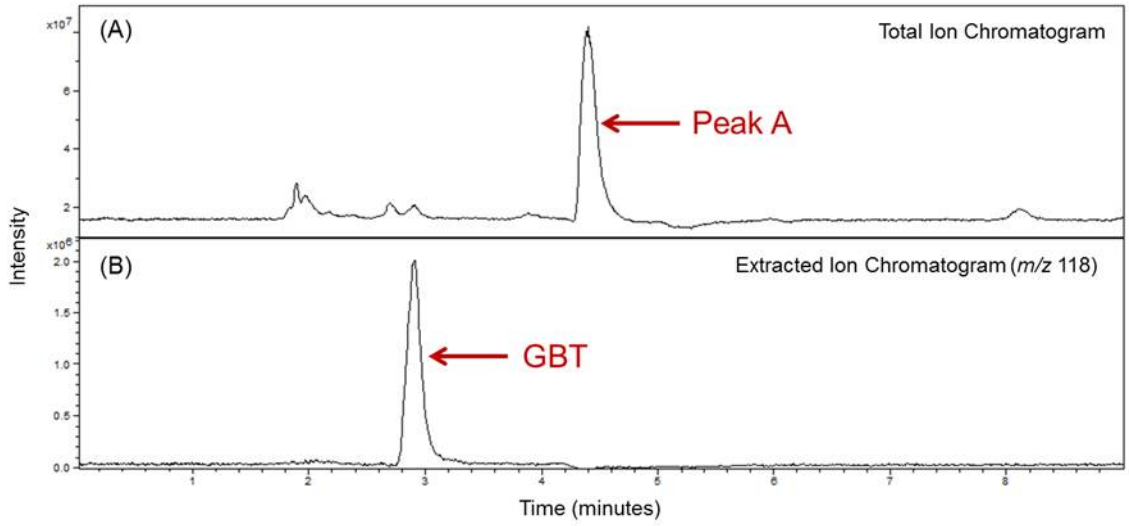

Figure 4.9: (A) Total ion chromatogram and (B) extracted ion chromatogram of *m/z* 118 from a 1 L sample extract from the Western English Channel, filter papers extracted and analysed by LC-MS according to Figure 4.1 except using mobile phase B: ammonium acetate: methanol: HPW: acetic acid (48.5: 2.1: 47.5: 0.1) with a final ammonium acetate concentration of 5 mM

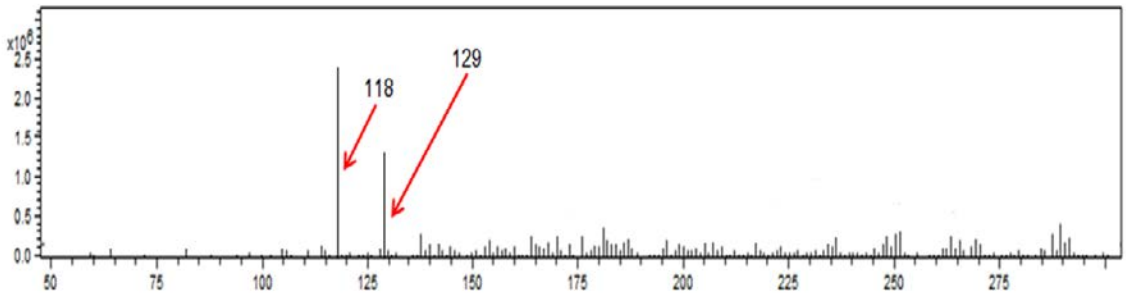

Figure 4.10: Mass spectrum (total ion count) recorded during elution and ionisation of GBT (*m/z* 118) in the ion source during analysis of natural sample by LC-MS according to Figure 4.9

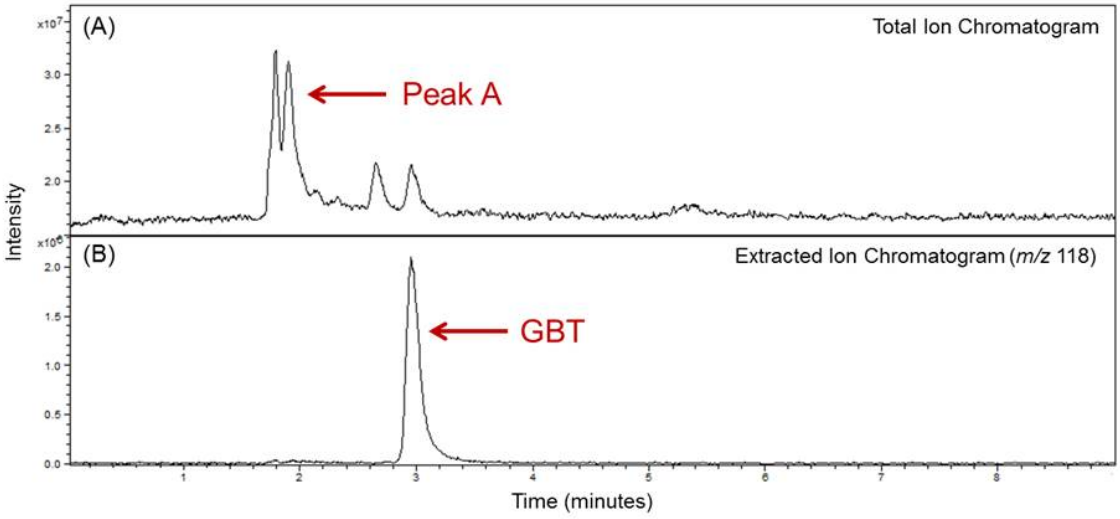

Figure 4.11: (A) Total ion chromatogram and (B) extracted ion chromatogram of *m/z* 118 from a 1 L sample extract from the Western English Channel, filter papers extracted and analysed by LC-MS according to Figure 4.1 except using mobile phase B: ammonium acetate: methanol: HPW: acetic acid (50.06: 0.42: 49.5: 0.02) with a final ammonium acetate concentration of 1 mM

During analysis with mobile phase B, the increased relative retention time of peak A compared to GBT reduced the presence of interfering ions derived from peak A, during elution of GBT. Ion suppression was thereby reduced. Based on the reduction in ion suppression and the improved peak shape, mobile phase composition B (Table 4.5) was selected for sample analysis.

As a result of the higher aqueous content, mobile phase composition B was more polar than that of the Airs and Archer (2010) mobile phase (polarities of 6.9 and 6.5, respectively, Table 4.6). To afford good chromatography, the polarity of injected solutions was required to match that of the mobile phase composition and the polarity of the extraction solvent (methanol: chloroform: water, 12**:**5**:**1, P=5.1) was not expected to be compatible with the higher aqueous content of the modified mobile phase. To this end the effect of polarity on standard variability was examined using calibration solutions. These were prepared using standard solutions in either the original (methanol: chloroform: water, 12**:**5**:**1, P=5.1) or modified (methanol: chloroform: water, 6**:**2.5**:**9.5, P=7.0) solvent compositions using mobile phase B (Table 4.5). The modified extraction solvent composition was expected to be more compatible as its polarity (P=6.9) was closer to that of mobile phase B.

Table 4.6: Polarity of mobile phase and extraction solvent compositions, including an estimate natural sample extract, polarity measured relative to test compounds

Composition	Polarity Index (P)
Airs and Archer (2010) mobile phase:	6.5
Mobile phase B:	6.9
Original extraction solvent: (methanol: chloroform: water, 12**:**5**:**1, P=5.1)	5.1
Modified extraction solvent: (methanol: chloroform: water, 2.4**:**1**:**3.8, P=7.0)	7.0
Natural sample extracts (approximated):	6.3-6.6

Four inter-day calibrations were performed and the variability in the peak area ratio (*m/z* 118/129) and lines of best fit were compared. The calibration solutions prepared in extraction solvent (methanol: chloroform: water, 12:5:1) showed a high degree of variability in the peak area ratio and the calculated lines of best fit (R^2 = 0.609). Notably, the points of intercept and gradients fluctuated considerably between calibrations (Figure 4.11). The calibration solutions prepared using the modified solvent composition (methanol: chloroform: water, 2.4**:**1**:**3.8) resulted in improved variability in the peak area ratio and the calculated lines of best fit (R^2 = 0.951). Any observed variability occurred between narrow limits and did not significantly affect the gradient or point of intercept. Based on the reduced variability the modified solvent composition was chosen for use during quantification of natural samples. A washing protocol was also employed to minimise contaminating ions (Chapter 7, Section 7.4.2).

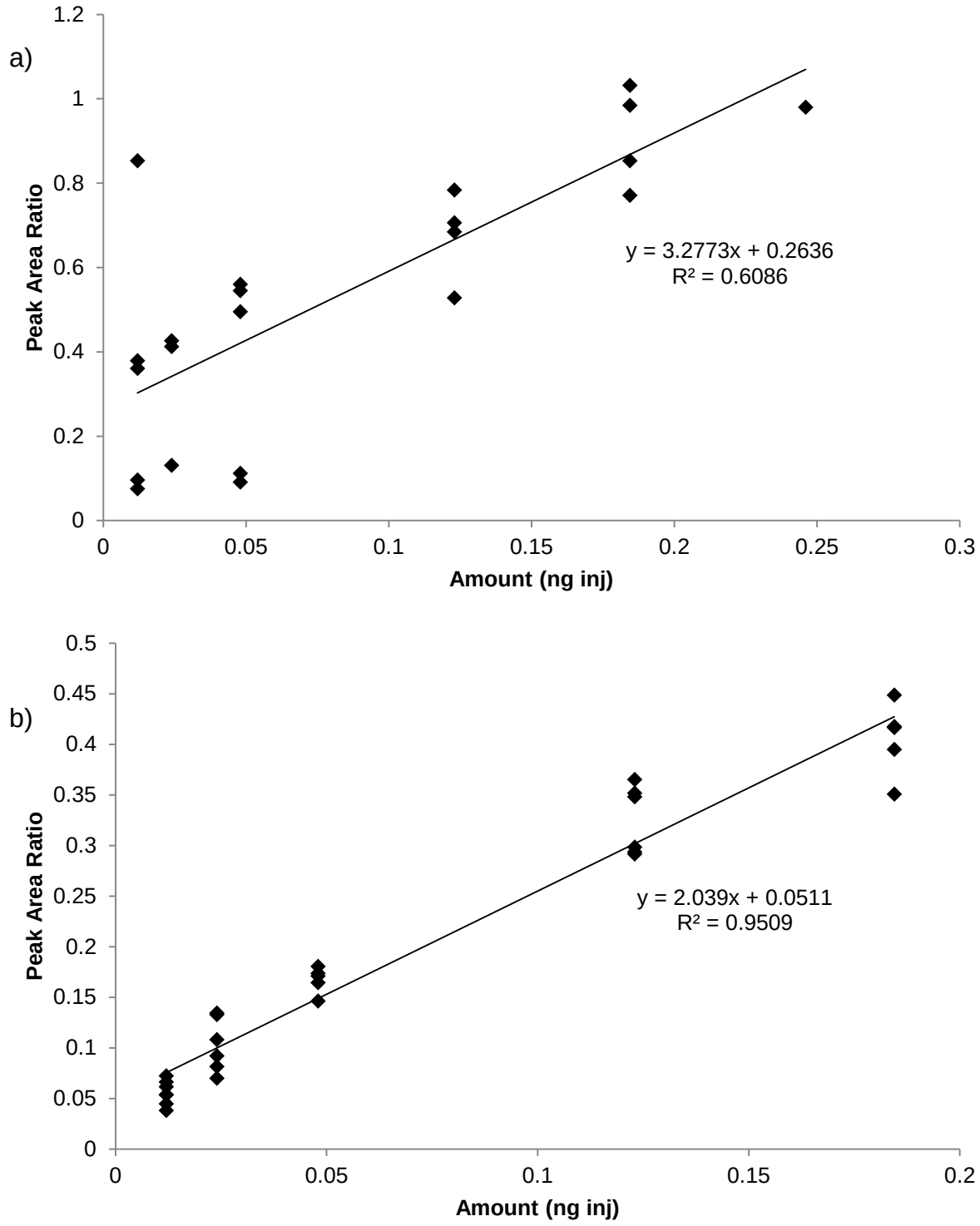

Figure 4.12: Calibration curves for GBT_p prepared in (A) extraction solvent (methanol: chloroform: water, 12:5:1) and (B) 50% extraction solvent/water (methanol: chloroform: water, 6:2.5:9.5)

The modified mobile phase and solvent composition reduced analyte suppression sufficiently to achieve an acceptable and reproducible GBT signal (*m/z* 118) during analysis of low volume samples. A 10 mL sample extract from station L4 analysed using both the Airs and Archer (2010) mobile phase and mobile phase B (Table 4.5) showed the marked differences in peak area (Figure 4.12). A clear peak was not evident in the analysis using the Airs and Archer (2010) mobile phase. In contrast, the GBT peak observed using mobile phase B was clear and permitted analysis of particulates collected from 10 mL seawater samples. The signal to noise ratio was improved along with the accuracy and consistency of peak integration. Furthermore, the analysis was not significantly affected by the number of samples injected.

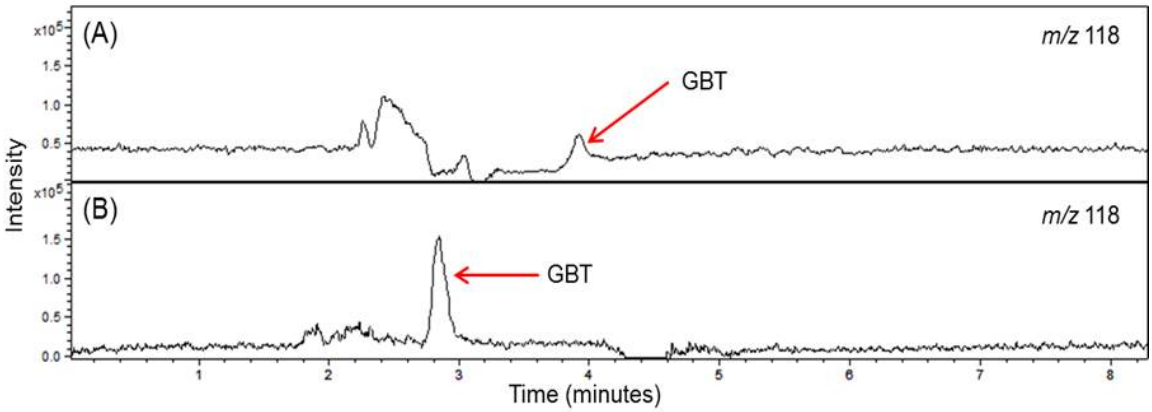

Figure 4.13: Extracted ion chromatogram (*m/z* 118) in two 10 mL samples from the Western English Channel analysed in: (A) Airs and Archer (2010) mobile phase and (B) mobile phase B, using LC-MS according to Figure 4.9 except in the mobile phase used

Particulate samples collected from station L4 were used to demonstrate that the modified analytical procedure was capable of analysing both 1 L and 10 mL water samples (Figure 4.13). The resulting chromatograms demonstrated the difference in peak size between extracts of both 1 L and 10 mL samples. However, the

filtration results, detailed in Section 4.2, indicated that 10 mL samples would give a more accurate GBT_p concentration and the modified analytical procedure made this possible.

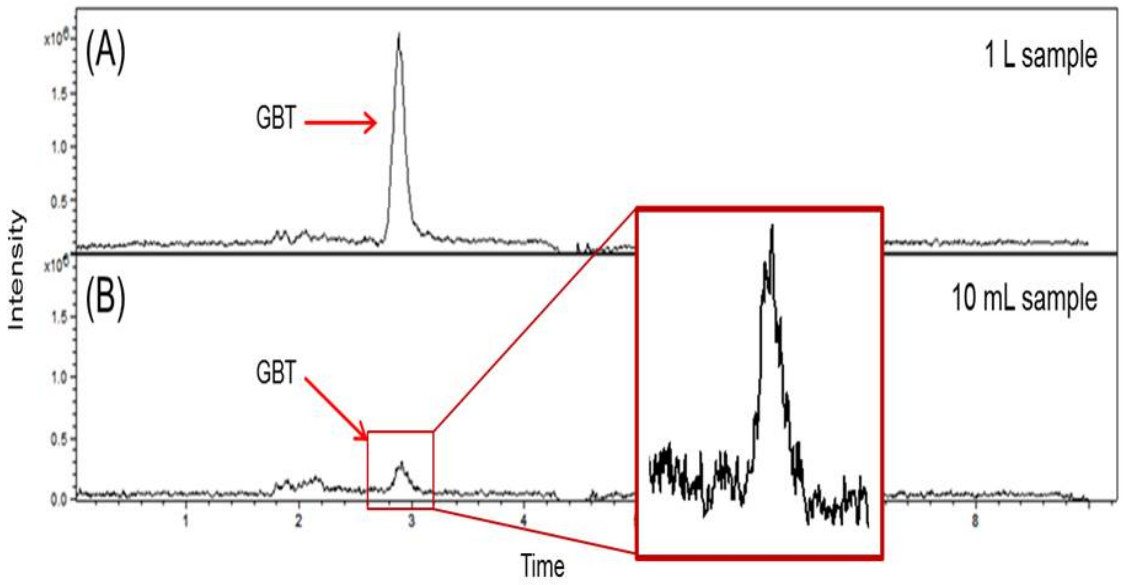

Figure 4.14: Extracted ion chromatogram (*m/z* 118) in: (A) a 1 L sample and (B) a 10 mL sample from the Western English Channel analysed using mobile phase B, filter papers were extracted and analysed by LC-MS according to Figure 4.9

4.5 Discussion and Conclusions

A marked filtration effect was evident during sampling for GBT_p using a range of sample volumes, with higher filter volumes resulting in reduced GBT_p concentrations. Filtration studies revealed that particulates collected from 10 mL samples consistently gave the highest GBT_p concentrations compared to the higher volumes sampled. Furthermore, variability in 10 mL samples was lower than for 1 L samples. These findings were consistent with reports of DMSP loss to the dissolved phase during filtration (Kiene and Slezak, 2006).

The effect of filtration volume on the observed GBT_p concentrations was thought to be caused by cell damage as a result of larger filter volumes, as cell rupture or leakage could lead to the loss of GBT_p to the dissolved phase. As a consequence, it appears that the resilience of phytoplankton cells is relevant to the sampling protocol. Previous work has shown that some phytoplankton species are more resilient than others to osmotic shock during filtration (Goldman and Dennett, 1985). The GBT_p concentrations determined for 1 L sample volumes may therefore be representative of the more resilient phytoplankton cells, whereas the GBT_p concentrations for 10 mL samples were expected to be more representative of the entire natural population in the sample. The filtration effects observed herein are important findings which have significant implications for sampling of natural phytoplankton communities to measure intracellular osmolytes.

Suppression of GBT ionisation during LC-MS analysis was apparent during processing of natural samples; this had implications for the sensitivity of the LC-

MS method and had a higher relative impact on the small volume samples. The ion suppression was addressed by modifying the mobile phase composition, affecting the relative elution position of GBT and interfering components, permitting analysis of the low volume samples to obtain more representative GBT_p concentrations.

The improved sampling and analytical approaches outlined in this chapter have enabled more accurate analysis of GBT_p. The effect of filtration volume, presented here, indicates that previous measurements, obtained using large sample volumes (2-4 L of seawater) may have significantly underestimated GBT_p concentrations in seawater. The maximum concentration of GBT_p observed at station L4 using large filter volumes (2-4 L) was 19 nmol dm^{-3} (Airs et al., unpublished data), which is over an order of magnitude lower than the highest concentration presented in this work (336 nmol dm^{-3}). During phytoplankton demise e.g. via a viral lysis event, GBT could represent a greater contribution to the labile DON pool than previously considered. Additionally, GBT is a precursor of the methylamines (King, 1988a) which are thought to be climatically active. For example, a recent study demonstrated that DMA concentrations above 3 ppt by volume enhanced nucleation rates in the atmosphere by more than a 1000-fold compared to ammonia. This enhancement was sufficient to explain the particle formation rates observed in the atmosphere. The elevated GBT measurements described herein may, therefore, have implications for a marine source of methylamines to the atmosphere.

Chapter 5

A study of particulate glycine betaine distributions in the Western English Channel

Chapter Outline

This chapter reports data from a seasonal study of particulate glycine betaine concentrations in the Western English Channel. Concentrations measured ranged from 2.0-484.3 nmol dm^{-3} depending on the sample size used, with large volume samples giving concentrations of 2.0-49.7 nmol dm^{-3} and small volume filtrations giving concentrations of 250.5-484.3 nmol dm^{-3}. Seasonal variability of GBT_p was evident with increased concentrations occurring in spring, summer and autumn. The data were analysed in conjunction with physico-chemical parameters and phytoplankton data; a number of potential contributors to GBT_p concentrations

5.1 Introduction

Glycine betaine is thought to be one of the most effective and widely used osmolytes in marine systems (Yancey et al., 1982). As a precursor of the methylamines it is also thought to have potential climatic relevance. Despite the potential biogeochemical importance of GBT, environmental knowledge of this compound is limited to only two published studies carried out in the Gulf of Maine (Keller et al, 2004) and the Western English Channel (Airs and Archer, 2010). Keller et al (2004) reported particulate GBT (GBT_p) concentrations of 0-15 nmol dm^{-3} from 4 depth profiles at 4 different sites in the Gulf of Maine. However, no typical distribution pattern was evident at any of the four sites. In the Stellwagen and Jordan Basins minimal concentrations were observed, with a 5 nmol dm^{-3} maximum observed at 5 m depth in the Jordan Basin. The depth profile at Georges Basin showed a surface maximum of 15 nmol dm^{-3} which decreased with depth. Conversely, in the Wilkinson Basin minimal concentrations of GBT_p were observed in surface waters which increased to approximately 15 nmol dm^{-3} at a depth of 100 m. In the second study, similar concentrations (15-18 nmol dm^{-3}) were observed in the Western English Channel using two different sampling techniques (Airs and Archer, 2010). A concentration of approximately 15 nmol dm^{-3} was observed in particulates collected from 150 mL samples using gravity filtration whilst particulates collected using gentle vacuum filtration gave a concentration of 18 nmol dm^{-3}. The same study reported GBT_p concentrations of 2.4 nmol dm^{-3} in the surface waters of the tropical North Atlantic Ocean and 1.5 nmol dm^{-3} at a depth of 30 m.

Both studies reported similar maximum concentrations (15-18 nmol dm^{-3}) in coastal surface waters with samples taken in oceanic waters giving lower concentrations (up to 2.4 nmol dm^{-3}). However, the absence of a clear trend and the scarcity of data on GBT_p has limited the understanding of GBT in marine systems. To further understand the role of GBT, a seasonal study was carried out at station L4 of the Western Channel Observatory, located in the Western English Channel. The seasonal variability of GBT_p was calculated and possible relationships with the physico-chemical parameters and phytoplankton abundances measured at station L4 were also investigated.

5.2 Sampling Strategy

A high resolution seasonal study of GBT_p concentrations was carried out from October 2012-October 2013 with samples collected weekly from the Western Channel Observatory long term monitoring station: L4 (50° 15.00'N, 4° 13.02'W). Particulates were collected using 10 mL (n=5) and 1 L (n=3) water samples. Water collected from the CTD and decanted into HDPE bottles, filled to over flowing and stored in the dark until sample processing (2-4 hours). Particulates were collected by gravity filtration using glass fibre filters (nominal pore size 0.7 µm), filter papers were then flask frozen in liquid nitrogen and stored at -80°C until analysis. Filters were solvent extracted (3 mL, methanol: HPW: chloroform) and clarified by centrifugation and 1 µL injected for analysis by LC-MS (Spherisorb ODS1 column, eluent run isocratically at 1 mL min-1. Mobile phase: acetonitrile: methanol: HPW: acetic acid (53: 21:

25: 1) with a final concentration of ammonium acetate of 50 mM, according to Airs and Archer (2010)). This strategy aimed to capture the seasonal variability in the GBT_p concentrations and to analyse the relationship between the 1 L and 10 mL sample concentrations throughout the sampling period.

5.3 Sampling Site

Station L4 in the Western English Channel (WEC) sits at the boundary of oceanic (Atlantic Ocean) and neritic (Eastern English Channel) waters (Southward et al., 2004). Station L4 is a long-term monitoring station which is characteristic of temperate coastal waters. The water is well-mixed during the autumn and winter months when the sea surface temperature (SST) is approximately 8°C and nutrients are relatively abundant (Smyth et al., 2010). Spring and summer months are characterised by a weak stratification of the water column accompanied by a decline in nutrient concentration and an increase in SST which typically peaks at 18°C. Inorganic nutrients become relatively depleted but the waters remain productive and support algal blooms from spring through to autumn. Although remote from the river Tamar, it is recognised that the riverine input does influence the water at L4 with pulses of fresh water from the Tamar affecting the salinity (Southward et al., 2004). *In situ* sampling takes place weekly and measurements include nutrient concentrations, phytoplankton abundance and pigment concentrations.

5.4 Physicochemical parameters measured in the Western English Channel October 2012-October 2013

The sea surface temperature (SST) varied from 7.26-17.45°C during the sampling period (Oct 2012- Oct 2013), reaching a minimum in March and a maximum in July. This was similar to the long-term trend observed at L4 where the SST reached a minimum of 9.1°C in March and an average maximum of 16.4°C in August (Figure 5.1) (Smyth et al., 2010). The onset of stratification was evident in June (Figure 5.2) and the salinity was 34.98 ± 0.2 PSU (Figure 5.1).

Chlorophyll *a* concentrations peaked in May (3.34 mg m^{-3}) with the lowest concentrations observed from December to March (0.35 mg m^{-3}). This concentration range was similar to the average chlorophyll concentration range of 0.5-2 mg m^{-3}, however concentrations as high as 8 mg m^{-3} have been observed previously (Smyth et al., 2010).

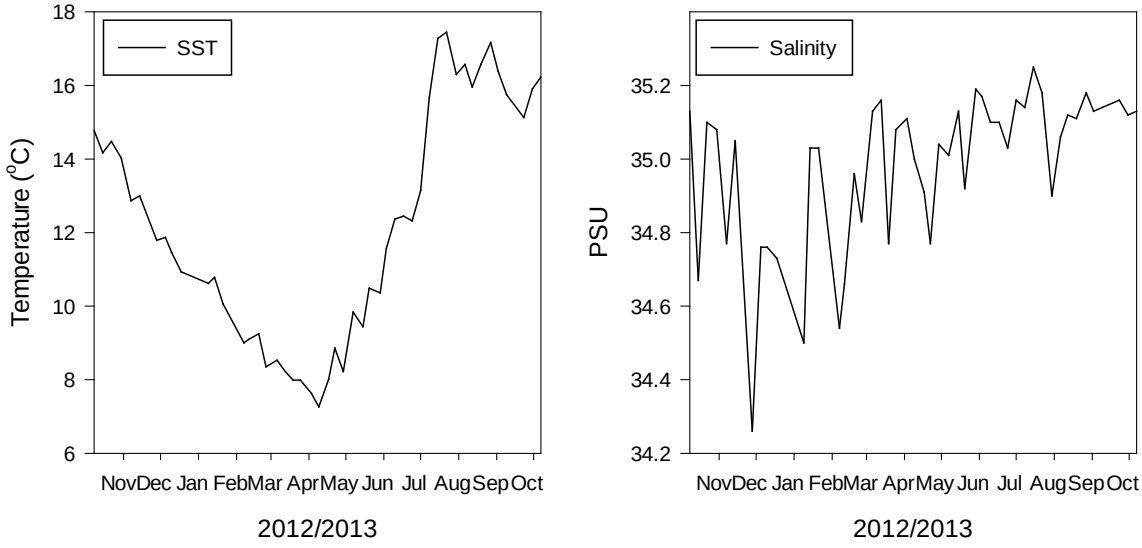

Figure 5.1: SST and salinity measured at station L4 during October 2012-October 2013

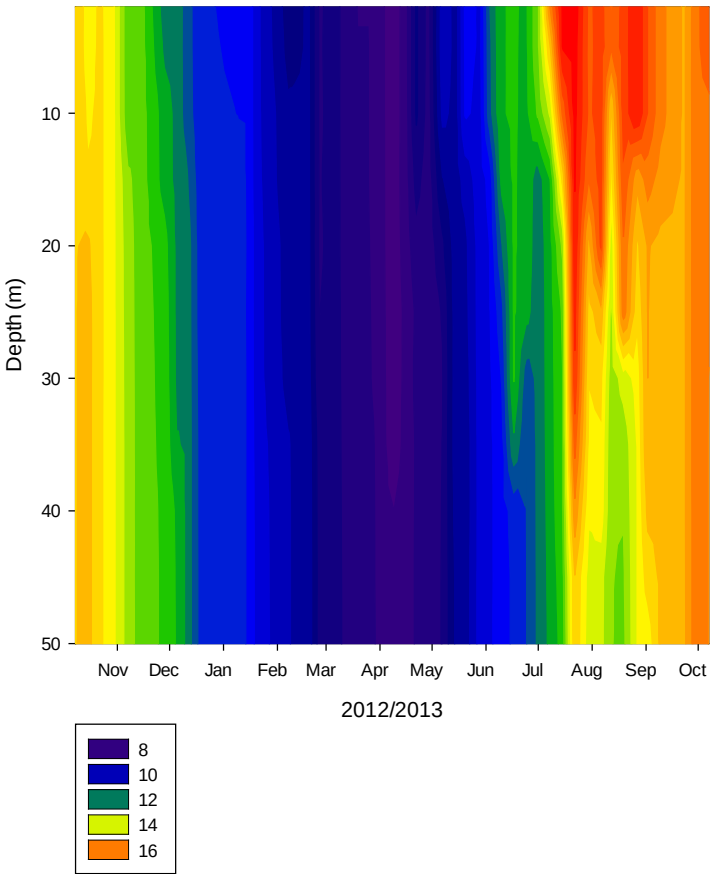

Figure 5.2: Depth profile of water temperature measured at station L4 during October 2012-October 2013

Inorganic nutrient concentrations at L4 showed clear seasonal patterns, generally increasing over the winter months when the water column was well-mixed and rapidly depleting to trace levels during the summer months following stratification (Figure 5.3) (Smyth et al., 2010). Nitrate concentrations varied between undetected (<0.02 µmol dm^{-3}) in June and 9.36 µmol dm^{-3} in February, the latter value being higher than the average maximum (8 µmol dm^{-3}) at station L4 (Smyth et al., 2010). Silicate concentrations ranged from 0.17 µmol dm^{-3} in July to 5.96 µmol dm^{-3} in November. This concentration is similar to the average maximum of 5 µmol dm^{-3} routinely observed in January (Smyth et al., 2010). Phosphate concentrations ranged from undetected (<0.02 µmol dm^{-3}) in July to 0.56 µmol

dm^{-3} in February, while nitrite concentrations varied from undetectable (<0.01 µmol dm^{-3}) in June and August to 1.18 µmol dm^{-3} in October 2013. A pre-spring bloom nitrite peak (0.26 µmol dm^{-3}) was observed, consistent with previous data at station L4. Ammonia concentrations ranged from undetectable (<0.02 µmol dm^{-3}) in August to 0.7 µmol dm^{-3} in May.

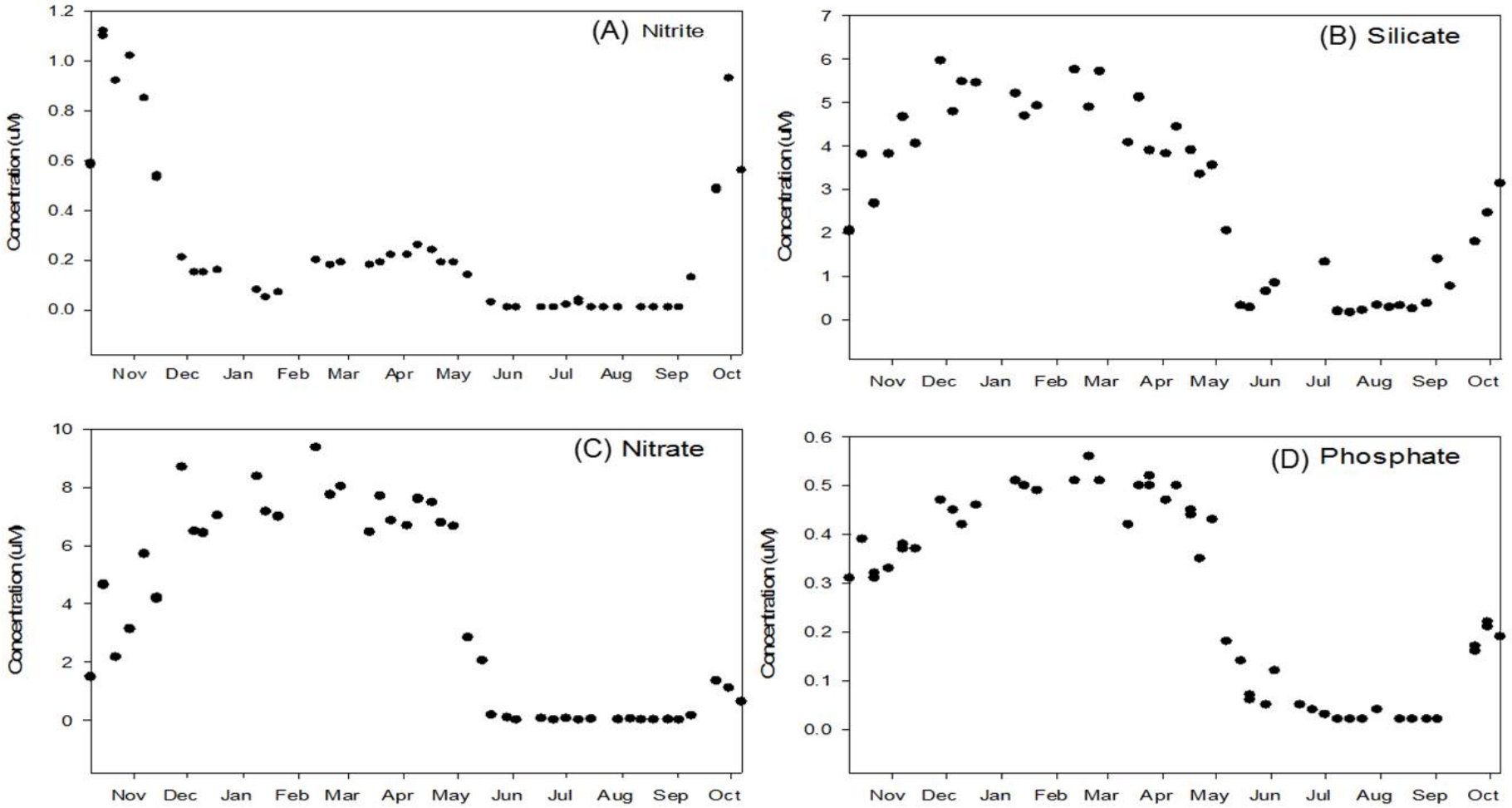

Figure 5.3: Surface water inorganic nutrient concentrations of: (A) nitrite, (B) silicate, (C) nitrate and (D) phosphate measured at station L4 during October 2012-October 2013

5.5 Particulate glycine betaine concentrations in the Western English Channel

To analyse the seasonal variability of GBT_p concentrations in the WEC, weekly samples of particulates isolated from 1 L and 10 mL water samples were analysed. Filtration studies, detailed in Chapter 4, indicated that collecting particulates from 1 L seawater samples might cause damage to the cells and result in loss of GBT_p to the dissolved phase. It was hypothesised that the GBT_p observed in the 1 L samples represented a non-labile pool of GBT_p that is not easily lost. A complete time series of 1 L samples was analysed to elucidate the seasonal variability of this non-labile GBT_p. Small volume (10 mL) filtration was thought to impose less stress on the cells, reducing the amount of GBT_p lost to the dissolved phase. A selection of 10 mL samples was analysed to try and elucidate the seasonal variability of this, more complete, GBT_p pool and the relationship between small and large volume sample concentrations.

The 1 L particulate samples analysed provided a full seasonal sample set (n=42) covering October 2012 to October 2013 (Figure 5.4). The concentrations of GBT_p in these samples ranged from a minimum of 2.0 nmol dm-3 in January 2013 to a maximum of 49.7 nmol dm^{-3} in October 2013. The highest concentration observed was more than double the previous maximum (18 nmol dm^{-3}) reported for station L4 (Airs and Archer, 2010). Seasonal variation was observed with maxima occurring in the spring, summer and autumn periods, which are typical periods of phytoplankton blooms at L4.

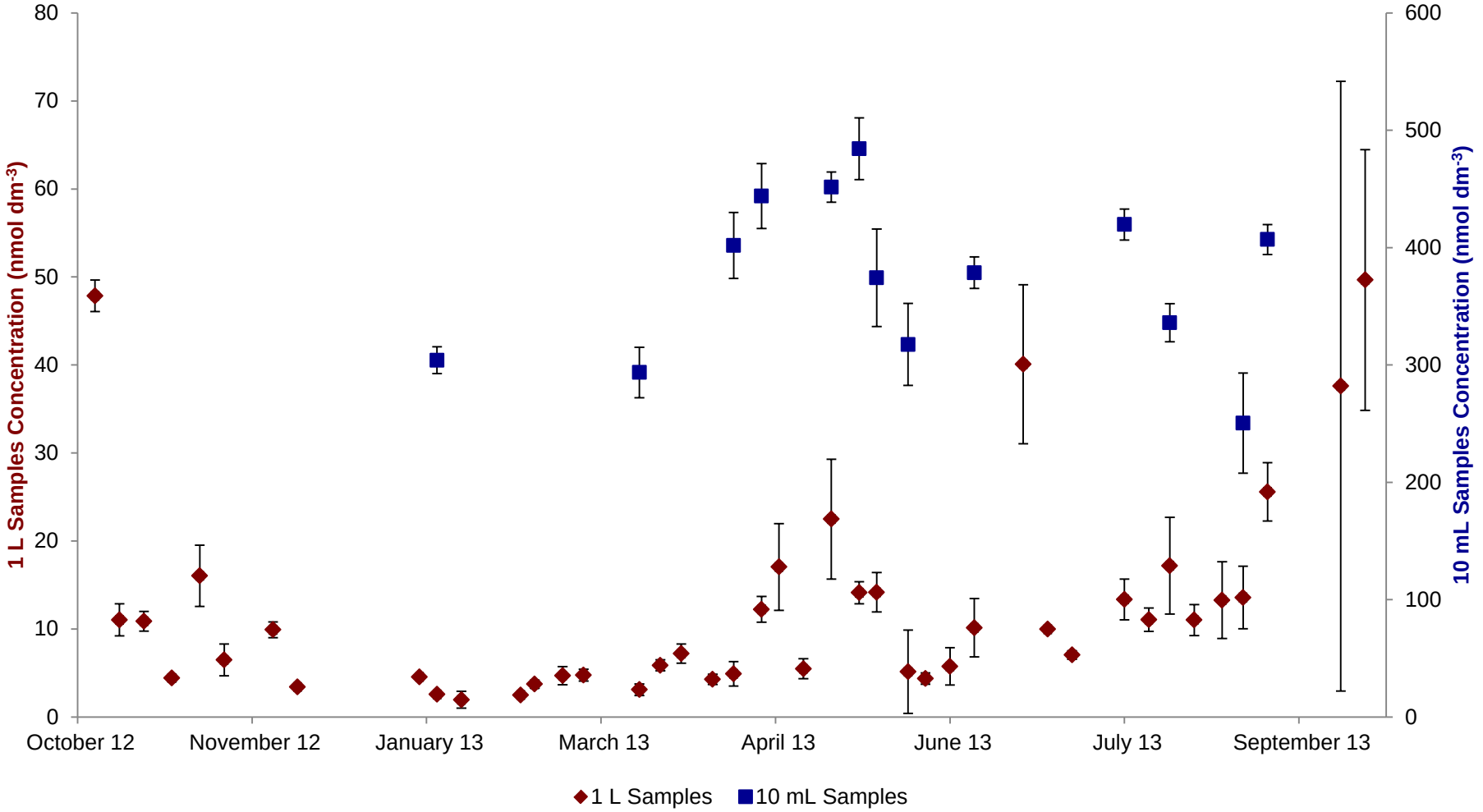

Figure 5.4: Seasonal GBT_p concentrations measured at station L4 extracted from particulate samples obtained by filtering 10 mL and 1 L water samples during October 2012-October 2013, concentrations and statistical analysis detailed in Appendix 1

Notably, the autumn peak, present in both 2012 and 2013, was particularly intense. With the exception of the concentrations observed on 30th September 2013, when a blocked filtration system affected the variability, the calculated RSDs varied from 0.4-48.8% with an average RSD of 21.4%. The 1 L samples were thought to be susceptible to cell damage during filtration. The damage to the cells was likely to be inconsistent and would, therefore, contribute to the variability observed. Although the average RSD for the 1 L samples was frequently high, the standard deviations showed minimal variation about the mean, with the exception of a few points. It was observed that the variability frequently coincided with high GBT_p concentrations. This was attributed to more GBT_p being available to be retained or lost during the filtration step.

The 10 mL particulate samples analysed covered the period of January-September 2013 (n=13) (Figure 5.4) with the smaller data set due to sample loss during processing. The concentrations ranged from a minimum of 250.5 nmol dm^{-3} in early September to a maximum of 484.3 nmol dm^{-3} in May. These concentrations were over an order of magnitude higher than any previous GBT_p concentration observed in natural samples. Where there was sufficient coverage the 10 mL concentrations mirrored the trends observed for the 1 L data set. Notably, the spring increase observed in the 1 L data set was repeated in the 10 mL samples. With the exception of the 250 nmol dm^{-3} data point, measured in early September, the two data sets significantly correlated (Regression: F=5.15 with df=1 and p=0.047, R^2=34%). The 250 nmol dm^{-3} data point represented the lowest measured GBT_p concentration. When

analysed, the samples from this data point showed poor chromatography with small, poorly defined peaks and poor peak shape; as such it may represent an erroneous data point. The 10 mL data set did not provide sufficient coverage of the autumn and winter months to provide adequate information on GBT_p concentrations in the winter period, and whether the peak in concentration observed in the 1 L data set during October 2012 and 2013 also occurred in the 10 mL samples. The GBT_p maxima in the 1 L data set occurred in October 2012 and 2013. If this pattern was replicated in the 10 mL sample set it is possible that higher concentrations than 484 nmol dm^{-3} could have been observed. The variability in the 10 mL data set was lower, with an average RSD of 6.6% compared to 21.4% in the 1 L samples. In addition, a smaller range of variability was observed (2.9-17.0%). Filtration of 10 mL samples was thought to place the collected cells under less stress than the filtration of 1 L samples and, as such, cause less cell damage. Since the damage inflicted would be unpredictable and inconsistent, the samples collected using the gentler method would be expected to exhibit less variability.

The 10 mL samples exhibited a narrow range of GBT_p concentrations, with the lowest concentration observed in excess of 250 nmol dm^{-3}. The concentration observed in January 2013 of (304 nmol dm^{-3}) coincided with a low GBT_p concentration (4.5 nmol dm^{-3}) in the 1 L data set. A minimum concentration of 304 nmol dm^{-3} in the low biomass winter period was deemed unlikely. It was considered possible that the ion suppression in conjunction with the small GBT signal, discussed in detail in Chapter 4, contributed to the high minimum values observed. Notably,

previous 10 mL measurements in February 2011, before the ion suppression became problematic, gave concentrations of 30 nmol dm^{-3} (Chapter 4). This indicated that the ion suppression, in combination with the small GBT signal observed in 10 mL samples, was increasing the effective limit of detection and reducing the method's ability to quantify potentially low concentrations. However, an average concentration of 335 nmol dm^{-3} was observed in samples collected during March 2012 (Chapter 4). These samples were also analysed during a period of lower ion suppression. This concentration, measured before the ion suppression became problematic, provides evidence that high concentrations could be measured during relatively low biomass periods and that the high concentrations should not necessarily be discounted. The limited coverage of the winter period in the 10 mL data set made it difficult to ascertain if there was a systematic problem.

The seasonal variability observed in this study showed similar trends to a seasonal study of GBT_p carried out in 2006-2007 using particulates collected from 2-3 L water samples at station L4 (Airs et al., unpublished data). The 2006-2007 seasonal study showed three periods of increased GBT_p concentration. The first period showed a peak in GBT_p concentration of 11 nmol dm^{-3} in spring, which was followed by a late summer peak of 14.3 nmol dm^{-3} and finally, an autumn increase to 19.1 nmol dm^{-3}. Both the 2006-2007 and 2012-2013 data sets exhibited a similar seasonal pattern of increases in GBT_p concentrations during spring and in the late summer with the largest peak in GBT_p concentrations observed in autumn. The three data sets also showed a clear stepwise increase

in observed GBT_p concentrations with decreasing filter volumes. Particulates collected from 2-3 L samples gave a maximum concentration of 19.1 nmol dm^{-3}, this maximum concentration is less than half the maximum concentration (49 nmol dm^{-3}) observed in particulates collected from 1 L samples. Both the 1 L and 2-3 L sample concentrations were an order of magnitude lower than the maximum concentration observed in particulates collected from 10 mL samples (484 nmol dm^{-3}).

5.6 Particulate glycine betaine concentrations and environmental variables

A BIO-ENV analysis of the potential contribution of environmental variables to observed GBT_p concentrations was carried out using PRIMER-E software. The environmental variables analysed included: SST, salinity, inorganic nutrients (nitrate, nitrite, phosphate, silicate and ammonium), Chl *a*, phytoplankton carbon and nitrogen (POC and PON) and dissolved organic nitrogen (DON). The only significant environmental variable selected by the BIO-ENV analysis was Chl *a* which potentially contributed 24.8% to the variability observed in the GBT_p concentrations.

5.6.1 Particulate glycine betaine concentrations and chlorophyll

Based on the BIO-ENV analysis, pigment concentrations, analysed using HPLC, were interrogated for potential relationships to GBT_p concentrations from the 1 L sample set. Pigment samples were collected from the CTD and filtered (GF/F) on board the boat and the filters flash frozen in liquid nitrogen and stored at -80°C before analysis by HPLC. A significant, positive correlation was found between the Chl *a* and GBT_p concentrations (Figure 5.5, Regression: $F=25.08$ with $df=1$ and $p<0.0001$, $R^2= 39.8\%$). The positive correlation provided evidence for phytoplankton as a source of GBT_p. A study of $DMSP_t$ at the same site that found no significant relationship with Chl *a* (Archer et al., 2009), and concluded that with seasonal taxonomic succession, the relative investment in Chl *a* and DMSP accumulation altered. In contrast, the positive correlation between Chl *a* and GBT_p concentrations indicates a significant contribution from several phytoplankton groups throughout the year.

In addition to being nitrogen-containing, a GBT molecule also contains 5 carbon atoms. Consequently, in addition to requiring a nitrogen source, GBT production would also require a source of fixed carbon, which could be provided, via photosynthesis, by chlorophyll. Furthermore, GBT has been implicated in protecting cells in higher plants and cyanobacteria against photo-oxidative stress and photo-inhibition by protecting Photosystem II (PSII) (Kondo et al., 1999; Papageorgiou and Murata, 1995; Prasad and Saradhi, 2004). Increased levels of GBT were associated with the accelerated recovery of the PSII complex from a photo-inhibited state in transgenic *Brassica juncea* (Prasad and Saradhi, 2004) and with a reduction in the amount of toxic oxygen species produced under high light stress in higher plants and cyanobacteria (Papageorgiou and Murata, 1995). Further studies used the cyanobacterium *Synechococcus*, engineered to over produce and accumulate GBT, to demonstrate that the modified cells were more tolerant to light than the control cells. Though this light protecting potential has not been demonstrated in phytoplankton, GBT could be required during periods of high light to protect the cells against photo-inhibition.

The GBT_p: Chl *a* ratio, a proxy for intracellular GBT concentration relative to light-harvesting capacity, was calculated (g: g) and plotted as a function of time for both the 1 L and 10 mL sample sets (Figure 5.6). The calculated ratios for the 1 L data set varied from 0.24-3.1 with the highest values occurring in the summer months and in October 2012. Interestingly, though both October 2012 and October 2013 had very similar GBT_p concentrations, the calculated ratio during October 2013 was approximately two thirds of that calculated in October 2012. The calculated ratios for the 10 mL data set varied from 103-724 and, where

there was sufficient coverage (limited coverage due to sample loss), mirrored the ratios calculated for the 1 L data set.

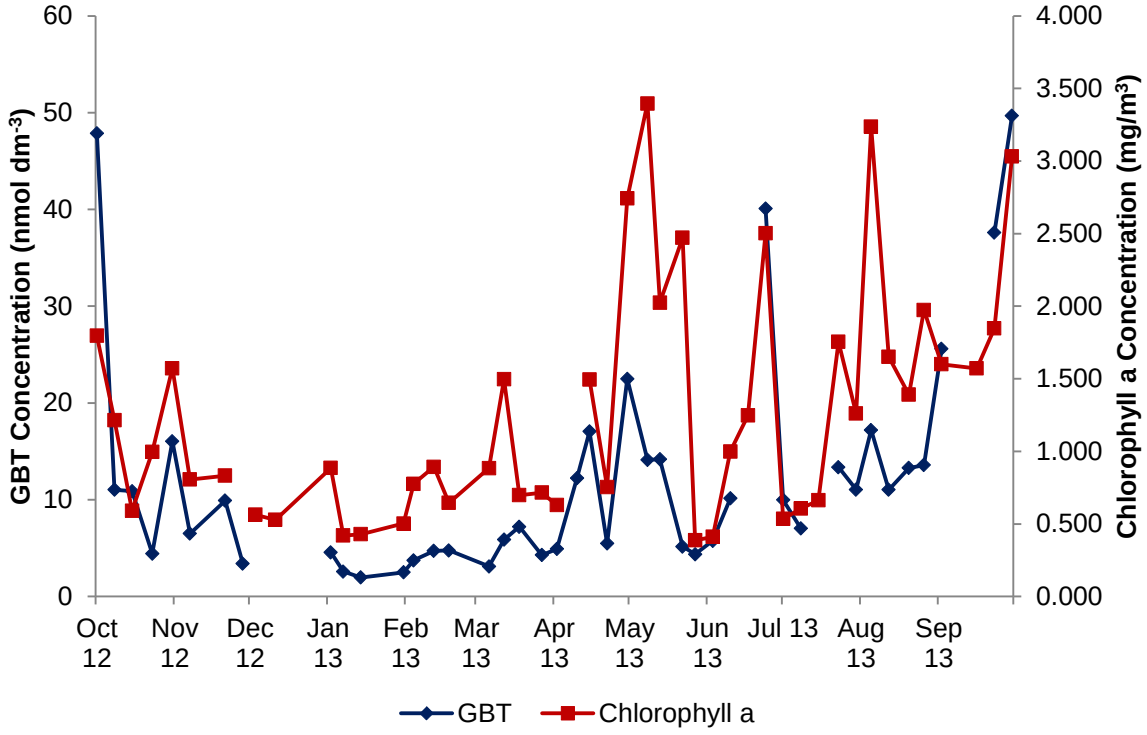

Figure 5.5: Seasonal chlorophyll *a* and GBTp (1 L samples) concentrations measured at station L4 during October 2012-October 2013

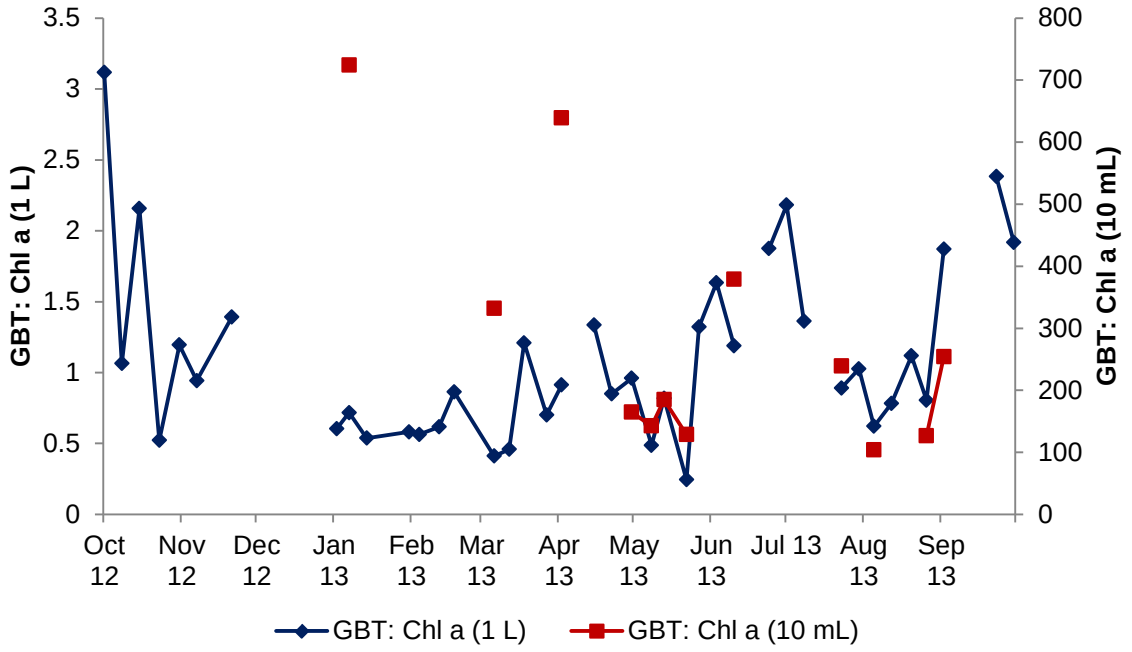

Figure 5.6: Calculated ratio GBT: Chl a (g:g) measured at station L4, (October 2012-October 2013)

Ten additional primary pigments were analysed for coincidence with GBT_p concentrations (Table 5.1). Of the ten pigments tested, seven pigments showed a significant positive correlation with GBT_p concentrations. The seven pigments were then further interrogated for particular correlations with increases in GBT_p concentration. Concentrations of the pigments increased during the spring bloom period and during August 2013, both of which were periods where the phytoplankton biomass increased.

Two further notable increases in GBT_p concentrations occurred during the spring bloom period and August 2013. The increase in GBT_p concentration in early July coincided with a *Prorocentrum cordatum* bloom. Increases in concentrations of four primary pigments were coincident with the July increase: chlorophyll *b*, chlorophyll *c*, diadinoxanthin and peridinin. Of these four, the most notable correlation was with peridinin. Peridinin concentrations remained low throughout the year except for 1st July 2013 when the concentration peaked briefly at 1.04 mg m^{-3}. Peridinin is a specific biomarker for Type 1 Dinophyta (Jeffrey and Wright, 2006). The second notable increase in GBT_p concentration occurred during October 2013. Peaks in chlorophyll b and alloxanthin concentrations were coincident with this increase. Alloxanthin is present in cryptophytes and some dinoflagellates such as *Dinophysis*; however no significant concentrations of either were observed during the October 2013 period.

Table 5.1: Regression analysis of 11 pigment concentrations with GBT_p concentrations at Station L4.

Pigment	p value	Correlation
Total Chlorophyll *a*	< 0.0001	Y
Total Chlorophyll *b*	0.002	Y
Total Chlorophyll *c*	0.004	Y
Carotenes	< 0.0001	Y
Alloxanthin	0.011	Y
19'-butanoyloxyfucoxanthin	0.48	N
Diadinoxanthin	0.006	Y
Fucoxanthin	0.001	Y
19'-hexanoloxyfucoxanthin	0.068	N
Peridinin	0.005	Y
Zeaxanthin	0.446	N

GBT showed positive correlations with carotenoids that have been assigned a photoprotective role (carotenes, alloxanthin and diadinoxanthin) as well as those that are considered to be photosynthetic (fucoxanthin and peridinin) (Table 5.1) (Hooker et al., 2005). GBT did not correlate, however, with all photoprotective or photosynthetic carotenoids. GBT is therefore not expected to play the same functional role across different classes. Notably, both GBT (from this study) and DMSP (Archer et al., 2009) had a positive relationship with the photoprotective xanthophyll compound diadinoxanthin.

5.6.2 Particulate glycine betaine and phytoplankton carbon

An analysis of the ratio of GBT_p to phytoplankton biomass carbon (phytC, g: g), measured using phytoplankton biomass was carried out for both the 1 L and 10 mL data sets (Figure 5.7). Phytoplankton abundance was analysed by light microscopy using water collected from station L4 and allowed to settle for 48 hours. Cell volumes were calculated according to Kovala and Larrance (1996) and these values converted to carbon according to Menden-Deuer and Lessard

(2000) (Section 7.5.1). For the 1 L data set the ratio varied throughout the year with highest ratios occurring in April and October 2013. These were periods when GBT_p comprised a higher proportion of the phytC in the water. These high ratios also coincide with high Chl *a* measurements; this could potentially mean that a higher proportion of available carbon was being used for GBT_p synthesis in phytoplankton. For the 10 mL data set the ratio varied throughout the year with the highest ratios occurring in January and April 2013, there were no data points corresponding with the high October ratios observed in the 1 L data set. However, the GBT_p concentration used to calculate the January ratio was considered analytically unreliable.

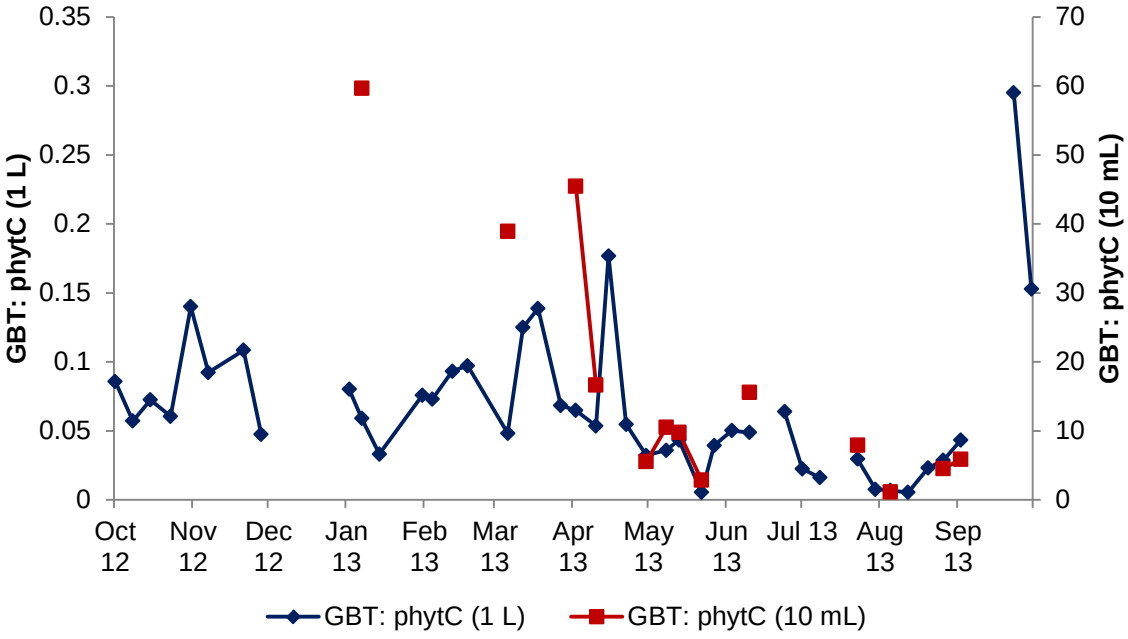

Figure 5.7: Ratio of GBT_p: phytC (g: g) calculated for the 1 L and 10 mL GBT data sets, using calculated phytoplankton carbon biomass

The ratio of GBT: phytC and Chl *a*: phytC (both g:g) showed a close relationship between the two, providing further evidence of a phytoplankton source of GBT (Figure 5.8).

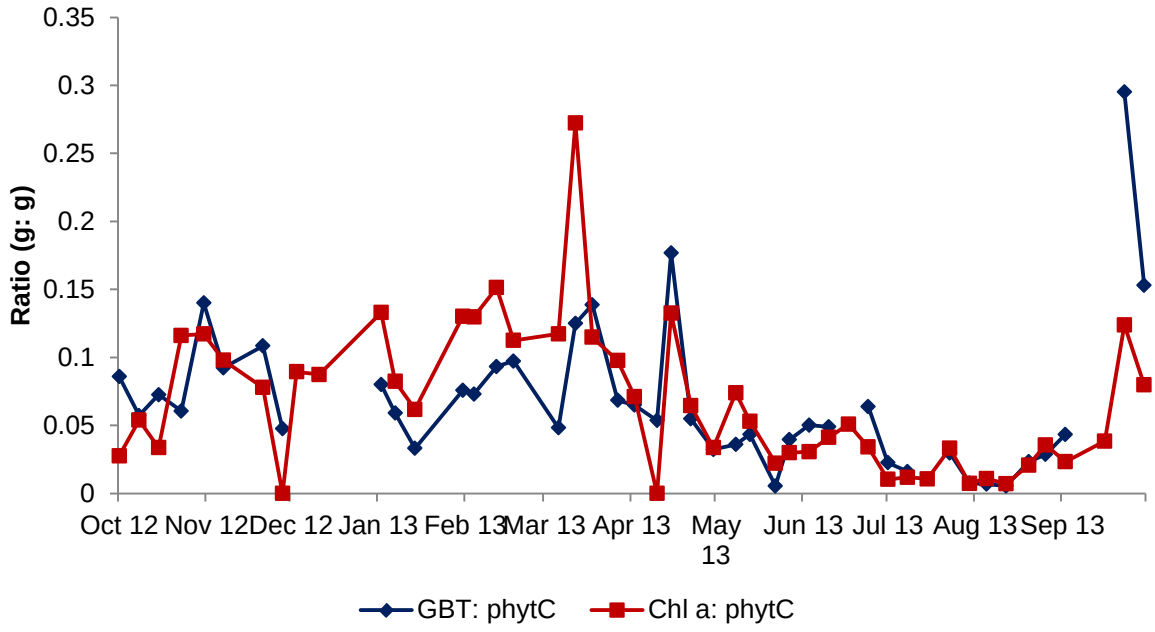

Figure 5.8: Ratio of GBT_p: phytC and Chl *a*: phytC (g: g) calculated for the 1 L data set, using calculated phytoplankton carbon biomass

5.6.3 Particulate glycine betaine and PAR

GBT has been proposed to protect cells against photo-inhibition and photo-oxidative stress. To test the potential effect of light on GBT_p production, the observed GBT_p concentrations were compared with the photosynthetically active radiation (PAR), the amount of light available for photosynthesis, measured at a depth of 2 m at station L4 using a Chelsea sensor attached to the CTD. The two data sets did not show a significant correlation (Regression: F=0.27 with df=1 and p=0.605, R^2=0.7%) (Figure 5.9).

The PAR was compared with the calculated ratio of GBT_p: Chl *a* (Figure 5.10). A regression analysis showed no significant correlation between the two data sets (Regression: F=0.003 with df=1 and p=0.87, R^2=0.1%) however there were some notable dates where high PAR coincided with high GBT_p: Chl *a* ratios during April, June and July 2013. This is in contrast with the study of $DMSP_t$ at the same

site; DMSP: Chl *a* positively correlated with PAR at station L4 (Archer et al., 2009), which may indicate that the two osmolytes may play different intracellular roles.

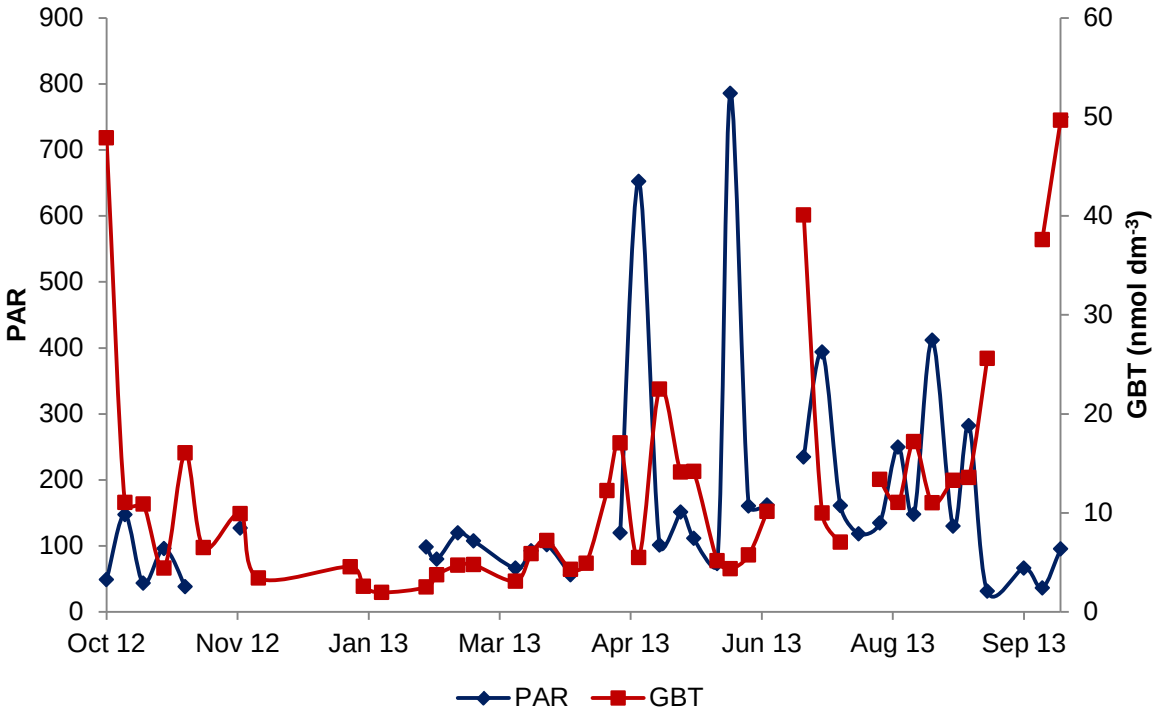

Figure 5.9: GBT_p concentration and PAR measured at station L4, October 2012-October 2013

The GBT_p: Chl *a* ratio is used as a proxy for intracellular GBT concentration relative to light-harvesting capacity (Archer et al., 2009). The three periods identified where high PAR coincided with a high GBT_p: Chl *a* ratio could indicate that the production of GBT compared to Chl a was increased in response to a cellular requirement for photo-protection.

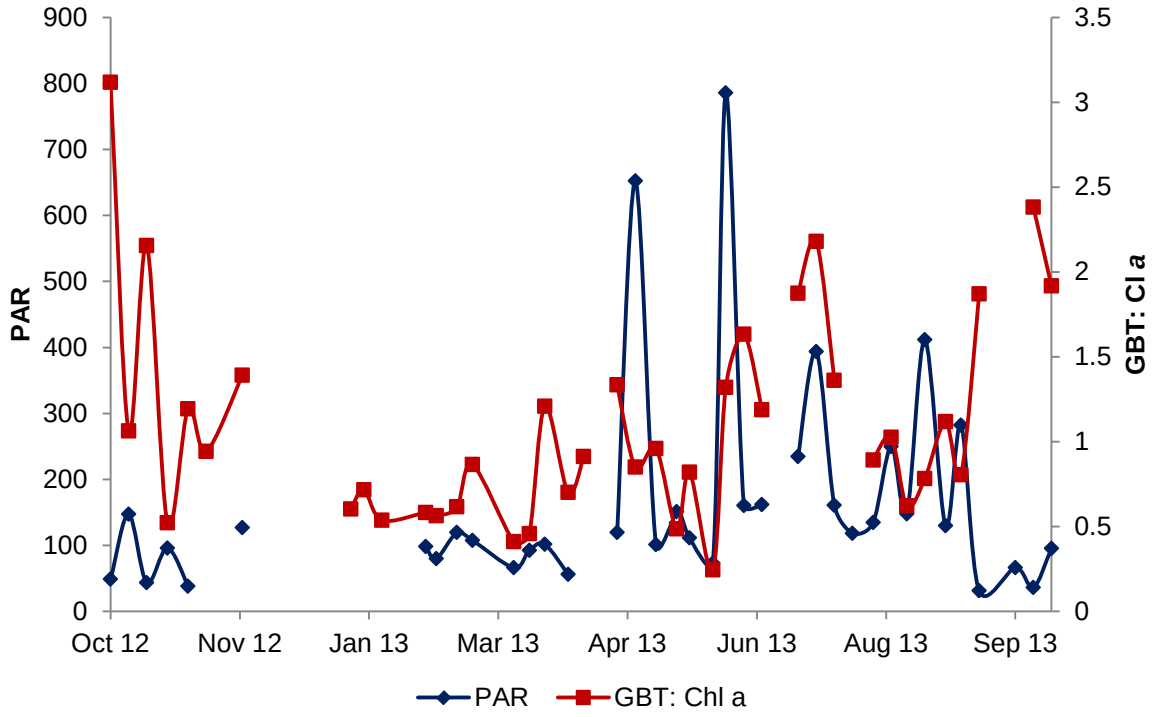

Figure 5.10: Calculated GBT_p: Chl a ratio and the PAR measured at station L4, October 2012-October 201

5.6.4 Particulate glycine betaine and salinity

As a compatible solute one of GBTs primary roles is to protect cells against changes in salinity (Welsh, 2000). Salinity at station L4 varies little compared to other environments, such as estuaries (Smyth et al., 2010). No significant relationship was found between GBT_p concentration and salinity at L4 (Figure 5.11). During a particularly wet season in November 2012, a sharp drop in salinity to 34.26 PSU was observed (28th November 2012); however, only a small peak in GBT_p concentration of 9.9 nmol dm^{-3} was observed (Figure 5.11). Therefore an effect of salinity variation on GBT production was not observed at L4.

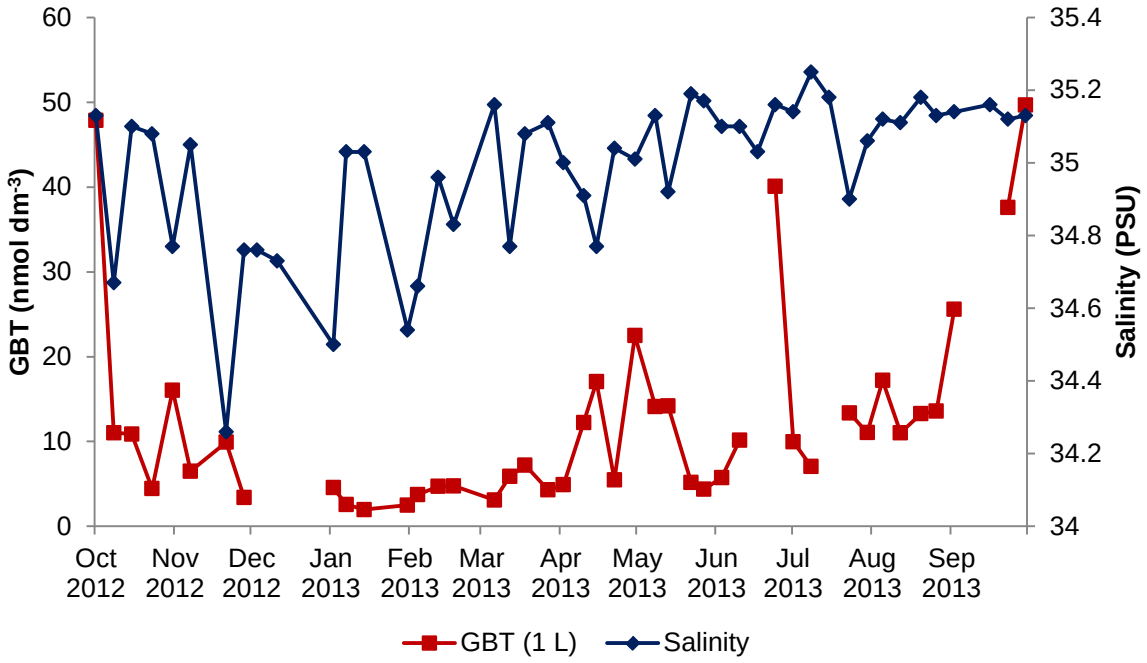

Figure 5.11: Salinity and GBT_p concentrations measured at station L4, October 2012-October 2013)

5.6.5 Particulate glycine betaine and mixed layer depth

The calculated mixed layer depth (MLD) was analysed in conjunction with the 1 L GBT_p data set to identify relationships. Formation of an MLD intensifies the levels of PAR experienced by phytoplankton in the near-surface waters. The MLD depth was calculated according to Kara et al. (2000) using temperature data collected from the CTD (Section 7.5.7). Spring peaks in GBT_p concentration were observed before the formation of a mixed layer (Figure 5.12). Two peaks in GBT_p concentration on the 7th May 2013 and 1st July 2013 were found to coincide with periods of shallow MLD, potentially due to higher light intensity stimulating phytoplankton (Figure 5.12). Following the breakdown of stratification and loss of the MLD a marked increase in GBT_p concentrations was observed from 30th September 2013. This could have resulted from the breakdown of stratification, and mixing of nutrient rich bottom water which increased GBT_p production (Figure 5.12).

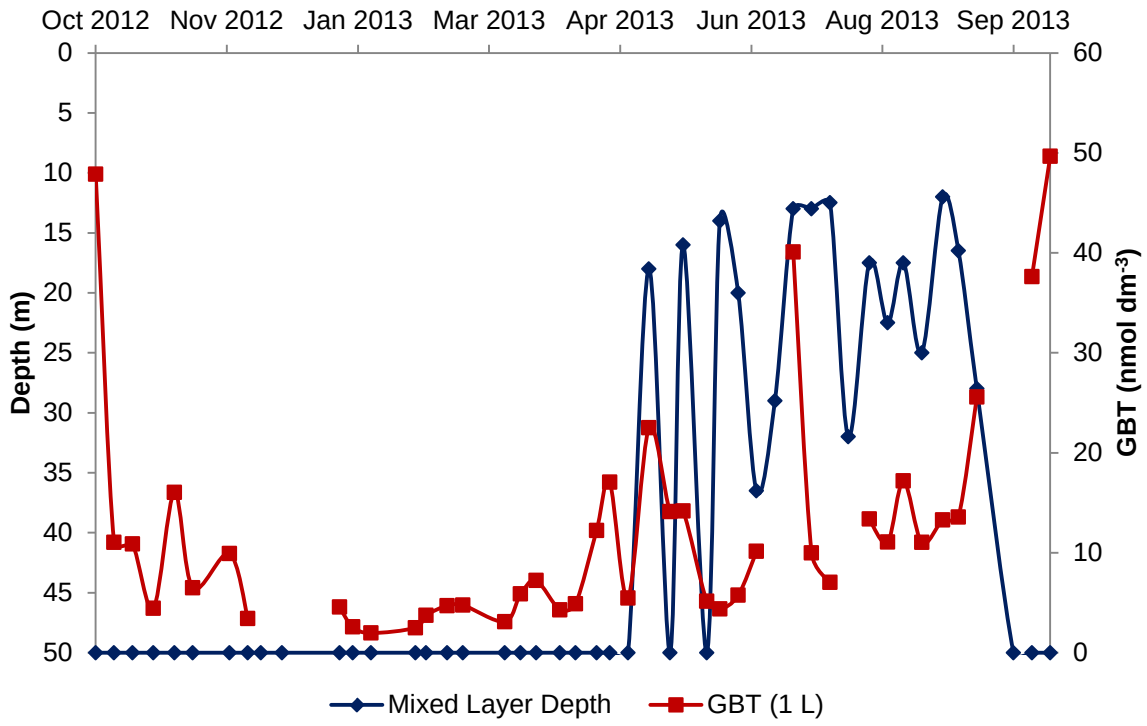

Figure 5.12: Calculated mixed layer depth and GBT_p concentration at station L4, October 2012-October 2013

5.7 Contributors to standing stocks of glycine betaine

The data set for the 1 L samples provided a comprehensive insight into the seasonal variability of GBT_p at station L4. Although not representing the true GBT_p concentrations, the significant correlation between the 1 L and 10 mL concentrations indicated that the relative changes in the concentrations for 1 L samples could be used for comparison with environmental variables.

5.7.1 Particulate glycine betaine concentrations and their relationship to phytoplankton assemblage at station L4

The 1 L data set was analysed in conjunction with the phytoplankton assemblage at station L4, analysed by microscopy and converted to carbon biomass (Section 7.5.1) to identify any potential contributors to the GBT_p concentration. Comparisons of the GBT_p concentration with the total phytoplankton biomass, the total diatom biomass and the total dinoflagellate biomass were carried out (Figure 5.13). Some correspondence was observed between GBT_p and phytoplankton biomass, for example during April and May 2013; however no simple relationship was identified so a statistical approach was applied.

The phytoplankton biomass was analysed for correlations with the maxima in GBT_p concentrations using a BV-STEP analysis carried out using PRIMER-E software. An initial analysis of data from the entire year was carried out using the top 10% of species contributing to the phytoplankton assemblage. This analysis identified five species that could potentially contribute up to 26% of the variability observed in the 1 L GBT_p dataset: *Chaetoceros socialis*, *Pseudo-nitzschia "delicatissima"*, *Prorocentrum cordatum*, *Calyptrosphaera* and *Thalassiosira* (approximate size 60 µm) (Figure 5.14 and Figure 5.15). *Chaetoceros socialis* and *Pseudo-nitzschia "delicatissima"* blooms were observed in May, July and September 2013 coincident with increases in GBT_p concentration (Figure 5.14). Additionally, an intense *Prorocentrum cordatum bloom* coincided with a sharp peak in GBT_p concentration in July 2013 (Figure 5.15). Blooms in the coccolithophore *Calyptrosphaera* coincided with small increases in GBT_p concentrations in the autumn and winter periods (Figure 5.15).

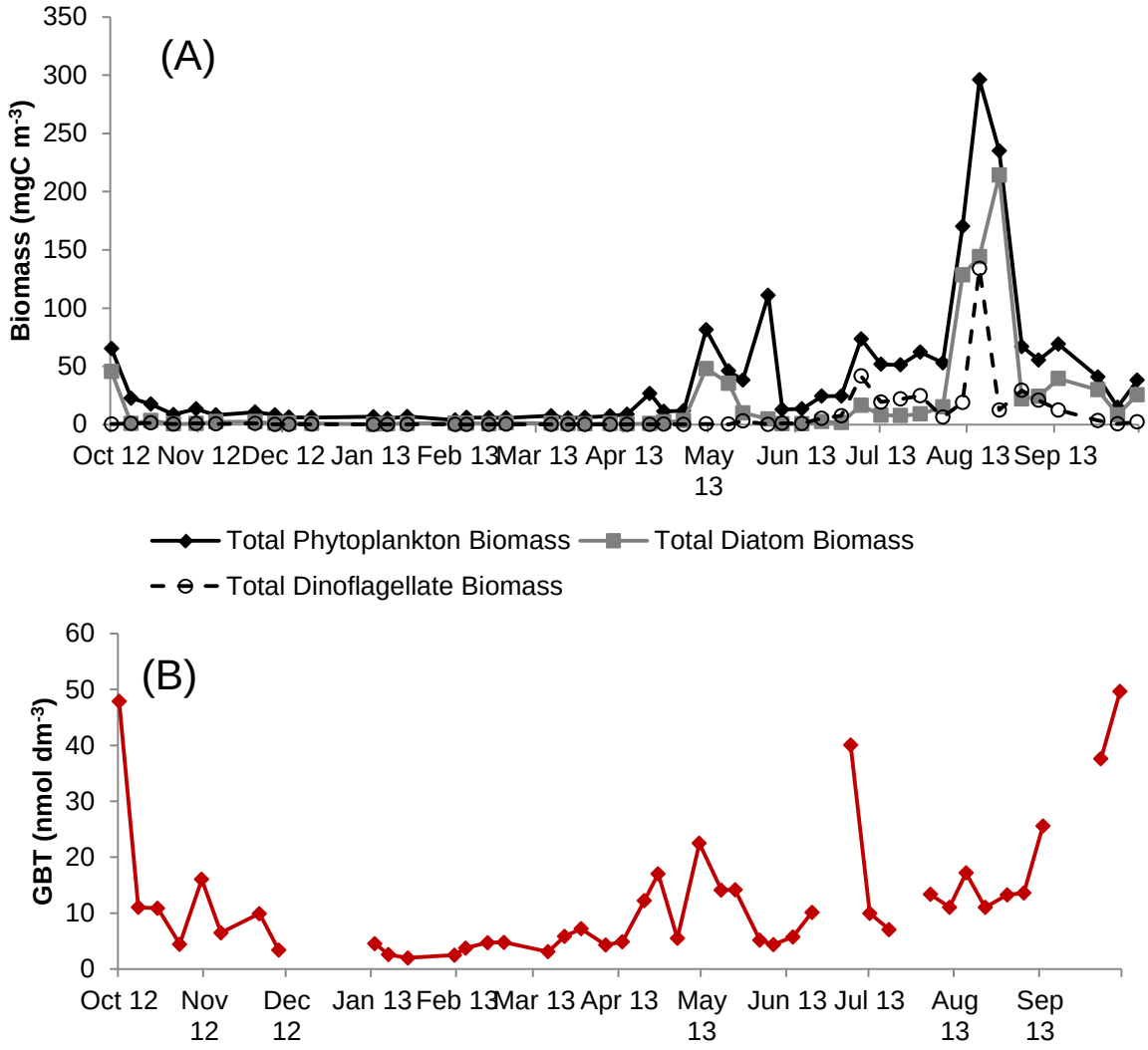

Figure 5.13: Total (A) total phytoplankton biomass, total diatom biomass and total dinoflagellate biomass and (B) 1 L GBT_p concentration measured at station L4 during October 2012-October 2013

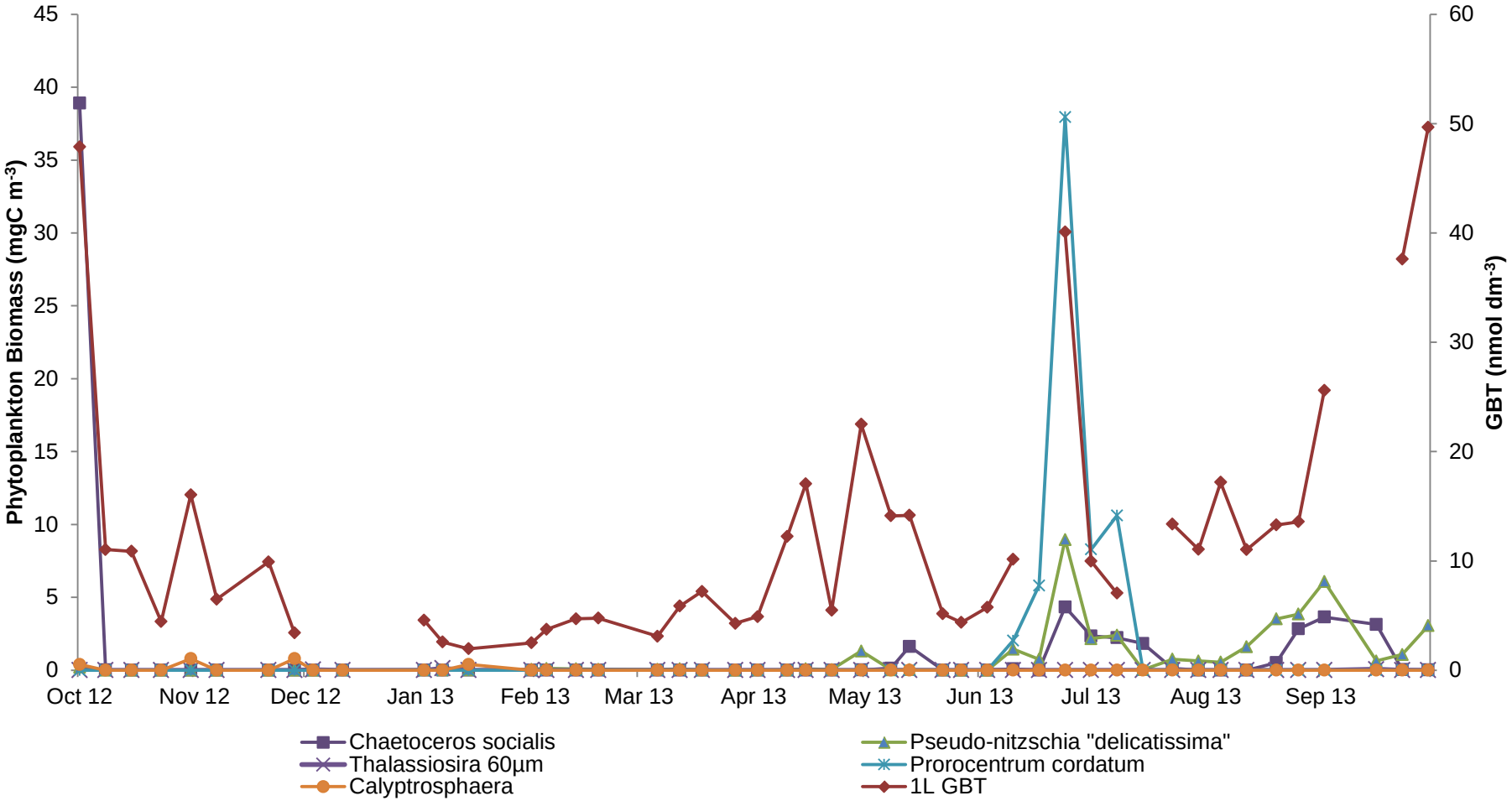

Figure 5.14: 1 L GBT_p concentrations and significant phytoplankton species biomass, identified using the BV-STEP statistical test, at station L4 during October 2012-October 2013

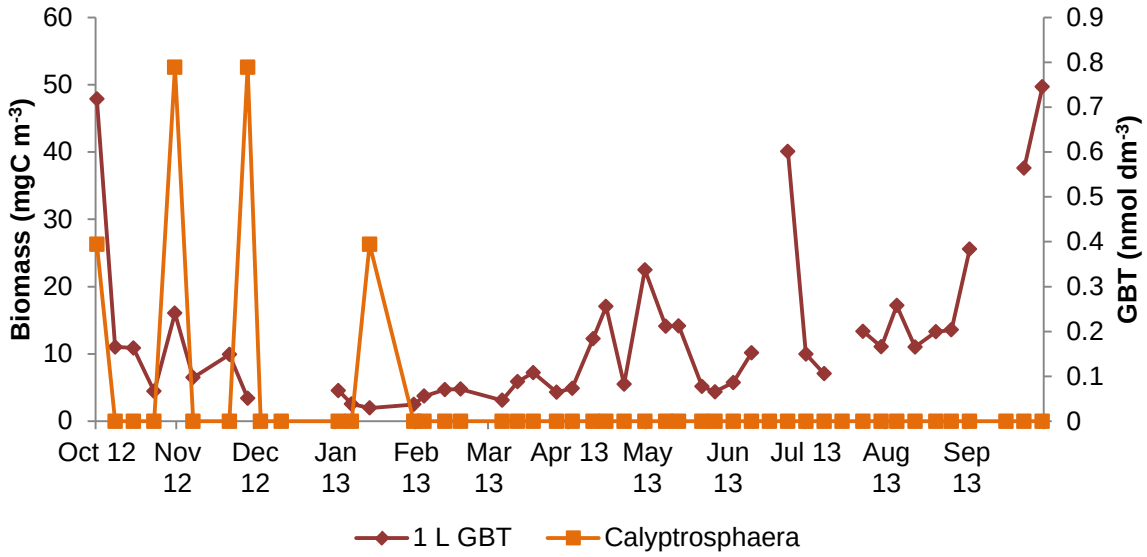

Figure 5.15: 1 L GBT_p concentrations and *Calyptrosphaeara* biomass at station L4 during October 2012-October 2013

In-depth analysis of the contribution of certain phytoplankton species to the measured GBT_p concentrations were carried out using the BV-STEP analysis of the entire phytoplankton data set for spring (March-May), summer (June-August) and autumn (September-November). The analysis for the spring period identified ten phytoplankton species that could have contributed up to 73% of the variability observed in the GBT_p concentration during that period (Figure 5.16). Three notable contributions were observed from *Rhizosolenia styliformis*, *Chaetoceros curvisetus* and *Pseudo-nitzschia "delicatissima"* during April and May 2013. *Rhizosolenia styliformis* abundance was observed to coincide with two peaks in GBT_p concentrations of 17.0 nmol dm^{-3} in April and 22.5 nmol dm^{-3} in May. *Pseudo-nitzschia "delicatissima"* and *Chaetoceros curvisetus* were observed to coincide with the May increase in GBT_p concentration (22.5 nmol dm^{-3}). Culture studies demonstrated the presence of GBT (<0.01pg GBT $cell^{-1}$) in *Chaetoceros gracilis* but not in *Chaetoceros didymus* (Spielmeyer et al., 2011). These culture

studies supported the hypothesis that *Chaetoceros* may be GBT- producing and so could have contributed to the GBT_p concentrations observed at station L4.

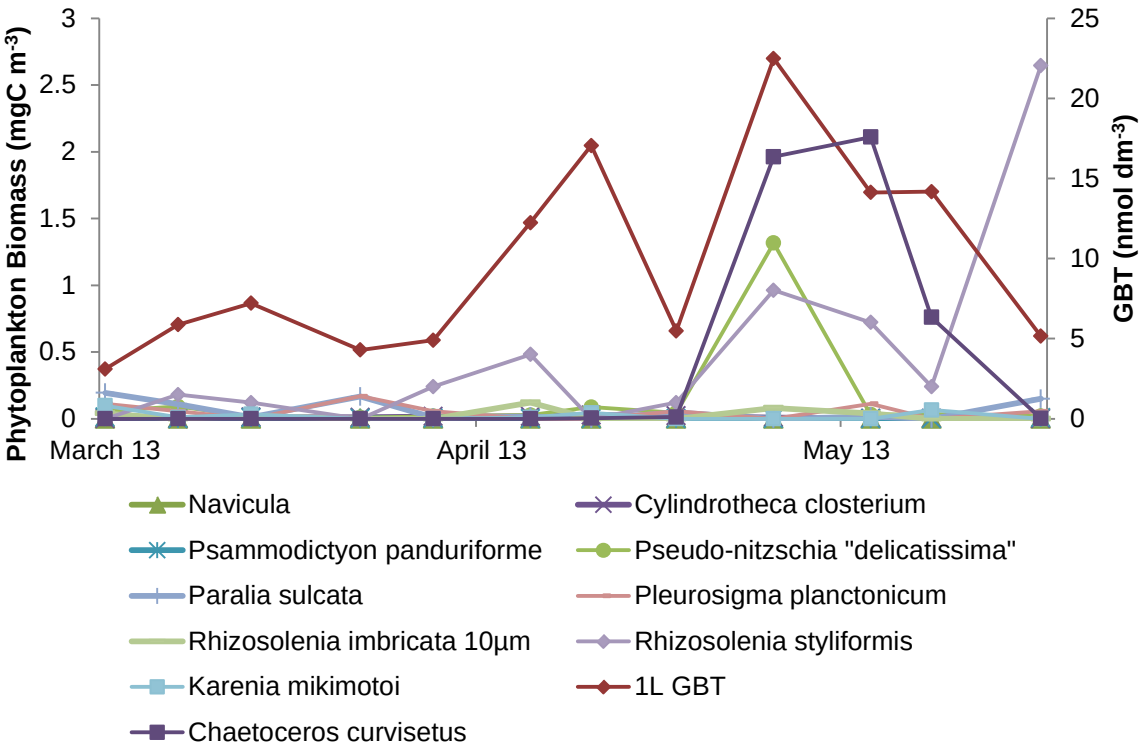

Figure 5.16: 1 L GBT_p concentrations and significant phytoplankton species, identified using the BV-STEP statistical test, during spring at station L4 during October 2012-October 2013

The BV-STEP analysis of the summer period (June-August) identified seven potential phytoplankton species that could have contributed up to 53% of the variability observed in the GBT_p concentration (Figure 5.17). Of the seven identified species, *Prorocentrum cordatum* was observed to correlate with the sharp increase in GBT_p concentration (40.1 nmol dm-3) with a brief, intense bloom in July. *Prorocentrum miniumum* in culture has been reported to contain GBT at 6.9 pg $cell^{-1}$ (Spielmeyer et al., 2011) a concentration substantially higher than any of the other 15 species analysed, consistent with *Prorocentrum* cells comprising a substantial contribution to the GBT_p concentration at station L4. A

brief bloom is typical of the dinoflagellate abundance at L4. The dinoflagellate levels are routinely low during the winter and spring months and increase during summer when the sea surface temperature increases, culminating in a brief late summer bloom (Widdicombe et al., 2010). In addition to the *Prorocentrum cordatum* bloom, there were four other notable phytoplankton blooms: *Pseudo-nitzschia "delicatissima"*, *Chaetoceros socialis*, *Gonyaulax spinifera* and *Leptocylindrus danicus* (Figure 5.17).

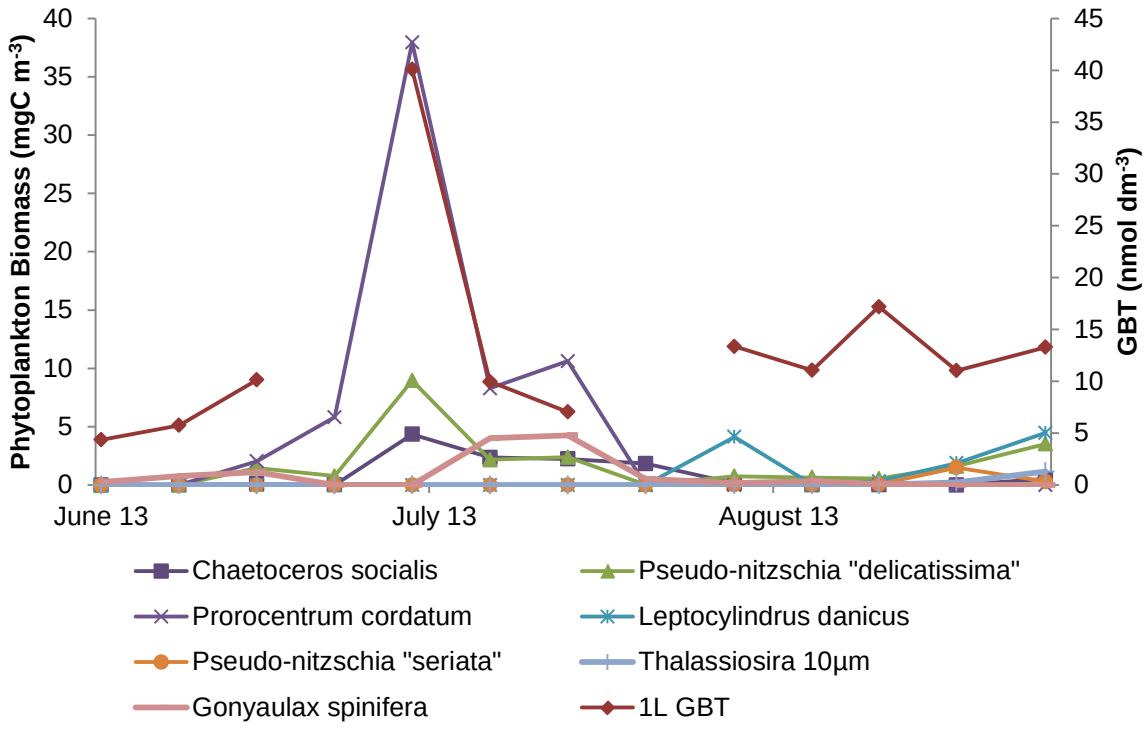

Figure 5.17: 1 L GBT_p concentrations and significant phytoplankton species, identified using the BV-STEP statistical test, during summer at station L4 during October 2012-October 2013

The BV-STEP analysis was carried out for the autumn period (October and November 2012 and September and early October 2013) and identified three phytoplankton species that could have contributed 53% of the variability observed in the GBT_p concentration (Figure 5.18). A *Chaetoceros socialis* bloom was

identified in October 2012 that coincided with the intense peak in GBT_p concentration. No phytoplankton species were observed to coincide with the October 2013 increase in GBT_p concentration.

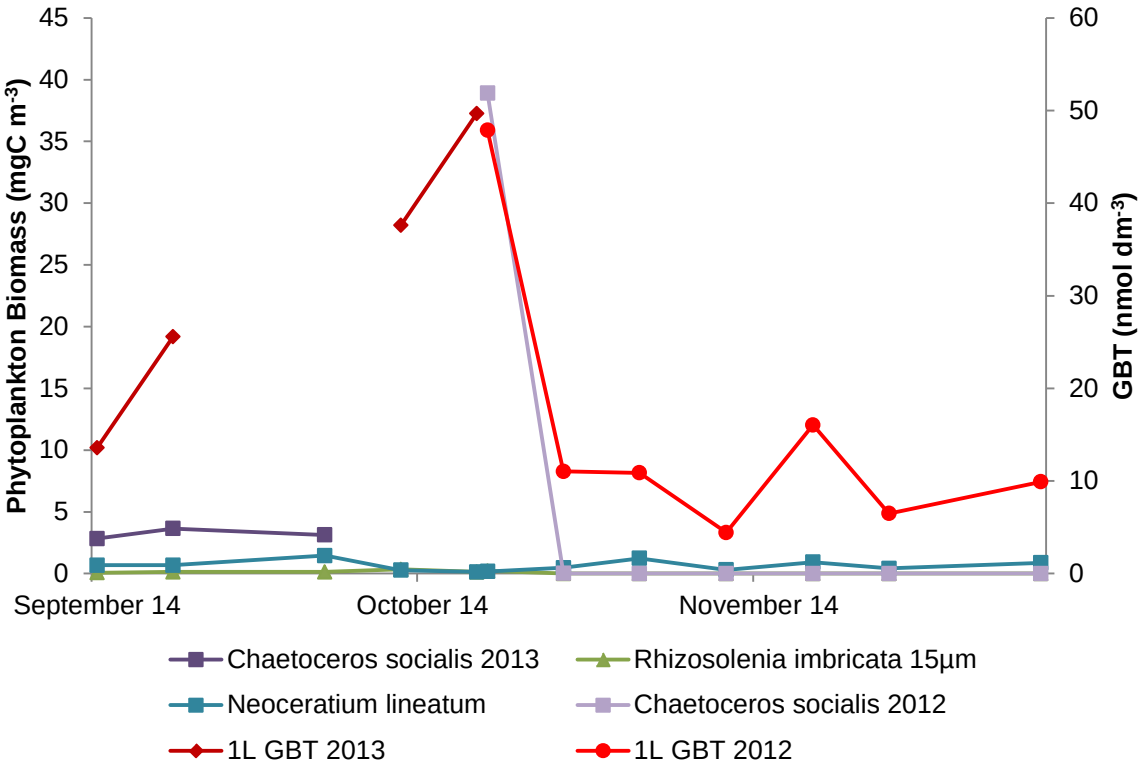

Figure 5.18: 1 L GBT_p concentrations and significant phytoplankton species, identified using the BV-STEP statistical test, during autumn at station L4 during October 2012-October 2013

Three *Phaeocystis* blooms were observed at station L4 using data collected by microscopy and flow cytometry. The first bloom occurred at the beginning of May 2013 and coincided with a relatively high GBT_p concentration. The second occurred in late May 2013 and coincided with a sharp decrease in GBT_p concentration (Figure 5.19). The third bloom occurred in late June, but there was no corresponding GBT_p concentration for that week. An increase in GBT_p concentration was

observed in the subsequent week but this was attributed to a *Prorocentrum cordatum* bloom.

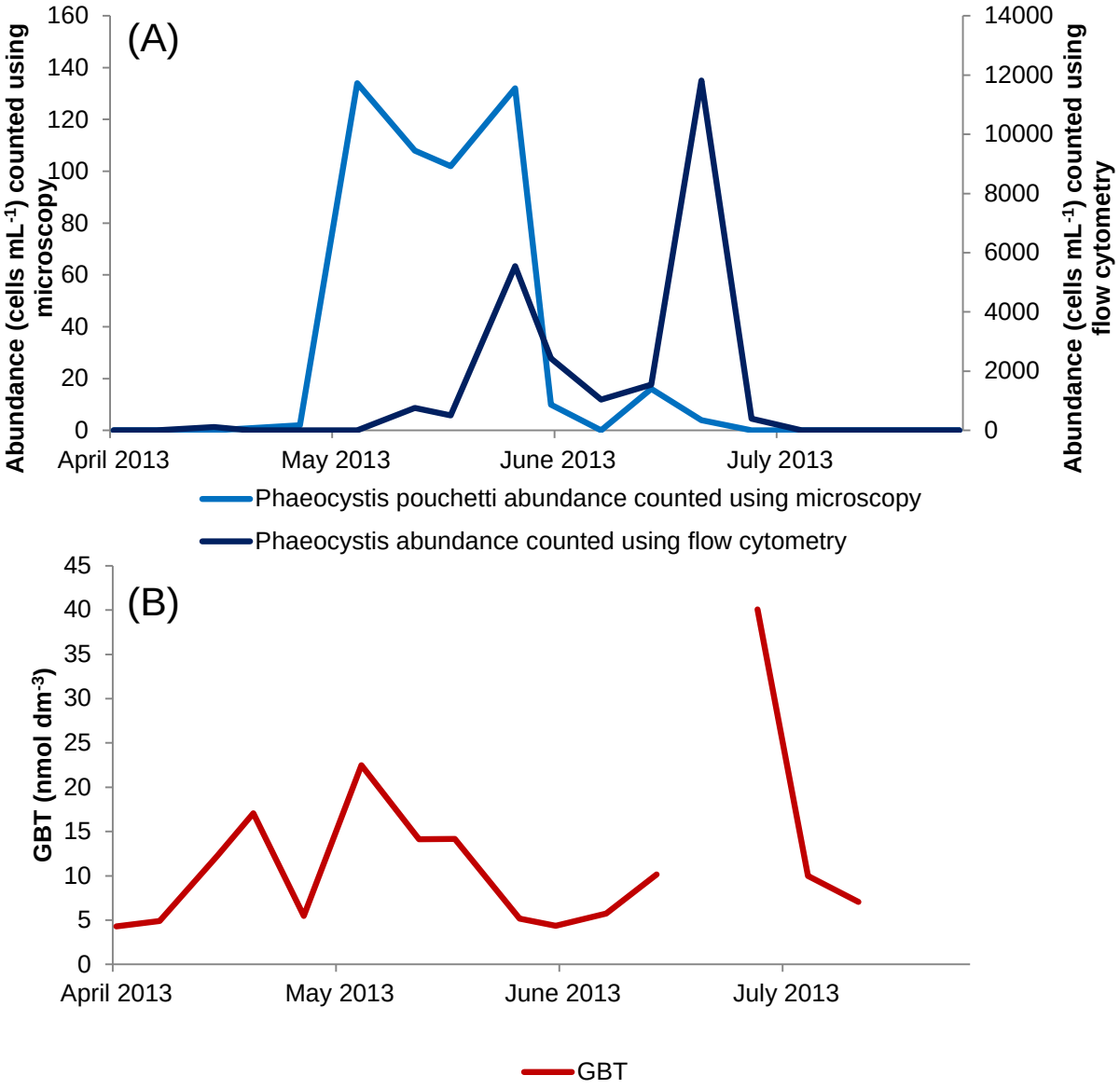

Figure 5.19: (A) Phaeocystis abundance at station L4 measured using flow cytometry and microscopy and (B) GBT concentrations, 1 L data set, April-July 2013

The *Phaeocystis* abundance did not demonstrate a clear relationship with GBT_p concentrations. Where there was corresponding GBT_p data the results were conflicting. In early May the *Phaeocystis* bloom coincided with a peak in GBT_p

concentration, however, in late May the *Phaeocystis* bloom coincided with a sharp decrease in GBT_p concentration. These conflicting observations indicated no clear relationship between *Phaeocystis* abundance and GBT_p concentration. The early May peak in GBT_p concentration had, however, been attributed to *Rhizosolenia styliformis*, *Chaetoceros curvisetus* and *Pseudo-nitzschia "delicatissima"* so it is possible that the early May *Phaeocystis* bloom did not contribute to the observed GBT_p concentrations. There are no known culture studies analysing GBT production by *Phaeocystis*. *Phaeocystis* is, however, a significant producer of DMSP (van Duyl et al., 1998) and, as such, its contribution to GBT concentrations is an important unknown.

Statistical analysis of both the environmental variables and phytoplankton assemblage showed that phytoplankton composition can partly explain the GBT_p concentrations observed. However, there are limitations to the microscopy approach (e.g. small cells can be missed). In addition, there are other potential sources of GBT_p, such as zooplankton and bacteria, which cannot be routinely quantified as separate fractions using the analytical method.

5.7.2 Particulate glycine betaine concentrations compared with nitrogen-containing nutrient levels measured in the Western English Channel

In addition to its role as a compatible solute in marine microbes, it is thought that GBT can be accumulated during periods of nitrogen abundance and stored for use during times of nitrogen scarcity. In a study looking at the relationship between GBT_p concentration and nitrogen availability, production or accumulation of GBT was demonstrated to be sensitive to nitrogen availability (Keller et al., 1999b). Significant amounts of GBT_p in cultures were only observed when the cells were nitrogen replete. This indicated that a degree of nitrogen abundance was required for GBT production. To elucidate relationships between nitrogen abundance and GBT_p at station L4, the GBT_p concentrations from the 1 L data set were compared with the concentrations of inorganic nitrogen species measured at station L4 (Figure 5.20).

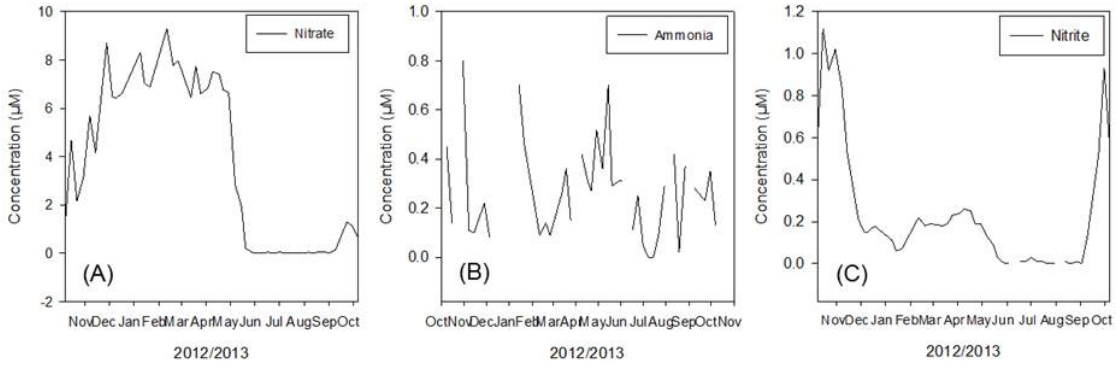

Figure 5.20: (A) Nitrate, (B) Ammonia and (C) Nitrite concentrations measured at station L4 during October 2012-October 2013

During the well-mixed winter period the nitrate concentrations were high, peaking at approximately 9 µmol dm^{-3}. A rapid depletion to below the limit of detection was evident following the spring bloom, with concentrations remaining low throughout the stratified spring-summer period. Nitrate is a potential contributor to

GBT production in the early spring bloom prior to the nitrate levels being exhausted. The addition of nitrate to nitrogen-limited cultures was shown to result in short term increases in GBT production in *Thalassiosira pseudonana, Emiliania huxleyi* and *Amphidinium carterae* (Keller et al., 1999a), indicating that nitrate concentrations could influence GBT production. The low nitrate concentrations during the summer and autumn months at station L4 would therefore have limited nitrate as a source of nitrogen for GBT production during this period. The increases in GBT_p observed during this period would, therefore, have likely been supported by other sources of fixed nitrogen.

The ammonium concentrations measured at L4 during October 2012-October 2013 revealed a number of spikes during the spring to autumn period; specifically during May-August, peaking at 0.7 µmol dm^{-3} in May. Ammonium is produced as both a waste product from cellular metabolism and a breakdown product of organic material. As such, its concentrations are likely to follow phytoplankton abundance. The importance of regenerated productivity and particularly ammonium regeneration to supporting microbial growth was demonstrated by Clark et al. (2014). Ammonium concentrations are likely to be particularly important during the summer when the phytoplankton community is considered nitrogen-limited, so during this period regenerated ammonium is likely to contribute to sustaining primary production and as a consequence, GBT production.

The seasonal nitrite concentrations at station L4 exhibit an intense autumn peak and a smaller spring-summer peak (Smyth et al., 2010). These seasonal trends

were observed in the nitrite data collected during the study period with a spring maximum of 0.22 µmol dm^{-3} in April and an autumn maximum of 1.18 µmol dm^{-3} in October. A similar trend was observed in the GBT_p concentrations. Notably, the substantial increase in nitrite concentrations in autumn coincided with the increase in GBT_p concentrations seen in the 1 L data set during both October 2012 and October 2013. This strong peak in nitrite concentration was attributed to enhanced nitrification of remineralised nitrogen following the breakdown of the late summer blooms and to the mixing of the high nitrite bottom water following the breakdown of the stratification (Smyth et al., 2010). The depth profile of nitrite concentrations at station L4 from October to December 2012 showed the accumulation of nitrite in the bottom waters as a result of the breakdown of late summer blooms. This accumulated nitrite then mixed with the rest of the water column following the breakdown of the stratification (Figure 5.21).

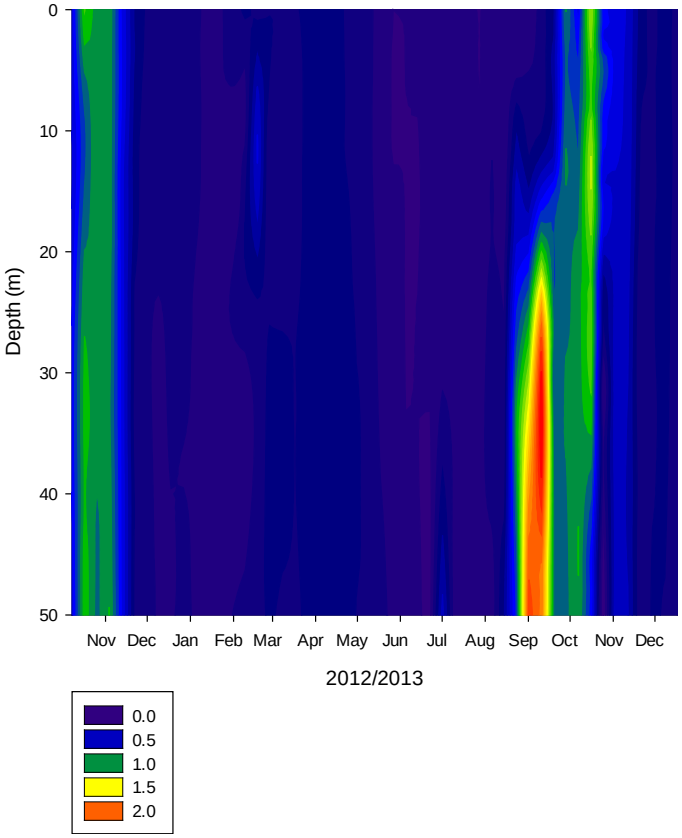

Figure 5.21: Depth profile of nitirite (µmol dm^{-3}) measured at station L4 during October 2012-Dec 2013

The substantial increase in GBT_p concentration in October 2013 could not be satisfactorily explained based on phytoplankton assemblage alone. The Chl *a* concentrations were found to significantly correlate with GBT_p during that period but no significant correlation was seen with phytoplankton biomass. However, this could be due to the microscopy approach missing smaller cells. Based on the lack of a significant biological contribution to the increase in GBT_p concentration it is possible that the nitrite availability was significant. The nitrite abundance may have allowed excess GBT_p production or accumulation to occur to be stored for use during periods of nitrogen depletion. The increase in GBT_p concentrations would then be attributed to fewer cells accumulating more GBT_p as opposed to an increase in phytoplankton cells present.

Studies have shown that phytoplankton cells are capable of taking up nitrite during periods of nitrite abundance. Nitrite uptake has been demonstrated in the European Shelf Seas with uptake rates of up to 2.08 nmol N L^{-1} h^{-1} and in the Western English Channel with rates of up to 18 nmol N L^{-1} h^{-1} (Clark et al., 2014; Wafar et al., 2004). Although nitrite represents a small proportion of the DIN pool, maintaining the opportunistic ability to assimilate nitrite in the event of episodic events that cause mixing of the water and introduction of nitrite from the bottom waters to the surface water would give phytoplankton species a competitive advantage (Wafar et al., 2004). This could be particularly relevant at station L4 where an annual short-lived peak in nitrite concentrations is observed in autumn.

In addition to the inorganic nitrogen containing nutrients, DON was considered as a potential source of fixed nitrogen for GBT production. When analysed there was no significant relationship observed between GBT_p and DON concentrations (Figure 5.22).

The DON concentrations rivalled and often exceeded the combined DIN concentrations at L4, particularly during the summer (Figure 5.22). As such, even though no significant correlation was observed, DON could still be a significant contributor of fixed nitrogen for GBT synthesis. Up to 70% of DON is thought to be bioavailable to support phytoplankton growth (Bronk, 2002). The bioavailability of DON is particularly important during the summer at station L4 when inorganic nutrient concentrations become depleted. A study in Randers Fjord in Denmark used ^{15}N labelled algal derived DON to mimic the uptake of DON (Veuger et al., 2004). The observed uptake rates for the algal derived DON in spring were

similar to those of ammonium and, in summer, exceeded the total uptake of ammonium, nitrate, urea and dissolved free amino acids. Uptake studies in the Western English channel showed urea (a dominant form of DON) uptake rates of approximately 15 nmol N L^{-1} h^{-1} (Wafar et al., 2004). Though not as high as the ammonium and nitrate uptake rates (approximately 45 and 48 nmol N L^{-1} h^{-1} respectively) these rates were comparable to the nitrite uptake rates measured (18 nmol N L^{-1} h^{-1}) at the same site.

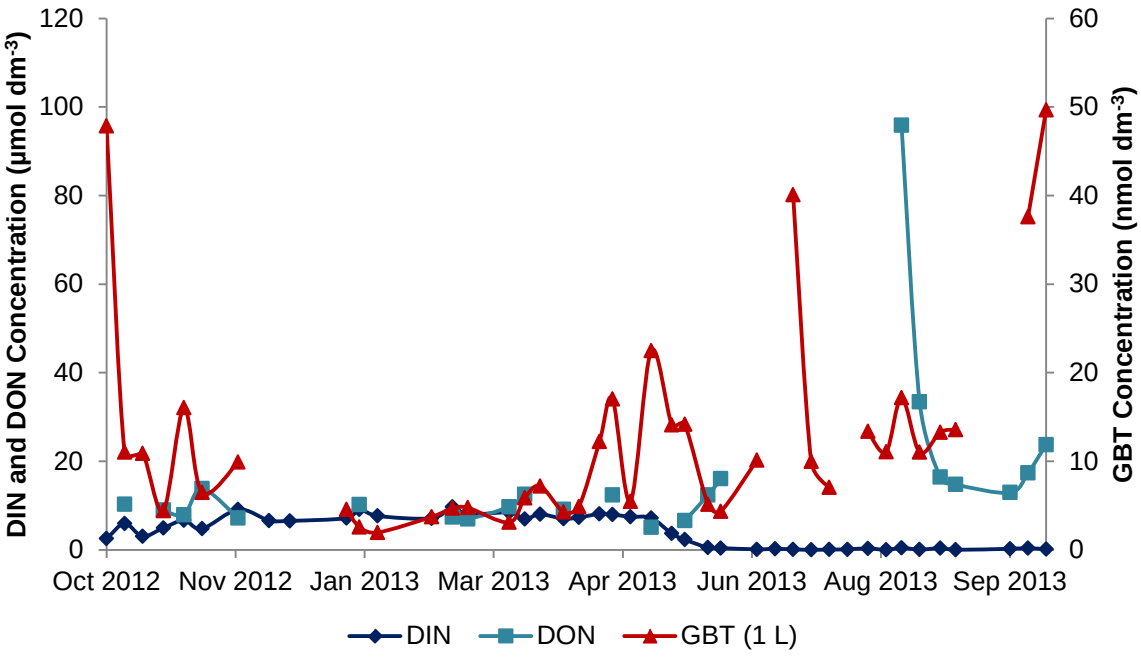

Figure 5.22: GBT_p and DON concentrations observed at station L4, October 2012-October 2013

Culture studies carried out to analyse the effect of DON on phytoplankton growth found that replacement of 50 % of the nitrate concentration with DON increased GBT_p production or accumulation in all three species analysed (*Emiliania huxleyi*, *Chaetoceros* and *Prorocentrum minimum*) (Fitzsimons et al., personal communication). For example, *Emiliana huxleyi* was cultured in triplicate with and without added DON. The concentration of GBT_p observed in cultures

approximately doubled with the addition of DON to the culture medium from 0.19 fmol cell^{-1} to 0.36 fmol cell^{-1} (Fitzsimons et al., personal communication). An extrapolation of this finding to the L4 seasonal study suggests that, the DON present could have supported the phytoplankton blooms and production of GBT during the summer period, when nitrate levels were low.

5.8 The ratio between particulate glycine betaine concentrations observed in 10 mL and 1 L samples and its relationship to the phytoplankton assemblage

Filtration studies carried out to elucidate the effect of filtration volume on observed concentration highlighted the need to investigate the potential effect of phytoplankton assemblage at station L4 on the results observed. Goldman and Dennett (1985) demonstrated that some phytoplankton species were more fragile and, as such, more susceptible to osmotic shock during filtration. For example, diatoms, with their rigid cell walls, were identified as being far less susceptible to osmotic shock and subsequent breakage during filtration than other more fragile species. This variable resilience to filtration indicated that the changing phytoplankton assemblage at L4 would likely affect the observed GBT_p concentration. The seasonal study provided the ideal opportunity to examine the affect the natural population had on the filtration effect already observed.

A comparison of the 10 mL and 1 L data sets was used to elucidate the effect of the fragility of the natural population on the GBT_p concentrations observed. If the phytoplankton assemblage did affect the concentrations observed then the effect would be apparent in the 1 L data set where the large volumes filtered were expected to damage any fragile cells present. A regression analysis of the two data sets (10 mL and 1 L) was carried out and a significant correlation observed (Regression: $F=5.15$ with $df=1$ and $p=0.047$, $R^2=34\%$) (Figure 5.23A). Both data sets followed the same general trend but a degree of variability was observed. The ratio of GBT_p in 1 L samples to the 10 mL samples was calculated and

plotted as a function of time (January – September 2013) (Figure 5.23B). A cluster of values was observed around May 2013 and it was hypothesised that the spring bloom was affecting the calculated ratio. Based on the results presented in Goldman and Dennett (1985) the calculated ratio was compared with the diatom and dinoflagellate biomass by plotting as a function of time (Figure 5.23B). The cluster of points observed during May 2013, which showed a smaller difference between the 1 L and 10 mL concentrations, coincided with a bloom in diatom biomass. This indicated that the presence of diatoms reduced the loss of GBT_p occurring in the 1 L filtrations. The influence of diatom biomass on the calculated ratio was not so pronounced during the August increase in diatom biomass. This was attributed to co-occurring high dinoflagellate biomass, which was absent in May 2013. The presence of the dinoflagellates, which are hypothesised to be affected by filtration, may have contributed to the results and obscured the effect of the diatoms.

A preliminary regression analysis of the calculated ratio and the diatom biomass showed a significant negative correlation, with the exception of two points (Regression: $F=6.86$ with $df=1$ and $p=0.028$, $R^2=43.2\%$). The first point coincided with the January data point which was considered suspicious due to analytical problems with that data point. The second point coincided with the exceptionally high dinoflagellate biomass observed in August 2013. This may be a result of the presence of dinoflagellates obscuring the effect of the diatoms. The significant correlation indicated that, the higher the diatom biomass the smaller the difference between the 1 L and 10 mL sample concentrations, which was attributed to the resilience of diatom cells. However, it is important to note that the

periods of high diatom abundance coincided with periods of high GBT_p concentrations, when the 1 L samples show higher observed concentrations. Consequently, it was possible that the difference was not due to differences in phytoplankton assemblage but to the higher 1 L GBT_p concentrations. Nonetheless, it was expected that the 1 L samples, which are more affected by the natural phytoplankton assemblage, would affect the calculated ratio. The smaller volume (10 mL) filtrations were thought to minimise the stress placed on the cells. Therefore there was no expectation of observing the effect of phytoplankton resilience on measured concentrations in this data set. Consequently, it was the 1 L data set that was expected to exhibit the variations that would impact upon the calculated ratio. A more comprehensive data set would be required allow firm conclusions to be reached but the initial data presented here indicated that the natural phytoplankton assemblage does impact on the filtration effect observed.

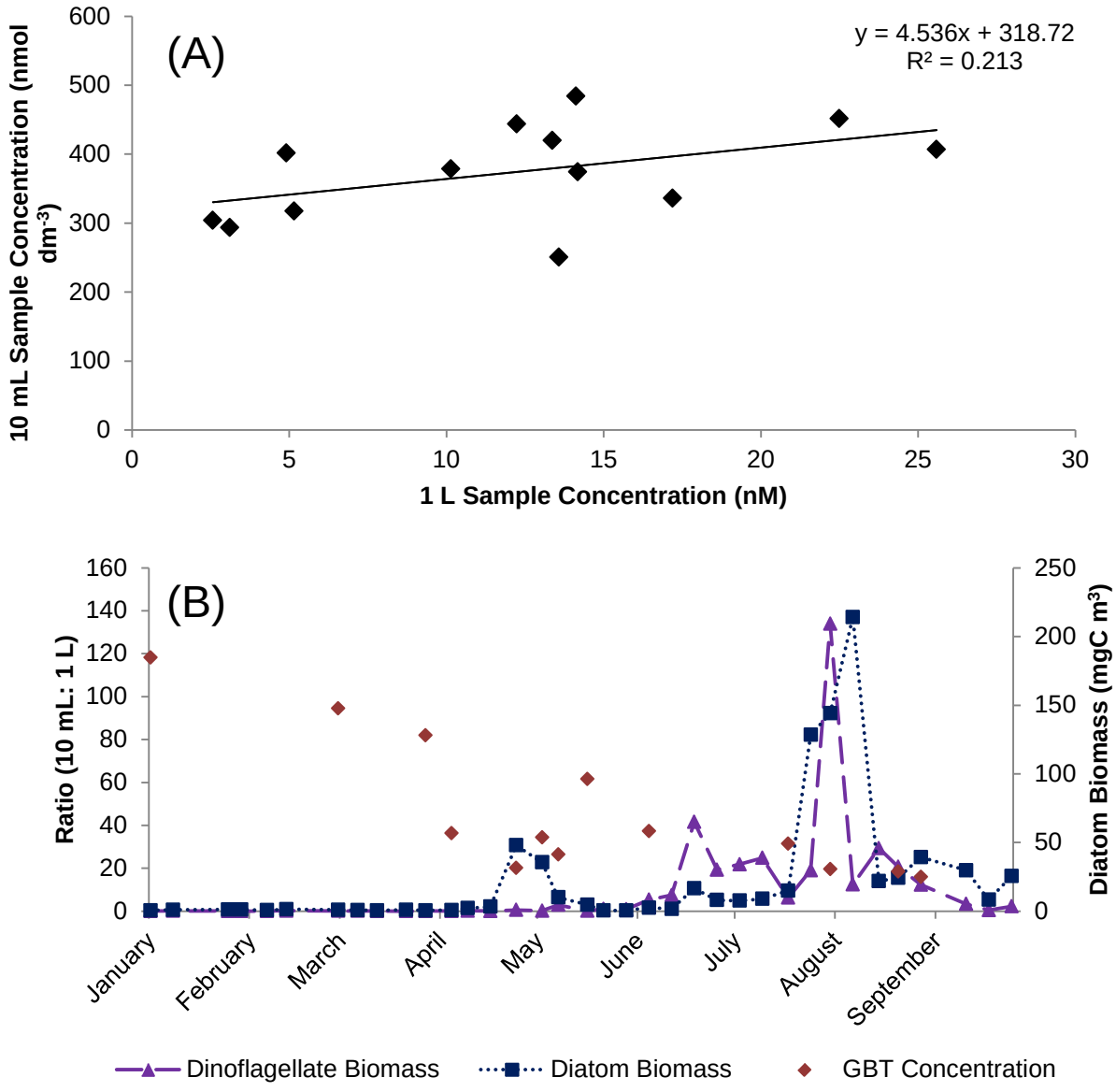

Figure 5.23: (A) Correlation between 1 L and 10 mL samples, (B) Ratio of GBT_p in 1 L: 10 mL samples and diatom and dinoflagellate biomass

5.9 Particulate glycine betaine and the nitrogen cycle

In light of the exceptionally high GBT_p concentrations observed during this study, the potential contribution of GBT to the organic nitrogen pool was evaluated. Seasonal average PON and DON concentrations were compared with GBT_p concentrations (Figure 5.24). The percentage contribution of the GBT_p to the PON and DON pools was then calculated, using the 10 mL sample data.

The GBT_p concentrations from the 10 mL samples contributed 0.55-0.85% to the PON pool, with the highest contribution observed in spring and the lowest observed in summer. GBT_p collected from 10 mL samples contributed 0.94-3.86% to the DON pool, with the highest contribution observed in spring and the lowest in summer. As the DON pool is smaller than the PON pool cell GBT_p, if released, would contribute a larger percentage to this pool.

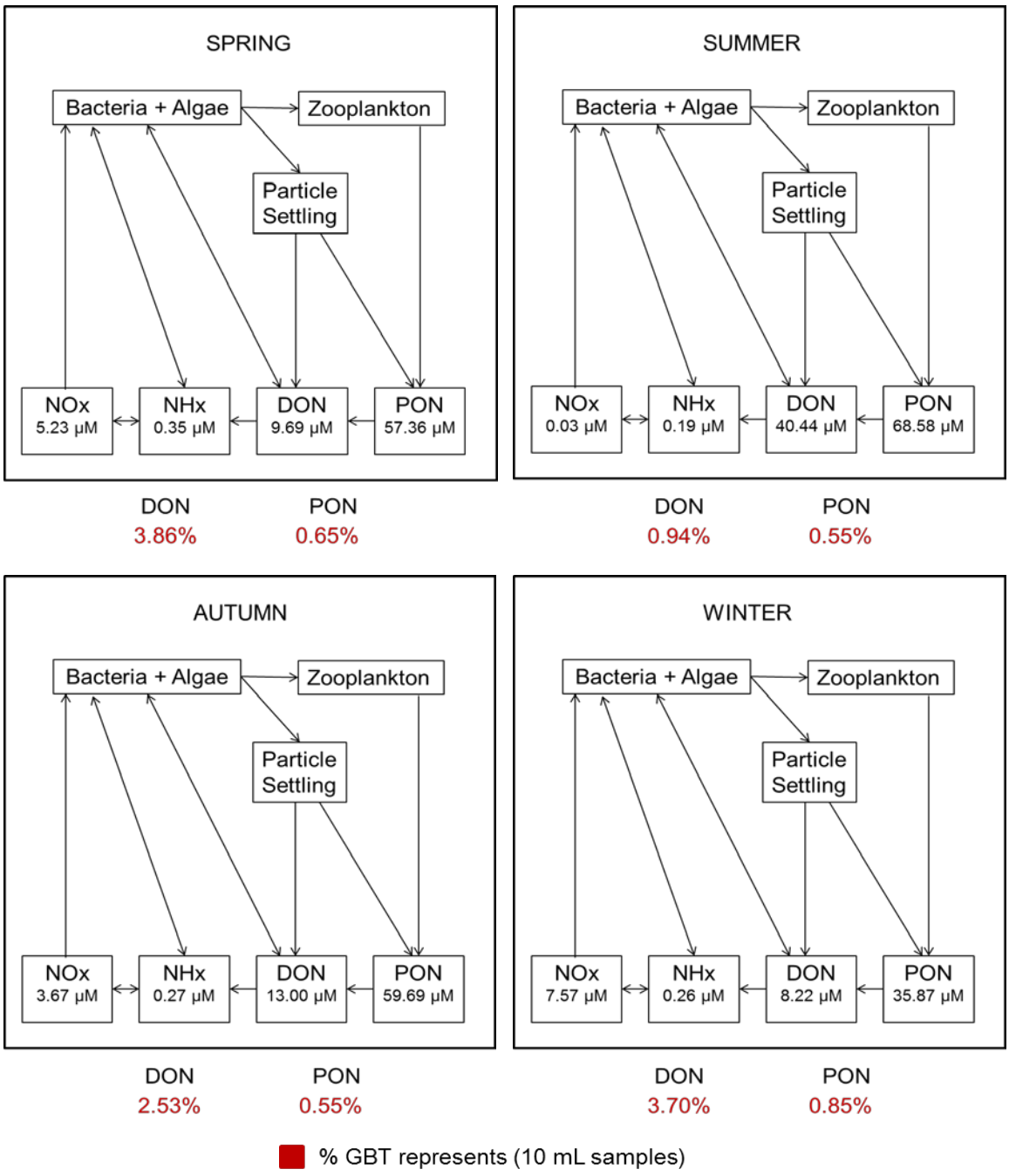

Figure 5.24: A section of the marine nitrogen cycle, adapted from Worsfold et al. (2008). NOx, NHx, DON and PON concentrations from 2012-2013 are shown along with the calculated contribution (%) of GBT_p to the DON and PON pools

The percentage of DON that GBT_p could represent if fully released from the cells (e.g. via a viral lysis event) was calculated and plotted as a function of time (Figure 5.25). The GBT_p concentrations could account for almost 6% of the total DON pool at station L4. Interestingly, the range of values (1-6%, Figure 5.25) is

similar to values reported from investigations of the MAs in marine sediments. DMA and TMA extracted from marine sediments made up approximately 0.5-5% of total organic nitrogen in coastal sediments, depending on the extraction method used (Lee, 1988; Lee and Olson, 1984). The pool extracted using hydrochloric acid accounted for approximately 0.5% of total organic nitrogen (Lee and Olson, 1984), whereas HF extractions contributed 5% (Lee, 1988).

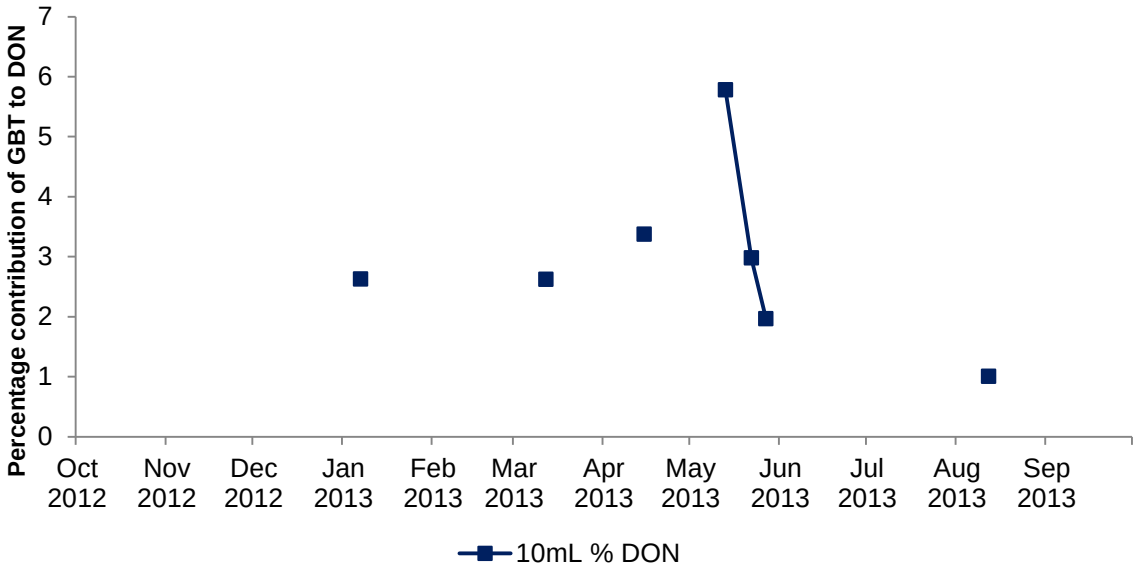

Figure 5.25: Concentrations of GBT_p in 10 mL samples measured as a percentage of dissolved organic nitrogen at station L4, October 2012-October 2013, calculated based on the limited 10 mL GBT_p and DON concentrations

The high GBT_p concentrations measured during this study have contributed to further molecular characterisation of the DON pool in coastal waters. While DON makes up a considerable proportion of total dissolved nitrogen (60-69%), a substantial proportion is still unidentified at the molecular level (Bronk, 2002). With average DON concentrations in coastal waters of approximately 10 µmol dm^{-3}, GBT_p concentrations of approximately 500 nmol dm^{-3} may comprise an important, labile sub-pool of DON (Bronk, 2002).

5.10 Particulate glycine betaine concentrations and measured dissolved methylamine concentrations in the Western English Channel

A selection of 1 L seawater samples from the spring bloom period and fresh samples from April 2014 were analysed for dissolved methylamines (MAs) using a newly developed SPME-GC-NPD method (Chapter 3). Samples collected during the spring bloom in 2013 were sampled and filtered (GF/F, n=3) after 2-3 hours then frozen in HDPE bottles until analysis. When analysed, these samples contained unquantifiable levels of the MAs throughout the spring bloom period (Figure 5.26).

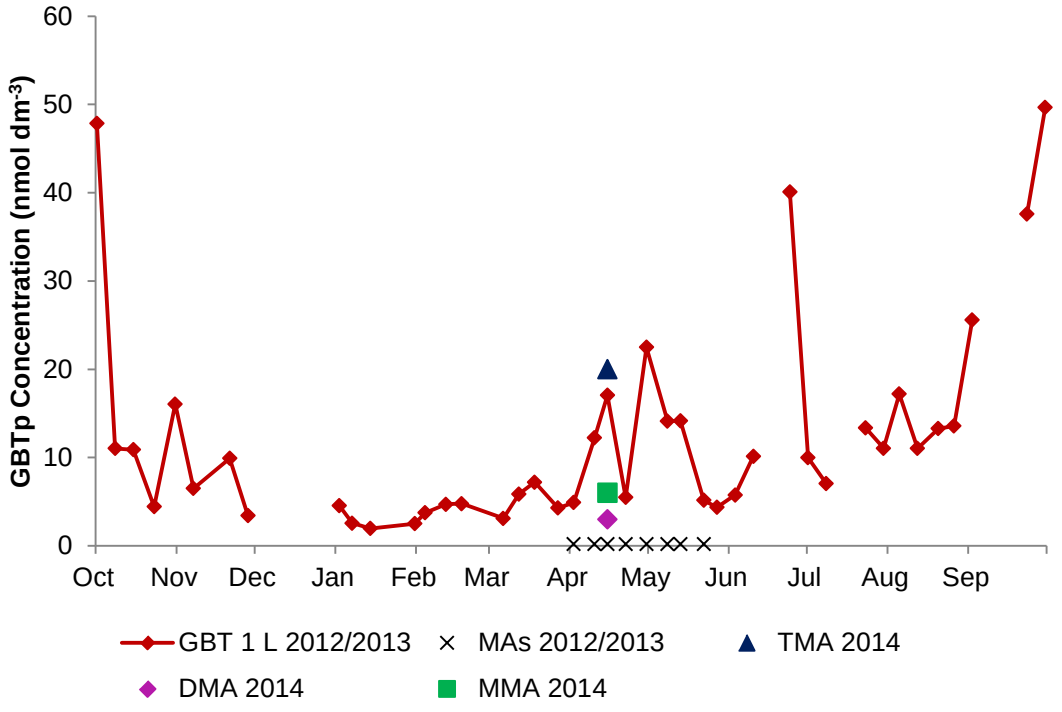

Figure 5.26: 1L GBT_p concentrations and dissolved MA presence measured at station L4 during October 2012-October 2013 and in April 2014. X represents unquantifiable presence of the 3 MAs. The 2014 concentrations represent one sample

The water samples collected during April 2014 were filtered immediately after collection and acidified. Concentrations of 20 nmol dm^{-3}, 3 nmol dm^{-3} and 6 nmol dm^{-3} for TMA, DMA and MMA respectively were observed (Figure 5.26). These values were approximately similar to those found by Gibb et al. (1995) of approximately 0.05-38 nmol dm^{-3} in coastal waters.

The MAs are thought to be climatically active and contribute to the acid-base chemistry in the atmosphere. They are believed to behave analogously to dimethyl sulphide (DMS) which contributes to the production of new aerosols in the atmosphere. The low concentrations of GBT_p observed previously (Airs and Archer, 2010; Keller et al., 2004) have meant that DMSP has historically been considered more significant to climate chemistry. A seasonal study of total DMSP ($DMSP_t$) at station L4 found reported concentrations of 3-127 nmol dm-3 (Archer et al., 2009). The GBT_p concentrations observed in the 10 mL data set are considerably higher than the $DMSP_t$ levels observed at the same site.

GBT is thought to have two primary breakdown pathways: anaerobic degradation to the MAs and aerobic degradation to glycine. The higher concentrations of GBT_p observed in this study means that, under conditions where anaerobic degradation can take place, significant levels of MAs could be produced. Anaerobic degradation involves two pathways. Anaerobic fermentation produces TMA and acetate, with further degradation to DMA and MMA (King, 1984; Welsh, 2000). The second pathway involves sequential demethylation by: homoacetogens and sulphate reducers (Heijthuijsen and Hansen, 1989; Möller et al., 1984; Müller et al., 1981; van der Maarel et al., 1996) and proceeds via two

key intermediates: dimethylglycine and sarcosine. Aerobic degradation has been primarily studied in terrestrial bacteria and occurs via a series of demethylation reactions catalysed by GBT methyltransferase and dimethylglycine oxidase and dehydrogenase to produce glycine (Chlumsky et al., 1995; Smith et al., 1988; Wargo et al., 2008). However, there is no experimental evidence to demonstrate that marine microorganisms use this pathway for GBT oxidation. The genomes of many marine Roseobacter clade bacteria and SAR11 strains, known to be capable of GBT metabolism (Carini et al., 2013; Chen et al., 2011; Sun et al., 2011), contain neither GBT methyltransferase nor dimethylglycine oxidase/dehydroeganse. Therefore the microbial pathways for GBT degradation need further investigation.

5.11 Discussion and Conclusions

The results detailed here represent a significant step forward in the understanding of GBT_p in coastal waters. The 1 L sample set allowed an in-depth analysis of the seasonal variability and potential physicochemical contributors to the changes in concentration. Significant phytoplankton blooms were identified, including a dinoflagellate bloom of *Prorocentrum cordatum* on 1st July 2013 in late summer which was thought to contribute to a GBT_p concentration of 40.1 nmol dm-3 in the 1 L dataset (Figure 5.16). Potential contributions from the phytoplankton species were identified using a statistical approach. The species identified as important contributors to the GBT_p concentrations observed can be used to direct future culture studies to further understand the production of GBT. Additional work could look at the potential contributions from zooplankton and bacteria to the GBT_p pool, perhaps using size fractionation of the entire microbial community.

The 10 mL sample set did not provide a full times series but where there was sufficient coverage; it mirrored the seasonal variability of the 1 L data set, notably the increase in GBT_p concentration during the spring bloom. The 10 mL GBT_p concentrations were over an order of magnitude higher than all previous concentrations measured in natural samples. The highest GBT_p concentration previously observed was 19 nmol dm^{-3} at station L4 (Airs et al., unpublished data) and was measured using particulates collected from 2-3 L of water. The highest concentration measured using the 10 mL sample volumes was 484.3 nmol dm^{-3} in May 2013. This data point coincided with the spring bloom period. There were no 10 mL samples for the period of the October increase in concentration

observed in the 1 L samples. The maximum GBT_p concentrations observed could potentially contribute a substantial portion of the unidentified DON pool.

Chapter 6

Discussion and Future Work

Chapter Outline

This chapter provides an evaluation of the study, which comprised: 1) the development of a method for quantification of the methylamines; 2) the optimisation of sampling and analysis protocols for glycine betaine; 3) a seasonal study of particulate glycine betaine. In addition, potential areas for future work are identified.

6.1 Discussion

This project aimed to improve our understanding of the cycling of methylated amines in marine systems and their potential climatic relevance. Previous investigations in this field were limited by the analytical challenges associated with the quantitative and reproducible determination of these compounds, and this project has made significant breakthroughs in analytical capability. An SPME-GC-NPD method for quantifying the MAs in aqueous samples was developed and tested, while a published technique for the sampling and analysis of GBT_p was significantly improved, with the sampling strategy modified to allow representative samples to be collected. The application of these methods has resulted in a seasonal dataset for particulate GBT and demonstrated a potential method for the measurement of dissolved MAs which can already be applied at low nmol dm^{-3} levels of MAs in seawater. The seasonal study of GBT has further demonstrated the potential importance of this compound to marine algae, while the addition of a robust and sensitive method for the MAs' determination means that important questions about the abundance, turnover and possible climatic role for these analytes can now be addressed.

6.1.1 Filtration artefacts

The optimisation of filtration volume has allowed the collection of precise, reproducible data on GBT_p levels, and has highlighted the need to question each step of an analytical protocol and ensure it is robust before continuing. A future advance might be to further reduce the filtration volume; for example, a sample volume of 3.5 mL was recommended for the filtration and analysis of dissolved DMSP ($DMSP_d$) (Kiene and Slezak, 2006). Although the optimised 10 mL volume

for GBT_p is almost 3 times greater than the 3.5 mL used for $DMSP_d$, a further reduction in filtration volume may make a quantifiable analyte signal more difficult to achieve. A potential approach could involve filtering multiple small volumes which could then form a composite sample for subsequent analysis. This would reduce the filtration volume without decreasing the amount of particulate matter collected. However, this approach would introduce further sampling handling and the potential for additional error. Sample filtration is likely to introduce some form of error or artefact and ideally a new sampling approach would remove the need for filtration. In addition, if a method for the quantification of dissolved GBT (GBT_d) could be developed then loss of GBT_p to the dissolved phase could be confirmed. A method for GBT_d analysis would also allow the quantification of standing stock concentrations and could be used in studies of GBT uptake and turnover by microbial communities. This would allow elucidation of production and turnover mechanisms.

In addition to understanding the role of microbial communities in GBT cycling, further understanding of the contributors to GBT production is required. This includes identifying the key GBT producers and the relationship between GBT production and nitrogen availability, including the cellular function of GBT and the conditions which stimulate its production.

With GBT_p concentrations of more than 480 nmol dm^{-3} observed in the Western English Channel during the seasonal time series, it may represent an underestimated contribution to the labile DON pool. As a result its contribution to the nitrogen cycle, and marine MA production and cycling, warrants further

investigation. Studies of GBT_p uptake have demonstrated that microbial communities rapidly assimilate and process GBT (0.5-11 hours), with turnover attributed predominantly to bacteria (Kiene and Hoffmann Williams, 1998). In addition, microbial turnover of the MAs was observed to occur within a similar timeframe, and this was attributed to uptake by bacteria that had not been removed by filtration. The microbial turnover rates of GBT and the MAs raise the question of whether low dissolved concentrations are truly representative of low standing concentrations or whether the methylated amine species are actually being rapidly transferred and turned over. The measurement of uptake and turnover of GBT and the MAs in real samples using isotopically-labelled substrates is one option for improving our understanding of this area of N-cycling.

6.1.2 MA analysis

An understanding of MA abundance and turnover in marine systems is necessary to begin to understand their potential importance to climate regulation. MAs, while less abundant than ammonia in the atmosphere, are proposed to make a disproportionately significant contribution to particle nucleation due to their more basic nature, particularly DMA (Almeida et al., 2013). This highlights the importance of taking a methodical, evidence-based approach to understanding their potential climatic relevance. Following the publication of the CLAW hypothesis in 1987, a paradigm shift in science took place and considerable resources have since been invested in understanding the contribution of dimethyl sulphide to cloud condensing nuclei (Charlson et al., 1987). More recent studies, however, have indicated that DMS does not play as much of a key role in particle nucleation in the atmosphere as previously thought (Woodhouse et al., 2010).

This further highlights the need to take an evidence-based approach to understanding the potential importance of MAs to particle nucleation in the atmosphere, including: 1) quantification of standing stocks of the MAs in marine waters; 2) identifying and measuring water-atmosphere pathways and fluxes; 3) understanding controls on MA production and subsequent impacts on atmospheric MA concentrations. In parallel to these analyte specific tasks, an improved understanding of the initial steps of particle nucleation in the atmosphere, and how this particle nucleation might affect local, regional and global climate regulation, is needed.

This work presents significant analytical breakthroughs in our ability to quantify methylated amines in marine systems. Two methods have been developed and optimised, SPME-GC and LC-MS, for the analysis of the MAs and GBT_p, respectively, facilitating future studies aimed at gaining a better understanding of MAs' and GBT cycling in marine systems. A robust estimate of spatial GBT and MA standing concentrations can be achieved and temporal studies should then be focused on understanding how their concentrations vary with time and season. The statistical analysis of the contributions of phytoplankton species to GBT_p concentrations can be used to direct future culture studies and identify key GBT producers. Mechanistic studies of uptake and turnover and of production processes (i.e. environmental conditions affecting GBT production and the identification of key biosynthetic pathways) are further key components of a complete understanding of the cycling and role of methylated amine species in marine systems.

Chapter 7

Experimental Procedures

7.1 Chemicals and Cleaning

7.1.1. Cleaning

All glassware was soaked overnight in 10% Decon and rinsed in high purity water (HPW) and allowed to dry. Glassware was then soaked overnight in 10% hydrochloric acid and rinsed in HPW and allowed to dry before use

7.1.2 Chemicals

Methylamine Analysis

Trimethylamine hydrochloride (CAS number 75-50-3), dimethylamine hydrochloride (CAS number 124-40-3) and monomethylamine hydrochloride (CAS number 74-89-5) were purchased from Acros Organics. Methanol (67-56-1; HPLC grade), pyridine (CAS number 110-86-1), triethylamine (CAS number 121-44-8), sodium chloride (CAS number 7647-14-5, analytical reagent grade) and sodium hydroxide (CAS number 1310-73-2, analytical reagent grade) were purchased from Fisher Scientific.

Single standard stock solutions (100 mmol dm^{-3}) were prepared from the hydrochloride salt of each MA. The solutions were acidified, refrigerated and stored for up to a month.

Glycine betaine analysis

GBT, carboxy-N,N,N-trimethylmethanaminium (CAS number 590-46-5), was obtained from Sigma-Aldrich as betaine hydrochloride. A deuterated internal standard (ISTD), d_{11}- glycine betaine [$(CD_3)_3N^+CD_2COO^-$; Mr 128], was purchased from CK Gas Products. Acetonitrile (75-05-8), methanol (67-56-1), chloroform (67-66-3) (all HPLC grade) were purchased from Fisher Scientific.

Acetic acid (64-19-7) and ammonium acetate(631-61-8) (LC-MS eluent additives) were also purchased from Fisher Scientific.

7.2 Natural Sample Collection

Surface water was collected at station L4, 10 km offshore in the Western English Channel (http://www.westernchannelobservatory.org.uk/l4/) from the non-toxic supply aboard the RV Plymouth Quest.

7.2.1 Methylamine sample collection

Samples (1 L) were either immediately filtered using 47 mm GF/F filter papers (0.7 µm pore size) acidified with concentrated hydrochloric acid and stored chilled until analysis, or transported back to the laboratory (approx. 2 h) to be filtered and stored frozen until analysis.

7.2.2 Glycine betaine sample collection

Water was kept in the dark and transported back to the laboratory (approx. 2 h), where particulates were collected by gravity filtration onto 47 mm GF/F filter papers, these were flash frozen in liquid nitrogen and stored at -80°C until analysis

7.3 Sample Extraction

7.3.1 Solid phase micro-extraction procedure for methylamine preconcentration

Polydimethylsiloxane/divinylbenzene (PDMS/DVB) fibres (Sigma Aldrich) were housed within a manual solid phase microextraction (SPME) holder. Water samples were modified to pH 13 with 10M NaOH solution (20 mL). The ionic strength of the solution was controlled by saturating the water with NaCl (300 and 350 g L^{-1} for seawater and HPW, respectively). Water samples (1 L) were then heated in a 1 L volumetric flask and maintained at 60°C for the extraction period. This step was initially carried out using a water bath and subsequently with an aluminium foil-lagged Pyrex beaker on a stirrer hotplate. The fibre was exposed to the headspace of the samples for 0.5-12 h during optimisation; the extraction time chosen was 2.5 h.

7.3.2 Solvent extraction of glycine betaine

Filter containing particulates were transferred to narrow glass tubes to which 3 mL of extraction solvent (methanol: chloroform: water, 2.4: 1: 3.8, P=7.0) containing the internal standard was added. The extracts were left overnight at 4°C and clarified using centrifugation (4 minutes, 20 000g).

7.4 Sample Analysis

7.4.1 Methylamine analysis

GC Conditions

An Agilent 6890 nitrogen-phosphorus detector was used throughout the project, initially connected to a Thames Restek Rxi-5Sil MS column (30 m × 0.2 mm × 0.25 µm) and subsequently with a CP Volamine column (60 m × 0.32 mm). The inlet was used in splitless mode with the injector temperature set to 270°C, and the gas pressure to 9.5 psi (655 millibar). The detector temperature was set to 300°C. The H_2, air and nitrogen (make up gas) flow rates were 2, 60 and 5 mL min^{-1}, respectively.

GC Maintenance

The analytical column was removed from the oven every 3-6 months and small portions of the front and back of the column removed in case of column contamination. This was followed by an instrument blank run to condition the column and ensure there was no contamination.

Analysis

After extraction the fibre was desorbed in the GC inlet using a narrow SPME liner. Specially designed SPME inlet liners and predrilled septa were used (Sigma Aldrich) with the GC and replaced every 1-2 weeks to minimise potential blockages of the narrow SPME inlet liner. The inlet was heated to 270°C and the fibre was exposed for 5 minutes. The heating programme used is shown in Table 7.1.

Table 7.1: GC oven temperature programme used in conjunction with the SPME pre-concentration step.

Heating Programme:	°C/min	Next (°C/min)	Hold (minutes)
		50 (initial temp.)	2
Ramp 1	10	180	0
Ramp 2	15	260(final temp.)	5

Routine fibre blanks were analysed at the beginning and end of each analytical day, and between extractions to ensure that carry over did not occur between samples.

GC Calibration

Methylamine (MA) calibration solutions were diluted as required from a 100 mM stock solution. Calibration standard solutions were prepared by spiking MAs into 1 L of prepurged seawater to give final concentrations of 1 nmol dm^{-3}, 2.5 nmol dm^{-3}, 5 nmol dm^{-3} and 10 nmol dm^{-3}; these solutions were then extracted using SPME. Seawater used for calibration was purged as a precaution to strip out any MAs present. This was carried out by modifying the seawater to pH 12 with NaOH solution then purging with nitrogen gas for 3-5 hours. Triplicate analysis of each concentration was carried out and plotted as concentration versus peak area (Figure 7.1).

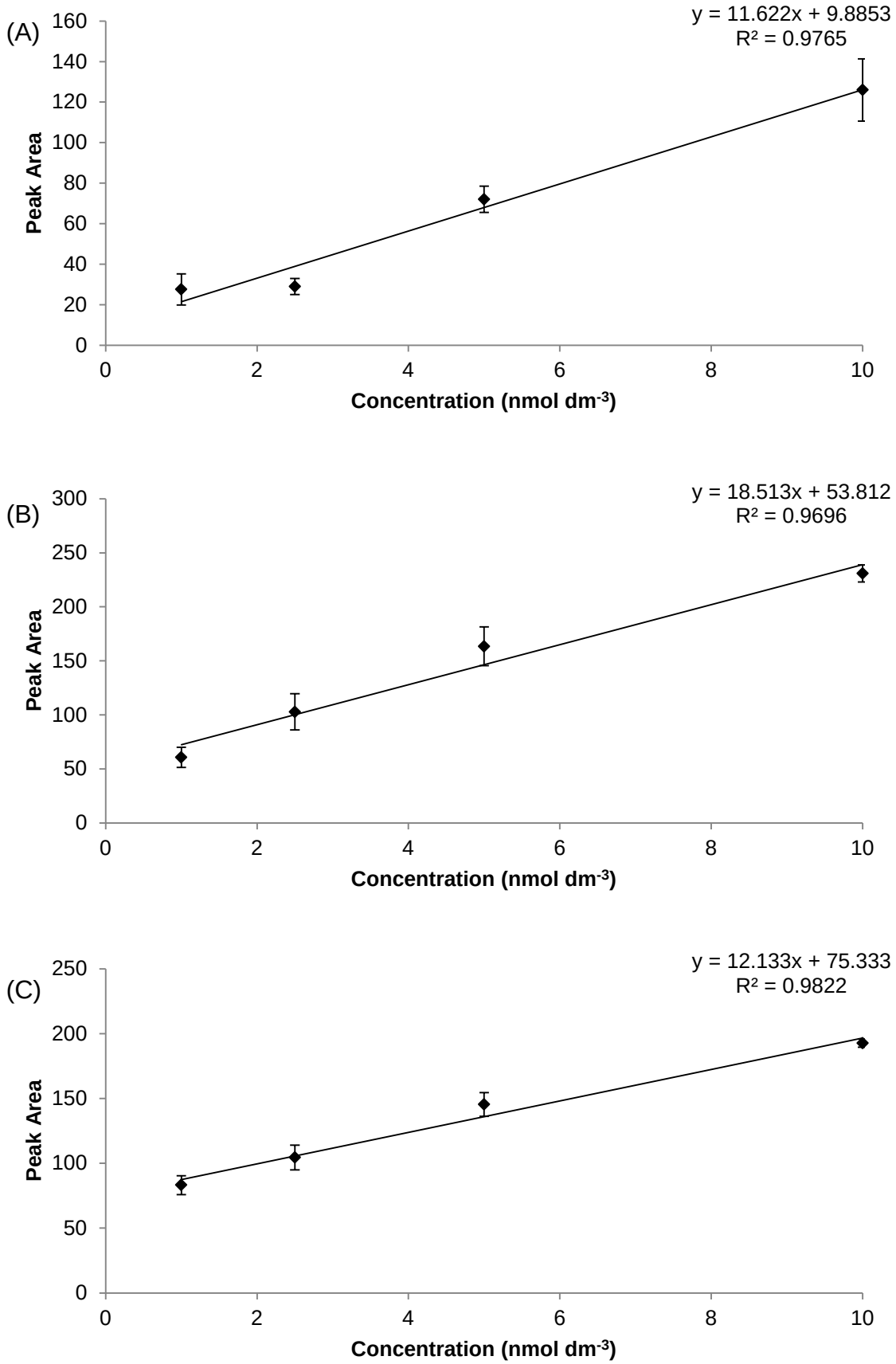

Figure 7.1: Calibration of: (A) MMA, (B) DMA and (C) TMA extracted from pre-purged seawater for 2.5 hours, heated at 60°C. Error bars denote 1 standard deviation (n=3)

7.4.2 Glycine betaine analysis

LC-MS conditions

The LC-MS system comprised an Agilent 1200 HPLC coupled via an ESI source to an Agilent 6330 ion trap LC-MS operated in the positive ion mode. The nebulizer pressure was set to 55 psi (379 millibar), drying gas flow was 12 L min^{-1}, and the drying gas temperature was 350 °C. A Spherisorb ODS1 250 × 4.6 mm, with µm particle size LC column (Waters) was used. The eluent was run isocratically at a flow rate of 1 mL min^{-1}. An injection program was used to exclude carryover, as recommended in the Agilent 1200 instrument handbook: 1. Needle wash in flush port 14 s; 2. Draw 1 µL from sample; 3. Needle wash vial 10 (HPW), 3 times; 4. Inject; 5. Wait 0.2 min; 6. Valve bypass; 7. Wait 0.2 min; 8. Valve mainpass; 9. Valve bypass; 10. Valve mainpass. Using this injection program, no carryover was detected in a blank sample run immediately after an injection containing 1620 pg GBT.

Mobile Phase for GBT Analysis

The original mobile phase (referred to in text as Airs and Archer mobile phase) composition was based on published methods for the analysis of a quaternary ammonium pesticide (Evans et al., 2000; Vahl et al., 1998), comprising acetonitrile : methanol : water : acetic acid (53 : 21 : 25 : 1), containing a final concentration of 50 mM ammonium acetate. The modified mobile phase composition (mobile phase B) developed to reduce ion suppression effects during GBT analysis comprised acetonitrile : methanol : water : acetic acid (50.06 : 0.42 : 49.5 : 0.02), and contained a final concentration of 1 mM ammonium acetate.

LC-MS tuning

A solution containing GBT hydrochloride in HPW was infused by a syringe pump at a flow rate of 5 µL min^{-1} into the HPLC solvent flow (1 mL min^{-1}) via a T piece connection adjacent to the LC-MS inlet. A prominent ion at *m/z* 118 was observed, corresponding to the protonated ion ($[M + H]^+$) of GBT. These ions were used to optimize the ion optics. Typical optimal settings were as follows: Capillary –1800 V, skimmer 33 V, capillary exit 150 V, octopole one 5.42 V, octopole two 0.83 V, octopole RF 50 Vpp, lens one –3.75 V, lens two –46 V.

LC-MS Calibration

Calibration curves for GBT were initially prepared in the solvent composition methanol: chloroform: HPW (12: 5: 1) and considered stable for one day. GBT was observed to be more stable in the solvent composition, methanol: chloroform: HPW (2.4**:** 1**:** 3.8) and this composition was subsequently used for standard preparation (Section 4.4). Analyses were performed in triplicate. The standard solutions of GBT were prepared at concentrations of 0.1, 0.2, 0.4, 1.0 and 1.6 µM. 1 µL injections of these solutions equated to 12, 24, 48, 123 and 185 pg of GBT on-column. Calibration solutions and samples were spiked with d_{11}-GBT equivalent to 197 pg in a 1 µL injection. The calibration curves were plotted as concentration versus peak area ratio (analyte: ISTD) (Figure 7.2). Once prepared, calibration solutions were stored at 4°C and were considered stable for 1 week.

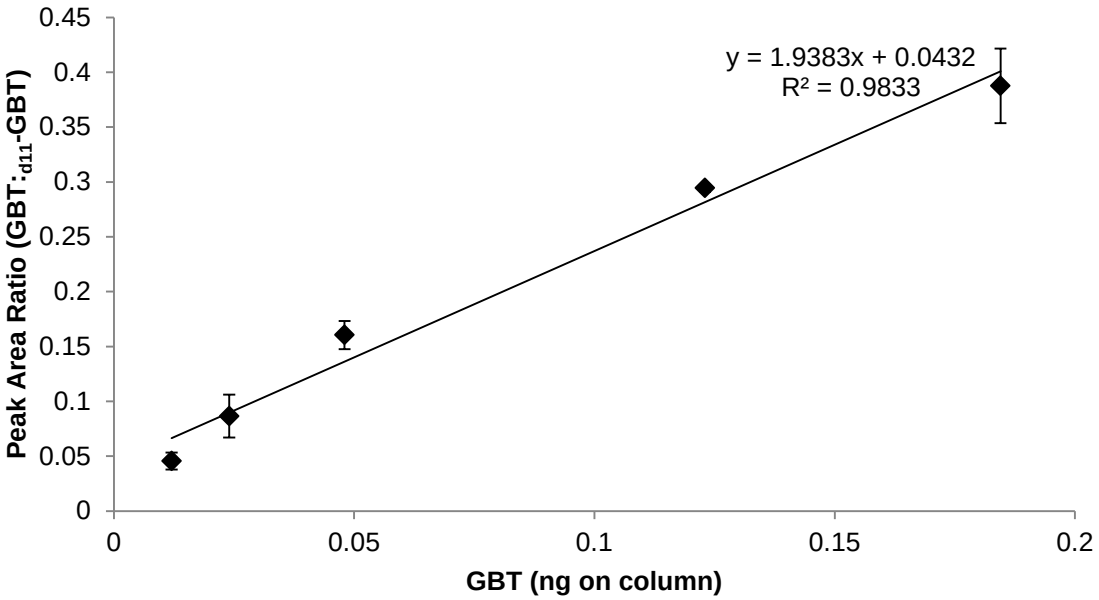

Figure 7.2: Calibration curve for GBT in the modified solvent composition (methanol: chloroform: HPW (2.4:1:3.8), error bars denote ±1SD (n = 3).

Wash protocol

To reduce the influence of observed ion suppression (discussed in Section 4.4) a cleaning regime was introduced to reduce the background levels of contaminating ions. The cleaning protocol comprised a polar wash (acetonitrile: HPW, 50:50) and an apolar wash (methanol: ethyl acetate: HPW, 19:80:1) of both the column and the electrospray ionisation source (ESI) source carried out periodically during the analytical day, and an isopropanol rinse of the ESI source at the end of every analytical day.

7.5 Seasonal study analysis

7.5.1 Phytoplankton abundance

Sampling and microscopy

Phytoplankton abundance was analysed as part of the L4 time series for the Western Channel Observatory at Plymouth Marine Laboratory. Phytoplankton samples were collected weekly at 10 m depth using a 10 L Niskin bottle. A 200 mL volume was immediately subsampled and fixed with 2% Lugol's iodine solution and a further 200 mL was subsampled and preserved with neutral formaldehyde. Samples were stored in cool, dark conditions, analysed using light microscopy and counted using the Utermöhl counting technique (Utermohl, 1958) using a Leica DM IRB inverted microscope. Between 10-100 mL of sample was settled for >48 hours and cells were identified, where possible, to species level. Cell volumes were calculated according to the equations of Kovala and Larrance (1996) and converted to carbon using the equations of Menden-Deuer and Lessard (2000).

Flow cytometric analysis of phytoplankton abundance was carried out at Plymouth Marine Laboratory. Flow cytometric analysis is based on the different light scattering and fluorescent properties of different groups of particles, which allows phytoplankton groups to be distinguished. Triplicate seawater samples from the surface, 10, 25 and 50 m were collected from station L4 using 0.25 L polycarbonate bottles. Samples were stored in cool dark conditions until analysis with a FACSort flow cytometer (Becton Dickinson) and a flow rate of 157 ± 6.4 mm^3 min^{-1}.

7.5.2 Nutrient analysis

Nutrient analysis was carried out at Plymouth Marine Laboratory. Triplicate seawater samples from surface, 10, 25 and 50 m were collected from station L4. Samples were stored in cool dark conditions until analysis. Dissolved inorganic phosphate was analysed using the method Murphy and Riley (1962), modified by Zhang and Chi (2002), where a phospho-molybdenum blue complex is formed by reaction with molybdate and ascorbic acid. Dissolved inorganic silicate was analysed by reaction with ammonium molybdate to form, primarily, silicomolybdic acid (Kirkwood, 1989). Total dissolved nitrate and nitrite concentrations were cumulatively analysed using a copper/cadmium column in ammonium chloride solution, which was used to reduce nitrate to nitrite. Nitrite ions were reacted with acidic sulphanilamide solution to produce a diazo compound, which then reacted with N-1-naphthylethylene diamine dihydrochloride (NEDD) to produce a reddish purple dye. The dye was analysed using a colorimeter (Brewer and Riley, 1965; Hansen and Koroleff, 2007). Nitrate concentrations were obtained by subtracting nitrite concentration from the combined total concentration. Ammonia analysis was based on the production of the indophenol-blue complex (Mantoura and Woodward, 1983).

7.5.3 Pigment analysis

Pigment analysis was carried out at Plymouth Marine Laboratory. Seawater (1-2 L) was collected and filtered on board the Plymouth Quest through a GF/F; the filter was flash frozen and stored in liquid nitrogen or at -80°C until analysis. The analytes were extracted in 2 mL acetone using an ultrasonic probe. Extracts were centrifuged (5 min at 4000 r.p.m), filtered through Teflon syringe filters (0.2 µm)

and analysed using reversed-phase HPLC with gradient elution (Zapata et al., 2000).

7.5.4 Dissolved organic nitrogen analysis

Dissolved organic nitrogen (DON) was calculated from total dissolved nitrogen (TDN) concentrations from analyses performed at Plymouth University. TDN was quantified using high temperature catalytic combustion on a Shimadzu TOC V analyser (Badr et al., 2003). Sample aliquots (100 µL) were injected onto a column containing a catalyst (0.5% platinum on aluminium oxide) and combusted at 720 °C. The NO in the combustion gas reacts with O_3 to produce the $NO_2^{\bullet}$ radical which chemiluminesces during decay to the ground state emitting light. The resulting signal is converted to a peak area and the TDN concentration calculated using external calibration and certified reference materials.

The DON concentration was calculated by subtracting the combined nitrite/nitrate concentrations and the ammonium concentration from each TDN concentration.

7.5.5 Particulate organic nitrogen

Particulate organic nitrogen (PON) was analysed at Plymouth Marine Laboratory. Triplicate 250 mL aliquots of seawater was prefiltered through a 200 µm mesh and then filtered through pre-ashed GF/Fs. The filters were dried at 60°C and acidified with sulphuric acid prior to analysis with a Thermoquest FlashEA 1112 elemental analyser.

7.5.6 Photosynthetically-active radiation and salinity

Photosynthetically active radiation (PAR) and salinity were measured using a Chelsea sensor attached to the sampling rosette and sampled by the R/V Plymouth Quest during visits to the L4 station.

7.5.7 Mixed layer depth

The mixed layer depth (MLD) was defined as 0.8°C from 10 m depth (Kara et al., 2000) and calculated using temperature data collected using the CTD data. The 10 m depth temperature was chosen as the initial reference temperature to eliminate possible bias due to 'skin effects' at the ocean surface. Based on data examined by Kara et al. (2000), the temperature at 10 m is very close to the SST.

7.6 Statistical analysis

Statistical analysis was carried out using Minitab 16 Statistical Software. Regression and ANOVA analysis were carried out; the normality of the residuals was tested using the Anderson-Darling test and an F-test was used to check the residuals for equal variance. Any data found to be non-normal was transformed using a Johnson Transformation and re-tested.

Concentrations of GBT_p, environmental variables and phytoplankton taxonomic data from the Western English Channel were analysed using the statistical package PRIMER v6 (Clarke and Gorley, 2006); statistical analyses are summarised below.

7.6.1 Data pre-treatment

The PRIMER software was used to replace missing data values with an average value calculated from the preceding and subsequent data points. All data was square root transformed to achieve optimal conditions for calculating Euclidean distance and Bray Curtis similarity matrices. Environmental variables were normalised to eliminate variation caused by different units and nominal scales.

7.6.2 BEST: BIO-ENV and BV-STEP tests

The multivariate statistical test BEST selects environmental variables (BIO-ENV) or species (BV-STEP) that best explain sample or community patterns observed (Clarke and Gorley, 2006). The BIO-ENV was used to test the potential relationship between environmental variables and GBT_p concentrations using all potential permutations. The BV-STEP test, utilising a stepwise search algorithm, was used to identify potential groups within the phytoplankton community that best explained the glycine betaine concentrations observed.

References

Abalos, M., Bayona, J.M. and Ventura, F., 1999. Development of a solid-phase microextraction GC-NPD procedure for the determination of free volatile amines in wastewater and sewage-polluted waters. Analytical Chemistry, 71(16): 3531-3537.

Abalos, M., Mas, R., Suc, V. and Bayona, J.M., 2001. Evaluation of capillary gas chromatography columns for the determination of free volatile amines after solid-phase microextraction. Chromatographia, 54(1-2): 109-113.

Abdul-Rashid, M.K., 1990. Studies of aliphatic amines and other volatile organic compounds in the marine environment, University of Liverpool.

Abdul Rashid, M.K., Riley, J.P., Fitzsimons, M.F. and Wolff, G.A., 1991. Determination of volatile amines in sediment and water samples. Analytica Chimica Acta, 252(1-2): 223-226.

Airs, R.L. and Archer, S.D., 2010. Analysis of glycine betaine and choline in seawater particulates by liquid chromatography/electrospray ionization/mass spectrometry. Limnology and Oceanography-Methods, 8: 499-506.

Aldrich, S., A practical guide to quantitation with solid phase microextraction, Bulletin 929, Bellefont.

Almeida, J., Schobesberger, S., Kurten, A., Ortega, I.K., Kupiainen-Maatta, O., Praplan, A.P., Adamov, A., Amorim, A., Bianchi, F., Breitenlechner, M., David, A., Dommen, J., Donahue, N.M., Downard, A., Dunne, E., Duplissy, J., Ehrhart, S., Flagan, R.C., Franchin, A., Guida, R., Hakala, J., Hansel, A., Heinritzi, M., Henschel, H., Jokinen, T., Junninen, H., Kajos, M., Kangasluoma, J., Keskinen, H., Kupc, A., Kurten, T., Kvashin, A.N., Laaksonen, A., Lehtipalo, K., Leiminger, M., Leppa, J., Loukonen, V., Makhmutov, V., Mathot, S., McGrath, M.J., Nieminen, T., Olenius, T., Onnela, A., Petaja, T., Riccobono, F., Riipinen, I., Rissanen, M., Rondo, L., Ruuskanen, T., Santos, F.D., Sarnela, N., Schallhart, S., Schnitzhofer, R., Seinfeld, J.H., Simon, M., Sipila, M., Stozhkov, Y., Stratmann, F., Tome, A., Trostl, J., Tsagkogeorgas, G., Vaattovaara, P., Viisanen, Y., Virtanen, A., Vrtala, A., Wagner, P.E., Weingartner, E., Wex, H., Williamson, C., Wimmer, D., Ye, P., Yli-Juuti, T., Carslaw, K.S., Kulmala, M., Curtius, J., Baltensperger, U., Worsnop, D.R., Vehkamaki, H. and Kirkby, J., 2013. Molecular understanding of sulphuric acid-amine particle nucleation in the atmosphere. Nature, 502(7471): 359-363.

Andreae, M.O., 1986. The Ocean as a Source of Atmospheric Sulfur Compounds. In: P. Buat-Menard (Editor), The Role of Air-Sea Exchange in Geochemical Cycling. D. Reidel Publishing Compnay, Dordrecht, pp. 331-362.

Antitila, T., Vehkamaki, H., Napari, I. and Kulmala, M., 2005. Effect of ammonium bisulphate formation on atmospheric water-sulfuric acid-ammonia nucleation. Boreal Environment Research, 10: 511-523.

Archer, S., Cummings, D., Llewellyn, C. and Fishwick, J., 2009. Phytoplankton taxa, irradiance and nutrient availability determine the seasonal cycle of DMSP in temperate shelf seas. Marine Ecology Progress Series, 394: 111-124.

Arthur, C.R. and Rigler, F.H., 1967. A possible source of error in the ^{14}C method of measuring primary productivity. Limnology and Oceanography, 12(1): 121.

Badr, E.A., Achterberg, E.P., Tappin, A.D., Hill, S.J. and Braungardt, C.B., 2003. Determination of dissolved organic nitrogen in natural waters using high-temperature catalytic oxidation. TrAC Trends in Analytical Chemistry, 22(11): 819-827.

Balch, W.M., 1986. Exploring the mechanism of ammonium uptake in phytoplankton with an ammonium analogue, methylamine. Marine Biology, 92: 163-171.

Ball, S.M., Hanson, D.R., Eisele, F.L. and McMurry, P.H., 1999. Laboratory studies of particle nucleation: Initial results for H2SO4, H2O, and NH3 vapors. Journal of Geophysical Research: Atmospheres, 104(D19): 23709-23718.

Bates, R.G. and Pinching, G.D., 1984. Acidic dissociation constant of the ammonium ion at 0 to 50°C, and the base strength of ammonia. Journal of Research of the National Bureau of Standards US, 4: 419-430.

Benner, R., Biddanda, B., Black, B. and McCarthy, M., 1997. Abundance, size distribution, and stable carbon and nitrogen isotopic compositions of marine organic matter isolated by tangential-flow ultrafiltration. Marine Chemistry, 57(3–4): 243-263.

Berman, T., 1973. Modifications in filtration methods for the measurement of inorganic ^{14}C uptake by photosynthesising algae. Journal of Phycology, 9: 327-330.

Berman, T. and Bronk, D.A., 2003. Dissolved organic nitrogen: a dynamic participant in aquatic ecosystems. Aquatic Microbial Ecology, 31(3): 279-305.

Bernard, T., Pocard, J.-A., Perround, B. and Le Rudulier, D., 1986. Variations in the response of salt-stressed Rhizobium strains to betaines. Archives of Microbiology, 143(4): 359-364.

Bicknell, B. and Owens, J.D., 1980. Utilisation of methyl amines as nitrogen sources by non- methylotrophs Journal of General Microbiology, 117: 89-96.

Biziuk, M. and Przyjazny, A., 1996. Methods of isolation and determination of volatile organohalogen compounds in natural and treated waters. Journal of Chromatography A, 733(1–2): 417-448.

Boch, J., Kempf, B., Schmid, R. and Bremer, E., 1996. Synthesis of the osmoprotectant glycine betaine in Bacillus subtilis: characterization of the gbsAB genes. Journal of Bacteriology, 178(17): 5121-9.

Bonfiglio, R., King, R.C., Olah, T.V. and Merkle, K., 1999. The effects of sample preparation methods on the variability of the electrospray ionization response for model drug compounds. Rapid Communications in Mass Spectrometry, 13(12): 1175-1185.

Booth, I.R. and Higgins, C.F., 1990. Enteric bacteria and osmotic stress; intracellular potassium glutamate as a secondary signal of osmotic stress. FEMS Microbiology Reviews, 75: 239-246.

Brewer, P.G. and Riley, J.P., 1965. The automatic determination of nitrate in sea water. Deep Sea Research and Oceanographic Abstracts, 12(6): 765-772.

Bronk, D.A., 2002. Dynamics of DON. In: D.A. Hansell and C.A. Carlson (Editors), Biogeochemistry of Marine Dissolved Organic Matter. Academic Press, San Diego.

Budd, J.A. and Spencer, C.P., 1968. The utilisation of alkylated amines by marine bacteria Marine Biology, 2: 92-101.

Burg, M.B. and Ferraris, J.D., 2008. Intracellular Organic Osmolytes: Function and Regulation. The Journal of Biological Chemistry, 283(12): 7309-7313.

Bushaw-Newton, K.L. and Moran, M.A., 1999. Photochemical formation of biologically available nitrogen from dissolved humic substances in coastal marine systems. Aquatic Microbial Ecology, 18(3): 285-292.

Bushaw, K.L., Zepp, R.G., Tarr, M.A., Schulz-Jander, D., Bourbonniere, R.A., Hodson, R.E., Miller, W.L., Bronk, D.A. and Moran, M.A., 1996. Photochemical release of biologically available nitrogen from aquatic dissolved organic matter. Nature, 381(6581): 404-407.

Bzdek, B.R., Ridge, D.P. and Johnston, M.V., 2011. Reactivity of methanesulfonic acid salt clusters relevant to marine air. Journal of Geophysical Research-Atmospheres, 116.

Cape, J.N., Cornell, S.E., Jickells, T.D. and Nemitz, E., 2011. Organic nitrogen in the atmosphere — Where does it come from? A review of sources and methods. Atmospheric Research, 102(1-2): 30-48.

Capone, D.G. (Editor), 2008. Nitrogen in the Marine Environment. Academic Press, London.
Carini, P., Steindler, L., Beszteri, S. and Giovannoni, S.J., 2013. Nutrient requirements for growth of the extreme oligotroph /`Candidatus Pelagibacter ubique/' HTCC1062 on a defined medium. ISME J, 7(3): 592-602.
Carpenter, L.J., Archer, S.D. and Beale, R., 2012. Ocean-atmosphere trace gas exchange. Chemical Society Reviews, 41(19): 6473-6506.
Cavalieri, A. and Huang, A.C., 1981. Accumulation of proline and glycinebetaine in Spartina alterniflora Loisel. in response to NaCl and nitrogen in the marsh. Oecologia, 49(2): 224-228.
Chafer-Pericas, C., Campins-Falco, P. and Herraez-Hernandez, R., 2006. Comparative study of the determination of trimethylamine in water and air by combining liquid chromatography and solid-phase microextraction with on-fiber derivatization. Talanta, 69(3): 716-723.
Chafer-Pericas, C., Herraez-Hernandez, R. and Campins-Falco, P., 2004. Liquid chromatographic determination of trimethylamine in water. Journal of Chromatography A, 1023(1): 27-31.
Challenger, F., 1951. Biological methlyation. Advances in Enzymology, 12: 429-491.
Charlson, R.J., Lovelock, J.E., Andreae, M.O. and Warren, S.G., 1987. Oceanic phytoplankton, atmospheric sulphur, cloud albedo and climate. Nature, 326: 655-661.
Chen, Y., 2012. Comparative genomics of methylated amine utilization by marine Roseobacter clade bacteria and development of functional gene markers (tmm, gmaS). Environmental Microbiology, 14(9): 2308-2322.
Chen, Y., Patel, N.A., Crombie, A., Scrivens, J.H. and Murrell, J.C., 2011. Bacterial flavin-containing monooxygenase is trimethylamine monooxygenase. Proceedings of the National Academy of Sciences, 108(43): 17791-17796.
Chlumsky, L.J., Zhang, L. and Jorns, M.S., 1995. Sequence Analysis of Sarcosine Oxidase and Nearby Genes Reveals Homologies with Key Enzymes of Folate One-carbon Metabolism. Journal of Biological Chemistry, 270(31): 18252-18259.
Clark, D.R., Brown, I.J., Rees, A.P., Somerfield, P.J. and Miller, P.I., 2014. The influence of ocean acidification on nitrogen regeneration and nitrous oxide production in the North-West European shelf sea. Biogeosciences Discuss., 11(2): 3113-3165.
Clarke, K.R. and Gorley, R.N., 2006. PRIMER v6: User Manual, PRIMER-E, Plymouth.
Csonka, L.N., 1989. Physiological and genetic responses of bacteria to osmotic stress. Microbiological Reviews, 53(1): 121-147.
Dacey, J.W.H. and Wakeham, S.G., 1986. Oceanic Dimethylsulfide: Production During Zooplankton Grazing on Phytoplankton. Science, 233(4770): 1314-1316.
daCosta, K.-A., Vrbanac, J.J. and Zeisel, S.H., 1990. The measurement of dimethylamine, trimethylamine, and trimethylamine N-oxide using capillary gas chromatography-mass spectrometry. Analytical Biochemistry, 187(2): 234-239.
Dawit, M., Williams, I.D. and Fitzsimons, M.F., 2001. Determination of 1-aminopropan-2-one, a dissolved sewage component, in water samples. Water Research, 35(5): 1135-1140.
de Zeeuw, J., Vonk, N., Buyten, J., Heijnsdijk, P. and Clarisse, R., 2000. The analysis of volatile amines by capillary gas chromatography. CAST: Chromatography and Separation Technology, 16: 5-8.
de Zeeuw J., V.N., Buyten J., Heijnsdijk P., Clarisse R.,, 2000. The analysis of volatile amines by capillary gas chromatography. CAST: Chromatography and Separation Technology, 16: 5-8.
Demeestere, K., Dewulf, J., De Witte, B. and Van Langenhove, H., 2007. Sample preparation for the analysis of volatile organic compounds in air and water matrices. Journal of Chromatography A, 1153(1–2): 130-144.

Deshnium, P., Gombos, Z., Nishiyama, Y. and Murata, N., 1997. The action in vivo of glycine betaine in enhancement of tolerance of Synechococcus sp. strain PCC 7942 to low temperature. Journal of Bacteriology, 179(2): 339-44.
Dewulf, J. and Van Langenhove, H., 1999. Anthropogenic volatile organic compounds in ambient air and natural waters: a review on recent developments of analytical methodology, performance and interpretation of field measurements. Journal of Chromatography A, 843(1–2): 163-177.
Dickson, D.M.J. and Kirst, G.O., 1986. The role of beta-dimethylsulphoniopropionate glycine betaine and homarine in the osmoacclimation of platymonas-subcordiformis Planta, 167(4): 536-543.
Dziubek, A.M. and Kowal, A.L., 1984. Effect of magnesium hydroxide on chemical treatment of secondary effluent under alkaline conditions, Proceedings of Water Reuse Symposium III. AWWA Research Foundation, San Diego.
Ellison, S.L.R. and Williams, A. (Editors), 2012. Eurachem/CITAC guide: Quantifying Uncertainty in Analytical Measurements.
Erupe, M.E., Viggiano, A.A. and Lee, S.H., 2011. The effect of trimethylamine on atmospheric nucleation involving H2SO4. Atmos. Chem. Phys., 11(10): 4767-4775.
Evans, C.S., Startin, J.R., Goodall, D.M. and Keely, B.J., 2000. Improved sensitivity in detection of chlormequat by liquid chromatography–mass spectrometry. Journal of Chromatography A, 897(1–2): 399-404.
Facchini, M.C., Decesari, S., Rinaldi, M., Carbone, C., Finessi, E., Mircea, M., Fuzzi, S., Moretti, F., Tagliavini, E., Ceburnis, D. and O'Dowd, C.D., 2008. Important Source of Marine Secondary Organic Aerosol from Biogenic Amines. Environmental Science & Technology, 42(24): 9116-9121.
Fitzsimons, M.F., Dawit, M., Revitt, D.M. and Rocha, C., 2005. Effects of early tidal inundation on the cycling of methylamines in inter-tidal sediments. Marine Ecology-Progress Series, 294: 51-61.
Fitzsimons, M.F., Jemmett, A.W. and Wolff, G.A., 1997. A preliminary study of the geochemistry of methylamines in a salt marsh. Organic Geochemistry, 27(1-2): 15-24.
Fitzsimons, M.F., Millward, G.E., Revitt, D.M. and Dawit, M.D., 2006. Desorption kinetics of ammonium and methylamines from estuarine sediments: Consequences for the cycling of nitrogen. Marine Chemistry, 101(1-2): 12-26.
Fowlis, I., 1995. Gas Chromatography: analytical chemistry by open learning. John Wiley & Sons, Chichester.
Galinski, E.A. and Trüper, H.G., 1982. Betaine, a compatible solute in the extremely halophilic phototrophic bacterium Ectothiorhodospira halochloris. FEMS Microbiology Letters, 13(4): 357-360.
Gibb, S.W., 1994. Trace Determination of Ammonia and Methylamines by Flow Injection Extraction-Ion Chromatography in Estuarine and Marine Environments, University of East Anglia.
Gibb, S.W., Mantoura, R.F.C. and Liss, P.S., 1995. Analysis of ammonia and methylamines in natural waters by flow-injection gas diffusion coupled to ion chromatography. Analytica Chimica Acta, 316(3): 291-304.
Gibb, S.W., Mantoura, R.F.C. and Liss, P.S., 1999a. Ocean-atmosphere exchange and atmospheric speciation of ammonia and methylamines in the region of the NW Arabian Sea. Global Biogeochemical Cycles, 13(1): 161-178.
Gibb, S.W., Mantoura, R.F.C., Liss, P.S. and Barlow, R.G., 1999b. Distributions and biogeochemistries of methylamines and ammonium in the Arabian Sea. Deep Sea Research Part II: Topical Studies in Oceanography, 46(3–4): 593-615.
Goldman, J.C. and Dennett, M.R., 1985. Susceptibility of some marine phytoplankton species to cell breakage during filtration and post-filtration rinsing. Journal of Experimental Marine Biology and Ecology, 86(1): 47-58.

Gorham, J., 1984. Separation of plant betaines and their sulphur analogues by cation-exchange high-performance liquid chromatography. Journal of Chromatography A, 287: 345-351.
Gronberg, L., Lovkvist, P. and Jonsson, J.A., 1992. Measurment of aliphatic amines in ambient air and rainwater. Chemosphere, 24(10): 1533-1540.
Hansen, H.P. and Koroleff, F., 2007. Determination of nutrients, Methods of Seawater Analysis. Wiley-VCH Verlag GmbH, pp. 159-228.
Hanson, A.D., Rathinasabapathi, B., Chamberlin, B. and Gage, D.A., 1991. Comparative physiological evidence that beta-alanine betaine and choline-o-sulfate act as compatible osmolytes in halophytic limonium species. Plant Physiology, 97(3): 1199-1205.
Harrison., R.M. (Editor), 1992. Understanding Our Environment: An Introduction to Environmental Chemistry and Pollution. The Royal Society of Chemistry, Cambridge.
Heijthuijsen, J.H.F.G. and Hansen, T.A., 1989. Anaerobic degradation of betaine by marine Desulfobacterium strains. Archives of Microbiology, 152(4): 393-396.
Herraez-Hernandez, R., Chafer-Pericas, C., Verdu-Andres, J. and Campins-Falco, P., 2006. An evaluation of solid phase microextraction for aliphatic amines using derivatization with 9-fluorenylmethyl chloroformate and liquid chromatography. Journal of Chromatography A, 1104(1-2): 40-46.
Hidy, G.M., 1984. Aerosols: An Industrial and Environmental Science. Academic, San Diego.
Higgins, C.F., Cairney, J., Stirling, D.A., Sutherland, L. and Booth, I.R., 1987. Osmotic regulation of gene expression: ionic strength as an intracellular signal? Trends in Biochemical Sciences, 12(0): 339-344.
Holm, P.I., Ueland, P.M., Kvalheim, G. and Lien, E.A., 2003. Determination of choline, betaine, and dimethylglycine in plasma by a high-throughput method based on normal-phase chromatography-tandem mass spectrometry. Clinical Chemistry, 49(2): 286-294.
Hooker, S.B.L., Van Heukelem, L., Thomas, C.S., Claustre, H., Ras, J., Schluter, L., Perl, J., Trees, C., Stuart, V., Head, E., Barlow, R., Sessions, H., Clementson, L., Fishwick, J., Llewellyn, C. and Aiken, J., 2005. The Second SeaWiFS HPLC Analysis Round-Robin Experiment (SeaHARRE-2). NASA Tech. Memo.
Hottiger, T., Boller, T. and Wiemken, A., 1987. Rapid changes of heat and dessication tolerance correlated with changes in trehalose content in *Saccharomyces cerevisiae* cells subjected to temperature shifts. FEBS Letters, 220: 113-115.
Hunter, E.P.L. and Lias, S.G., 1998. Evaluated Gas Phase Basicities and Proton Affinities of Molecules: An Update. Journal of Physical and Chemical Reference Data, 27(3): 413-656.
IPCC, 2007. Contribution of Working Group I to the Fourth Assessment Report of the Intergovernmental Panel on Climate Change, Intergovernmental Panel on Climate Change, Cambridge.
Jakubowska, N., Polkowska, Ż., Namieśnik, J. and Przyjazny, A., 2005. Analytical Applications of Membrane Extraction for Biomedical and Environmental Liquid Sample Preparation. Critical Reviews in Analytical Chemistry, 35(3): 217-235.
Jakubowska, N., Zygmunt, B., Polkowska, Ż., Zabiegała, B. and Namieśnik, J., 2009. Sample preparation for gas chromatographic determination of halogenated volatile organic compounds in environmental and biological samples. Journal of Chromatography A, 1216(3): 422-441.
Jeffrey, S.W. and Wright, S.W., 2006. Photosynthetic pigments in marine microalgae: insights from cultures and the sea. In: S. Rao (Editor), Algal cultures, analogues of blooms and applications. Science Publishers, Enfield, pp. 33-90.
Jönsson, J.Å. and Mathiasson, L., 2001. Memrane extraction in analytical chemistry. Journal of Separation Science, 24(7): 495-507.

Kara, A.B., Rochford, P.A. and Hurlburt, H.E., 2000. An optimal definition for ocean mixed layer depth. Journal of Geophysical Research: Oceans, 105(C7): 16803-16821.
Karl, D.M. and Michaels, A.F., 2001. Nitrogen Cycle. In: J.H. Steele (Editor), Encyclopedia of Ocean Sciences (Second Edition). Academic Press, Oxford, pp. 32-39.
Keller, M.D., Kiene, R.P., Matrai, P.A. and Bellows, W.K., 1999a. Production of glycine betaine and dimethylsulfoniopropionate in marine phytoplankton. II. N-limited chemostat cultures. Marine Biology, 135(2): 249-257.
Keller, M.D., Kiene, R.P., Matrai, P.A. and Bellows, W.K., 1999b. Production of glycine betaine and dimethylsulfoniopropionate in marine phytoplankton. I. Batch cultures. Marine Biology, 135(2): 237-248.
Keller, M.D., Matrai, P.A., Kiene, R.P. and Bellows, W.K., 2004. Responses of coastal phytoplankton populations to nitrogen additions: dynamics of cell-associated dimethylsulfoniopropionate (DMSP), glycine betaine (GBT), and homarine. Canadian Journal of Fisheries and Aquatic Sciences, 61(5): 685-699.
Kiene, R.P. and Hoffmann Williams, L.P., 1998. Glycine betaine uptake, retention and degradation by microorganisms in seawater. Limnology and Oceanography, 43(7): 1592-1603.
Kiene, R.P., Hoffmann Williams, L.P. and Walker, J.E., 1998. Seawater microorganisms have a high affinity glycine betaine uptake system which also recognizes dimethylsulfoniopropionate. Aquatic Microbial Ecology, 15(1): 39-51.
Kiene, R.P. and Slezak, D., 2006. Low dissolved DMSP concentrations in seawater revealed by small-volume gravity filtration and dialysis sampling. Limnology and Oceanography-Methods, 4: 80-95.
King, G.M., 1984. Metabolism of Trimethylamine, Choline, and Glycine Betaine by Sulfate-Reducing and Methanogenic Bacteria in Marine Sediments. Applied and Environmental Microbiology, 48(4): 719-725.
King, G.M., 1988a. Distribution and Metabolism of Quaternary Amines in Marine Sediments. In: T.H. Blackburn and J. Sorensen (Editors), Nitrogen Cycling in Coastal Marine Environments. SCOPE. John Wiley and Sons Ltd, Chichester, pp. 143-173.
King, G.M., 1988b. Methanogenesis from Methylated Amines in a Hypersaline Algal Mat. Applied and Environmental Microbiology, 54(1): 130-136.
King, R., Bonfiglio, R., Fernandez-Metzler, C., Miller-Stein, C. and Olah, T., 2000. Mechanistic investigation of ionization suppression in electrospray ionization. Journal of the American Society for Mass Spectrometry, 11(11): 942-950.
Kirkwood, D.S., 1989. Simulataneous determination of selected nutrients in seawater.
Koc, H., Mar, M.-H., Ranasinghe, A., Swenberg, J.A. and Zeisel, S.H., 2002. Quantitation of Choline and Its Metabolites in Tissues and Foods by Liquid Chromatography/Electrospray Ionization-Isotope Dilution Mass Spectrometry. Analytical Chemistry, 74(18): 4734-4740.
Kondo, Y., Sakamoto, A., Nonaka, H., Hayashi, H., Saradhi, P.P., Chen, T.H. and Murata, N., 1999. Enhanced tolerance to light stress of transgenic Arabidopsis plants that express the codA gene for a bacterial choline oxidase. Plant Molecular Biology, 40(2): 279-288.
Kovala, P.E. and Larrance, J.D., 1996. Comparison of phytoplankton cell numbers, cell volume, cell surface and plasma volume, per metre, from microscopic counts, University of Washington, Seattle.
Kuenzler, E.J. and Ketchum, B.H., 1962. Rate of phosphorus uptake by *Phaeodactylum tricornutum*. Biological Bulletin, 123: 134-145.
Kulmala, M., 2003. How particles nucleate and grow. Science, 302(5647): 1000-1001.
Kulmala, M., Vehkamäki, H., Petäjä, T., Dal Maso, M., Lauri, A., Kerminen, V.M., Birmili, W. and McMurry, P.H., 2004. Formation and growth rates of ultrafine atmospheric particles: a review of observations. Journal of Aerosol Science, 35(2): 143-176.

Kuráň, P. and Soják, L., 1996. Environmental analysis of volatile organic compounds in water and sediment by gas chromatography. Journal of Chromatography A, 733(1–2): 119-141.
Kurten, T., Loukonen, V., Vehkamaki, H. and Kulmala, M., 2008. Amines are likely to enhance neutral and ion-induced sulfuric acid-water nucleation in the atmosphere more effectively than ammonia. Atmospheric Chemistry and Physics, 8(14): 4095-4103.
Laakso, L., Gagné, S., Petäjä, T., Hirsikko, A., Aalto, P.P., Kulmala, M. and Kerminen, V.M., 2007. Detecting charging state of ultra-fine particles: instrumental development and ambient measurements. Atmos. Chem. Phys., 7(5): 1333-1345.
Lamark, T., Kaasen, I., Eshoo, M.W., Falkenberg, P., McDougall, J. and Strøm, A.R., 1991. DNA sequence and analysis of the bet genes encoding the osmoregulatory choline—glycine betaine pathway of Escherichia coli. Molecular Microbiology, 5(5): 1049-1064.
Lean, D.R.S. and Burnison, B.K., 1979. An evaluation of errors in the ^{14}C method of primary production measurement. Limnology and Oceanography, 24(5): 917-925.
Lee, C., 1988. Amino Acid and Amine Biogeochemistry in Marine Particulate Material and Sediments. In: T.H. Blackburn and J. Sorensen (Editors), Nitrogen Cycling in Coastal Marine Environments. SCOPE. John Wiley and Sons Ltd, Chichester, pp. 125-141.
Lee, C. and Olson, B.L., 1984. Dissolved, exchangeable and bound aliphatic amines in marine sediments: initial results. Organic Geochemistry, 6(0): 259-263.
Lee, S. and Fuhrman, J.A., 1987. Relationships between Biovolume and Biomass of Naturally Derived Marine Bacterioplankton. Applied and Environmental Microbiology, 53(6): 1298-1303.
Liang, C., Zhang, X.Y., Luo, Y., Wang, G.P., Zhou, Q. and Wang, W., 2009. Overaccumulation of glycine betaine alleviates the negative effects of salt stress on wheat. Russian Journal of Plant Physiology, 56(3): 370-376.
Liss, P.S., Hatton, A.D., Malin, G., Nightingale, P.D. and Turner, S.M., 1997. Marine sulphur emissions. Philosophical Transactions of the Royal Society of London. Series B: Biological Sciences, 352(1350): 159-169.
Liss, P.S. and Slater, P.G., 1974. Flux of Gases across the Air-Sea Interface. Nature, 247(5438): 181-184.
Lomstein, B.A., Jensen, A.-G.U., Hansen, J.W., Andreasen, J.B., Hansen, L.S., Berntsen, J.r. and Kunzendorf, H., 1998. Budgets of sediment nitrogen and carbon cycling in the shallow water of Knebel Vig, Denmark. Aquatic Microbial Ecology, 14(1): 69-80.
Mantoura, R.F.C. and Woodward, E.M.S., 1983. Optimization of the indophenol blue method for the automated determination of ammonia in estuarine waters. Estuarine, Coastal and Shelf Science, 17(2): 219-224.
Menden-Deuer, S. and Lessard, E.J., 2000. Carbon to volume relationships for dinoflagellates, diatoms, and other protist plankton. Limnology and Oceanography, 45(3): 569-579.
Merrill, D.T. and Jorden, R.M., 1975. Lime-Induced Reactions in Municipal Wastewaters. Journal (Water Pollution Control Federation), 47(12): 2783-2808.
Mirzaei, H., Brusniak, M.-Y., Mueller, L.N., Letarte, S., Watts, J.D. and Aebersold, R., 2009. Halogenated Peptides as Internal Standards (H-PINS): Introduction of an MS-based internal standard set for liquid chromatography-mass spectrometry. Molecular & Cellular Proteomics, 8(8): 1934-1946.
Möller, B., Oßmer, R., Howard, B., Gottschalk, G. and Hippe, H., 1984. Sporomusa, a new genus of gram-negative anaerobic bacteria including Sporomusa sphaeroides spec. nov. and Sporomusa ovata spec. nov. Archives of Microbiology, 139(4): 388-396.

Moran, M.A. and Zepp, R.G., 1997. Role of photoreactions in the formation of biologically labile compounds from dissolved organic matter. Limnology and Oceanography, 42(6): 1307-1316.
Muller, C., Iinuma, Y., Karstensen, J., van Pinxteren, D., Lehmann, S., Gnauk, T. and Herrmann, H., 2009. Seasonal variation of aliphatic amines in marine sub-micrometer particles at the Cape Verde islands. Atmospheric Chemistry and Physics, 9(24): 9587-9597.
Müller, E., Fahlbusch, K., Walther, R. and Gottschalk, G., 1981. Formation of N,N-Dimethylglycine, Acetic Acid, and Butyric Acid from Betaine by Eubacterium limosum. Applied and Environmental Microbiology, 42(3): 439-445.
Murphy, J. and Riley, J.P., 1962. A modified single solution method for the determination of phosphate in natural waters. Analytica Chimica Acta, 27(0): 31-36.
Nadykto, A., Yu, F., Jakovleva, M., Herb, J. and Xu, Y., 2011. Amines in the Earth's Atmosphere: A Density Functional Theory Study of the Thermochemistry of Pre-Nucleation Clusters. Entropy, 13(2): 554-569.
Nadykto, A.B., Herb, J., Yu, F. and Xu, Y., 2014. Enhancement in the production of nucleating clusters due to dimethylamine and large uncertainties in the thermochemistry of amine-enhanced nucleation. Chemical Physics Letters, 609(0): 42-49.
Nadykto, A.B. and Yu, F., 2007. Strong hydrogen bonding between atmospheric nucleation precursors and common organics. Chemical Physics Letters, 435(1–3): 14-18.
Nagata, T. and Kirchman, D.L., 1996. Bacterial degradation of protein adsorbed to model submicron particles in seawater. Marine Ecology Progress Series, 132: 241-248.
Nalewajko, C. and Lean, D.R.S., 1972. Retention of dissolved compounds by membrane filters as an in the ^{14}C method of primary production measurement. Journal of Phycology, 8: 37-43.
Nyyssölä, A., Kerovuo, J., Kaukinen, P., von Weymarn, N. and Reinikainen, T., 2000. Extreme Halophiles Synthesize Betaine from Glycine by Methylation. Journal of Biological Chemistry, 275(29): 22196-22201.
Pailleux, F. and Beaudry, F., 2012. Internal standard strategies for relative and absolute quantitation of peptides in biological matrices by liquid chromatography tandem mass spectrometry. Biomedical Chromatography, 26(8): 881-891.
Papageorgiou, G. and Murata, N., 1995. The unusually strong stabilizing effects of glycine betaine on the structure and function of the oxygen-evolving Photosystem II complex. Photosynthesis Research, 44(3): 243-252.
Pawliszyn, J., 1997. Solid Phase Microextraction: Theory and Practice. Wiley, New York.
Pocard, J.-A., Vincent, N., Boncompagni, E., Smith, L.T., Poggi, M.-C. and Rudulier, D.L., 1997. Molecular characterization of the bet genes encoding glycine betaine synthesis in Sinorhizobium meliloti 102F34. Microbiology, 143(4): 1369-1379.
Poolman, B. and Glaasker, E., 1998. Regulation of compatible solute accumulation in bacteria. Molecular Microbiology, 29(2): 397-407.
Prasad, K.V.S.K. and Saradhi, P.P., 2004. Enhanced tolerance to photoinhibition in transgenic plants through targeting of glycinebetaine biosynthesis into the chloroplasts. Plant Science, 166(5): 1197-1212.
Record Jr, M.T., Courtenay, E.S., Cayley, D.S. and Guttman, H.J., 1998. Responses of E. coli to osmotic stress: large changes in amounts of cytoplasmic solutes and water. Trends in Biochemical Sciences, 23(4): 143-148.
Ryther, J.H. and Dunstan, M.W., 1971. Nitrogen, phosphorus and eutrophication in the coastal marine environment. Science, 171: 1008-1012.
Schuster, S., Arrieta, J.M. and Herndl, G.J., 1998. Adsorption of dissolved free amino acids on colloidal DOM enhances colloidal DOM utilization but reduces amino acid uptake by orders of magnitude in marine bacterioplankton. Marine Ecology Progress Series, 166: 99-108.

Sharp, J.H., 1983. The distribution of inorganic nitrogen and dissolved and particulate nitrogen in the sea. In: E.J.a.C. Carpenter, D. (Editor), Nitrogen in the Marine Environment. Academic press, new York, pp. 1-38.
Silva, R.C., Aguiar, P.M.S. and Augusto, F., 2004. Coupling of Dynamic Headspace Sampling and Solid Phase Microextraction. Chromatographia, 60(11-12): 687-691.
Skoog, D.A., West, D.M., Holler, F.J. and Crouch, S.R., 2004. Fundamentals of Analytical Chemistry. Brooks/Cole, Belmont.
Smith, L.T., Pocard, J.A., Bernard, T. and Le Rudulier, D., 1988. Osmotic control of glycine betaine biosynthesis and degradation in Rhizobium meliloti. Journal of Bacteriology, 170(7): 3142-3149.
Smith, R.M. and Martell, A.E., 1975. Critical Stability Constants, 2. Plenum, New York.
Smyth, T.J., Fishwick, J.R., AL-Moosawi, L., Cummings, D.G., Harris, C., Kitidis, V., Rees, A., Martinez-Vicente, V. and Woodward, E.M.S., 2010. A broad spatio-temporal view of the Western English Channel observatory. Journal of Plankton Research, 32(5): 585-601.
Southward, A.J., Langmead, O., Hardman-Mountford, N.J., Aiken, J., Boalch, G.T., Dando, P.R., Genner, M.J., Joint, I., Kendall, M.A., Halliday, N.C., Harris, R.P., Leaper, R., Mieszkowska, N., Pingree, R.D., Richardson, A.J., Sims, D.W., Smith, T., Walne, A.W. and Hawkins, S.J., 2004. Long-Term Oceanographic and Ecological Research in the Western English Channel, Advances in Marine Biology. Academic Press, pp. 1-105.
Spielmeyer, A., Gebser, B. and Pohnert, G., 2011. Dimethylsulfide sources from microalgae: Improvement and application of a derivatization-based method for the determination of dimethylsulfoniopropionate and other zwitterionic osmolytes in phytoplankton. Marine Chemistry, 124(1-4): 48-56.
Spielmeyer, A. and Pohnert, G., 2010. Direct quantification of dimethylsulfoniopropionate (DMSP) with hydrophilic interaction liquid chromatography/mass spectrometry. Journal of Chromatography B, 878(31): 3238-3242.
Spielmeyer, A. and Pohnert, G., 2012. Influence of temperature and elevated carbon dioxide on the production of dimethylsulfoniopropionate and glycine betaine by marine phytoplankton. Marine Environmental Research, 73(0): 62-69.
Storey, R. and Jones, R.G.W., 1977. Quaternary ammonium compounds in plants in relation to salt resistance. Phytochemistry, 16(4): 447-453.
Strom, A.R., 1979. Biosynthesis of trimethylamine oxide in calanoid copepods. seasonal changes in trimethylamine monooxygenase activity. Marine Biology, 51(1): 33-40.
Strom, A.R., 1980. Biosynthesis of trimethylamine oxide in *Calanus Finmarchicus.* Properties of soluble trimethylamine monooxygenase. Comparative Biochemical Physiology, 65B: 243-249.
Sun, J., Steindler, L., Thrash, J.C., Halsey, K.H., Smith, D.P., Carter, A.E., Landry, Z.C. and Giovannoni, S.J., 2011. One Carbon Metabolism in SAR11 Pelagic Marine Bacteria. PLoS ONE, 6(8): e23973.
Swinnerton, J.W., Linnenbom, V.J. and Cheek, C.H., 1962. Determination of Dissolved Gases in Aqueous Solutions by Gas Chromatography. Analytical Chemistry, 34(4): 483-485.
Thurman, H. and Burton, E., 2001. Introductory Oceanography. Prentice Hall, New Jersey.
Torpo, L., Kurtén, T., Vehkamäki, H., Laasonen, K., Sundberg, M.R. and Kulmala, M., 2007. Significance of Ammonia in Growth of Atmospheric Nanoclusters. The Journal of Physical Chemistry A, 111(42): 10671-10674.
Turner, S.M., Malin, G., Liss, P.S., Harbour, D.S. and Holligan, P.M., 1988. The seasonal variation of dimethylsulphide and dimethylsylphoniopropionate concentrations in nearshore waters. Limnology and Oceanography, 33: 364-375.

Utermohl, H., 1958. Zur Vervollkommnung der quantitativen Phytoplankton-Methodik. Mitteilungen Internationale Vereinigung für Theoretische und Angewandte Limnologie, 9: 1-38.
Vahl, M., Graven, A. and Juhler, R.K., 1998. Analysis of Chlormequat residues in grain using liquid chromatography-mass spectrometry (LC-MS/MS). Fresenius' Journal of Analytical Chemistry, 361(8): 817-820.
van der Maarel, M.J., Jansen, M., Haanstra, R., Meijer, W.G. and Hansen, T.A., 1996. Demethylation of dimethylsulfoniopropionate to 3-S-methylmercaptopropionate by marine sulfate-reducing bacteria. Applied and Environmental Microbiology, 62(11): 3978-84.
van Duyl, F.C., Gieskes, W.W.C., Kop, A.J. and Lewis, W.E., 1998. Biological control of short-term variations in the concentration of DMSP and DMS during a Phaeocystis spring bloom. Journal of Sea Research, 40(3–4): 221-231.
Van Neste, A., Duce, R.A. and Lee, C., 1987. Methylamines in the marine atmosphere. Geophysical Research Letters, 14(7): 711-714.
VandenBoer, T.C., Markovic, M.Z., Petroff, A., Czar, M.F., Borduas, N. and Murphy, J.G., 2012. Ion chromatographic separation and quantitation of alkyl methylamines and ethylamines in atmospheric gas and particulate matter using preconcentration and suppressed conductivity detection. Journal of Chromatography A, 1252(0): 74-83.
Velasco-García, R., Mújica-Jiménez, C., Mendoza-Hernández, G. and Muñoz-Clares, R.A., 1999. Rapid Purification and Properties of Betaine Aldehyde Dehydrogenase from Pseudomonas aeruginosa. Journal of Bacteriology, 181(4): 1292-1300.
Veuger, B., Middelburg, J.J., Boschker, H.T.S., Nieuwenhuize, J., van Rijswijk, P., Rochelle-Newall, E.J. and Navarro, N., 2004. Microbial uptake of dissolved organic and inorganic nitrogen in Randers Fjord. Estuarine, Coastal and Shelf Science, 61(3): 507-515.
Wafar, M., L'Helguen, S., Raikar, V., Maguer, J.-F. and Corre, P.L., 2004. Nitrogen uptake by size-fractionated plankton in permanently well-mixed temperate coastal waters. Journal of Plankton Research, 26(10): 1207-1218.
Wargo, M.J., Szwergold, B.S. and Hogan, D.A., 2008. Identification of Two Gene Clusters and a Transcriptional Regulator Required for Pseudomonas aeruginosa Glycine Betaine Catabolism. Journal of Bacteriology, 190(8): 2690-2699.
Weast, R.C. (Editor), 1986. Handbook of Chemistry and Physics. CRC Press, Boca Raton.
Welsh, D.T., 2000. Ecological significance of compatible solute accumulation by micro-organisms: from single cells to global climate. FEMS Microbiology Reviews, 24(3): 263-290.
Weretilnyk, E.A. and Hanson, A.D., 1989. Betaine aldehyde dehydrogenase from spinach leaves: Purification, in vitro translation of the mRNA, and regulation by salinity. Archives of Biochemistry and Biophysics, 271(1): 56-63.
Wheeler, P. and Hellebust, J.A., 1981. Use of methylammonium as an ammonium analogue in nitrogen transport and assimilation studies with *Cyclotella criptica* Journal of Phycology, 16: 328-334.
Widdicombe, C.E., Eloire, D., Harbour, D., Harris, R.P. and Somerfield, P.J., 2010. Long-term phytoplankton community dynamics in the Western English Channel. Journal of Plankton Research, 32(5): 643-655.
Winfrey, M.R. and Ward, D.M., 1983. Substrates for sulfate reduction and methane production in intertidal sediments. Applied and Environmental Microbiology, 45(1): 193-199.
Woodhouse, M.T., Carslaw, K.S., Mann, G.W., Vallina, S.M., Vogt, M., Halloran, P.R. and Boucher, O., 2010. Low sensitivity of cloud condensation nuclei to changes in the sea-air flux of dimethyl-sulphide. Atmos. Chem. Phys., 10(16): 7545-7559.

Worsfold, P.J., Monbet, P., Tappin, A.D., Fitzsimons, M.F., Stiles, D.A. and McKelvie, I.D., 2008. Characterisation and quantification of organic phosphorus and organic nitrogen components in aquatic systems: A review. Analytica Chimica Acta, 624(1): 37-58.

Yancey, P., Clark, M., Hand, S., Bowlus, R. and Somero, G., 1982. Living with water stress: evolution of osmolyte systems. Science, 217(4566): 1214-1222.

Yang, X.H., Lee, C. and Scranton, M.I., 1993. Determination of nanomolar concentrations of individual dissolved low molecular weight amines and organic acids in seawater. Analytical Chemistry, 65(5): 572-576.

Yang, X.H., Scranton, M.I. and Lee, C., 1994. Seasonal-variations in concentration and microbial uptake of methylamines in estuarine waters. Marine Ecology-Progress Series, 108(3): 303-312.

Zapata, M., RodrÃ-guez, F. and Garrido, J.L., 2000. Separation of chlorophylls and carotenoids from marine phytoplankton: a new HPLC method using a reversed phase C8 column and pyridine-containing mobile phases. Marine Ecology Progress Series, 195: 29-45.

Zhang, J.-Z. and Chi, J., 2002. Automated analysis of nanomolar concentrations of phosphate in natural waters with liquid waveguide. Environmental Science & Technology, 36(5): 1048-1053.

Zhong, Z., Li, G., Luo, Z. and Zhu, B., 2012. Multi-channel purge and trap system coupled with ion chromatography for the determination of alkylamines in cosmetics. Analytica Chimica Acta, 715(0): 49-56.

Appendix 1. Seasonal particulate glycine betaine concentrations measured in the Western English Channel (October2012- October 2013)

	1L samples			10mL samples		
Date	Average Concentration (nM)	Standard Deviation	Relative Standard Deviation (%)	Average Concentration (nM)	Standard Deviation	Relative Standard Deviation (%)
08/10/2012	47.86	1.78	3.72			
15/10/2012	11.04	1.83	16.54			
22/10/2012	10.88	1.11	10.17			
30/10/2012	4.44	0.41	9.27			
07/11/2012	16.05	3.49	21.76			
14/11/2012	6.50	1.81	27.80			
28/11/2012	9.91	0.91	9.16			
05/12/2012	3.41	0.16	4.64			
09/01/2013	4.56	0.30	6.68			
14/01/2013	2.57	0.20	7.65	304.02	11.42	3.76
21/01/2013	1.97	0.96	48.79			
07/02/2013	2.50	0.07	2.77			
11/02/2013	3.74	0.45	12.15			
19/02/2013	4.71	1.03	21.95			
25/02/2013	4.77	0.68	14.25			
13/03/2013	3.11	0.66	21.23	293.63	21.55	7.34
19/03/2013	5.87	0.63	10.67			
25/03/2013	7.21	1.09	15.10			
03/04/2013	4.29	0.59	13.69			
09/04/2013	4.90	1.39	28.42	401.91	28.05	6.98
17/04/2013	12.24	1.47	12.03	443.90	27.66	6.23
22/04/2013	17.05	4.94	28.94			
29/04/2013	5.48	1.13	20.67			
07/05/2013	22.49	6.81	30.26	451.54	12.90	2.86
15/05/2013	14.12	1.24	8.79	484.29	26.37	5.44
20/05/2013	14.17	2.25	15.85	374.36	41.59	11.11
29/05/2013	5.16	4.73	91.78	317.52	34.87	10.98
03/06/2013	4.37	0.64	14.56			
10/06/2013	5.75	2.12	36.87			
17/06/2013	10.14	3.31	32.65	378.62	13.41	3.54
01/07/2013	40.09	9.04	22.55			
08/07/2013	9.97	0.04	0.39			
15/07/2013	7.05	0.48	6.86			
30/07/2013	13.37	2.32	17.32	419.73	13.17	3.14
06/08/2013	11.06	1.33	12.06			
12/08/2013	17.20	5.49	31.93	336.05	16.28	4.84
19/08/2013	11.03	1.76	15.99			

27/08/2013	13.28	4.35	32.75			
02/09/2013	13.58	3.55	26.17	250.49	42.59	17.00
09/09/2013	25.59	3.32	12.97	406.93	12.75	3.13
30/09/2013	37.60	34.64	92.11			
07/10/2013	49.67	14.81	29.82			